



Diver, Louise A. (2014) *Molecular studies of CYP17A1 gene regulation and its association with hypertension*. PhD thesis.

<https://theses.gla.ac.uk/5016/>

Copyright and moral rights for this work are retained by the author

A copy can be downloaded for personal non-commercial research or study, without prior permission or charge

This work cannot be reproduced or quoted extensively from without first obtaining permission in writing from the author

The content must not be changed in any way or sold commercially in any format or medium without the formal permission of the author

When referring to this work, full bibliographic details including the author, title, awarding institution and date of the thesis must be given

Enlighten: Theses

<https://theses.gla.ac.uk/>
research-enlighten@glasgow.ac.uk



Molecular studies of *CYP17A1* gene regulation and its association with hypertension.

Louise A. Diver MSc. BSc (Hons)

Thesis submitted for the degree of Doctor of Philosophy to the
University of Glasgow

Institute of Cardiovascular and Medical Sciences
College of Medical, Veterinary and Life Sciences
University of Glasgow

March 2014

© Louise A. Diver 2014

Abstract

Human essential hypertension is a highly heritable disorder with complex aetiology and is a major risk factor for cardiovascular events such as ischaemic heart disease and stroke. A combination of multiple environmental and lifestyle factors contribute to blood pressure variation alongside a strong genetic component. Only a small proportion of the genetic factors that regulate blood pressure in the population are currently known, although there is strong evidence that the adrenal cortex and the steroid hormones it produces contribute. Several research strategies have been utilised to dissect the genetic aetiology of hypertension, including candidate gene studies and association studies. Two recent genome-wide association studies aimed to identify variations associated with altered blood pressure and hypertension. A total of ten variants were identified with genome-wide significance after a combined analysis between the two consortia, including a polymorphism located within intron 3 of the *CYP17A1* gene. This variant was reported to be associated with a systolic blood pressure increase of 1.16 mmHg. The *CYP17A1* gene codes for a dual-function enzyme (17 α -hydroxylase/17,20 lyase) expressed primarily in the adrenal cortex and gonads that plays a key role in the steroidogenic pathway. Mutations in its coding region and splice sites are known to cause a rare form of congenital adrenal hyperplasia, suggesting that more common genetic variations at this locus might result in more subtle effects on blood pressure.

A detailed examination of the variation across the *CYP17A1* locus was required to establish patterns of linkage disequilibrium and is presented in Chapter 3. Some information on the polymorphic variation in this region was already available in public databases but precise details on linkage disequilibrium and the corresponding haplotype blocks were lacking. The entire *CYP17A1* gene was directly sequenced, including approximately 2.5kb upstream from the transcriptional start site, in 62 subjects drawn from a normotensive population. Polymorphic variations were identified mainly in the promoter and introns. Two seemingly unrelated blocks of SNPs were identified as being worthy of follow-up investigations, particularly those located in the promoter region, as these could be responsible for alterations in the transcriptional activity of the gene. A total of seven promoter polymorphisms were then genotyped in a larger hypertensive population where the relationship between SNPs was less clear.

In Chapter 4 the effect of *CYP17A1* genotype on intermediate corticosteroid phenotype is explored in a hypertensive population. Corticosterone, cortisol and androgen production were not significantly altered in the population when stratified by genotype for each polymorphism. However when further split by gender, increased cortisol excretion rates were found to associate with the minor allele at position -362 in males and at positions -1204 and -2205 in females. Ratios of various corticosteroid intermediary metabolites were also compared as indices of *CYP17A1* enzymatic activity. Ratios of THDOC:THS were significantly reduced in the presence of the minor allele at positions -34, -1204 and -2205, suggesting increased 17 α -hydroxylase efficiency. In addition, aldosterone excretion was significantly elevated in individuals with CC genotype at position -1877; an indirect genotype-dependent effect has been speculated.

A bioinformatic search was conducted to identify putative transcription factor binding sites at the polymorphic locations. This is presented in Chapter 5. This confirmed the hypothesis that single base changes at each of the seven polymorphic sites could lead to altered transcriptional activity. Using reporter gene assays *in vitro*, the G allele at position -362 (rs248658) associated with greater transcriptional activity than the A allele. The T allele at position -1877 (rs138009835) was transcriptionally less active than its alternative C allele. Similarly, the C allele at position -2205 (rs2150927) showed lower activity than the T allele. These data provide strong evidence that common variation at this locus may be of functional significance.

The studies in Chapter 6 investigate a potential regulatory role of microRNA (miRNA) at the *CYP17A1* locus. MiRNAs are a class of small non-coding RNA molecules that have recently emerged as novel post-transcriptional regulators of gene expression. They function by targeting the 3' untranslated region (3'UTR) of specific mRNAs and cause repression either through mRNA destabilisation followed by degradation, or by mRNA translational repression. Previous research utilised a siRNA approach to knock down Dicer, a protein required for miRNA maturation, and noted significantly increased *CYP17A1* mRNA levels in the H295R human adrenocortical cell line. The investigation presented here cross-referenced bioinformatic analysis with microarray expression data in order to predict which adrenal miRNAs are most likely to regulate *CYP17A1* expression. Predicted miRNAs also shown to be differentially expressed between normal and

diseased adrenal tissue were then selected for further analysis. *In vitro* investigation involved artificial manipulation of the specific miRNA levels in H295R cells followed by measurement of *CYP17A1* mRNA levels. Increased amounts of hsa-miR-320a significantly raised *CYP17A1* mRNA levels, although subsequent reporter construct assays showed that this was not due to direct miRNA binding of the *CYP17A1* 3'UTR. The studies in this chapter are the first to demonstrate miRNA-mediated regulation of *CYP17A1* expression.

In summary, this work aimed to investigate polymorphic variation in the human *CYP17A1* gene and its association with hypertension. Patterns of linkage disequilibrium across the *CYP17A1* gene were identified and the association of several polymorphisms with intermediate corticosteroid phenotype examined. The functional effects of candidate polymorphisms have also been assessed *in vitro*. Further studies will be required to determine whether observed changes in transcriptional activity are the direct result of altered transcription factor binding at polymorphic sites. Finally, the role of miRNA in the post-transcriptional regulation of *CYP17A1* has been confirmed.

Table of Contents

Abstract	1
List of Tables	9
List of Figures	12
Publications	15
Acknowledgements	16
Author's Declaration	17
Abbreviations	18
1 Introduction.....	22
1.1 Blood Pressure and Hypertension	23
1.1.1 Physiological Regulation of Blood Pressure	23
1.1.2 Essential Hypertension.....	26
1.1.2.1 Environmental Risk Factors	26
1.1.2.2 Genetic Risk Factors	27
1.1.3 Genetic Basis of Hypertension	28
1.1.3.1 Candidate Gene Analysis.....	28
1.1.3.2 Linkage Analysis & Genome-Wide Association Studies	31
1.2 The Steroidogenic Pathway	37
1.2.1 The Adrenal Glands.....	38
1.2.1.1 Products of the Adrenal Cortex.....	39
1.2.1.2 Synthesis of Steroid Hormones.....	44
1.2.1.3 Metabolism and Excretion of Steroid Hormones	49
1.3 The <i>CYP17A1</i> Gene	51
1.3.1 17α -Hydroxylase / 17, 20 Lyase	52
1.3.2 Molecular Structure	54
1.3.3 The Role of <i>CYP17A1</i> in Hypertension	55
1.3.3.1 <i>CYP17A1</i> Monogenic Disorders	55
1.3.3.2 Polymorphic Variation.....	58
1.4 Transcriptional Regulation.....	62
1.4.1 Gene Transcription	62
1.4.2 Studies on Transcriptional Regulation of Adrenal <i>CYP17A1</i>	63
1.4.2.1 ACTH Effect on Transcription	67
1.5 Post-Transcriptional Regulation.....	68
1.5.1 MicroRNA.....	69
1.5.1.1 Discovery.....	69
1.5.1.2 Nomenclature	70
1.5.1.3 MiRNA Synthesis in Animals.....	70
1.5.1.4 Target Recognition.....	73

1.5.1.5	Gene-Silencing Mechanisms / Repression Mechanisms	73
1.5.1.6	miRNAs and the Human Adrenal Gland	76
1.6	Aims:	78
2	Methods.....	79
2.1	General Laboratory Practice	80
2.2	Sequencing the <i>CYP17A1</i> Gene in Normotensive and Hypertensive Populations	80
2.2.1	Study Subjects	80
2.2.1.1	Adrenal Function Study	80
2.2.1.2	MRC British Genetics of Hypertension Study.....	80
2.2.2	Determination of Nucleic Acid Quantity and Quality	81
2.2.3	PCR of <i>CYP17A1</i>	81
2.2.4	Agarose Gel Electrophoresis	83
2.2.5	PCR Product Purification	83
2.2.6	Sequencing Reaction	84
2.2.7	Sequencing Reaction Purification	85
2.2.8	Automated Cycle Sequencing	85
2.2.9	Data Analysis	86
2.3	Cell Culture.....	86
2.3.1	Cryopreservation	87
2.3.2	Maintenance of Established Cell Lines.....	87
2.3.3	Counting Cells.....	88
2.3.4	Stimulation of H295R Cells	88
2.4	RNA Isolation & DNase Digestion	88
2.5	Reverse Transcription	89
2.6	Quantitative Real-Time Polymerase Chain Reaction.....	90
2.6.1	Universal ProbeLibrary	90
2.6.2	miScript qRT-PCR System.....	92
2.6.3	qRT-PCR Data Analysis	93
2.7	Reporter Constructs	94
2.7.1	pEZX - 3'UTR Reporter Construct	94
2.7.2	pGL3 - 5' Regulatory Region Reporter Construct.....	94
2.7.2.1	Site-Directed Mutagenesis.....	94
2.7.3	Transformation of Competent Cells.....	95
2.7.4	Small Scale DNA Purification.....	96
2.7.5	Large Scale DNA Purification.....	97
2.7.6	Verification of Plasmids.....	98
2.7.6.1	Restriction Endonuclease Digestion	98
2.7.6.2	Plasmid Sequencing	98

2.8	Transient Cell Line Transfection	99
2.8.1	5' Regulatory Region Reporter Construct Transfection	99
2.8.2	3'UTR Reporter Construct Transfection	100
2.8.2.1	Preparation of Small Molecules	100
2.8.2.2	3'UTR Reporter Construct Co-transfection	100
2.8.2.3	Small Molecule Transient Transfection.....	101
2.9	Dual Reporter Luciferase Assay	102
2.10	Statistical Analysis	102
3	Characterisation of Genetic Variation at the Human <i>CYP17A1</i> Locus	103
3.1	Introduction	104
3.2	Aims	104
3.3	Methods	105
3.3.1	Subjects.....	105
3.3.1.1	SNP Discovery Phase.....	105
3.3.1.2	Hypertensive Population.....	105
3.3.2	Sequencing	105
3.3.3	Statistical Analysis.....	106
3.4	Results.....	106
3.4.1	SNP Discovery Phase.....	106
3.4.1.1	PCR of <i>CYP17A1</i>	106
3.4.1.2	Polymorphism Identification	107
3.4.1.3	Linkage Disequilibrium.....	111
3.4.1.4	Haplotype Analysis.....	119
3.4.2	Hypertensive Population.....	121
3.4.2.1	Promoter Region Variation in the <i>CYP17A1</i> Gene	121
3.4.2.2	Linkage Disequilibrium and Haplotype Analysis	122
3.5	Discussion	125
3.6	Conclusions	128
4	Investigation of the Phenotypic Consequences of <i>CYP17A1</i> Promoter Region Polymorphisms on Corticosteroid Production in a Hypertensive Population.	129
4.1	Introduction	130
4.2	Aims	132
4.3	Methods	132
4.3.1	Study Subjects	132
4.3.2	Urinary Corticosteroid Metabolite Measurements	133
4.3.3	Data Analysis	133
4.4	Results.....	133
4.4.1	Demographics	134

4.4.2	Association of Genotype with Urinary Corticosteroid Metabolite Excretion Rates and Patterns.....	138
4.5	Discussion	158
4.6	Conclusions	164
5	<i>In Vitro</i> Studies of <i>CYP17A1</i> Transcription.....	165
5.1	Introduction	166
5.2	Aims	167
5.3	Bioinformatics.....	168
5.3.1	Methods	168
5.3.2	Results.....	169
5.3.3	Discussion	179
5.4	Reporter Gene Assays	182
5.4.1	Methods	182
5.4.2	Results - Assessment of Allele Transcriptional Activity	185
5.4.2.1	Restriction Digestion of Plasmids.....	185
5.4.2.2	Confirmation of Mutations.....	185
5.4.2.3	Transcriptional Activity <i>in vitro</i>	188
5.4.3	Results - Assessment of Haplotype Transcriptional Activity	193
5.4.3.1	Verification of Plasmids.....	193
5.4.3.2	Transcriptional Activity <i>in vitro</i>	195
5.4.4	Discussion	198
5.5	Conclusions	200
6	Investigating the Role of MicroRNAs in the Regulation of <i>CYP17A1</i> Expression.....	201
6.1	Introduction	202
6.2	Aims	203
6.3	Materials and Methods	204
6.3.1	Bioinformatic Analysis.....	204
6.3.1.1	Identification of miRNA Genes Located Within <i>CYP17A1</i> Sequence	204
6.3.1.2	Investigation of the Evolutionary Sequence Conservation of <i>CYP17A1</i> 3'UTR	204
6.3.1.3	Bioinformatic miRNA Target Prediction.....	204
6.3.2	Assessment of miRNA Expression in Normal Adrenal Tissue and APA Tissue	205
6.3.3	Pre-miR™ or Anti-miR™ Transfection of H295R Cells.....	205
6.3.4	Investigation of miRNA Binding to 3'UTR Reporter Construct.....	206
6.3.5	Statistical Analysis.....	206
6.4	Results.....	207
6.4.1	Identification of miRNAs Originating from <i>CYP17A1</i> Locus	207

6.4.2	Analysis of the 3'UTR of the <i>CYP17A1</i> Gene.....	208
6.4.3	Identification of Putative miRNA Binding Sites in <i>CYP17A1</i>	208
6.4.4	Adrenally-Expressed miRNAs Predicted to Bind <i>CYP17A1</i> 3'UTR....	211
6.4.5	Assessment of miRNA Effect on <i>CYP17A1</i> mRNA Abundance.....	214
6.4.6	Assessment of pEZX Reporter Construct as an Experimental Tool..	223
6.4.7	miRNA Targeting to the 3'UTR of <i>CYP17A1</i> mRNA.....	224
6.4.8	Further Investigation of miR-320a in Steroidogenesis.....	226
6.4.9	Bioinformatic Analysis to Identify Putative miRNA Binding Sites in the 3'UTRs of <i>POR</i> and <i>CYP5A</i>	228
6.5	Discussion	230
7	General Discussion	240
8	Appendices	247
8.1	Appendix 1.....	247
8.2	Appendix 2.....	251
9	References	253

List of Tables

Table 1-1 Monogenic disorders featuring hypertension.	30
Table 1-2 Examples of linkage studies in hypertension.	32
Table 1-3 Summary of results from meta-analysis of CHARGE and Global BP-Gen.	34
Table 1-4 Genes within a block of SNPs in linkage disequilibrium.....	37
Table 1-5 Identities and abbreviations of key adrenal steroids.....	40
Table 1-6 Major corticosteroid hormones and their urinary metabolites.....	50
Table 1-7 Characteristics of CAH arising from mutations in steroidogenic genes.	56
Table 2-1 Primer sequences for gene expression assays.	91
Table 2-2 Primer assay molecules.	92
Table 2-3 Pre-miR™ and Anti-miR™ molecules.	100
Table 2-4 siRNA targeted to <i>CYP17A1</i> 3'UTR.	100
Table 3-1 Characteristics of polymorphisms identified by sequencing across the human <i>CYP17A1</i> locus in subjects from the Adrenal Function Study population.	109
Table 3-2 Characteristics of polymorphisms genotyped across the human <i>CYP17A1</i> locus in a subset of the BRIGHT cohort.	121
Table 4-1 Number of individuals with each genotype at the seven <i>CYP17A1</i> promoter SNPs.	134
Table 4-2 Demographic data on the BRIGHT study subgroup.....	135
Table 4-3 Demographic data on the BRIGHT study subgroup stratified by -34 genotype.....	135
Table 4-4 Demographic data on the BRIGHT study subgroup stratified by -362 genotype.....	135
Table 4-5 Demographic data on the BRIGHT study subgroup stratified by -804 genotype.....	136
Table 4-6 Demographic data on the BRIGHT study subgroup stratified by -1204 genotype.....	136
Table 4-7 Demographic data on the BRIGHT study subgroup stratified by -1488 genotype.....	136
Table 4-8 Demographic data on the BRIGHT study subgroup stratified by -1877 genotype.....	137
Table 4-9 Demographic data on the BRIGHT study subgroup stratified by -2205 genotype.....	137
Table 4-10 Urinary corticosteroid excretion rates of the BRIGHT study subgroup.	138
Table 4-11 Urinary corticosteroid excretion rates of the BRIGHT study subgroup stratified by -34 genotype.....	143
Table 4-12 Urinary corticosteroid excretion rates of the BRIGHT study subgroup stratified by -362 genotype.	143
Table 4-13 Urinary corticosteroid excretion rates of the BRIGHT study subgroup stratified by -804 genotype.	143
Table 4-14 Urinary corticosteroid excretion rates of the BRIGHT study subgroup stratified by -1204 genotype.....	144
Table 4-15 Urinary corticosteroid excretion rates of the BRIGHT study subgroup stratified by -1488 genotype.....	144
Table 4-16 Urinary corticosteroid excretion rates of the BRIGHT study subgroup stratified by -1877 genotype.....	144
Table 4-17 Urinary corticosteroid excretion rates of the BRIGHT study subgroup stratified by -2205 genotype.....	145

Table 4-18 Ratios of urinary corticosteroid excretion rates of the BRIGHT study subgroup stratified by -34 genotype.	147
Table 4-19 Ratios of urinary corticosteroid excretion rates of the BRIGHT study subgroup stratified by -34 genotype.	148
Table 4-20 Ratios of urinary corticosteroid excretion rates of the BRIGHT study subgroup stratified by -362 genotype.	148
Table 4-21 Ratios of urinary corticosteroid excretion rates of the BRIGHT study subgroup stratified by -804 genotype.	149
Table 4-22 Ratios of urinary corticosteroid excretion rates of the BRIGHT study subgroup stratified by -1204 genotype.	149
Table 4-23 Ratios of urinary corticosteroid excretion rates of the BRIGHT study subgroup stratified by -1488 genotype.	150
Table 4-24 Ratios of urinary corticosteroid excretion rates of the BRIGHT study subgroup stratified by -1877 genotype.	150
Table 4-25 Ratios of urinary corticosteroid excretion rates of the BRIGHT study subgroup stratified by -2205 genotype.	151
Table 4-26 THAlDo excretion of the BRIGHT study subgroup.	152
Table 4-27 THAlDo excretion of the BRIGHT study subgroup stratified by -34 genotype.	152
Table 4-28 THAlDo excretion of the BRIGHT study subgroup stratified by -362 genotype.	152
Table 4-29 THAlDo excretion of the BRIGHT study subgroup stratified by -804 genotype.	152
Table 4-30 THAlDo excretion of the BRIGHT study subgroup stratified by -1204 genotype.	153
Table 4-31 THAlDo excretion of the BRIGHT study subgroup stratified by -1488 genotype.	153
Table 4-32 THAlDo excretion of the BRIGHT study subgroup stratified by -1877 genotype.	153
Table 4-33 THAlDo excretion of the BRIGHT study subgroup stratified by -2205 genotype.	153
Table 4-34 Demographic data on the BRIGHT study subgroup stratified by combinations of alleles (Group 1 vs. Group 2).	155
Table 4-35 Urinary corticosteroid excretion rates of the BRIGHT study subgroup stratified by combinations of alleles (Group 1 vs. Group 2).	155
Table 4-36 Demographic data on the BRIGHT study subgroup stratified by combinations of alleles (Group 1 vs. Group 2+3).	156
Table 4-37 Urinary corticosteroid excretion rates of the BRIGHT study subgroup stratified by combinations of alleles (Group 1 vs. Group 2+3).	156
Table 4-38 Ratios of THDOC:THS of the BRIGHT study subgroup stratified by combinations of alleles (Group 1 vs. Group 3).	157
Table 5-1 Sequences entered into bioinformatic searches for putative transcription factor binding around sites of polymorphic variation.	169
Table 5-2 Number of transcription factor binding sites predicted by each database for the flanking sequence of each polymorphism.	170
Table 5-3 Transcription factors predicted to bind to each polymorphism irrespective of allele.	171
Table 5-4 Transcription factors predicted to bind only the T allele or the C allele at position -34 of <i>CYP17A1</i>	172
Table 5-5 Transcription factors predicted to bind only the A allele or the G allele at position -362 of <i>CYP17A1</i>	173
Table 5-6 Transcription factors predicted to bind only the G allele or the A allele at position -804 of <i>CYP17A1</i>	174

Table 5-7 Transcription factors predicted to bind only the T allele or the C allele at position -1204 of <i>CYP17A1</i>	175
Table 5-8 Transcription factors predicted to bind only the C allele or the G allele at position -1488 of <i>CYP17A1</i>	176
Table 5-9 Transcription factors predicted to bind only the C allele or the T allele at position -1877 of <i>CYP17A1</i>	177
Table 5-10 Transcription factors predicted to bind only the C allele or the T allele at position -2205 of <i>CYP17A1</i>	178
Table 5-11 Transcription factors implicated in the regulation of <i>CYP17A1</i>	179
Table 5-12 Haplotypes found in the promoter region of <i>CYP17A1</i> and their frequencies in the Adrenal Function Study population and subset of the BRIGHT cohort.	183
Table 6-1 Bioinformatic databases used for miRNA target prediction.	205
Table 6-2 Number of precursor and mature miRNA sequences found within <i>CYP17A1</i> introns.	207
Table 6-3 Genomic location information required for miRNA sequence prediction.	207
Table 6-4 Bioinformatic miRNA target site predictions for <i>CYP17A1</i> 3'UTR.....	210
Table 6-5 Identities of miRNAs with putative binding sites in the <i>CYP17A1</i> 3'UTR, coding sequence and 5'UTR.....	210
Table 6-6 Database prediction, sequence and genomic co-ordinates and base pair-matching for selected miRNAs.	213
Table 6-7 qRT-PCR expression of selected miRNAs in H295R cells.	214
Table 6-8 Bioinformatic miRNA target site predictions for <i>CYP5A</i> and <i>POR</i> 3'UTRs.	229
Table 8-1 Primers used to amplify and sequence 2.4kb of <i>CYP17A1</i> promoter in AFS and BRIGHT cohorts.	247
Table 8-2 Expand high fidelity PCR system cycling conditions.	247
Table 8-3 Primers used to amplify and sequence exonic regions of <i>CYP17A1</i> in the AFS cohort.	248
Table 8-4 Thermo-Start <i>taq</i> DNA polymerase PCR enzyme kit cycling conditions.	248
Table 8-5 Primers used to amplify and sequence intronic regions of <i>CYP17A1</i> in the AFS cohort.	249
Table 8-6 Primers used for site-directed mutagenesis of pGL3-17 reporter construct.....	250
Table 8-7 Primers used for sequencing of pGL3-17 (and mutated) reporter constructs.....	250
Table 8-8 Primers used for sequencing of pEZX reporter constructs.	250

List of Figures

Figure 1-1 Factors involved in the regulation of arterial pressure.	25
Figure 1-2 The Renin-Angiotensin System.	25
Figure 1-3 Cross-sectional illustration of the layers of the adrenal gland.	38
Figure 1-4 The cyclopentanoperhydrophenanthrene structure.	39
Figure 1-5 The chemical structure of cholesterol.	39
Figure 1-6 Hypothalamic pituitary axis regulation of cortisol secretion.	42
Figure 1-7 Human corticosteroid biosynthetic pathway.	46
Figure 1-8 Structures of intermediate compounds involved in 17 α -hydroxylase and 17, 20 lyase reactions.	47
Figure 1-9 A schematic representation of the systems of electron transfer.	49
Figure 1-10 Diagram showing the exon/intron structure of <i>CYP17A1</i> gene.	54
Figure 1-11 Mutations known to cause 17 α -hydroxylase/17, 20 lyase deficiency.	57
Figure 1-12 Transcription factor binding sites characterised in the human adrenally-expressed <i>CYP17A1</i> promoter region.	64
Figure 1-13 Overview of miRNA biogenesis and post-transcriptional repression mechanisms.	71
Figure 2-1 Typical PCR resulting from a gradient of annealing temperatures. ...	82
Figure 3-1 PCR fragments from 6 different AFS samples.	107
Figure 3-2 Sequence analysis of the human <i>CYP17A1</i> gene.	108
Figure 3-3 Positions of the 36 variations identified across the human <i>CYP17A1</i> locus.	110
Figure 3-4 Linkage disequilibrium plot of all polymorphisms identified in the human <i>CYP17A1</i> gene.	112
Figure 3-5 Linkage disequilibrium plot of polymorphisms with minor allele frequency >0.05 identified in the human <i>CYP17A1</i> gene.	113
Figure 3-6 Linkage disequilibrium plot of <i>CYP17A1</i> promoter polymorphisms (D' values).	115
Figure 3-7 Linkage disequilibrium plot of <i>CYP17A1</i> promoter polymorphisms (r^2 values).	115
Figure 3-8 Linkage disequilibrium plot of <i>CYP17A1</i> promoter polymorphisms with MAF >0.05 (D' values).	116
Figure 3-9 Linkage disequilibrium plot of <i>CYP17A1</i> promoter polymorphisms with MAF >0.05 (r^2 values).	116
Figure 3-10 Linkage disequilibrium plot of six <i>CYP17A1</i> promoter polymorphisms (D' values).	117
Figure 3-11 Linkage disequilibrium plot of six <i>CYP17A1</i> promoter polymorphisms (r^2 values).	117
Figure 3-12 Linkage disequilibrium plot of four variants found across the <i>CYP17A1</i> locus (D' values).	118
Figure 3-13 Linkage disequilibrium plot of four variants found across the <i>CYP17A1</i> locus (r^2 values).	118
Figure 3-14 Schematic representation of haplotypes generated from LD Block 1 polymorphisms.	120
Figure 3-15 Schematic representation of haplotypes generated from LD Block 2 polymorphisms.	120
Figure 3-16 Linkage disequilibrium plot of common promoter polymorphisms genotyped in a subset of the BRIGHT cohort (D' values).	123
Figure 3-17 Linkage disequilibrium plot of common promoter polymorphisms genotyped in a subset of the BRIGHT cohort (r^2 values).	123

Figure 3-18 Schematic representation of haplotypes present in 2.4kb of the <i>CYP17A1</i> promoter region in a subset of the BRIGHT cohort.....	124
Figure 4-1 Physiological consequences of treatment with a selective <i>CYP17A1</i> inhibitor e.g. abiraterone acetate.	132
Figure 4-2 Correlation between excretion rates of total cortisol and total corticosterone metabolites.	139
Figure 4-3 Correlation between excretion rates of total androgen and total corticosterone metabolites.	140
Figure 4-4 Correlation between excretion rates of total cortisol and total androgen metabolites.....	141
Figure 5-1 Transcription factor binding sites characterised in the human adrenally-expressed <i>CYP17A1</i> promoter region.	166
Figure 5-2 pGL3-17 - the <i>CYP17A1</i> promoter reporter construct.	184
Figure 5-3 Restriction endonuclease digestion of pGL3-17 and seven mutated constructs.....	186
Figure 5-4 Sequence analysis of pGL3-17 mutated plasmids.	187
Figure 5-5 Assessment of relative levels of reporter construct activities.	188
Figure 5-6 Basal expression of mutated reporter constructs relative to opposing allele.	190
Figure 5-7 Stimulated expression of mutated reporter constructs relative to opposing allele.....	192
Figure 5-8 Restriction endonuclease digestion of pGL-17 haplotype reporter constructs.....	194
Figure 5-9 Schematic representation of alleles present in each haplotype reporter construct.....	194
Figure 5-10 Basal expression of haplotype reporter constructs.	196
Figure 5-11 Stimulated expression of haplotype reporter constructs.....	196
Figure 5-12 Basal versus stimulated expression of haplotype reporter constructs.	197
Figure 6-1 Mammalian evolutionary sequence conservation of <i>CYP17A1</i> 3'UTR.	209
Figure 6-2 Venn diagram of miRNAs expressed in normal adrenal tissue and APA predicted to bind to the 3'UTR of <i>CYP17A1</i>	212
Figure 6-3 Expression analysis of miRNA predicted to bind to <i>CYP17A1</i> 3'UTR.	212
Figure 6-4 Assessment of A) <i>CYP17A1</i> mRNA abundance and B) mature miRNA levels post-transfection with specific pre-miRs™ in H295R cells grown in basal conditions.....	216
Figure 6-5 Assessment of A) <i>CYP17A1</i> mRNA abundance and B) mature miRNA levels post-transfection with specific anti-miRs™ in H295R cells grown in basal conditions.....	218
Figure 6-6 Assessment of <i>CYP17A1</i> mRNA abundance in H295R cells grown under basal conditions or stimulated with 1mM (Bu) ₂ CAMP.	219
Figure 6-7 Assessment of A) <i>CYP17A1</i> mRNA abundance and B) mature miRNA levels post-transfection with specific pre-miRs™ in H295R cells stimulated with (Bu) ₂ CAMP.	221
Figure 6-8 Assessment of A) <i>CYP17A1</i> mRNA abundance and B) mature miRNA levels post-transfection with specific anti-miRs™ in H295R cells stimulated with (Bu) ₂ CAMP.	222
Figure 6-9 siRNA verification of the pEZX-17 reporter construct.	223
Figure 6-10 Effect of miR-320a targeting on the luciferase activity of the pEZX-17 reporter construct.....	225
Figure 6-11 Effect of miR-34c-3p targeting on the luciferase activity of the pEZX-17 reporter construct.	225

Figure 6-12 Assessment of A) <i>CYP11A1</i> mRNA abundance and B) mature miRNA levels post-transfection in H295R cells grown in basal conditions.	227
Figure 6-13 Venn diagrams showing microRNAs expressed in normal adrenal tissue and APA tissue that are predicted to bind the 3'UTRs of A) <i>POR</i> and B) <i>CYB5A</i>	229

Publications

Original articles

Robertson S, Mackenzie SM, Alvarez-Madrado S, Diver LA, Lin J, Stewart PM, Fraser R, Connell JM, Davies E. MicroRNA-24 is a novel regulator of aldosterone and cortisol production in the human adrenal cortex. *Hypertension*. 2013 Sep; 62(3):572-8.

McManus F, Sands W, Diver L, MacKenzie SM, Fraser R, Davies E, Connell JM. APEX1 regulation of aldosterone synthase gene transcription is disrupted by a common polymorphism in humans. *Circulation Research*. 2012 Jul 6;111(2):212-9.

Abstracts and awards

Diver LA, Alvarez-Madrado S, Lin J, Wood S, MacKenzie SM, Connell JM, Davies E. MicroRNA-24 is a post-transcriptional regulator of the human *CYP11B1* and *CYP11B2* genes. *Endocrine Reviews* Vol. 34 2013.

The Endocrine Society's 95th Annual Meeting. Poster Communication.

Diver LA, Wood S, MacKenzie SM, Connell JM, Davies E. The role of miR-320a in the regulation of *CYP17A1* and *CYP11A1* expression. *Endocrine Reviews* Vol. 34 2013.

The Endocrine Society's 95th Annual Meeting. Featured Poster Presentation.

Diver LA, Alvarez-Madrado S, Lin J, Wood S, MacKenzie SM, Connell JM, Davies E. Validation of *CYP11B1* and *CYP11B2* regulation by microRNA-24. *Endocrine Abstracts* Vol. 31 2013.

Society for Endocrinology BES 2013. Poster Prize Nominee.

Diver LA, Alvarez-Madrado S, McManus F, MacKenzie SM, Connell JM, Davies E. Transcriptional efficiency of the *CYP17A1* gene is affected by common genetic variations in the 5' regulatory region. *Hypertension* Vol. 30 e-sup1 2012

24th Scientific Meeting of the International Society of Hypertension. Oral Communication

Diver LA, Alvarez-Madrado S, McManus F, MacKenzie SM, Connell JM, Davies E. Polymorphic variation in the 5' regulatory region of the *CYP17A1* gene affects transcriptional efficiency. *Endocrine Reviews* Vol. 33 2012.

The Endocrine Society's 94th Annual Meeting. Poster Communication.

Diver LA, Alvarez-Madrado S, McManus F, MacKenzie SM, Connell JM, Davies E. *CYP17A1* transcription efficiency is significantly altered by two common upstream polymorphisms.

ADRENAL 2012. Exceptional Abstract Scholarship Award Winner

Diver LA, McManus F, Sands W, MacKenzie SM, Fraser R, Connell JM, Davies E. Aldosterone synthase (*CYP11B2*) expression is negatively regulated by APEX1: a novel transcription factor in adrenal steroidogenesis.

ADRENAL 2012. Poster Communication.

Diver LA, Wood S, MacKenzie SM, Connell JM, Davies E. Modulation of *CYP17A1* gene expression by miR-320. *Endocrine Reviews* Vol. 32 2011.

The Endocrine Society's 93rd Annual Meeting. Presidential Poster Prize Nominee.

Acknowledgements

I would like to express my gratitude to all who have contributed to my PhD experience. Firstly, thank you to my supervisors, Prof. Eleanor Davies and Dr. Scott MacKenzie for giving me the opportunity to work in your research group and for all your expertise, guidance and support. I owe a special thank you to Prof. Robert Fraser for all his assistance and constant encouragement throughout the writing process and to Prof. John Connell and Dr. Marie Freel for their continued mentorship. I would also like to thank Dr. Claire Hastie, Dr. John McClure and Lesley Graham for their analytical, statistical and laboratory advice and Dr. Frances McManus for allowing me access to her Adrenal Function Study and patiently training me in the first few months.

This thesis would not have been possible without the help, support and patience of my colleagues, Samantha, Stacy and Elaine. You have each contributed significantly to my development as a scientist. Samantha, I am very grateful for your endless support and advice, your attention to detail is something I could really learn from. Stacy, thank you for sharing your highly skilled lab techniques and for your continued encouragement from Australia. Elaine, thank you for your assistance in seeking out the BRIGHT samples and keeping me organised in the lab. The three of you are more than just colleagues, you are friends for life.

A big thank you also to my office-mates Zaki, Dashti, Sophia, Scott and Omar; we shared a lot of ups and downs as well as many lunches along the way! Thanks also to students Clare, Izah, Junjun, Heather, Kris, Sithu and Marie-Louise for allowing me to assist you in your projects enabling me to develop my teaching abilities. Jim, our daily football chats were a welcome release from failed experiments and laboratory stress and Carole, thanks for the cakes!

Finally, I would like to express my appreciation to my family, Mum, Dad, Nana, Papa, Steven, Tracey, Bradley, Kerry, Gran, Frances, Thomas and to Ian, by dedicating this thesis to them. Their love, support and encouragement has made this all possible.

Author's Declaration

I declare that the work presented in this thesis is, to the best of my knowledge and belief, original and my own work, unless otherwise stated in the text. This work has not been submitted previously for a higher degree. It was carried out under the supervision of Professor Eleanor Davies and Dr. Scott MacKenzie in the Institute of Cardiovascular and Medical Sciences at the British Heart Foundation Glasgow Cardiovascular Research Centre.

Louise A. Diver
March 2014

Abbreviations

(Bu)₂cAMP	Dibutyryl cAMP
17BHS1/3	17 β -hydroxysteroid dehydrogenase type 1/3
17-OH-P	17-hydroxyprogesterone
17-OH-PREG	17-hydroxypregnenolone
18-OH-B	18-hydroxycorticosterone
3β-HSD	3 β -hydroxysteroid dehydrogenase
3β-HSD2	3 β -hydroxysteroid dehydrogenase type 2
3'UTR	3 prime untranslated region
5'UTR	5 prime untranslated region
A	Adenosine
ACA	Adrenocortical adenoma
ACC	Adrenocortical carcinoma
ACE	Angiotensin Converting Enzyme
ACTB	β -actin gene
ACTH	Adrenocorticotrophin Hormone
Ad^o	Adrenodoxin
A'dione	Androstenedione
Ad^r	Adrenodoxin
AETIO	Aetiocholanolone
AFS	Adrenal Function Study
Ago1-4	Argonaute Protein 1-4
AGT	Angiotensinogen gene
Aldo	Aldosterone
AME	Apparent Mineralocorticoid Excess
ANDRO	Androsterone
AngII	Angiotensin II
ANOVA	Analysis of variance
APA	Aldosterone-producing adenoma
AS3MT	Arsenite methyltransferase gene
AT1	Angiotensin type 1 receptor
AT2	Angiotensin type 2 receptor
aTHB	Allotetrahydrocorticosterone
aTHF	Allotetrahydrocortisol
ATP2B1	Plasma membrane calcium-transporting ATPase 1 gene
AU	Arbitrary units
B	Corticosterone
BMI	Body mass index
BP	Blood pressure
bp	base pairs
BRIGHT	British Genetics of Hypertension
C	Cholesterol
C	Cytosine
C10orf26	Chromosome 10 open reading frame 26
C10orf32	Chromosome 10 open reading frame 32
C17	Carbon 17
C19	Carbon 19
C21	Carbon 21
CAH	Congenital adrenal hyperplasia
cAMP	Cyclic adenosine monophosphate
CASZ1	Castor zinc finger 1 gene
CBG	Corticosteroid-binding globulin
cDNA	Complementary DNA
cfu	Colony-forming unit
CHARGE	Cohorts for Heart and Aging research in Genome Epidemiology
CMV	Cytomegalovirus

CNNM2	Cyclin M2 gene
COUP-TF	Chicken ovalbumin upstream promoter- transcription factor
CRH	Corticotrophin-releasing hormone
CSK-ULK3	CSK-ULK 3 gene
C_t	Cycle threshold
CYB5A	Cytochrome b5 gene
CYP11A1	Cholesterol side-chain cleavage gene
CYP11B1	11 β -hydroxylase gene
CYP11B2	Aldosterone synthase gene
CYP17A1	17 α -hydroxylase/17,20 lyase gene
CYP19A1	Aromatase gene
CYP21A1	21-hydroxylase gene
CYP450	Cytochrome P450 enzymes
DASH	Dietary approaches to stop hypertension
DAX1	Dosage-sensitive sex reversal adrenal hypoplasia critical region on chr X gene 1
DBP	Diastolic blood pressure
Dcp2	Decapping enzyme 2
DGCR8	DiGeorge Syndrome Critical Region in Gene 8
DHA	Dehydroepiandrosterone
DHEA	Dehydroepiandrosterone
DHEAS	Dehydroepiandrosterone sulphate
DLRA	Dual Luciferase Reporter Assay
DMSO	Dimethyl sulphoxide
DNA	Deoxyribonucleic acid
dNTPs	Deoxynucleotide triphosphates
DOC	11-deoxycorticosterone
dsDNA	Double-stranded deoxyribonucleic acid
E	Cortisone
EDTA	Ethylenediamine tetra-acetic acid
eIF	Eukaryotic initiation factor
EMSA	Electromobility shift assay
EPIC-Norfolk	European prospective investigation into cancer-the Norfolk cohort
F	Cortisol
FAD	Flavin adenine dinucleotide
FAM	Fluorescein
FCS	Foetal calf serum
FDX1	adrenodoxin
FDXR	adrenodoxin reductase
FGF5	Fibroblast growth factor 5 gene
FMN	Flavin mononucleotide
G	Guanine
g	G-force (relative centrifugal force)
GC/MS	Gas chromatography mass spectrometry
GRA	Glucocorticoid Remediable Aldosteronism
GREs	Glucocorticoid-responsive elements
GW182	Glycine-tryptophan protein of 182 kD
GWAS	Genome-wide association study
HoxD10	Homeobox D10 transcription factor
HPSF	High purity salt free
HSD11B2	11 β -hydroxysteroid dehydrogenase
HWE	Hardy-Weinberg equilibrium
IGF1R	Insulin-like growth factor 1 receptor
INTERSALT	International Study of Salt and Blood Pressure
ITGA9	Integrin alpha-9 gene
ITS	Insulin-transferrin-selenium
IU	International Unit
IUPAC	International Union of Pure and Applied Chemistry
K⁺	Potassium ions

kb	Kilobases
kD	KiloDaltons
LARII	Luciferase assay buffer II
LB	Luria broth
LC:MS/MS	Liquid chromatography tandem mass spectrometry
LD	Linkage disequilibrium
LOD	Logarithm of the odds
MAF	Minor allele frequency
Mb	Megabases
miRISC	miRNA-induced silencing complex
miRNA	Micro ribonucleic acid (microRNA)
MKP-1	Mitogen-activated protein kinase phosphatase-1
MR	Mineralocorticoid receptor
mRNA	Messenger ribonucleic acid
<i>MTHFR</i>	Methylenetetrahydrofolate reductase gene
Na ⁺	Sodium ions
NAD	Nicotinamide adenine dinucleotide
NADPH	Nicotinamide adenine dinucleotide phosphate
NF-1	Nuclear-factor 1
NHANES III	National health and nutrition examination survey III
<i>NR3C2</i>	Nuclear receptor subfamily 3 gene (MR gene)
<i>NR5A1</i>	SF1, Steroidogenic factor 1
<i>NT5C2</i>	5'-nucleotidase cytosolic 2 gene
<i>OPAL1</i>	Outcome predictor in acute leukaemia 1 gene
P	Progesterone
PABP	Poly A binding protein
PACT	Protein activator of PKR
p-bodies	Processing-bodies
PBS	Phosphate buffered saline
PCOS	Polycystic ovary syndrome
PCR	Polymerase chain reaction
pEZX	Reporter construct
pGL3	Reporter construct
PKA	Protein kinase A
PLB	Passive lysis buffer
<i>PNMT</i>	Phenylethanolamine N-methyl-transferase
Pol II	RNA polymerase II
<i>POR</i>	P450 oxidoreductase gene
PREG	Pregnenolone
Pre-miRNA	Preliminary miRNA
Pri-miRNA	Primary miRNA
PRKRA	Protein kinase interferon-inducible double stranded RNA-dependent activator
PSF	Polypyrimidine-tract-binding protein-associated factor
qRT-PCR	Quantitative reverse transcription polymerase chain reaction
QTL	Quantitative trait locus
RAAS	Renin-angiotensin-aldosterone system
Ran-GTP	Ras-related nuclear protein-guanosine-5'-triphosphate
RAS	Renin-angiotensin system
REST	Repressor element 1-silencing transcription factor
RISC	RNA-induced silencing complex
RLC	RNA-induced silencing complex (RISC) loading complex
RLU	Relative light units
RNA	Ribonucleic acid
RNAi	RNA interference
rpm	Revolutions per minute
RQ	Relative quantification
RT	Reverse transcription
S	11-deoxycortisol

S1P	Sphingosine-1-phosphate
SBP	Systolic blood pressure
SEM	Standard error of the mean
SF-1	Steroidogenic factor 1
SHBG	Sex hormone-binding globulin
siRNA	short interfering ribonucleic acid
SNP	Single nucleotide polymorphism
SOC	Super optimal broth with catabolite repression
SPRI	Solid phase reversible immobilisation
SREBP-1	Sterol regulatory element binding protein 1
SULT2A1	Sulfotransferase
SV40	simian virus 40
T	Thymine
TBE	Tris/Borate/EDTA
TBP	TATA-binding protein
TE	Tris/EDTA
TESS	Transcription Element Search System
THA	Tetrahydro-11-dehydrocorticosterone
THAldo	Tetrahydroaldosterone
THB	Tetrahydrocorticosterone
THDOC	Tetrahydrodeoxycorticosterone
THE	Tetrahydrocortisone
THF	Tetrahydrocortisol
THS	Tetrahydrodeoxycortisol
T_m	Melting temperature
TRBP	Tar RNA binding protein
TSS	Transcription start site
U	Uracil
U	Unit
UPL	Universal ProbeLibrary
UV	Ultraviolet
V	Voltage
v/v	Volume/volume
w/v	Weight/volume
WBP1L	WW domain binding protein 1-like gene
WHR	Waist-hip ratio
WTCCC	Wellcome Trust Case Control Consortium
XRN-1/2	5'-3' exoribonuclease 1/2
ZF	Zona fasciculata
ZG	Zona glomerulosa
ZR	Zona reticularis

1 Introduction

High blood pressure affects around one-third of adults worldwide and is a major risk factor for cardiovascular events such as ischaemic heart disease and stroke. The exact cause of essential hypertension is unknown; however it is known that both environmental and genetic factors play key roles in the regulation of blood pressure and it is possible that variations in either of these may predispose to hypertension. A clearer understanding is required of why and how hypertension develops in individuals so that the probability of its onset can be assessed accurately and its consequences pre-empted. The following sections outline the components of blood pressure, the numerous factors that control them and, briefly, the nature of the damage caused by hypertension. This is followed by a more detailed examination of factors predisposing to hypertension and their study.

1.1 Blood Pressure and Hypertension

Arterial blood pressure is the pressure exerted by the circulating blood on vessel walls. Blood pressure is highest when the heart contracts, known as systolic blood pressure (SBP) and lowest when the heart relaxes, the diastolic blood pressure (DBP). Blood pressure is a continuous trait and therefore selecting an upper normal limit is arbitrary. A desirable adult level might be 120/80 (Chobanian *et al.*, 2003).

Recently, recommendations for the management of hypertension have been updated whereby thresholds for pharmacological intervention are clearly defined (James *et al.*, 2013). Treatment should be provided for individuals in the general population ≥ 60 years when SBP ≥ 150 mmHg or DBP ≥ 90 mmHg. The same threshold for DBP is recommended for treatment in the general population < 60 years, however, expert opinion suggests pharmacological intervention when SBP ≥ 140 mmHg.

1.1.1 Physiological Regulation of Blood Pressure

Several physical factors are involved in the regulation of blood pressure, which, in turn, can be influenced by physiological and genetic factors, some of which are outlined in Section 1.1.2. Changes in blood pressure can arise from alterations in cardiac output, defined as heart rate multiplied by the stroke

volume. Also, peripheral resistance, i.e. diameter and smooth muscle tone of the arteries in which the blood is flowing, small arteries at the periphery and viscosity of the blood itself also affect arterial blood pressure. These components are mainly regulated by neural, endocrine and paracrine factors influencing kidney function and vascular tone (Figure 1-1). The regulation of fluid and electrolyte balance by the kidney is of primary importance in determining blood pressure (Guyton *et al.*, 1972; Guyton 1991). One key element affecting the efficiency of the kidney is angiotensin II (Ang II), the active product of the renin-angiotensin system (RAS) (Figure 1-2). In response to stimuli, such as low sodium, the enzyme renin is synthesised and released from juxtaglomerular cells, initiating an enzymatic cascade, converting angiotensinogen to angiotensin I. In turn, this is converted (predominantly within pulmonary vasculature) by the Angiotensin-Converting Enzyme (ACE) into the vasoconstrictor and primary active product angiotensin II. Ang II stimulates aldosterone production, increasing sodium re-absorption in the kidney, and contraction of vascular smooth muscle. Both tend to increase blood pressure. The action of Ang II is mediated through two receptors. Binding to the AT1 receptor promotes vasoconstriction and leads to increased sodium retention in the kidneys. Interaction of Ang II with the AT2 receptor, however, counteracts this effect by stimulating vasodilation (Unger 2002). This is an excellent illustration of how a detailed knowledge of a blood pressure-regulating system is valuable in the treatment of hypertension. Antagonists of ACE and blockers of angiotensin-receptor binding have found effective use. As outlined in Figure 1-1, there are many complex body systems and physiological factors which control the regulation of blood pressure. It is with one of these, adrenocortical activity, that this thesis is mainly concerned.

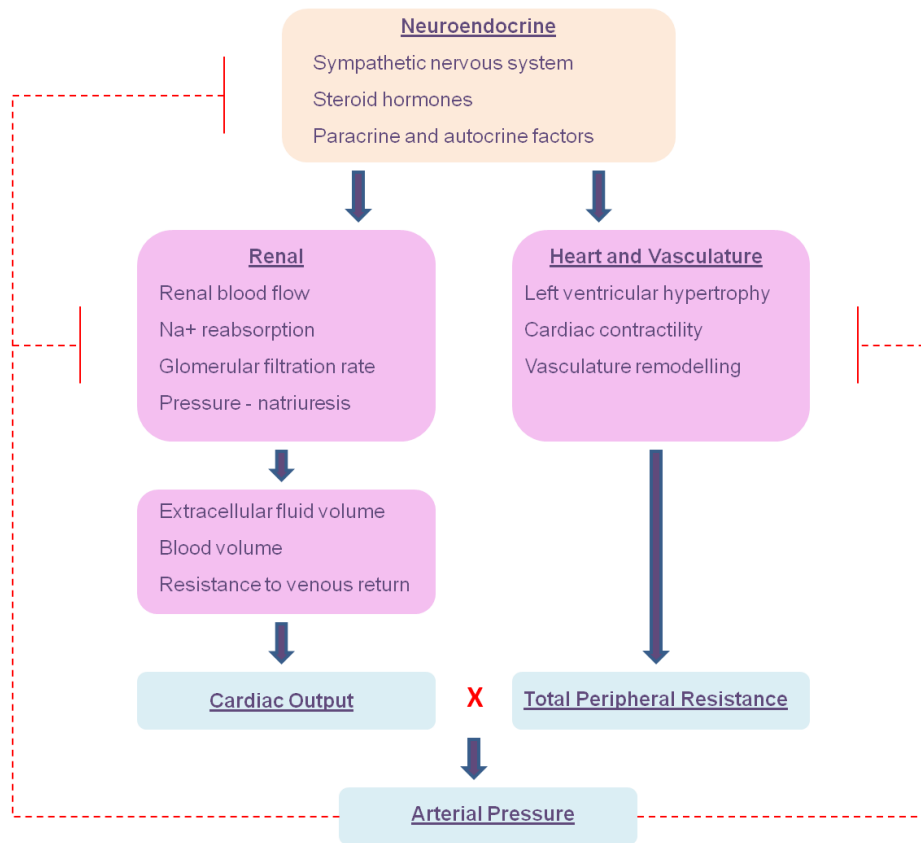


Figure 1-1 Factors involved in the regulation of arterial pressure.
 Arrows show interactions between the different factors; dashed lines indicate negative feedback.
 Adapted from Cowley (2006).

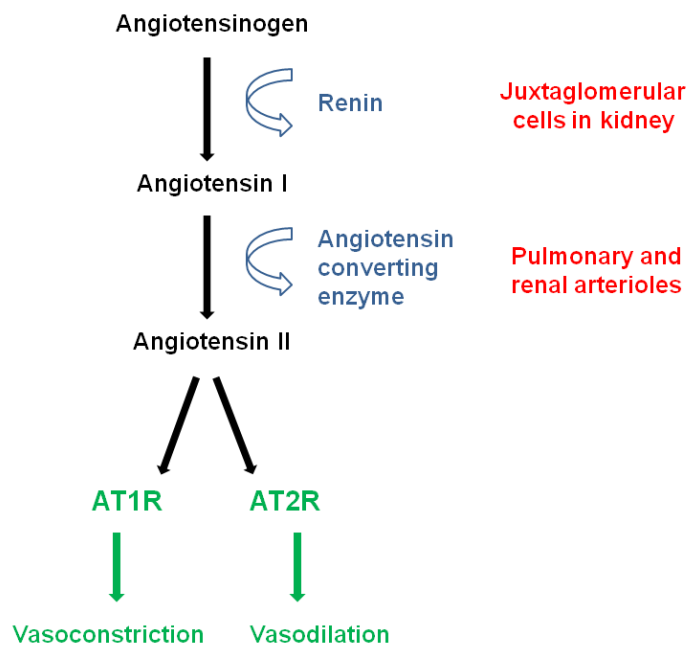


Figure 1-2 The Renin-Angiotensin System.
 AT1R: angiotensin II receptor type 1; AT2R: angiotensin II receptor type 2.

1.1.2 Essential Hypertension

In a small proportion (approximately 5%) of individuals, hypertension can be attributed to an underlying cause, such as renal, endocrine or neurological disorders. In the majority, however, no cause has yet been identified. This is classed as essential hypertension, also known as primary or idiopathic hypertension. Non-modifiable risk factors (e.g. age and gender) have been shown to have some influence on blood pressure; systolic blood pressure increases with age and men tend to have higher blood pressure than women (Franklin *et al.*, 2001; Chobanian *et al.*, 2003). For the development of essential hypertension, the greatest contribution probably arises from a combination of genetic and environmental factors. Diet, including salt intake, and lifestyle (exercise, smoking, alcohol intake etc.) are known contributory factors and are clearly modifiable (see Section 1.1.2.1). Still, about 35% of variation in blood pressure can be attributed to genetic factors (Ward 1990), with a positive family history significantly increasing relative risk of hypertension and cardiovascular disease (Ehret and Caulfield 2013; Williamson *et al.*, 2013). Importantly, environmental and genetic factors contribute separately and probably also interact with each other (see Section 1.1.2.1).

While most of this thesis will focus on the genetic influence and the pathophysiological mechanisms leading to hypertension, it is important to discuss briefly contributing environmental factors, since these will certainly modify genetic predisposal.

1.1.2.1 Environmental Risk Factors

Excess body weight, diet, lack of physical activity, stress and smoking have all been shown to associate with increased blood pressure.

There is compelling evidence that a high sodium intake correlates with increased blood pressure. The INTERSALT study examined urinary sodium and potassium excretion levels and their relationship with blood pressure in 10,079 individuals from 52 centres located in 32 different countries (Stamler *et al.*, 1989). It reported that increased sodium excretion had a significant positive association with increased blood pressure. These findings were corroborated by the EPIC-

Norfolk and NHANES III studies (Hajjar and Kotchen 2003; Khaw *et al.*, 2004). Intervention studies, like the DASH-Sodium Trial, varied sodium intake and evaluated its effect on blood pressure (Vollmer *et al.*, 2001). Here, decreasing sodium intake lowered blood pressure in both normotensive and hypertensive individuals.

The INTERSALT study also reported an inverse relationship between blood pressure and potassium excretion levels. The effects of dietary potassium were explored further through meta-analysis of thirty-three controlled trials by Whelton *et al.*, (1997). Potassium supplementation reduced both blood pressure and the requirement for medication.

Epidemiological studies have shown that populations with diets based on natural foods, which are low in sodium and high in potassium, have considerably lower rates of hypertension than those in industrialised areas with diets high in processed foods (Adroque and Madias 2007). The ability of various body systems to adapt to this balance change is important in maintaining blood pressure. This ability may be genetically determined and, as will be shown later, the adrenal cortex may be influential.

1.1.2.2 Genetic Risk Factors

Blood pressure is a highly heritable trait. Heritability for blood pressure has been reported as 15-40% for systolic blood pressure and 15-30% for diastolic blood pressure, with a combined rate of approximately 35% (Ward 1990). Population studies demonstrate that there is greater similarity in blood pressure levels within families than between families (Longini *et al.*, 1984). Furthermore, monozygotic twins have a greater concordance of blood pressure than dizygotic twins (Feinleib *et al.*, 1977). Several comparisons of blood pressure between biological and adopted siblings corroborate these findings; in a shared environment, biological siblings display greater similarity in blood pressure than their adopted counterparts (Biron *et al.*, 1976; Perusse *et al.*, 1989).

It is not surprising, since so many different physiological systems contribute to blood pressure, that essential hypertension is probably a heterogeneous condition in which small differences in the structure of genes coding for the

active proteins contribute to different degrees of final pressure. How might these contributing factors be identified and their relative contributions established? Various approaches are outlined in the next sections.

1.1.3 Genetic Basis of Hypertension

Various techniques have been employed to identify the genetic loci affecting blood pressure and to quantify their effects. Rare monogenic disorders of which hypertension is a feature provide a starting point, offering an insight into pathways and mechanisms involved in the development of hypertension. A summary of these is provided below. To investigate the genetic aetiology of hypertension, recent research strategies adopted include candidate gene studies and association studies. The progress and utility of each method is reviewed in the following sections.

1.1.3.1 Candidate Gene Analysis

High blood pressure has been the subject of research for more than a century and much is known of the systems contributing to its physiology and pathophysiology. It is therefore logical to study genes - 'candidate genes' - that code for key proteins within these systems. Predictably, some of these relate to the RAAS and, particularly relevant to this review, aspects of corticosteroidogenesis. The candidate gene approach has been used in many hypertension investigations, with varying degrees of success.

Angiotensinogen

The angiotensinogen gene (*AGT*) has been described in Section 1.1.1. Numerous single nucleotide polymorphisms (SNPs) have been identified in its coding and regulatory regions. Jeunemaitre *et al.* (1992) reported an association between the SNPs T174M and M235T and hypertension. However, attempts to replicate these findings produced conflicting results (see review by Dickson and Sigmund 2006). A meta-analysis of several case-control studies also failed to repeat these findings but did report that the T allele at position 235 correlates with increased relative risk of hypertension (Sethi *et al.*, 2003).

Angiotensin Converting Enzyme

The ACE gene encoding angiotensin converting enzyme (*ACE*) has a 287 base-pair insertion/deletion polymorphism within its intron 16 that has been associated with coronary artery disease, endothelial dysfunction and increased ACE plasma levels. Investigations attempting to identify associations between ACE and essential hypertension have, however, produced conflicting results. Some have reported a sex-specific correlation whereby an association of ACE with hypertension is seen only in men (O'Donnell *et al.*, 1998), while others have reported that there is no association at all (Jeunemaitre 2008). No definitive conclusion about the involvement of ACE gene variation in essential hypertension can be drawn at the moment.

Corticosteroidogenic Genes

The adrenal steroidogenic pathway is the focus of this thesis and several of its genes have also been studied as candidates. The *CYP11B1* and *CYP11B2* genes, which encode for 11 β -hydroxylase and aldosterone synthase respectively, catalyse the terminal stages of cortisol and aldosterone production in the adrenal gland (see Figure 1-7 later). Both have been implicated in the development of hypertension. A review of the studies involving these genes can be found in Section 1.3.3.1 and Section 1.3.3.2.

Monogenic Disorders of Hypertension

Studying monogenic or Mendelian forms of hypertension provides an insight into the underlying mechanisms that control blood pressure and can yield strong clues to aid identification of candidate genes. These rare disorders with high blood pressure account for around 1% of all hypertensive cases (Rafiq *et al.*, 2010) and are summarised in Table 1-1. It is of interest that salt and water metabolism is disturbed in nearly all cases. Again, the adrenal cortex features prominently.

Table 1-1 Monogenic disorders featuring hypertension.

AR: autosomal recessive; AD: autosomal dominant ACTH: adrenocorticotrophic hormone; ENaC: epithelial sodium channel.

Disorder	Gene	Inheritance Pattern	Clinical Features
AME (Mune and White 1996; Li <i>et al.</i> , 1998)	<i>HSD11B2</i>	AR	Decreased conversion of cortisol to cortisone leading to excess stimulation of MR. Patient has low aldosterone and suppressed renin.
CAH - subtype IV (Krone and Arlt 2009)	<i>CYP11B1</i>	AR	Decreased cortisol production, increased mineralocorticoid production. Increased androgen levels.
CAH - subtype V (Krone and Arlt 2009)	<i>CYP17A1</i>	AR	Decreased cortisol production, increased mineralocorticoid production. Decreased androgen levels.
GRA (Lifton <i>et al.</i> , 1992a; Lifton <i>et al.</i> , 1992b)	<i>CYP11B1</i> / <i>CYP11B2</i>	AD	Ectopic expression of aldosterone synthase controlled by ACTH leading to increased aldosterone/renin ratio.
Gordon's Syndrome (Wilson <i>et al.</i> , 2001)	<i>WNK1</i> <i>WNK4</i>	AD	Increased activity of Na-Cl co-transporter in distal nephron leading to excess sodium retention and hyperkalaemia.
Liddle's Syndrome (Hansson <i>et al.</i> , 1995)	<i>SCNN1B</i> <i>SCNN1G</i>	AD	Activation of ENaC leading to increased sodium reabsorption and plasma volume.

The study of these monogenic disorders emphasises that several distinct mechanisms can lead to high blood pressure through the common cause of increased sodium reabsorption and plasma volume expansion. Mutation of enzymes participating in the adrenal steroidogenic pathway (see Figure 1-7) leads to various monogenic disorders such as the syndrome of apparent mineralocorticoid excess (AME) and congenital adrenal hyperplasia (CAH). The genes responsible for CAH are of particular relevance to this thesis and are discussed in Section 1.3.3.1. An inactive 11 β -hydroxysteroid dehydrogenase type 2 (*HSD11B2*) enzyme is found in individuals with AME, preventing the conversion of cortisol to cortisone (Mune and White 1996; Li *et al.*, 1998). In the distal renal tubule, the mineralocorticoid receptor (MR) has the same affinity for cortisol and aldosterone so in AME patients; the MR is no longer protected from excess cortisol and is free to bind it. Patients with glucocorticoid-remediable aldosteronism (GRA) experience failure of the regulatory mechanisms to suppress aldosterone synthase, leading to volume-dependent hypertension and suppressed renin (Lifton *et al.*, 1992a; Lifton *et al.*, 1992b). GRA is caused by an unequal recombination event during meiosis that creates a hybrid gene composed of the *CYP11B1* ACTH-responsive promoter and the coding region of

aldosterone synthase (*CYP11B2*). In such cases, aldosterone production is controlled by ACTH rather than Angiotensin II, causing an increase in mineralocorticoid production and, subsequently, increased sodium reabsorption and potassium excretion. Finally, mutations in post-receptor mechanisms (e.g. Na-Cl and ENaC transporters) as in Gordon's syndrome and Liddle's syndrome are described as gain-of-function as they cause increased sodium and chloride retention and subsequent increased plasma volume (Hansson *et al.*, 1995; Wilson *et al.*, 2001).

There is no doubt that numerous studies of monogenic disorders that cause high blood pressure and subsequent investigations into the underlying causative mechanisms have furthered our knowledge of blood pressure regulation. This has prompted investigation of candidate genes in order to test their impact on essential hypertension.

The candidate gene approach has several disadvantages. It makes various assumptions. It requires prior knowledge of possible disease mechanisms and therefore does not explore unknown pathways. Many association studies produce conflicting results, with weak correlation significance that is difficult to replicate. Possible flaws in the experimental approach have been identified. Most candidate gene studies have been statistically underpowered due to relatively small sample sizes, so that the small genetic effects of individual systems may be missed. In response to these limiting factors, linkage analysis and genome-wide association studies were developed.

1.1.3.2 Linkage Analysis & Genome-Wide Association Studies

Linkage Analysis

Linkage analysis studies compare genetic markers within the entire genomic DNA of individuals drawn from families comprising both affected and unaffected members. The term linkage refers to the tendency of particular genetic loci to be co-inherited during meiosis.

Family-based genetic linkage studies take into account the proportion of the genome expected to be shared by two family members, e.g. siblings share

approximately 50% of their genomes. If both are affected by hypertension, the study design hypothesises that the alleles closest to a causative region on the chromosome will be shared more frequently. Such regions are identified as quantitative trait loci (QTL) and warrant further study. Linkage is assessed by logarithm of the odds (LOD) scores, where a positive LOD score is indicative of linkage. This should not be confused with the term ‘linkage disequilibrium’, used later in this thesis, which relates to the phenomenon seen in cohorts whereby two or more loci are found together in the same haplotype more often than by random chance, i.e. the non-random association of alleles. It is also useful to have knowledge of linkage disequilibrium (LD) patterns, as the allele under investigation may be in LD with others elsewhere on the chromosome.

In the last decade, various genetic linkage studies for hypertension have been conducted but few have achieved LOD scores of genome-wide significance, generally held to be $\text{LOD} \geq +3.0$. This arbitrarily-selected threshold indicated odds of 1000 to 1 that the linkage observed has not occurred by chance. Successful linkage studies are summarised in Table 1-2, although the lack of replication within the published literature is apparent (Binder 2007). The genetic heterogeneity of different study cohorts may be a key factor and, therefore, although linkage analysis has generated novel QTLs, its limited success and lack of reproducibility deem it less than ideal for studying the complex genetic contribution to hypertension. In some cases, single QTLs may constitute long portions of the genome and individual genes within such sections remain to be identified.

Table 1-2 Examples of linkage studies in hypertension.

Study	Chromosomal Region	Population
(Levy <i>et al.</i> , 2000)	17q (60-76cM)	Framingham Study
(Kristjansson <i>et al.</i> , 2002)	18q (80-94cM)	Icelandic cohort
(Allayee <i>et al.</i> , 2001)	4p (13-43cM)	18 Dutch families
(Angius <i>et al.</i> , 2002)	2p (26.5-27.1cM)	Hypertensive probands from isolated Sardinian village
(Caulfield <i>et al.</i> , 2003)	6q	Bright hypertensive sibling-pairs

Genome-Wide Association Studies

The currently favoured method for identifying genomic variation associated with hypertension is termed the genome-wide association study (GWAS). GWAS aims to identify genotype associations with a particular trait by examining variation across the entire genome. The successful completion of the Human Genome Project and the development of the International Hapmap Project, have provided greater understanding of variation within the human genome (Lander *et al.*, 2001; Venter *et al.*, 2001; Gibbs *et al.*, 2003). This knowledge, together with more advanced understanding of LD patterns within the genome, have meant that the genetic linkage analysis technique can be expanded to incorporate 'tagSNPs': a single SNP that represents a portion of a chromosome within an LD block. The development of microarray chips has enabled high-throughput genotyping of up to a million SNPs in thousands of subjects. A comparison of allele frequencies in cases and controls should therefore reveal any associations between variants and hypertension or other disease traits.

Despite the initial optimism surrounding this approach, early GWA studies failed to provide major insights into the genetic basis of hypertension. The Wellcome Trust Case Control Consortium (WTCCC) performed the first GWAS for hypertension and, although it identified several risk variants, genome-wide significance, $p < 5 \times 10^{-7}$, was not achieved (Burton *et al.*, 2007). The WTCCC study did, however, identify significant associations with other traits including coronary artery disease; this appeared to indicate that this method had the potential to identify associations with hypertension but that greater sample sizes would be required to attain sufficient statistical power to detect relatively small blood pressure effects. In addition, a greater number of chip probes achieving more detailed genomic coverage were recommended for future studies. Of concern to the WTCCC study was the discrepancy between the average age of the cases (68 years) and controls (48 years). This was a fundamental flaw in the study design, given that the risk of developing hypertension increases with age, it being likely that a significant proportion of the controls would develop the trait over the next 10-20 years. As a result, a more stringent recruitment process should be incorporated into future study designs.

Several other smaller GWA studies had little success (Org *et al.*, 2009; Sabatti *et al.*, 2009; Wang *et al.*, 2009). Both Wang *et al.* and Org *et al.* identified variants of significance only following meta-analyses that combined various cohorts, again confirming the need for very large cohorts.

To address this requirement, subject data sourced from various large international studies were combined. The Global BP-Gen consortium included 34,433 individuals from 17 studies (Newton-Cheh *et al.*, 2009) in which hundreds of thousands of common genetic variants had been genotyped. Computational imputation of 2.5 million SNPs were combined in a meta-analysis and analysed for their association with systolic and diastolic blood pressure and hypertension. The Cohorts for Heart and Ageing Research in Genome Epidemiology (CHARGE) BP consortium utilised 29,136 individuals of European descent from 6 studies (Levy *et al.*, 2009) in a large meta-analysis. An *in silico* comparison between the two studies was then performed in an attempt to replicate their findings. The Global BP-Gen study identified 8 SNPs attaining genome-wide significance: 3 for SBP and 5 for DBP. The CHARGE consortium reported 13 SNPs for SBP, 20 for DBP and 10 for hypertension, all with $p < 4 \times 10^{-7}$ for genome-wide significance. The results from the combined meta-analyses are summarised in Table 1-3. Variance in the levels of significance of each SNP obtained from these two studies may partly be explained by differences in the analytical methods as much as genetic heterogeneity between study populations.

Table 1-3 Summary of results from meta-analysis of CHARGE and Global BP-Gen.

SNP	Chromosome	Nearest Gene	Affected Phenotype	p-value
rs9815354	3	<i>ULK4</i>	DBP	2.54E-09
rs11014166	10	<i>CACNB2</i>	DBP	1.24E-08
rs1004467	10	<i>CYP17A1</i>	SBP	1.28E-10
rS381815	11	<i>PLEKHA7</i>	SBP	1.89E-09
rs2681472	12	<i>ATP2B1</i>	DBP	1.47E-09
rs3681492	12	<i>ATP2B1</i>	SBP	3.76E-11
rs3184504	12	<i>SH2B3</i>	SBP DBP	4.52E-09 2.58E-14
rs2384550	12	<i>TBX3/TBX5</i>	DBP	3.75E-08
rs6495122	15	<i>CSK/ULK3</i>	DBP	1.84E-10

Other studies are attempting to replicate these findings. Takeuchi *et al.*, (2010) conducted a GWAS in a Japanese cohort consisting of 25,826 individuals. Significant blood pressure and hypertension associations were identified with variants within the *MTHFR*, *FGF5*, *CYP17A1*, *ATP2B1* and *CSK-ULK3* genes, all previously reported by the Global BP-Gen and CHARGE studies. Two additional loci, located within the *CASZ1* and *ITGA9* genes, were also statistically significant. A smaller study of 3,210 Chinese Han participants replicated the significant association of four variants found in the CHARGE and BP-Gen studies (Liu *et al.*, 2011) identifying a similar effect size of both *CYP17A1* variants and the *MTHFR* intronic variant in relation to systolic blood pressure. The polymorphism located near *FGF5*, however, had a more pronounced effect in the Chinese Han population compared to the European cohorts. The authors acknowledge that the study was underpowered to detect significant associations with other previously reported variants. These results, while replicating the findings of the major GWA studies, suggest that the genetic contribution to the regulation of blood pressure is likely to be different between ethnic groups.

While pro-GWAS researchers view the latest findings as a substantial advancement in understanding the genetic basis of hypertension, there is a case for some criticism of the approach. Little more than a handful of new loci have been identified despite thousands of participants within the various studies and expensive analytical techniques. It is clear from GWAS results that the hypertensive effect size of each significant variant identified must be small (~1mmHg). Given the relatively low number of candidate genes reported, much of the heritability of hypertension remains unexplained. Furthermore, it is also clear that, for most of the genes identified, no clear mechanism has yet been derived. One important exception is *CYP17A1* (Section 1.3). GWA studies were designed to identify common alleles with frequencies above 5%, leaving the contribution from multiple rare alleles unexamined. Studying the effects of such rare alleles is difficult by this method as even large-scale combined meta-analyses, as described above, are underpowered for their detection.

The reported GWAS findings are also controversial as they fail to identify most of the genes already known to be involved in blood pressure regulation (e.g. those regulating renal sodium handling and the renin-angiotensin-aldosterone systems) inviting scepticism from some researchers. However the intent of linkage and

GWA studies is to identify individual influential genes that can then be studied more intensively.

CYP17A1

While some novel variants may offer promise for future research, the possibility remains that at least some of the reported variants are simply markers for other causative SNPs within the same LD block. While this may, of course, apply to the reported association with *CYP17A1*, the main focus of research in this thesis, more drastic changes to this gene are already known to affect blood pressure (see Section 1.3.3.1). The CHARGE consortium assessed 29,136 participants of European descent and reported that the major allele or polymorphism rs1004467, located within intron three of the *CYP17A1* gene, raises SBP by 1.05 mmHg, giving a p-value of 1.28E-10 in the BP-Gen combined meta-analysis. The Global BP-Gen study reported another highly significant SNP in their analysis of an initial 34,433 subjects, with rs11191548 giving a p-value of 3E-07. Their follow-up genotyping in an expanded cohort displayed a p-value of 9E-15 and *in silico* exchange with the CHARGE consortium provided p=9E-05. A combined analysis of all three stages examined by the BP-Gen consortium found that the major allele increased SBP by 1.16 mmHg (p=7E-24). The genome-wide significance of these loci was confirmed by Takeuchi *et al.*, (2010) in a large Japanese population and by Liu *et al.* (2011) in a modest Chinese Han cohort. The variant examined by the BP-Gen study, rs11191548, lies upstream of *CYP17A1* but is in LD with that reported by the CHARGE consortium, with this particular LD block spanning 6 genes. This is summarised in Table 1-4 (Gomez-Rubio *et al.*, 2010).

Table 1-4 Genes within a block of SNPs in linkage disequilibrium.

Gene	Strand	Function
<i>C10orf26</i> (also <i>WBP1L</i> and <i>OPAL1</i>)	Forward	Two protein-coding transcripts implicated in acute lymphoblastic leukaemia (Holleman <i>et al.</i> , 2006)
<i>CYP17A1</i>	Reverse	Crucial CYP450 enzyme involved in steroidogenesis
<i>C10orf32</i>	Forward	Two protein-coding transcripts with unknown function. Conserved across many species
<i>AS3MT</i>	Forward	Arsenic (3+ oxidation state) methyltransferase: associated with arsenic metabolism (Gomez-Rubio <i>et al.</i> , 2010)
<i>CNNM2</i>	Forward	Cyclin M2: Member of the ancient conserved domain-containing protein family important in magnesium homeostasis (Stuiver <i>et al.</i> , 2011)
<i>NT5C2</i>	Reverse	5' nucleotidase cytosolic 2: Encodes a hydrolase important in cellular purine metabolism (Pesi <i>et al.</i> , 2010)

The *CYP17A1* (17 α -hydroxylase/17,20 lyase) enzyme is part of a system of enzymes synthesising corticosteroids, compounds which participate in the control of intermediary metabolism, the immune system, salt and water homeostasis and - most relevant here - blood pressure. It also plays a key role in androgen and oestrogen synthesis. The *CYP17A1* gene therefore lies at a crucial point in the synthetic pathway that determines the balance of these various systems. Most importantly abnormalities in its function affect blood pressure. The following sections will explain the position, structure and function of the gene in the corticosteroid pathway, known disorders caused by mutations in the coding regions as well as an overview of the regulatory mechanisms that may contribute to altered expression and lead to a hypertensive phenotype.

1.2 The Steroidogenic Pathway

Steroid hormones are synthesised by endocrine glands and released into the blood circulation. The *CYP17A1* gene is primarily expressed in the cortex of the adrenal glands and gonadal tissue. The main focus of this section will be its role within the adrenal cortex.

1.2.1 The Adrenal Glands

The adrenal glands are pyramidal-shaped, functionally distinct endocrine glands situated above each kidney. Each gland is surrounded by an outer fibrous capsule and contains an outer cortex and inner medulla that are derived from two separate embryonic tissues and essentially function as separate glands. As shown in Figure 1-3 below, the cells of the adrenal medulla secrete the catecholamines, adrenaline, noradrenaline and dopamine, released under conditions including emotional excitement, stress and exercise; their function will not be discussed further. The adrenal cortex, on the other hand, can be further divided into three roughly concentric zones: the innermost section closest to the medulla is the zona reticularis (ZR). Next to that is the distinctly larger section of the zona fasciculata (ZF). The outermost layer is the zona glomerulosa (ZG), the principal product of which is the mineralocorticoid, aldosterone. Glucocorticoids, such as cortisol and corticosterone, and the adrenal androgens dehydroepiandrosterone (DHEA) and androstenedione are synthesised by the ZF and ZR. The terms glucocorticoid and mineralocorticoid are further defined in Section 1.2.1.1.



Figure 1-3 Cross-sectional illustration of the layers of the adrenal gland.
Image cannot be displayed due to copyright restrictions.

1.2.1.1 Products of the Adrenal Cortex

Steroid hormones are derived from a basic cyclopentanoperhydrophenanthrene structure (Figure 1-4). The numbering of the carbon atoms of the substrate cholesterol molecule is shown in Figure 1-5.

The principal steroid products and components of the adrenal cortex are outlined in Table 1-5. The relationships between these components and how they produce the end products is further described in Section 1.2.1.2.

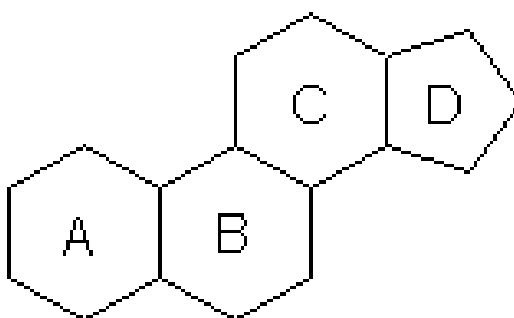


Figure 1-4 The cyclopentanoperhydrophenanthrene structure.

This basic structure is present in all steroid hormones. The rings are identified by letter according to the universally recognised International Union of Pure and Applied Chemistry (IUPAC).

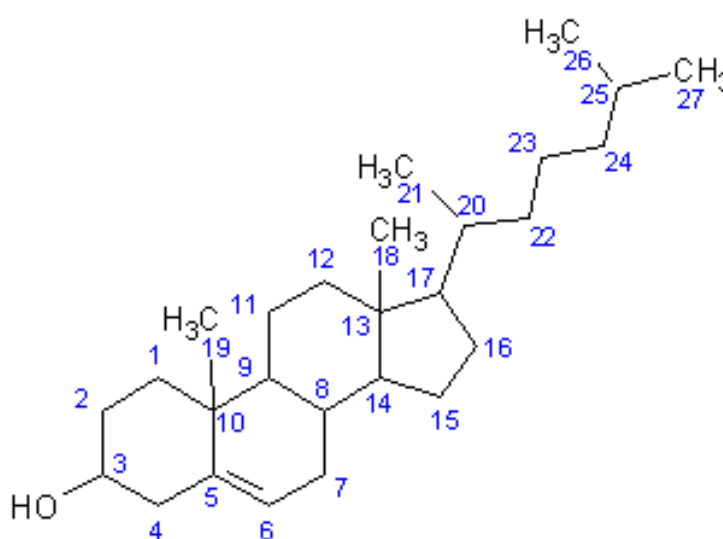


Figure 1-5 The chemical structure of cholesterol.

Cholesterol is the basic molecule from which steroid hormones are derived. The numbering of the carbon atoms is according to the International Union of Pure and Applied Chemistry (IUPAC).

Table 1-5 Identities and abbreviations of key adrenal steroids.

Common Name	Abbreviation	Systematic Name
Aldosterone	Aldo	11 β ,21-dihydroxy-18-al-pregn-4-ene-3, 20-dione
Androstenedione	A'dione	Androst-4-ene-3,17-dione
Cholesterol	C	Cholest-5-en-3 β -ol
Corticosterone	B	11 β ,21-dihydroxypregn-4-ene-3,20-dione
Cortisol	F	11 β ,17 α ,21-trihydroxypregn-4-ene-3, 20-dione
Dehydroepiandrosterone	DHEA/DHA	3 β -hydroxyandrost-5-ene-17-one
Pregnenolone	PREG	3 β -hydroxypregn-5-ene-20-one
Progesterone	P	pregn-4-ene-3,20-dione
11-Deoxycortisol	S	17 α ,21-dihydroxypregn-4-ene-3,20-dione
11-Deoxycorticosterone	DOC	21-hydroxypregn-4-ene-3,20-dione
17-Hydroxypregnenolone	17-OH-PREG	3 β -hydroxypregn-5-ene-20-one
17-Hydroxyprogesterone	17-OH-P	17 α -hydroxypregn-4-ene-3,20-dione
18-Hydroxycorticosterone	18-OH-B	11 β -21-dihydroxypregn-4-ene-3,20-dione-18-al

Mineralocorticoids

The mineralocorticoids help to regulate the extracellular balance of sodium and potassium in the body, the most potent being aldosterone. Mineralocorticoids bind to the mineralocorticoid receptor (MR) in the cytosol. The MR is encoded by the *NR3C2* gene and is expressed in many tissues including colon, kidney and heart. The specificity of the MR is poor as it exhibits an ability to bind both mineralocorticoids and glucocorticoids with equal affinity. The MR, however, can preferentially bind mineralocorticoids through its co-localisation with the 11 β -hydroxysteroid dehydrogenase type 2 (*HSD11B2*) enzyme (Edwards *et al.*, 1988; Funder *et al.*, 1988). This enzyme catalyses the conversion of cortisol to cortisone, which cannot bind the MR. The effects of mutant *HSD11B2* genes described in Section 1.1.3.1.

Glucocorticoids

Glucocorticoids, such as cortisol and corticosterone, are a class of steroid hormone released in response to stress. They are also key regulators of intermediary metabolism and the immune system, and essential in the maintenance of blood pressure and cardiovascular function. The glucocorticoid

exerts its effects by binding to the specific intracellular glucocorticoid receptor (GR) within target cells, forming a complex capable of activating transcription of target genes (Mangelsdorf *et al.*, 1995). For example, the binding of cortisol to the GR has been demonstrated to activate *cis*-acting elements called glucocorticoid response elements (GREs) located in or near hormone-responsive genes (Eberwine 1999). The GR is present in almost every vertebrate animal cell, hence the widespread importance of glucocorticoids in the regulation of whole-body homeostasis.

Of the glucocorticoids, cortisol predominates in humans and is under the control of the hypothalamic/pituitary axis, where corticotropin-releasing hormone (CRH) is released from the hypothalamus and stimulates the anterior pituitary to secrete adrenocorticotrophic hormone (ACTH). Circulating ACTH stimulates glucocorticoid production via the intracellular second messenger cyclic adenosine monophosphate (cAMP), which subsequently activates the protein kinase A pathway. This leads to the phosphorylation of various proteins and an increase in mRNA production. The resultant cortisol acts to inhibit CRH/ACTH production, thus creating a negative feedback loop (Figure 1-6). ACTH release from the pituitary gland exhibits a diurnal rhythm. Under normal circumstances, release of ACTH occurs in brief episodic bursts. These pulses of ACTH release are typically greatest in the early hours of the morning due to pulses of greater intensity (Veldhuis *et al.*, 1990). The amplitude of the pulses declines during the course of the day, an effect mirrored by levels of plasma cortisol.

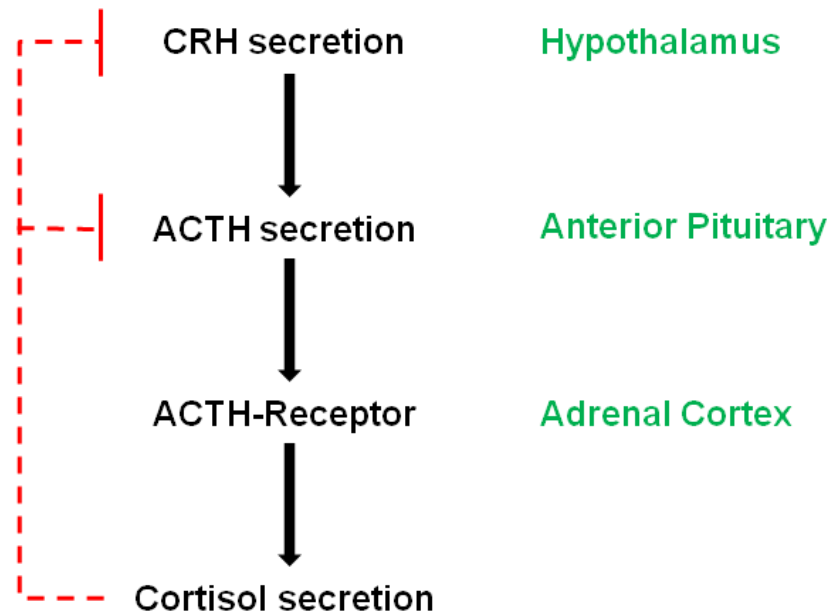


Figure 1-6 Hypothalamic pituitary axis regulation of cortisol secretion.
 CRH: corticotrophin-releasing hormone; ACTH: adrenocorticotrophic hormone.

Cortisol is produced in the zona fasciculata of the adrenal gland. The effects of excess cortisol on blood pressure are well-documented and contribute to increased cardiovascular risk (reviewed by Whitworth *et al.*, 2005). Surprisingly, however, there is little understanding of the mechanisms responsible for these effects. Glucocorticoid-induced hypertension is normally associated with increases in cardiac output or peripheral resistance and is only partly explained by excess sodium and water reabsorption through promiscuous activation of kidney MR (Whitworth *et al.*, 2000). Several studies attribute raised pressure to an increased sensitivity of tissues to cortisol, possibly due to mutant glucocorticoid receptors or impaired cortisol inactivation by type 2 11 β -hydroxysteroid dehydrogenase (Walker *et al.*, 1996; Walker 2007; Goodwin and Geller 2012). In addition, GR is present in vascular smooth muscle and *in vitro* studies of smooth muscle cells showed a significant increase in AT1 receptor gene expression following incubation with synthetic glucocorticoids (Sato *et al.*, 1994). As outlined in Section 1.1.1, the AT1 receptor is a key mediator of vasoconstriction effects and is expressed in the heart, blood vessels, lung, kidney and brain as well as the adrenal cortex.

The effect of glucocorticoids on other hormones has also been investigated in relation to blood pressure. Following the administration of exogenous glucocorticoids to a cohort of healthy male subjects, both systolic blood pressure and erythropoietin concentration increases significantly (Kelly *et al.*, 2000). Erythropoietin is a key regulator of red cell production, known to promote vasoconstriction and the proliferation of endothelial cells, and a positive correlation between it and total peripheral resistance had previously been shown (Langenfeld *et al.*, 1997). Glucocorticoid effects on catecholamine production have also been demonstrated. Conversion of adrenaline from noradrenaline in the adrenal cortex requires the enzyme phenylethanolamine N-methyl-transferase (PNMT), and the synthesis and activity of PNMT requires a very high intra-adrenal concentration of glucocorticoids (Wurtman and Axelrod 1965). However, it remains unclear whether levels of glucocorticoid in the healthy adult influence adrenaline effects on heart rate and blood pressure.

The inhibition of the vasodilator nitric oxide system is another candidate mechanism whereby glucocorticoids may affect blood pressure. In the body, nitric oxide has key roles in the control of vascular tone, dilating vessels and relaxing vascular smooth muscles, and hence reducing blood pressure. Administration of synthetic glucocorticoids *in vitro* (to human endothelial cells) and *in vivo* (to male Wistar-Kyoto rats) results in significantly lower transcript levels of nitric oxide synthase (Wallerath *et al.*, 1999). More recent studies, however, yield conflicting evidence (reviewed by Goodwin and Geller 2012); better understanding of glucocorticoid effects on the nitric oxide system and its contribution to blood pressure is clearly required.

Inappropriate levels of cortisol production are known to occur in rare disorders like Cushing's syndrome and Addison's disease. Cushing's syndrome is characterised by long-term high cortisol levels and is described in further detail below. Addison's disease is the result of cortisol deficiency, whereby the patients exhibit hypotension, hypoglycaemia and weight loss. Cortisol levels are also altered in individuals with congenital adrenal hyperplasia (described in Section 1.3.3.1).

Cushing's Syndrome

Patients with Cushing's syndrome and Cushing's disease exhibit myriad clinical features including persistent hypertension, weight gain, muscle weakness, diabetes mellitus and osteoporosis. Cushing's syndrome arises when the body has prolonged exposure to inappropriately high levels of glucocorticoids, and specifically cortisol. The causes can be exogenous or endogenous. Exogenous synthetic glucocorticoids are routinely administered clinically to treat other conditions such as asthma and rheumatoid arthritis (Wei *et al.*, 2004). Endogenous increases in cortisol production may arise in several ways. Pituitary tumours secreting excess ACTH cause approximately 70% of cases; this is termed Cushing's disease. Another 15% have adrenal tumours which secrete excess cortisol; Cushing's syndrome (Nieman and Ilias 2005). Patients within this category typically have normal to low levels of ACTH secretion due to the negative feedback system (Figure 1-6). Thus the terms Cushing's syndrome and Cushing's disease cannot be used interchangeably. The remaining 15% exhibit ectopic ACTH secretion from tumours located outside the pituitary/adrenal systems.

Adrenal Androgens

The adrenal androgens DHEA and, to a lesser extent, androstenedione, serve as precursors of testosterone and oestrogens. The most abundant product of the adrenal cortex is DHEAS, a sulphated version of DHEA, reversibly catalysed by the enzyme sulfotransferase (*SULT2A1*) in the adrenal glands and liver. DHEAS is more water soluble and stable than DHEA, and its measurement in plasma or urine is commonly used in the assessment of adrenal cancers and polycystic ovarian syndrome (Banaszewska *et al.*, 2003).

1.2.1.2 Synthesis of Steroid Hormones

Cholesterol is the precursor of all adrenal and gonadal steroid hormones. The ovaries secrete oestrogens and progestins, while the testes secrete mainly androgens. Despite the different products of these tissues, the biochemical pathways involved are remarkably similar. The presence or absence of the expression of specific enzymes within each tissue can account for differences in

their secretory capacities. Therefore, it is possible to provide a general outline of the major biosynthetic pathway applicable to these steroid-secreting glands, as shown in Figure 1-7.

The enzymes involved in the biosynthetic pathway are cytochrome P450 enzymes and hydroxysteroid dehydrogenases. To convert cholesterol to aldosterone (referred to later as the 17-deoxy-corticosteroid pathway) and cortisol (17-hydroxy-corticosteroid pathway), a series of reactions modify the pregnane structure and remove part of the side chain. Complete removal of the side chain is required for androgen and oestrogen synthesis. The focus of this thesis is on the *CYP17A1* gene within the adrenal cortex; the chemical changes that result from the action of this enzyme are depicted in Figure 1-8.

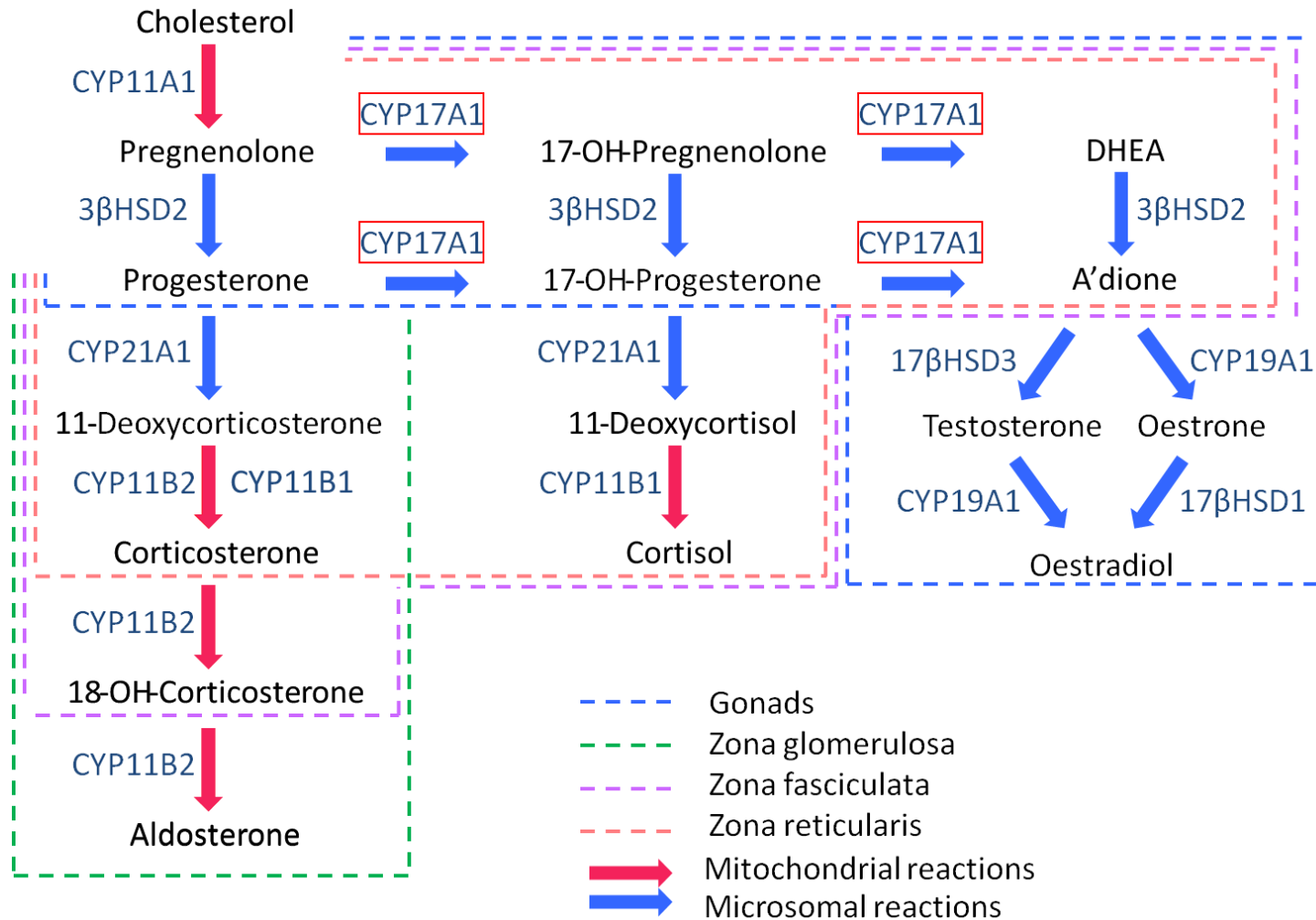


Figure 1-7 Human corticosteroid biosynthetic pathway.

Pathway of corticosteroid synthesis in the adrenal cortex, ovaries and testes. Dashed lines indicate where each reaction occurs. -OH: hydroxyl; A'dione: Androstenedione.

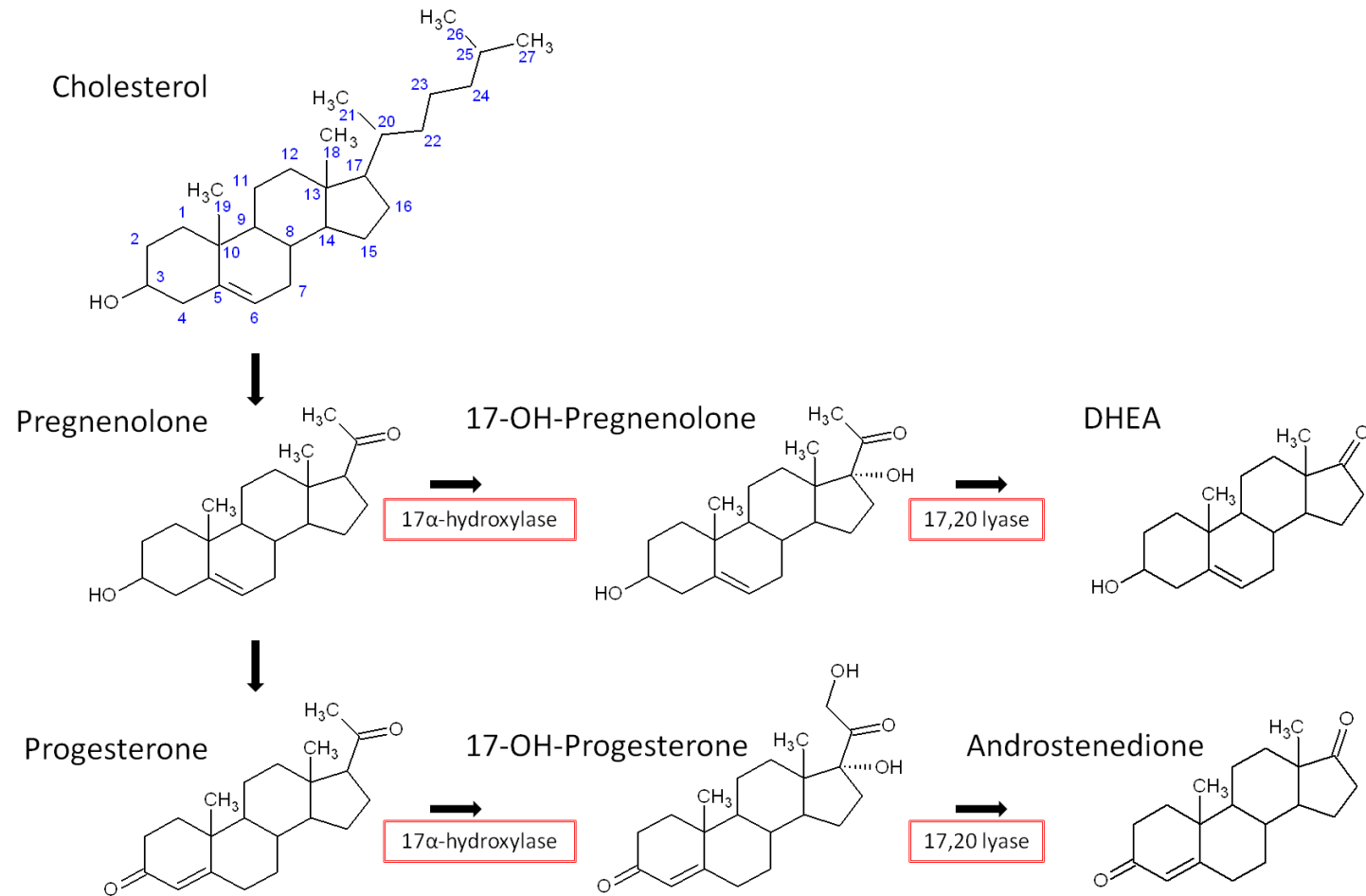
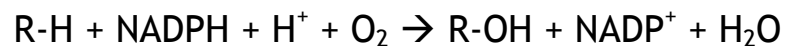


Figure 1-8 Structures of intermediate compounds involved in 17 α -hydroxylase and 17, 20 lyase reactions.
The carbon atoms are numbered on the cholesterol molecule.

Cytochrome P450 Enzymes

Cytochrome P450 enzymes (CYP450) are a large superfamily of haemoproteins present in a wide range of species; in human subjects, 57 putative functional genes exist (Nelson *et al.*, 2004). They catalyse reactions using molecular oxygen to oxidise many substrates and influence a wide range of cellular functions, including xenobiotic metabolism (drug degradation), lipid synthesis and steroid synthesis. CYP450 enzymes can be further classified on the basis of their location of action. Five cytochrome P450 enzymes participate in corticosteroid synthesis: *CYP11A1*, *CYP11B1* and *CYP11B2* are located in the mitochondria; *CYP17A1* and *CYP21A1* are associated with the endoplasmic reticulum and are termed microsomal.

In the adrenal glands and gonads, CYP450s catalyse a monooxygenase reaction, adding an oxygen atom into the steroid substrate R-H utilising an electron donor, usually nicotinamide adenine dinucleotide phosphate (NADPH). The locus and orientation of the resulting hydroxyl group are specific to the enzyme. The basic reaction stoichiometry is:



Mitochondrial and microsomal CYP450 enzymes use different mechanisms of electron transfer (Figure 1-9). Mitochondrial enzymes receive electrons via an electron transfer chain. Two electrons are transferred to the flavoprotein adrenodoxin (ferredoxin) reductase (*FDXR*) upon binding to NADPH, and are subsequently transferred to adrenodoxin (*FDX1*), a non-haem iron-sulphur protein (Miller 2005b). This then interacts and donates the electrons to the haem iron of the CYP450 before being transferred to the substrate. In contrast, microsomal CYP450s employ a single flavoprotein, P450 oxidoreductase (POR), with two flavins: flavinadenine dinucleotide (FAD) and flavin mononucleotide (FMN). In certain circumstances, cytochrome b5 can also be utilised in this process (Miller 2005b) (see Section 1.3.1). The differing electron transport mechanisms described above may play an important role in regulating enzymatic function. This applies to *CYP17A1* and will be further explained in Section 1.3.1.

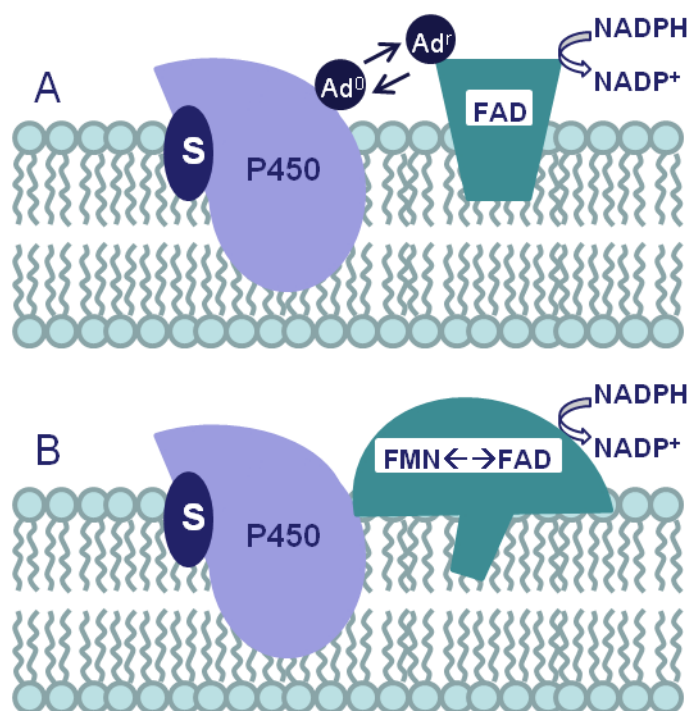


Figure 1-9 A schematic representation of the systems of electron transfer.

Panel A shows the mitochondrial system and Panel B the microsomal system. Adapted from Payne and Hales (2004). FAD: flavin adenine dinucleotide; FMN: flavin mononucleotide; Ad^r: adrenodoxin reductase; Ad^o: adrenodoxin; S: substrate

Hydroxysteroid Dehydrogenases

Hydroxysteroid dehydrogenases are non-metalloenzymes with two essential roles (reviewed by Payne and Hales 2004). Within the steroidogenic tissues, they are essential, particularly 3 β -hydroxysteroid dehydrogenase (3 β -HSD), for the biosynthesis of steroid hormones. They are also expressed in peripheral tissue, (e.g. the kidney), where they have a key role in steroid metabolism, e.g. *HSD11B2* (see Section 1.1.3.1). In contrast to cytochrome P450 enzymes, which are the products of individual genes, the dehydrogenases have several isoforms or isozymes, each encoded by a different gene. Each isoform has a specific expression pattern, cellular localisation and catalytic activity (reductase or dehydrogenase). All dehydrogenase enzymes utilise co-factors that donate or accept hydrogen molecules. For example, NAD⁺/NADP⁺ are co-factors for 3 β -HSD.

1.2.1.3 Metabolism and Excretion of Steroid Hormones

Following their synthesis in the endocrine glands, steroid hormones are released immediately into the bloodstream. Due to their lipophilic properties, steroid

molecules are usually bound to carrier proteins, for example, plasma albumin, corticosteroid-binding globulin (CBG) or the sex hormone-binding globulin (SHBG). Alternatively, they may be in a conjugated form within the circulation (linked to hydrophilic substances, such as sulphate or glucuronide derivatives). The unbound molecules, sometimes known as the ‘free fraction’, are considered the biologically active portion. Therefore, in addition to the rate of synthesis from the endocrine glands, the effective concentration of a steroid hormone can also be affected by the proportion of ‘free’ hormone, blood flow rate, and the rate of metabolism and excretion (i.e. clearance rate).

Steroid hormones must be inactivated after they have served their purpose in a tissue-specific setting. Peripheral steroid inactivation occurs mainly in the liver, but also may occur in the kidneys or within target tissues. For corticosteroids, this involves modifications to the chemical structure, commonly the saturation, or reduction, of the A ring. Inactive steroid hormones are usually then excreted as urinary metabolites. The corticosteroid metabolites are conjugated with glucuronic acid to increase water solubility. DHEA, on the other hand, is sulphated to form DHEAS. Urinary metabolite excretion rates can be used as a measure of steroid production although, interpretation of urinary steroid metabolite analyses is complicated by the fact that a single steroid hormone is converted to several metabolites and some metabolites originate from more than one hormone. The major corticosteroid hormones and their urinary metabolites are shown in Table 1-6.

Table 1-6 Major corticosteroid hormones and their urinary metabolites.

Steroid Hormone	Urinary Metabolite	Abbreviation
Cortisol	Tetrahydrocortisol allotetrahydrocortisol	THF aTHF
Cortisone	Tetrahydrocortisone	THE
Deoxycortisol	Tetrahydrodeoxycortisol	THS
Corticosterone	Tetrahydrocorticosterone allotetrahydrocorticosterone Tetrahydro-11-dehydrocorticosterone	THB aTHB THA
Deoxycorticosterone	Tetrahydrodeoxycorticosterone	THDOC
Aldosterone	Tetrahydroaldosterone	THAldo
Dehydroepiandrosterone	Dehydroepiandrosterone Androsterone Aetiocholanolone	DHEA/DHA ANDRO AETIO

The complex biosynthetic role of 17 α -hydroxylase / 17,20 lyase was shown in Figure 1-8. The following section examines this key steroidogenic phase in more detail.

1.3 The *CYP17A1* Gene

The *CYP17A1* gene encodes a dual-function cytochrome P450 (CYP450) enzyme expressed primarily in the adrenal cortex, ovarian thecal cells and testes (Chung *et al.*, 1987). This thesis focuses on its role within the adrenal cortex. The gene product of *CYP17A1*, often referred to as the 17 α -hydroxylase enzyme, functions as a hydroxylase in the zona fasciculata, converting pregnenolone and progesterone at carbon 17 (C17) to 17 α -hydroxypregnenolone and 17 α -hydroxyprogesterone respectively. In the zona reticularis, it functions as a 17,20-lyase on these hydroxylated products and cleaves the C17,20 bond, producing dehydroepiandrosterone (DHEA) and androstenedione (Figure 1-8). Evidence suggests DHEA is the predominant adrenal androgen product, with androstenedione formed through conversion of DHEA by the enzyme *3 β HSD2*, as opposed to conversion from 17 α -hydroxyprogesterone by *CYP17A1* (Auchus *et al.*, 1998). Until the 1980s, it was believed that 17 α -hydroxylase and 17,20 lyase were separate enzymes but biochemical studies in the pig revealed that the *CYP17A1* protein catalysed both reactions at a single active site (Nakajin and Hall 1981). Studies in other species yielded similar results. That both enzymatic activities were the result of a single gene in humans was confirmed in 1991 when non-steroidogenic cells were transfected with vectors containing the *CYP17A1* gene and both activities detected (Lin *et al.*, 1991). As described in Section 1.2.1.2, *CYP17A1* locates to the endoplasmic reticulum and therefore falls into the microsomal sub-group of CYP450 enzymes.

Scientific evidence indicates the importance of the *CYP17A1* gene in foetal development. Bair and Mellon (2004) used a specific vector to target and knockout *CYP17A1* in mice. In the first generation offspring, apparently healthy and fertile offspring were obtained. These were heterozygous for the *CYP17A1* knockout, meaning they had one copy of the gene (+/-). Subsequent breeding of the first generation offspring resulted in two categories of mice: (+/+) or (+/-).

Noticeably there were no (-/-) offspring. Further investigations established that mice homozygous for the knocked-out gene (-/-) experienced early embryonic lethality around day 7. The exact role of steroidogenesis in foetal development is unclear; however this study suggests that having at least one functional copy of *CYP17A1* is essential to life. The translation of these findings to humans is not straightforward as there are clear differences in steroidogenesis between rodents and humans. In humans, *CYP17A1* is expressed in the gonads and adrenal cortex, but not the placenta whereas, in rodents, it is expressed in the gonads and placenta but not the adrenals (Chung *et al.*, 1987; Durkee *et al.*, 1992; Greco and Payne 1994). Studies of *CYP17A1* expression within the human foetus are obviously difficult, although recent evidence indicates a possible novel role for *CYP17A1* in the development of the human nervous system. *CYP17A1* expression was detected in both the spinal cord and dorsal root ganglia in 9-11 week human foetuses (Schonemann *et al.*, 2012). The electron donor, *POR*, however, is not present. This opens new avenues of investigation concerning *CYP17A1* within the nervous system, termed 'neurosteroids', in order to elucidate its role in foetal development

CYP17A1 also plays a key role in later human development, particularly at adrenarche. Around the age of 6-8 years, the zona reticularis develops and results in a profound increase in adrenal DHEA synthesis (Nakamura *et al.*, 2009). The 17,20 lyase activity facilitates an increase in adrenal androgens, whilst 17 α -hydroxylase activity maintains glucocorticoid levels. Thus, the correct enzymatic expression and regulation are central to normal sexual maturity.

Finally, as noted previously in Section 1.1.3, mutation within the coding regions of the human gene are known to cause a significant reduction in enzymatic activity, resulting in individuals with congenital adrenal hyperplasia (CAH), a rare but severe disorder.

1.3.1 17 α -Hydroxylase / 17, 20 Lyase

The ratio of 17 α -hydroxylase activity to 17,20 lyase activity is important in determining the ratio of C21 to C19 steroids, which are the precursors of sex steroids (Miller 1988). Recent research has identified three important factors which influence this 'switch' in enzymatic function post-translationally. Being a

microsomal CYP450 type II enzyme, 17 α -hydroxylase/17,20 lyase receives electrons from NADPH via P450 oxidoreductase (POR). Initial research using the porcine model found *POR* to be more abundant in testes than the adrenal glands (as reviewed by Miller 2005a). As the testes have a higher ratio of lyase to hydroxylase activity, it was concluded that *POR* has a key role in the determination of this ratio. Further studies in yeast also implicated cytochrome b5 (*CYB5A*). They confirmed that *POR* is required for the hydroxylase and lyase reactions but that cytochrome b5 selectively enhances 17,20 lyase activity (Auchus *et al.*, 1998). The presence of cytochrome b5 alone is not sufficient for the enzyme to function; it acts as an allosteric facilitator and not as an electron donor. Cytochrome b5 is expressed in the zona reticularis of the adrenal gland (Yanase *et al.*, 1998) where it facilitates the production of DHEA and other androgens.

Understanding of the mechanisms behind the 17 α -hydroxylase / 17,20 lyase switch has been assisted by the study of patients with isolated 17,20 lyase deficiency. In this rare disorder, patients have normal 17 α -hydroxylase activity but absent or abnormal 17,20 lyase activity. The first proven case was in 1997, when it was reported that two Brazilian patients had each presented with hormonal levels suggestive of this disorder (Geller *et al.*, 1999). Each was homozygous for a different mutation in *CYP17A1* (R347H and R358Q). The mutants were investigated *in vitro* and, through the addition of excess cytochrome b5, lyase activity was partly restored (Geller *et al.*, 1999). The near-normal hydroxylase activity suggested that the active site was not altered by these mutations but rather the redox binding sites associated with electron transfer. Indeed, molecular modelling showed that these mutations altered the electrostatic charge of the protein, inhibiting its interaction with POR, and emphasising the importance of redox partner interactions in 17,20 lyase regulation (Auchus and Miller 1999).

The final recognised factor influencing the hydroxylase/lyase switch is cAMP. As described in Section 1.2.1.1, circulating ACTH activates adenylyl cyclase, which increases intracellular levels of cAMP, thereby promoting phosphorylation events through a cascade of events via the protein kinase A pathway. Phosphorylation is a relatively well-studied form of post-translational modification, whereby the addition or removal of phosphate groups (PO_4^{3-}) induces conformational changes

to the structure of a protein resulting in activation or deactivation of function. Phosphorylation sites have been identified on serine and threonine residues and shown to affect 17,20 lyase activity selectively (Zhang *et al.*, 1995), although the mechanisms underlying this enhancement are not fully understood and the specific phosphorylation sites are currently unknown (Souter *et al.*, 2006; Tee *et al.*, 2008; Wang *et al.*, 2010). It is hoped that the elucidation of such sites will provide further insight into the switch mechanism (Miller 2005a).

1.3.2 Molecular Structure

The human *CYP17A1* gene is located on the reverse strand of chromosome 10q24 (Sparkes *et al.*, 1991), spanning approximately 7000 base pairs. Transcription of the gene can generate three isoforms, although only one is known to produce protein. As depicted in Figure 1-10, the protein-coding gene consists of 8 exons which code for 508 amino acids. The locations of the intron/exon boundaries are conserved between species, confirming their functional importance.

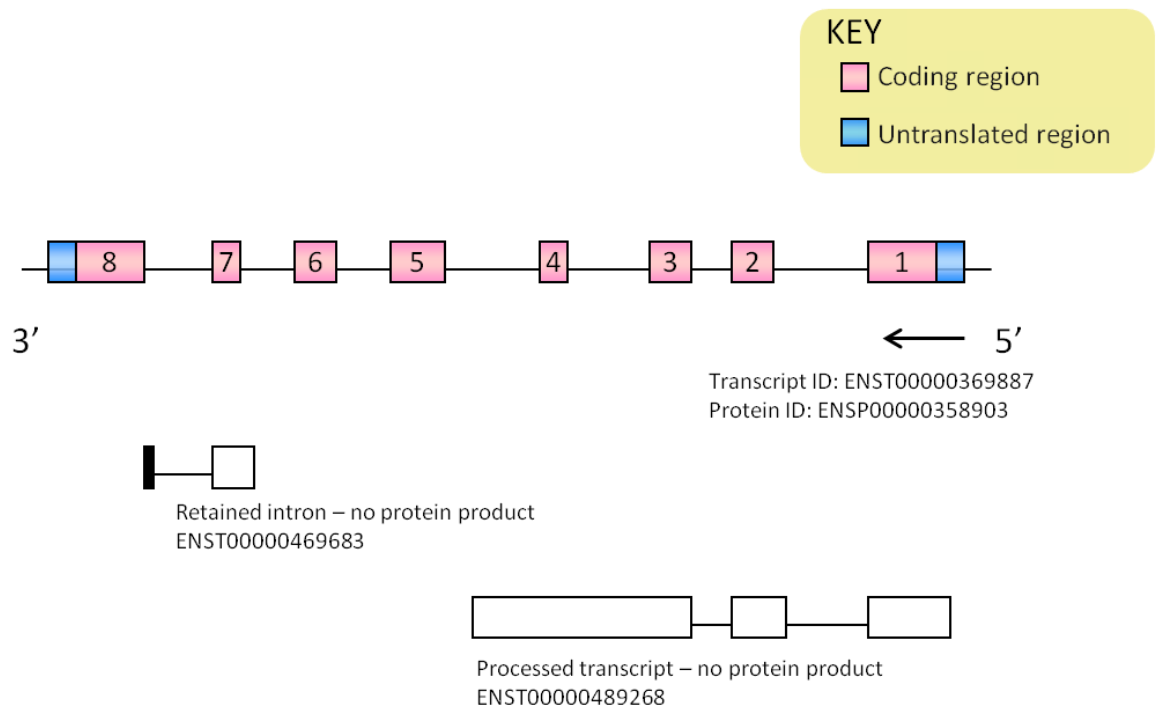


Figure 1-10 Diagram showing the exon/intron structure of *CYP17A1* gene.

1.3.3 The Role of *CYP17A1* in Hypertension

CYP17A1 has been identified as a candidate gene for the development of essential hypertension through recent GWAS and by the study of rare monogenic disorders (see Section 1.1.3). This section will review the relationship between the abnormal *CYP17A1* gene and blood pressure.

1.3.3.1 *CYP17A1* Monogenic Disorders

Congenital adrenal hyperplasia (CAH) is a rare disorder, first described by Biglieri *et al.* (1966). Around 1% of cases are caused by a deficient *CYP17A1* gene (New 2003). Mutations in other genes within the steroidogenic pathway also cause this condition; these and their resultant characteristics are described in Table 1-7. Patients with CAH have altered levels of mineralocorticoids, glucocorticoids and androgens, with varying severity depending on the causative mutation. A mutant *CYP17A1* gene causes defective androgen production which influences sexual development and maturation of the individual, and the reduction in glucocorticoids leads to increased ACTH production, which massively stimulates pathways that do not require the *CYP17A1* enzyme (see Figure 1-7). Affected females fail to undergo puberty or to develop secondary sex characteristics. Males develop as immature, phenotypic females. Excess 11-deoxycorticosterone (DOC), a weak mineralocorticoid, causes hypertension, hypokalaemia and patients have low aldosterone concentrations (Hahm *et al.*, 2003; Martin *et al.*, 2003). Paradoxically, low or absent cortisol is not lethal because the excessive levels of corticosterone provide a substitute. Mutations causing 17 α -hydroxylase/17,20-lyase deficiency are most often located within one of the eight exons although also, occasionally, at intronic splice sites (Figure 1-11).

Table 1-7 Characteristics of CAH arising from mutations in steroidogenic genes.

Gene	<i>CYP21A</i>	<i>CYP11B1</i>	<i>CYP11B2</i>	<i>CYP17A1</i>	<i>HSD3B2</i>
Enzyme	21-Hydroxylase	11 β -Hydroxylase	Aldosterone Synthase	17 α -Hydroxylase / 17,20 lyase	3 β -Hydroxysteroid dehydrogenase
Incidence	1:14,000	1:10,000	Rare	Rare	Rare
Ambiguous Genitalia	Females	Females	No	Males. No puberty in females	Males. Mild in females
Blood Pressure	↓	↑	↓	↑	↓
Mineralo-corticoids	↓	↑	↓	↑	↓
Glucocorticoids	↓	↓	Normal	↓	↓
Androgens	↑	↑	Normal	↓	↓ males ↑ females
Elevated Steroids	17-OH-P	DOC, 11-Deoxycortisol	Cortico-sterone	DOC, cortico-sterone	DHEA, 17-OH-Preg

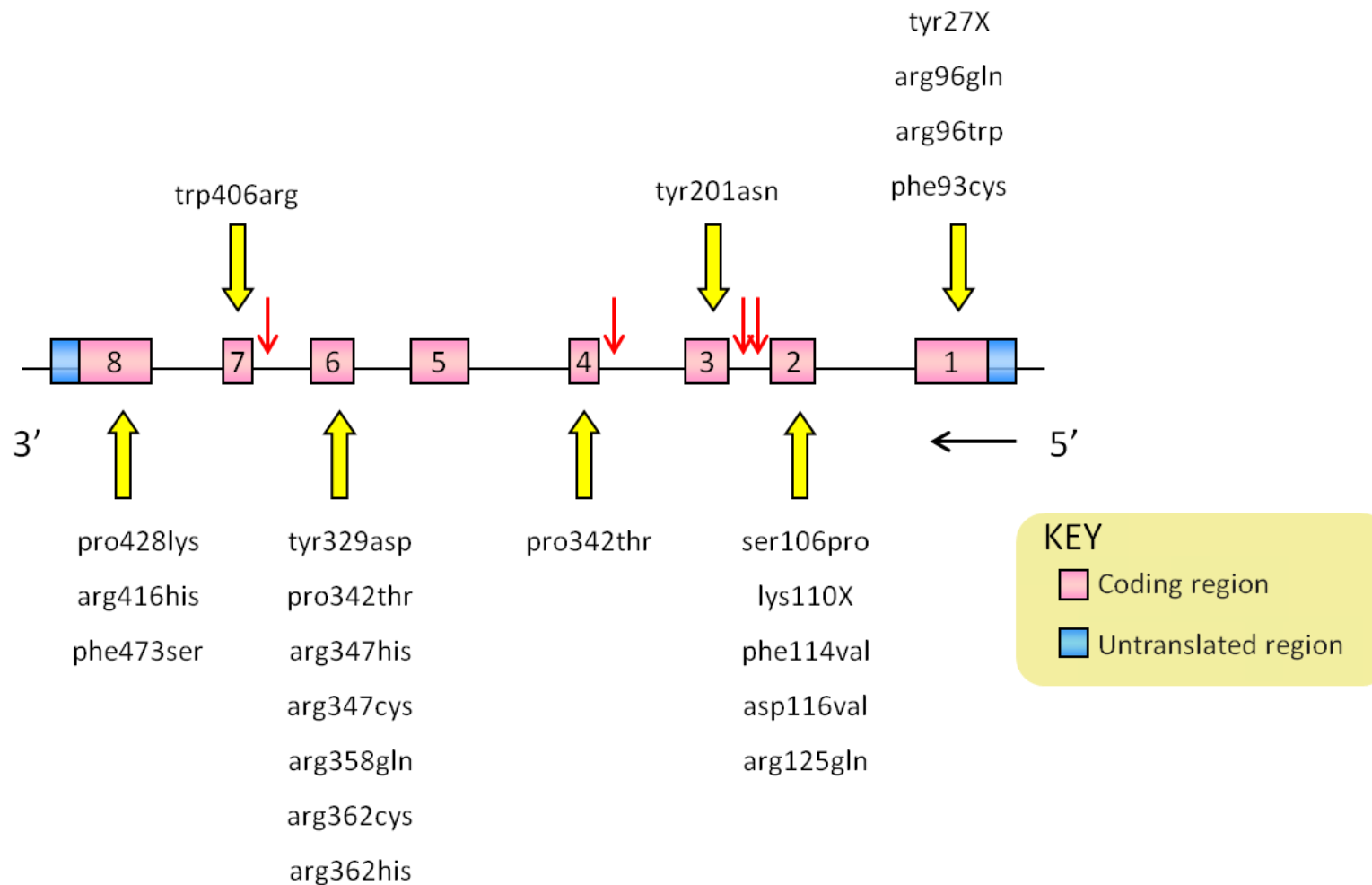


Figure 1-11 Mutations known to cause 17 α -hydroxylase/17, 20 lyase deficiency.

Mutations occurring within each exon are depicted by yellow arrows and the corresponding amino acid changes provided. Red arrows indicate the locations of mutations occurring within intronic splice sites.

Thus, aberrant activity of the *CYP17A1* gene product affects blood pressure. The cases described above result from severe changes in the structural gene and are rare. Given that the enzyme is crucial in controlling the substrate flow through the different arms of corticosteroid biosynthesis. It is plausible to suggest that smaller changes in structure (i.e. polymorphisms) might have more subtle effects that contribute to the much more common condition of essential hypertension.

There is little information on the relationship between *CYP17A1* activity and essential hypertension. Surprisingly, no specific studies have yet followed up on the GWAS findings (Section 1.1.3.2), which seems to obviate the purpose of such an expensive study. Several questions remain to be addressed. Firstly, does the GWAS correctly identify the *CYP17A1* locus as causative or is it merely a marker? Secondly, is there a functional polymorphism at this locus? Thirdly, can this polymorphism be related to hypertensive risk? It has been postulated that more common genetic variants may cause a very mild form of enzyme dysfunction (Levy *et al.*, 2009). This hypothesis is the basis of the work presented in this thesis. Do minor alterations in the expression of *CYP17A1* have the potential to disturb corticosteroidogenesis? The following sections review what is known of variation within the gene and how its expression is regulated.

1.3.3.2 Polymorphic Variation

Although the terms ‘mutation’ and ‘polymorphism’ are sometimes used interchangeably, in terms of this thesis, the conventional definitions are followed. Mutations are rare, with a frequency of <1% in the population and usually cause a “large” phenotypic alteration. Polymorphisms occur more frequently and are generally thought to cause little or no change to the structural gene, although such variations are now being studied in more detail in an attempt to explain complex polygenic disorders. The more common allele at a given locus is termed the major allele, and the rarer termed minor. Reported polymorphic variations are identified by ‘rs’ followed by a number, allocated by the dbSNP database (<http://www.ncbi.nlm.nih.gov/projects/SNP/>). Where polymorphisms are due to a single base change, they are known as single nucleotide polymorphisms (SNPs).

The association of polymorphic variants within the *CYP17A1* gene has recently been studied in disorders such as polycystic ovary syndrome (PCOS), breast and prostate cancer as well as obesity and premature male baldness. Women with PCOS have excess androgen secretion. Certain types of breast and prostate cancer are hormone-related. *CYP17A1* is a key enzyme involved in androgen biosynthesis, particularly in the ovaries and testes, and is therefore a candidate gene for these hormone-associated disorders.

Evidence from *in vitro* studies of thecal cells isolated from the human ovary show that transcription and expression of *CYP17A1* is significantly increased in individuals with PCOS (Wickenheisser *et al.*, 2000). This finding has led to numerous studies of association between PCOS and a T/C variant that lies 34 bases upstream from the *CYP17A1* transcriptional start site (rs743572). Results from such studies have been conflicting. Some PCOS case-control studies have reported a significant association with PCOS in patients homozygous for the minor C allele (Diamanti-Kandarakis *et al.*, 1999; Pusalkar *et al.*, 2009). The number of affected participants in these studies was ≤ 100 and were derived from Greek and Indian populations respectively. Other studies in a wide range of ethnic populations found no association with PCOS (Marszalek *et al.*, 2001; Kahsar-Miller *et al.*, 2004; Echiburu *et al.*, 2008; Park *et al.*, 2008; Unsal *et al.*, 2009; Chua *et al.*, 2012; Ramos Cirilo *et al.*, 2012). Some interesting findings, however, did arise from this research. Echiburu and colleagues failed to identify significant association of rs743572 with PCOS in a Chilean cohort, but did report a correlation between the minor C allele and increased body weight. In a Korean cohort of 134 affected individuals and 100 matched controls, Park *et al.* reported that a particular haplotype of *CYP17A1* SNPs, which included the major rs743573 T allele within the *CYP17A1* gene shows significant association with PCOS ($p=0.001$). A GWAS conducted using 744 PCOS cases, and replicated in over 3000 Chinese Han participants, identified three loci significantly associated with PCOS, but none were situated at the *CYP17A1* locus (Chen *et al.*, 2011). These rs743572 association studies had modest sample sizes and so, in 2012, a meta-analysis was conducted on 1320 PCOS cases and 1017 controls, from 10 different studies. This found no overall association in the combined group but sub-group analysis found the minor C allele to be a significant marker of PCOS risk in studies with ≤ 200 participants (Li *et al.*, 2012). The authors propose 'small-study

bias' as an explanation for the previous inconsistent findings, where selection bias is more likely to occur; small studies showing a small effect are less likely to be published. Alternatively, it may be the case that recruitment was inadequate and therefore case/control groups were not ideally matched.

Similar inconsistent and contradictory findings resulted from studies investigating association between rs743572 and hormone-related cancers such as breast and prostate cancer (Miyoshi and Noguchi 2003; Mononen and Schleutker 2009). In an attempt to provide a definitive conclusion, a large meta-analysis combined 24 breast cancer studies (Chen and Pei 2010). The authors hypothesised that the inconsistency and variability seen in previous studies might be due in part to contributions from other risk factors. The combined analysis revealed no association with breast cancer risk, but suggested that this was due largely to sample heterogeneity (e.g. age, ethnicity, tumour stage and grade). Further sub-group analyses provided evidence of a possible link between age at menarche, BMI, menopausal status, rs743573 and breast cancer risk. A meta-analysis examining prostate cancer risk was also conducted, combining 10 cohorts of European, Asian and African men (Ntais *et al.*, 2003) which, again, reported no significant association with rs743572. Sub-group analyses found that the minor allele associated with increased prostate cancer susceptibility but only in men of African descent. The quest to uncover the genetic alterations that predispose individuals to cancer and other disorders is a challenging task. While the studies discussed above are inconsistent and sometimes contradictory, such research highlights the need for a focused approach. Heterogeneity is an apparent issue in these types of studies and the necessity to assess other risk factors in such analyses is becoming ever clearer.

In considering the role of *CYP17A1* polymorphisms in hypertension, it is useful to assess other studies that associate hypertension with polymorphic sites within other steroidogenic genes. Polymorphisms G-1889C and A-1859G in *CYP11B1* have been associated with decreased 11 β -hydroxylase efficiency and with an altered transcriptional response to ACTH (Barr *et al.*, 2007). Variant T-344C in *CYP11B2* is the most commonly studied polymorphism in this region, displaying significant associations with altered plasma aldosterone levels and hypertension (Iwai *et al.*, 2007; Sookoian *et al.*, 2007). First described by White and Slutsker, this site corresponds to a steroidogenic factor-1 (SF-1) binding site, a

transcription factor involved in the regulation of many steroidogenic genes. Despite the C allele binding to SF-1 with significantly greater affinity than the T allele (White and Slutsker 1995; Bassett *et al.*, 2002), *in vitro* analysis has found this to have no effect on gene transcription (Clyne *et al.*, 1997; Bassett *et al.*, 2002). *CYP11B1* and *CYP11B2* lie in tandem on chromosome eight and many of the polymorphisms in this region are in strong LD i.e. there is non-random inheritance of alleles at these polymorphic sites. The lack of functional importance at this site led to the belief that it may simply be a marker for another functional allele, with which it is in LD. McManus and colleagues (2012) identified a possible functional variant at position -1651 of *CYP11B2* and found that the T allele at this site reduces transcriptional activity *in vitro* and associates with lower excretion rates of aldosterone in man. It is possible to draw some parallels between these studies and those of *CYP17A1* in hypertension and other disorders, which raises several questions. Are the SNPs reported by recent GWAS simply markers for a functional SNP located elsewhere in the region? Are the GWAS polymorphisms in LD with the commonly studied SNP rs743572? What influence might SNPs in the promoter region of a gene have on its expression and activity? What other factors could influence gene expression?

There are several mechanisms of gene regulation that may alter expression. As described in Section 1.3.3.1, mutations in the coding regions and splice sites have been reported to affect hydroxylase and/or lyase activity severely. Combined with the recent GWAS findings, it is therefore reasonable to hypothesise that common polymorphisms occurring throughout the gene may contribute to minor alterations in the structure and folding of the gene product and thus may account for some subtle changes in enzymatic activity. Furthermore, polymorphisms occurring immediately upstream of the transcription start site may affect the binding of necessary transcription factors, in a manner similar to other components of the steroidogenic pathway, as described above. In addition, the recent discovery of post-transcriptional regulation by microRNAs has opened new avenues of investigation mainly by mRNA destabilisation followed by degradation, or by mRNA translational repression. MicroRNAs (miRNAs) are short, non-coding RNAs of approximately 20 nucleotides, which inhibit gene expression. There is now an expanding list of thousands of known miRNAs, some of which have been implicated in the

regulation of genes involved in cancer and cardiovascular disease. The data presented in Chapters 5 and 6 of this thesis investigate both the transcriptional and post-transcriptional regulation of *CYP17A1*. Firstly, Sections 1.4 and 1.5 of this review explain these regulation mechanisms and summarise recent research concerning *CYP17A1* and the adrenal gland.

1.4 Transcriptional Regulation

In 1956, Francis Crick first described the ‘central dogma’ of molecular biology; the concept that DNA is transcribed to RNA, which is then translated to protein (Crick 1956). Gene transcription is an integral part of this process, regulated and controlled by many complex mechanisms, not all of which are fully understood.

1.4.1 Gene Transcription

RNA transcription is an essential and complex process, which utilises DNA as a template for RNA synthesis. The region immediately upstream (5’) of the transcriptional start site (TSS) is termed the promoter region. Typically, a distinct ‘core’ sequence known as the TATA-box, located within the promoter region in close proximity to the TSS, encodes a binding site for a transcription factor known as the TATA-binding protein (TBP). The binding of TBP promotes the association of various other transcription factors and the enzyme RNA polymerase II (Pol II), forming the pre-initiation complex. The hydrogen bonds of the DNA double helix are broken allowing Pol II to synthesise the RNA transcript in the 5’ to 3’ direction by pairing ribonucleotides complementary to those of the DNA nucleotides. RNA nucleotides differ from DNA nucleotides in two ways: DNA thymine bases are replaced by uracil bases in RNA, and the sugar-phosphate backbone of the nucleotides are comprised of a ribose sugar, as opposed to the deoxyribose of DNA. When transcription is complete, the hydrogen bonds of the RNA/DNA complex break, and the newly-formed RNA transcript is released.

The rate of transcription by the pre-initiation complex of a typical eukaryotic gene is regulated by complex mechanisms, often cell- or tissue-specific. Transcription rate can be modulated by the presence of proteins known as

activators and repressors. In addition, enhancer element sequences, which can be located almost anywhere in the genome, can interact with both activator and repressive proteins for further regulation (Banerji *et al.*, 1981; Barolo and Posakony 2002). The rate of transcription can be controlled by regulatory sequence elements up to 1 Mb away from the gene, as DNA looping will permit transcription factors bound there to lie in close physical proximity to the TSS (Maston *et al.*, 2006).

There are several other mechanisms of transcriptional control. DNA methylation is an epigenetic modification and is associated with transcriptional silencing. This can occur in two ways. Firstly, methylation of CG dinucleotides within CpG islands (CG-rich regions in the genome) can prevent transcription factors from binding to this region. Secondly, proteins that bind to methylated cytosines recruit co-repressor complexes which modify the chromatin structure and affect transcription initiation. Mechanisms that regulate chromatin structure, including histone modification, are beyond the scope of this thesis but do provide an alternative mechanism of transcriptional regulation. A general review is provided by Clouaire and Stancheva (2008).

Alterations in any of the mechanisms described above will affect the nature or rate of formation of the RNA transcript and lead to altered physiological effects of the gene's expression unless compensated for by another mechanism. Section 1.4.2 summarises studies of the transcriptional regulation of adrenal *CYP17A1*. While many of the pathways and transcription factors regulating this gene are likely to be the same in both the adrenal and gonadal glands, some would be expected to be different to meet their unique hormonal demands.

1.4.2 Studies on Transcriptional Regulation of Adrenal *CYP17A1*

Considerable research interest has focused on the transcriptional regulation of *CYP17A1* because of its branchpoint role in glucocorticoid and androgen synthesis and its implication in rare but severe disorders. Reporter construct studies have found that approximately 60-80% of the basal transcriptional regulation of *CYP17A1* can be accounted for by the 227 base pairs immediately upstream of the TSS (Lin *et al.*, 2001). Numerous interacting factors have been

identified (Figure 1-12). The majority of these have been reviewed by Sewer and Jagarlapudi (2009) and the best understood are described below.

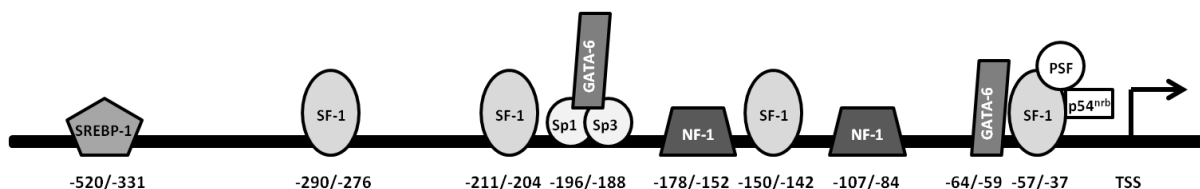


Figure 1-12 Transcription factor binding sites characterised in the human adrenally-expressed *CYP17A1* promoter region.

DNA binding regions are provided beneath each transcription factor. SREBP-1: sterol regulatory element binding protein 1; SF-1: steroidogenic factor 1; Sp1/3: specificity protein-1/3; GATA-6: family member 6 of GATA transcription factor family; NF-1: nuclear factor 1; TSS: transcription start site.

Steroidogenic Factor-1

The orphan nuclear receptor, steroidogenic factor-1 (SF-1) (also known as NR5A1), is the best characterised transcription factor in adrenal steroidogenesis. Disruption of the gene encoding SF-1 in mice has demonstrated its importance in adrenal and gonadal development and in sexual differentiation (Luo *et al.*, 1994). As evidenced by a heterozygous mutation in its gene, it is likely that SF-1 is essential to these processes in humans also (Achermann *et al.*, 1999). Reporter construct studies identified both basal and cAMP-responsive elements within the first 63bp immediately upstream from the transcriptional start site of *CYP17A1* (Rodriguez *et al.*, 1997). A SF-1 binding site has been identified within this region at -57/-37, where a complex containing SF-1, p54^{nrB} (RNA and DNA-binding protein) and the polypyrimidine-tract-binding protein-associated factor (PSF) have been shown to bind (Sewer *et al.*, 2002). This complex appears to be crucial in cAMP-dependent activation of *CYP17A1* transcription. Repression of transcription occurs upon the recruitment of the corepressor mSin3A by PSF. Upon cAMP stimulation, however, mSin3A is released from the SF-1/ p54^{nrB}/ PSF complex, and transcription of *CYP17A1* is activated. *In vitro* studies produce differing results. Studies of the human adrenocortical cell line H295R found that the binding of SF-1 alone is not sufficient to induce transcription of the human

gene; the entire SF-1/ p54^{nrb}/ PSF complex is required. On the other hand, similar experiments involving the transfection of reporter constructs containing the human *CYP17A1* promoter into mouse adrenocortical Y1 cells require only the binding of SF-1 (Rodriguez *et al.*, 1997). This highlights the need to study regulation of steroidogenic genes in homologous cell systems.

Through experiments on the human foetal adrenal gland, Hanley and colleagues (2001) identified three additional functional SF-1 binding sites in the human gene. These are located -150/-142, -211/-204 and -290/-276 bases upstream from the TSS of *CYP17A1*. The authors also provide evidence that the nuclear receptor DAX1 (dosage-sensitive sex reversal, adrenal hypoplasia congenita, critical region on the X chromosome gene 1) represses transcriptional activation of SF-1 in a dose-dependent manner. However, it is unclear from these studies whether a direct interaction occurs between SF-1 and DAX1. Furthermore, there is evidence of DAX1 expression within the adult adrenal gland (Shibata *et al.*, 2003). These data support the role of DAX1 as a transcriptional repressor: in deoxycorticosterone-producing adenomas, Western blot analyses show both *CYP17A1* and SF-1 protein levels to be significantly reduced relative to those from normal adrenal tissue, while DAX1 levels are substantially increased. This supports the hypothesis that DAX1 has an inhibitory effect on SF-1 and, subsequently, *CYP17A1* production. The same authors also presented evidence of association between SF-1 and chicken ovalbumin upstream promoter-transcription factors (COUP-TFs). In the bovine *CYP17* promoter, COUP-TF was shown to bind the same region as SF-1, but acted as a transcriptional repressor as opposed to SF-1, which activated transcription (Shibata *et al.*, 2003). The role of COUP-TF in the human *CYP17A1* promoter is unclear, although expression profiles from cortisol-producing adenomas show both COUP-TFI and COUP-TFII levels to be significantly reduced, while *CYP17A1* is significantly increased.

It is clear from the above review that SF-1 is an important regulator of human *CYP17A1* both in the developing embryonic and adult adrenal cortex. There have been some attempts to elucidate the mechanisms and transcriptional elements SF-1 exploits to exert transcriptional control but much of this puzzle has yet to be solved. Nevertheless the studies comparing expression of various transcription factors in both normal and diseased adrenal tissue have proved a useful tool to aid in the explanation of altered enzymatic expression in adrenal disorders.

GATA-6

GATA-6 is a member of a family of zinc-finger transcription factors (GATA 1-6). Primarily expressed in the zona reticularis of the adrenal cortex, GATA-6 is believed to play a key role in adrenal androgen biosynthesis at the gene transcription level (Jimenez *et al.*, 2003). Interestingly, another member of the GATA family, GATA-4, has been shown to be expressed in human gonadal tissue, alongside GATA-6, but not in adrenal tissue; this suggests GATA-6 may be of importance in adrenal androgen production (Kiiveri *et al.*, 2002). *In vitro* studies in H295R cells co-transfected reporter constructs containing the *CYP17A1* promoter alongside an expression vector containing the GATA-6 coding region. This increased promoter activity 6-fold, but this effect could not be replicated in a non-steroidogenic cell line (Jimenez *et al.*, 2003). This indicates that GATA-6 requires other transcriptional elements to produce this effect.

Study of the GATA transcription factor family's role in gene promoters of importance in gonadal tissue identified a functional GATA-4 site within the promoter of SF-1 (Tremblay and Viger 2001). It is possible that GATA-6 promotes transcription of *CYP17A1* in a similar manner in the zona reticularis of the adrenal cortex. The combined effect of GATA-6 and SF-1 has been examined *in vitro*. Using non-steroidogenic cells, transfection of both SF-1 and GATA-6 expression plasmids increases *CYP17A1* promoter activity when compared to GATA-6 alone. Furthermore, promoter activity is increased to levels similar to those observed following transfection with GATA-6 alone in steroidogenic cells (Jimenez *et al.*, 2003). These data suggest that there is greater induction of *CYP17A1* transcription in the presence of both SF-1 and GATA-6, although evidence of a direct interaction between the two within adrenal tissue is lacking.

Within the promoter region of *CYP17A1*, there is an apparent GATA binding site at -64/-59, but mutation of this site in reporter construct studies does not affect transcription in the presence of GATA-4 or GATA-6 (Flück and Miller 2004). Instead, the authors present evidence that the ability of GATA-4 or GATA-6 to induce transcription requires interaction with the Sp1 transcriptional element within the Sp1:Sp3 complex site. The Sp1:Sp3 binding site is located -196/-188 bases upstream of *CYP17A1* TSS (Lin *et al.*, 2001).

Furthermore, GATA-6 has also been shown to associate with SF-1 in the transcriptional regulation of cytochrome b5 (Flück and Miller 2004; Huang *et al.*, 2005), providing additional evidence of its importance in 17, 20 lyase expression and subsequent adrenal androgen production.

NF-1

Binding sites for the transcription factor nuclear factor 1 (NF-1) have been identified and confirmed at positions -107/-85 and -178/-152 of the *CYP17A1* proximal promoter region using electrophoretic mobility shift assays (EMSAs) (Lin *et al.*, 2001). Mutation at both sites halved transcriptional activity *in vitro*, indicating that these transcriptional elements play a key role in the regulation of *CYP17A1* transcription.

1.4.2.1 ACTH Effect on Transcription

In the zona fasciculata, the peptide hormone adrenocorticotropin (ACTH) increases levels of the intracellular second-messenger cAMP via activation of adenylyl cyclase. This results in the activation of the cAMP-mediated protein kinase A (PKA) pathway and a subsequent increase in the transcription of steroidogenic genes. The direct targets of the PKA pathway are still to be elucidated but it appears to promote binding of transcription factors to cAMP-responsive sequences within the promoters of steroidogenic genes.

It has been shown that both basal (required for constitutive expression) and cAMP-responsive elements are located within the 63 bases immediately upstream of the *CYP17A1* TSS (Rodriguez *et al.*, 1997). As described above, a complex containing the transcription factor SF-1 binds to a site located at position -57/-50 of the human *CYP17A1* promoter and regulates expression in the adrenal cortex. Aside from the regulatory control exerted by PSF through its recruitment and release of mSin3A, the phosphorylation state of SF-1 plays a key role in the stimulation of transcription by ACTH/cAMP. SF-1 is dephosphorylated following cAMP stimulation of the H295R adrenocortical cell line (Sewer and Waterman 2002). Mitogen-activated protein kinase phosphatase-1 (MKP-1) has been identified as an essential phosphatase in this process (Sewer and Waterman 2003). Both mRNA and protein levels of MKP-1 are increased upon stimulation

with cAMP *in vitro* and, importantly, the increase in MKP-1 expression immediately precedes increased *CYP17A1* expression, suggesting a role in cAMP-dependent expression of *CYP17A1* (Sewer and Waterman 2003). The authors therefore postulate that MKP-1 is responsible for the dephosphorylation of SF-1 and the subsequent increase in *CYP17A1* transcription but evidence of direct associations is lacking, meaning that there may be a number of intermediary factors involved in this process.

Further studies have identified roles for sterol regulatory element binding protein 1 (SREBP-1) and other proteins in cAMP-induced *CYP17A1* expression (Ozbay *et al.*, 2006). A binding site for SREBP has been identified within the region -520/-331 upstream of the *CYP17A1* TSS (Figure 1-12). Activation of the PKA pathway following stimulation by ACTH decreases intracellular levels of numerous sphingolipids, which are essential components of cellular plasma membranes. This decrease triggers the release of sphingosine-1-phosphate (S1P) which promotes the recruitment of the SREBP-1 transcription factor to the site upstream of *CYP17A1* (Ozbay *et al.*, 2006).

Thus, much information on a complex mixture of factors is available. How many other such factors exist, how they are organised into a clear scheme of regulation and, importantly, how they differ between organs, remain to be discovered.

1.5 Post-Transcriptional Regulation

RNA interference (RNAi) is a naturally-occurring process used by cells to post-transcriptionally silence or diminish the effect of a gene by hastening the destruction of its mRNA products. RNAi was first observed in plants (Napoli *et al.*, 1990), when scientists introduced a pigment-producing gene to intensify petal colour. Instead, the resulting petals were colourless. The molecular mechanisms behind this gene silencing effect - a Nobel-prize-winning discovery - were fully described by Fire *et al.* (1998). RNAi uses short, non-coding, double-stranded RNA, which binds to a complementary region on messenger RNA,

leading to post-transcriptional gene silencing. Similar single-stranded molecules were shown to have a modest effect by comparison.

Following its discovery, RNAi has become a powerful research tool, with several classes of small RNA molecules now commonplace in research. Short interfering RNA (siRNA) is frequently used and relevant to the class of molecules described in this thesis: microRNA (miRNA).

1.5.1 MicroRNA

MicroRNAs (miRNAs) are a class of small non-coding RNA molecules, approximately 20-25 nucleotides in length. They are thought to play key roles in various human disease pathologies, including several cancers (Lu *et al.*, 2005; Suzuki *et al.*, 2009). The role of miRNAs in post-transcriptional gene regulation will be discussed in the following sections, as well as what is known about their involvement in human adrenal disease.

1.5.1.1 Discovery

The inaugural miRNA, *lin-4*, was first described by Lee *et al.* (1993). Conducting their research in the nematode worm *C.elegans*, Lee and colleagues established that the product of the *lin-4* gene was not translated into a peptide product but instead generated a small non-coding RNA that displayed sequence complementarity to a 3' untranslated region (3'UTR) section of *lin-14* mRNA. The LIN-14 protein is critical to the timing of larval events in *C.elegans*. The first functional characterisation of a miRNA was published in the same issue of *Cell* by Wightman *et al.* (1993), showing that *lin-4* binds directly, though imperfectly, to the 3'UTR of *lin-14*, reducing protein production. The importance of these studies was not fully appreciated until the discovery of a second miRNA some seven years later. Reinhart *et al.* (2000) described the importance of the 21-nucleotide RNA molecule, *let-7*, in coordinating the timing of *C. elegans* development and noted its conservation across species.

The turn of the millennium saw a vast increase in miRNA-mediated gene regulation research, with the latest release of miRBase (v. 19, August 2012, see Section 1.5.1.2) listing 25,141 mature miRNA entries across 193 species.

1.5.1.2 Nomenclature

When a research article describing a novel and experimentally-validated miRNA is submitted for publication, the miRNA sequence is entered confidentially into the miRBase database (formally Rfam) for official naming (<http://microrna.sanger.ac.uk/>) (Griffiths-Jones 2006). Strict expression and biogenesis criteria must be met to ensure the finding is a novel miRNA, and not another form of small RNA, e.g. siRNA (Ambros *et al.*, 2003). Each miRNA is first identified by species - e.g. hsa (human) or mmu (mouse) - and then numbered according to time of submission, with mature sequences labelled 'miR' and precursor hairpins 'mir' (Griffiths-Jones *et al.*, 2006). Identical sequences found in different species are assigned the same numbers. Identical sequences found within a species but arising from different genomic locations are given numerical suffixes (e.g. hsa-miR-1-1, hsa-miR-1-2). MiRNAs with similar sequences are grouped into a 'miRNA family' and have an additional lowercase letter to aid identification (e.g. hsa-miR-320a, hsa-miR-320b, hsa-miR-320c). Mature miRNAs derive from a hairpin precursor (see section 1.5.1.3) and it is therefore possible for a miRNA to originate from either arm of the hairpin pre-miRNA. The current nomenclature for such miRNAs assigns either a -5p or -3p suffix, depending on whether the miRNA was generated from the 5' or 3' hairpin arm (e.g. hsa-miR-34c-5p and hsa-miR-34c-3p). Before this particular nomenclature was developed, some early studies assigned an asterisk to the apparently non-functional miR from the hairpin as a means of differentiating between the two miRs (e.g. hsa-let-7c and hsa-let-7c*)(Griffiths-Jones 2004).

1.5.1.3 MiRNA Synthesis in Animals

MiRNAs are synthesised in a multistep process, summarised in Figure 1-13 and outlined in the following sections. The majority of known miRNA genes are located in intergenic or intronic regions of chromosomes, with a smaller proportion being transcribed from exonic regions (Lau *et al.*, 2001; Rodriguez *et al.*, 2004).

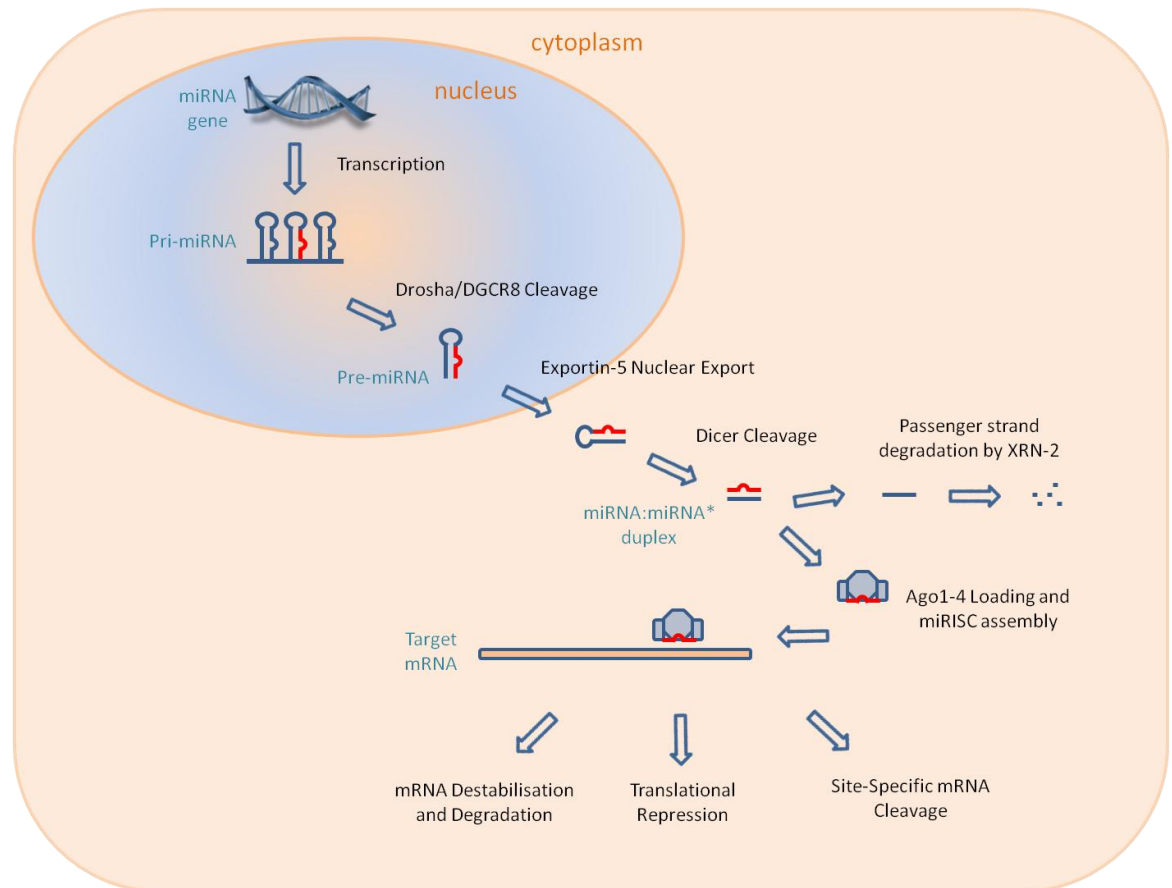


Figure 1-13 Overview of miRNA biogenesis and post-transcriptional repression mechanisms.

MicroRNA genes are transcribed in the nucleus as primary transcripts (Pri-miRNA) before being processed into ~70 nucleotide pre-miRNAs by Drosha endonuclease. The pre-miRNA is transported from the nucleus into the cytoplasm by Exportin-5 where it is processed further by Dicer. The mature miRNA (red) is then loaded into Argonaute 1-4 and assembled into the miRNA-induced silencing complex (miRISC), which is subsequently guided to the 3'UTR of the target mRNA. mRNA translation is then inhibited through one or more repressive mechanisms, including mRNA cleavage, degradation and translational repression.

Nuclear Processing

A miRNA is initially transcribed in the nucleus as part of a longer primary transcript (Pri-miRNA) by RNA polymerase II or, less commonly, RNA polymerase III (Lee *et al.*, 2004; Borchert *et al.*, 2006). Such transcripts are usually several kilobases in length and contain stem loop structures. These stem loop structures include the miRNA double stranded stem, imperfectly paired and linked by a small terminal loop. They are cleaved at the stem by a microprocessor complex to produce a 70-nucleotide hairpin structure, termed the pre-miRNA (Lee *et al.*, 2003). This microprocessor complex is a multi-protein complex in which the key components are Drosha and DGCR8 (DiGeorge Syndrome Critical Region in Gene 8) (Lee *et al.*, 2003; Landthaler *et al.*, 2004). DGCR8 binds to the stem of the structure, thus guiding the RNase III enzyme to cleave the double-stranded stem around 11 basepairs from the stem-base, generating a 5'-phosphate group and a two-nucleotide 3'-overhang at the cleavage site (Basyuk *et al.*, 2003). (Invertebrates utilise 'Pasha' in place of DGCR8. This will not be discussed further (Denli *et al.*, 2004)).

Nuclear-Cytoplasm Transportation

Following cleavage by the microprocessor complex, pre-miRNAs are transported into the cytoplasm for further processing. Transportation occurs through nuclear pore complexes via the Ran guanosine triphosphate (Ran-GTP)-dependent nuclear transport receptor, Exportin-5 (Yi *et al.*, 2003; Bohnsack *et al.*, 2004). Lund *et al.* (2004) propose that only pre-miRNAs of defined length and structure can be efficiently transported by Exportin-5 from the nucleus, where Ran-GTP levels are high, to the cytoplasm, where the relatively low levels of Ran-GTP trigger release of the pre-miRNA from Exportin-5.

MiRNA Induced Silencing Complex (miRISC)

Following action by Dicer ('dicing'), unwinding of the strands is catalysed by an as yet unidentified RNA helicase and the guide strand incorporated into an Ago 1-4 protein complex, while the passenger strand is degraded by the enzyme XRN-2. The guide strand is preferentially incorporated into the miRISC, the strand of choice being that with the less stable 5' end being chosen (Khvorova *et al.*,

2003). Following Argonaute 1-4 loading, the miRNA guides miRISC to its target mRNA (Section 1.5.1.4) and mRNA repression initiates (Section 1.5.1.5). There is now some evidence of instances where the passenger strand can be incorporated into the miRISC and a functional miRNA is produced. The REST and Co-REST transcription factors, which are important in Huntington's disease, have been shown to be co-regulated by hsa-miR-9 and hsa-miR-9* (Packer *et al.*, 2008). It is not clear how often these instances occur, although, aside from the less thermostable strand being preferred, the presence of a 5'uridine base (5'U) appears to promote loading into the miRISC complex (Seitz *et al.*, 2011).

1.5.1.4 Target Recognition

Classical miRNA action causes repression of the mRNA by direct binding of its 3'UTR. The majority of miRNAs are believed to act in this manner although there is some evidence of miRNA targeting and binding to the coding regions and 5'UTRs (Duursma *et al.*, 2008; Orom *et al.*, 2008). The miRNA sequence serves as a target recognition motif, steering the miRISC to the 3'UTR of the target mRNA. The bulges in the structure of the miRNA often lead to imperfect base-pairing. The development of bioinformatic databases has led to the identification of a region known as the 'seed site'. This refers to nucleotides 2-7 from the 5' end of the miRNA. This region is often evolutionarily conserved and is now the basis for generating target predictions (Lewis *et al.*, 2005). *In silico* analyses predicting mRNA targets of specific miRNAs on the basis of miRNA:mRNA pairing must therefore be evaluated with caution. Perfect base-pairing complementarity between miRNA and mRNA leads to site-specific mRNA endonucleolytic cleavage, similar to siRNA silencing, and is very much more common in plants than in animals. Imperfect base-pairing, however, causes repression either through mRNA destabilisation followed by degradation, or by mRNA translational repression (summarised in Section 1.5.1.5)

1.5.1.5 Gene-Silencing Mechanisms / Repression Mechanisms

The mechanisms behind miRNA-mediated repression are not fully understood. As explained in the previous section, the two currently accepted models in animals involve translational repression and mRNA destabilisation and degradation.

Translational Repression

Reviews of recent evidence suggest that there are several different modes of mRNA translational repression (Filipowicz *et al.*, 2008; Gu and Kay 2010). Translation is a complex, multi-step process facilitating the conversion of mRNA to protein. Typically, translation begins with a complex initiation step whereby the 5' terminal cap structure, m⁷GpppN (where N is any nucleotide), of the mRNA is recognised by and interacts with the eIF4E subunit of the eukaryotic translation initiation factor 4F (eIF4F). Various subtypes of eIF are involved at this stage and facilitate the recruitment of the 40S ribosomal subunit (Kapp and Lorsch 2004). The eIF complex also associates with the polyadenylate-binding protein (PABP), bound to the adenylation site at the 3' end of the mRNA, which brings together both ends of the transcript, effectively 'circularising' the mRNA (Wells *et al.*, 1998). This circular formation increases translation initiation efficiency and the 40S ribosomal subunit begins to scan the mRNA for the AUG start codon. The elongation process can then occur upon recruitment of the 60S ribosomal subunit, regulated by various elongation factor proteins (Kapp and Lorsch 2004). The termination process occurs when the stop codon is reached, where upon translation release factors trigger the dissociation of the ribosomal subunits from the mRNA.

There is much evidence to suggest that miRNA-mediated translational repression can occur at various stages in the complex translation process. A brief summary is provided below:

1. Competition for 5'-cap binding: Eulalio *et al.* (2008) contradicted previous evidence that miRISC competed with eIF4E for 5'-cap binding by proposing that GW182 (Protein with multiple glycine (G)-tryptophan (W) repeats, molecular mass 182 kD), recruited by Ago 1-4 in miRISC, was in fact responsible. Failure of subunit eIF4E binding therefore causes repression at the translation initiation stage.
2. Inhibition of 60S subunit recruitment: Chendrimada *et al.* (2007) showed that the 60S ribosomal subunit interacts with eIF6 and proposed that one or both of these proteins interact with miRISC, thus inhibiting 40S-60S interaction and causing translational repression. There is conflicting

evidence as to the exact mechanisms. However, the published data are consistent with the theory that translational repression can occur post-initiation.

3. Premature ‘ribosomal drop-off’: Petersen *et al.* (2006) suggested that the presence of miRISC prompts early ribosomal dissociation from the mRNA in the elongation stage of translation. Guo *et al.* (2010) corroborated this proposal with a large ribosomal profiling study *in vitro*. These and similar studies demonstrate miRNA-mediated post-initiation translational repression.

mRNA Destabilisation

Destabilisation of mRNA occurs when the poly (A) tail is shortened (Wu *et al.*, 2006). This deadenylation of the mRNA increases its instability and inhibits translation initiation by preventing the binding of PABPs (Poly(A)-binding proteins). Catalysed by exosomes, mRNA degradation and decay then occurs in a 3'-5' direction. Alternatively, destabilisation may cause removal of the 5'm⁷GpppN cap by Dcp2 enzyme, allowing 5'-3' decay. Both mechanisms block circularisation of the mRNA, thus decreasing translational initiation efficiency. These mRNAs may then accumulate in cellular processing bodies (P-bodies), which lack the machinery necessary for translation (Valencia-Sanchez *et al.*, 2006) and are degraded by XRN1 and other exonucleases (Behm-Ansmant *et al.*, 2006). Research suggests that the protein GW182, a component of P-bodies, associates with the Ago 1-4 complex within miRISC, thus promoting their transition from cytoplasm to P-bodies (Eystathioy *et al.*, 2002; Behm-Ansmant *et al.*, 2006). Interestingly, Bhattacharyya *et al.*, (2006) proposed a mechanism whereby, under certain cellular conditions, mRNA could be released from the P-body back into the cytoplasm to undergo translation. This gives credence to the notion that miRNAs act more as ‘fine-tuners’ of mRNA levels than simply as ‘on-off’ switches.

There is conflicting evidence as to whether translational repression and mRNA destabilisation are entirely independent processes or whether they are interlinked in certain situations (reviewed by Filipowicz *et al.*, 2008).

Understanding the exact mechanisms behind mRNA repression by miRNA is essential, particularly if miRNA is to be considered for therapeutic use.

1.5.1.6 miRNAs and the Human Adrenal Gland

Various studies have shown the importance of microRNAs in adrenal development and maintenance in mice (Bernstein *et al.*, 2003; Huang and Yao 2010), but the effects of miRNAs in the human adrenal gland are less well studied. Wood (2011) used a siRNA approach to knock down Dicer, the protein vital for miRNA maturation, in the H295R human adrenocortical carcinoma cell line, and studied the effects on levels of steroidogenic mRNAs. Interestingly, only those encoding cytochrome P450 enzymes in the pathway were affected (*CYP11A1*, *CYP21A1*, *CYP17A1*, *CYP11B1*, *CYP11B2*). Steroid production was also significantly altered, with the end products aldosterone and cortisol, together with many intermediate compounds in their biosynthesis, all increased relative to control cells (DOC, corticosterone, 18-OH corticosterone). These results were consistent with canonical miRNA action, whereby lower levels of mature miRNAs lead to increased target mRNA levels and result in more abundant product. These data support a significant regulatory role for miRNAs in human steroidogenesis.

In 2008, Romero *et al.* identified miR-21 as a key modulator of aldosterone production. Overexpression of miR-21 *in vitro* significantly increased aldosterone production and cell proliferation in H295R cells. These findings support the role of miR-21 in both corticosteroid production and oncogenesis. This study, however, made little attempt to identify possible target genes of miR-21 or to suggest a regulatory mechanism by which miR-21 causes increased aldosterone production and cell proliferation.

Robertson *et al.* (2013) provides a comprehensive study of the effects of miR-24 on aldosterone and cortisol production, as well as identifying and confirming target genes. This work builds on its previous abstract publication (Wood *et al.*, 2011) which showed that mRNA levels of *CYP11B1* and *CYP11B2* mRNA were significantly increased after siRNA knockdown of Dicer *in vitro*. MiRNAs predicted to bind both mRNAs were identified and cross-referenced with miRNA expression profiles derived from both normal human adrenal tissue and aldosterone-producing adenoma (APA) tissue. Overexpression and inhibition studies revealed

that miR-24 significantly alters *CYP11B1* and *CYP11B2* mRNA levels as well as aldosterone and cortisol production *in vitro*. Experiments utilising reporter constructs mutated at the predicted seed site confirmed that miR-24 binds the 3'UTRs of each mRNA at sites identified by bioinformatic programs. The alterations in mRNA should also be reflected at the protein level but the high homology of the two genes has so far prevented the generation of specific antibodies. Nonetheless, these data set a benchmark for future research into miRNA regulation of corticosteroidogenesis.

The majority of published research concerning miRNA in the adrenal gland concerns miRNA expression profiles in adrenal tumours (Soon *et al.*, 2009; Patterson *et al.*, 2011; Schmitz *et al.*, 2011). These studies suggest that various miRNAs are dysregulated in adrenocortical carcinomas or adenomas. The definition of a miRNA profile specific to a certain type of growth would hold the potential to aid in the diagnosis of adrenocortical tumours, using miRNA as prognostic markers (reviewed by Singh *et al.*, 2012).

It is clear from this review of recent evidence that miRNAs are important regulators of adrenal function. Thus, their small, fine-tuning effects must be added to the better understood influences, such as those that modulate expression through interaction with the gene promoter. It is important to understand the balance between these controls both in normal and disordered physiology. Previous studies have shown that small changes in the activity of *CYP11B1* and *CYP11B2* may contribute to the slow, inexorable rise in blood pressure which may establish essential hypertension (Barr *et al.*, 2007; Freel *et al.*, 2007; McManus *et al.*, 2012). How else might the adrenal cortex be involved?

1.6 Aims:

Recent genome-wide association studies linked a locus within *CYP17A1* to greater risk of increased systolic blood pressure. While many studies investigating association of *CYP17A1* genetic variation with androgen-related disorders such as breast and prostate cancers and polycystic ovary syndrome have been published, few have investigated its association with blood pressure. The position of this gene in the steroidogenic pathway, with its ability sequentially to catalyse 17 α -hydroxylase and 17,20 lyase reactions, makes it crucial to the modulation of adrenocortical output between corticosteroids and androgens. The work presented in this thesis tests the hypothesis that common genetic variation in both the 5' and 3' regulatory regions of the *CYP17A1* gene lead to subtle changes in blood pressure. There follows an account of a programme of experimental work that addresses each of these facets. Its major aims were as follows:-

- To identify the pattern of linkage disequilibrium across the *CYP17A1* gene and examine the association of *CYP17A1* polymorphisms with hypertension in a Caucasian population
- To investigate *in vitro* the functional effects of candidate polymorphisms located in the promoter region of *CYP17A1* in order to determine their likely effects on glucocorticoid and androgen production.
- To investigate a potential role for microRNA in the post-transcriptional regulation of the *CYP17A1* gene.

2 Methods

This chapter provides a detailed outline of the general laboratory practices and experimental methods used to perform the work described in this thesis. Some methods are common to more than one chapter; specific materials and methods section are also provided within each individual results chapter.

2.1 General Laboratory Practice

A laboratory coat and latex powder-free gloves were worn during all procedures. Hazardous substances were handled in accordance with Control of Substances Hazardous to Health regulations, with laboratory facemasks, spectacles and fume hoods used where necessary. All equipment and reagents were of the highest available grades.

2.2 Sequencing the *CYP17A1* Gene in Normotensive and Hypertensive Populations

2.2.1 Study Subjects

2.2.1.1 Adrenal Function Study

DNA samples from normotensive volunteers were analysed from the Adrenal Function Study (AFS), previously conducted by Dr. Frances McManus (n=60). An automated method had been used for DNA extraction (Gentra System Autopure LS, Large Sample Nucleic Acid Purification Automated DNA extraction, QIAGEN, U.K.) according to the manufacturer's instructions and DNA had been stored for approximately six months at -20°C prior to use.

2.2.1.2 MRC British Genetics of Hypertension Study

The MRC BRitish Genetics of HyperTension (BRIGHT) cohort is a large multicentre study comprising 3500 affected sibling-pairs (sib-pairs) and 3000 parent-offspring trios (TDTs). The data presented in Chapter 4 of this thesis relates to 511 unrelated hypertensive individuals from the sib-pair group for whom corticosteroid and androgen profiles were available. A detailed account of the recruitment of the sib-pair group was previously described by Caulfield *et al.*, (2003). In brief, blood pressure values of 150/100 mmHg or higher, based on one reading, or 145/90 mmHg, as a mean of three readings, were required for inclusion in the study with onset of hypertension diagnosed before age 60 years

in at least one sibling. DNA was extracted by the BRIGHT consortium, as described at http://www.brightstudy.ac.uk/info/sop_9000666.html#processing.

2.2.2 Determination of Nucleic Acid Quantity and Quality

Both the quantity and quality of nucleic acids (RNA or DNA) were assessed using a Nanodrop® ND-1000 spectrophotometer (Labtech International Ltd, U.K.) with ND-1000 v3.1.0 software. 2µl of each sample is loaded on to the end of a fibre optic cable and, when the arm of the instrument is lowered, the sample is brought into contact with a second fibre optic cable, causing the liquid to bridge a specific gap between the two fibre optic ends. Light is then passed through the sample and sample concentrations are provided onscreen. Purity of the sample can be assessed using the additional information provided onscreen: the 260/280 value is a ratio of sample absorption at 260nm and 280nm, with values of 1.8 and 2.0 considered optimal for DNA and RNA respectively. Nuclease-free water is used as a reference.

2.2.3 PCR of CYP17A1

Primers were designed to amplify DNA at least 2 kilobases upstream from the transcriptional start site, encompassing the promoter/enhancer region of the *CYP17A1* gene. Exons were amplified either singly or in pairs using primers previously published by Lin *et al.* (1991) and Monno *et al.* (1993), with a reverse primer designed to amplify the 3'UTR specifically. Primers to amplify the introns were designed as necessary, with all newly-designed primers based on published sequences (www.ensembl.org/index.html) and checked for specificity via the BLAST database (<http://blast.ncbi.nlm.nih.gov/Blast.cgi>). All primers were obtained from Eurofins MWG Operon (Germany) and had undergone High Purity Salt Free (HPSF) purification. Sequences are provided in Appendix 1. The promoter region PCR was performed on a 96-well Dyad Disciple™ sample block powered by the PTC-0221 thermal cycler with heated lid (MJ Research, MA, U.S.A.) using the Expand High Fidelity PCR System (Roche Diagnostics Ltd, Burgess Hill, U.K.). All introns, exons and 3' untranslated regions of the gene were amplified using the Thermo-Start *Taq* DNA Polymerase PCR Enzyme Kit (Thermo Fisher Scientific, U.K.), and performed on the Multi Block System Satellite 0.2 Thermo Cooler (Thermo Fisher Scientific, U.K.). Specific protocols

for each PCR system are shown below. DNA samples were diluted to a working stock of 5ng/ μ l with nuclease-free water.

Expand High Fidelity PCR System

Reagent	Volume per reaction	Final concentration
dNTPs	2.00 μ l	80 μ M each
Forward primer (10 μ M)	0.75 μ l	300nM
Reverse primer(10 μ M)	0.75 μ l	300nM
Expand High Fidelity Taq DNA polymerase	0.75 μ l	2.6U
Expand High Fidelity Buffer with MgCl ₂ (10x)	2.50 μ l	1x
Nuclease-free water	13.25 μ l	
Genomic DNA (5ng/ μ l)	5.00 μ l	25ng

Thermo-Start Taq DNA Polymerase PCR Enzyme Kit

Reagent	Volume per reaction	Final Concentration
dNTPs	5.00 μ l	200 μ M each
Forward primer (10 μ M)	1.30 μ l	500nM
Reverse primer (10 μ M)	1.30 μ l	500nM
Thermostart taq (5U/ μ l)	0.25 μ l	1.25U
Thermostart Buffer (10x)	2.50 μ l	1x
MgCl ₂ (25mM)	1.50 μ l	1.5mM
Nuclease-free water	8.15 μ l	
Genomic DNA (5ng/ μ l)	5.00 μ l	25ng

A temperature gradient was used to optimise all PCR annealing temperatures, with a typical gradient result shown in Figure 2-1. Individual PCR conditions can be found in Appendix 1.

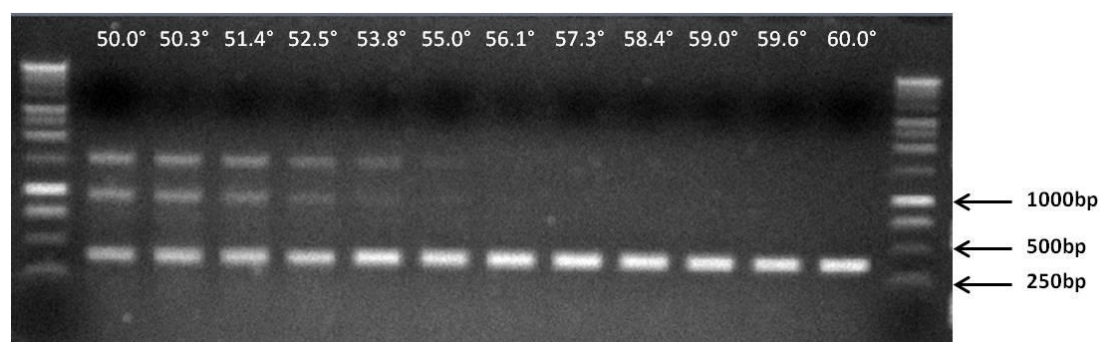


Figure 2-1 Typical PCR resulting from a gradient of annealing temperatures. The intended product size is 397 bp and is resolved on a 1% agarose gel.

2.2.4 Agarose Gel Electrophoresis

Agarose gel electrophoresis was used to separate DNA fragments resulting from PCR or restriction digestion. A 1% agarose gel was prepared by adding 1g of (w/v) Ultrapure agarose (Invitrogen, Paisley, U.K.) to 100ml of Tris/Borate/EDTA (TBE) (10mM Tris, 10mM boric acid, 10mM EDTA, pH 8.3) and heating in a microwave oven for approximately 100 seconds. 1 μ l of ethidium bromide (10mg/ml) (Sigma-Aldrich, Poole, U.K.), which intercalates with DNA and fluoresces under UV light, was added to the liquid gel in a fume hood before pouring the whole mixture into a gel mould with Teflon comb and allowed to set for 15-30 minutes. After setting, the gel was submerged in a standard electrophoresis tank in 1x TBE buffer and the comb removed. Equal amounts of samples were combined with loading dye (0.02% bromophenol blue, 0.02% xylene cyanol and 2.5% glycerol) and loaded into the wells alongside an appropriate marker: either 1kb or 100bp DNA size ladder (Promega, Wisconsin, U.S.A.). The gel was resolved at a constant 90V for 45 minutes. DNA fragments were visualised and captured on a molecular Imager ChemiDoc(TM) XRS+ Imaging system and Multi-Analyst software v 1.1 (both Bio-Rad Laboratories, Hemel Hempstead, U.K.), scanning with UV light at 302nm.

2.2.5 PCR Product Purification

The AMPure purification method (Agencourt, Beverly, MA, U.S.A.) was used to separate PCR products from unincorporated dNTPs, primers, primer dimers, salts and other contaminants left over from the PCR reaction, in preparation for the subsequent sequencing reaction. For 25 μ l PCR reactions, 36 μ l of resuspended AMPure reagent was added to each PCR product and vortexed. The mixture was collected at the bottom of the wells in the PCR plate by brief centrifugation and incubated at room temperature for 5 minutes to allow PCR products of at least 100 base pairs (bp) to bind to magnetic beads in the AMPure reagent. The PCR plate was then placed on a solid phase reversible immobilisation (SPRI) magnet for 10 minutes. With the magnetic beads (along with the DNA) bound to the magnet, the remaining liquid was removed by inversion. With the plate remaining on the magnet, 150 μ l of 70% ethanol was added to each sample for a total of 30 seconds and this, again, was removed by inversion. To ensure that no ethanol remained, the plate, while still on the magnet, was inverted onto a

piece of tissue and briefly centrifuged. The plate was then removed from the magnet and allowed to dry at room temperature for at least 20 minutes. 40µl of nuclease-free water was added to each sample and then vortexed in order to elute the DNA from the magnetic beads. The plate was returned to the magnet for at least 10 minutes and a small volume of this final solution (specified in Section 2.2.6) was used as template for the sequencing reaction.

2.2.6 Sequencing Reaction

PCR products and plasmid DNA were sequenced using BigDye Terminator v3.1 Cycle Sequencing chemistry (Applied Biosystems, Warrington, U.K.) which utilises a technique based on the dideoxy chain termination method of sequencing. Varying volumes of DNA template were used, depending on the preceding PCR. Sequencing reaction mixtures were set up in 96-well PCR plates consisting of the following components:

Reagent	Volume per Reaction (µl)
ABI PRISM Big Dye v3.1 Sequencing Buffer (5x)	3.5
ABI PRISM Big Dye Termination v3.1 Ready Reaction Mix	0.5
Sequencing Primer (3.2µM)	1.0
DNA template:	
<i>e.g. Plasmid 100-200ng</i>	
<i>PCR product (High Fidelity Taq) 2µl</i>	Variable
<i>PCR product (Thermostart Taq) 5µl</i>	
Nuclease-free water	Up to final volume of 20

Sequencing primers are synthetic oligonucleotides designed to produce overlapping fragments of the desired region. As with the PCR primers described in Section 2.2.3, primers were based on published sequences, checked for specificity, and obtained commercially in HPSF form. Sequences of individual sequencing primers can be found in Appendix 1. Primers were designed for each opposing strands in order to increase the reliability of results. The program for each reaction was chosen based on the melting temperatures (T_m) of the sequencing primers: BIGSEQ50 for primers with $T_m < 60^\circ\text{C}$ and BIGSEQ60 for primers with $T_m > 60^\circ\text{C}$, the conditions of which are shown below:

BIGSEQ50			BIGSEQ60		
Time	Temperature	Cycles	Time	Temperature	Cycles
45 secs	96 °C		45 secs	96 °C	25
25 secs	50 °C	25	4 mins	60 °C	
4 mins	60 °C				

2.2.7 Sequencing Reaction Purification

The CleanSEQ purification method (Agencourt, Beverly, MA, U.S.A.) was used to remove components of the sequencing reaction from the sample prior to automated cycle sequencing. For 20µl sequencing reactions, 10µl of resuspended CleanSEQ reagent was added to each sequencing reaction product, followed by 62µl of 85% ethanol, and vortexed. The mixture was collected at the bottom of the wells in the PCR plate by brief centrifugation and placed on a SPRI magnet for 10 minutes. The remaining liquid was removed by inversion and discarded before 150µl of 85% ethanol was added to each sample. After 30 seconds the ethanol was removed by inversion before being briefly centrifuged in the same orientation. The plate was then removed from the magnet and allowed to dry at room temperature for at least 20 minutes. 40µl of nuclease-free water was added to each sample and then vortexed in order to elute the DNA from the magnetic beads. The plate was returned to the magnet and 20µl of DNA sample transferred to a bar-coded plate for sequencing.

2.2.8 Automated Cycle Sequencing

Automated cycle sequencing was performed on an ABI 3730 DNA analyser (Applied Biosystems, Foster City, CA, U.S.A). Genomic DNA sequencing results were analysed using SeqScape v2.2 genotyping software (Applied Biosystems, Foster City, CA, U.S.A) and plasmid DNA sequencing results using CLC Genomics Workbench v4.9 (CLC Bio, Swansea, U.K.). For both software programmes, sequences were aligned to a reference sequence based on those published for the *CYP17A1* gene (www.ensembl.org/index.html) and those provided by the manufacturer for reporter constructs (Sections 2.7.1, 2.7.2).

2.2.9 Data Analysis

CYP17A1 gene sequencing data from both the AFS Cohort and BRIGHT sib-pair subset were analysed using Haploview software version 4.2 (<http://www.broad.mit.edu/mpg/haploview>) (Barrett *et al.*, 2005). This software enabled the pattern of linkage disequilibrium, Hardy-Weinberg equilibrium and haplotype structure to be determined.

2.3 Cell Culture

Cells were cultured under sterile conditions using class II biological vertical laminar flow safety cabinets (Holten Safe 2010). Cabinets were cleaned before and after use with 1% Rely+On™ Virkon® (DuPont, Herts, U.K.), 70% ethanol and dH₂O. All fluid and plastic waste was decontaminated by soaking in 10% H₂O₂ for 24 hours. Fluids were then discarded through domestic waste drains and plastics incinerated. Cells were grown in a monolayer in 25cm², 75cm² and 150cm² culture flasks with vented caps (Corning Life Sciences, Amsterdam, the Netherlands) with normal growth medium, as detailed below, and incubated in a humidified chamber at 37°C with 5% CO₂.

The H295R (strain 2) human adrenocortical tumour cell line were a generous gift from Professor William Rainey (Medical College of Georgia, U.S.A). These cells were maintained in Dulbecco's modified Eagles medium (DMEM) with F12, 1:1 (Invitrogen, Paisley, U.K.) supplemented with 2.5% Ultrosor G (Pall Bioscience, France), 1% insulin-transferrin-selenium (ITS) (BD Biosciences, Oxford, U.K.) and 1% penicillin/streptomycin: 1IU penicillin, 100µg/ml streptomycin (Invitrogen, Paisley, U.K.).

HeLa cells, an immortalised human cell line derived from a cervical cancer were purchased from the European Collection of Animal Cell Cultures (Porton Down, Wiltshire, U.K.) and were maintained in DMEM (Invitrogen, Paisley, U.K.) supplemented with 10% (v/v) foetal calf serum (FCS), 2mM L-glutamine (Sigma-Aldrich, Poole, U.K), 100mM sodium pyruvate (Sigma-Aldrich, Poole, U.K.) and 1% penicillin/streptomycin: 1IU penicillin, 100µg/ml streptomycin (Invitrogen, Paisley, U.K.)

2.3.1 Cryopreservation

For long-term storage, cells were harvested as described in Section 2.2.2 but resuspended in complete growth medium supplemented with sterile 10% (v/v) dimethyl sulphoxide (DMSO) (Thermo Fisher Scientific, Loughborough, U.K.) to prevent the formation of ice crystals. Cell suspensions were aliquoted into 2ml cryopreservation vials and cooled at a constant $-1^{\circ}\text{C}/\text{minute}$ to -80°C using isopropanol and a Nalgene Cryo container (Thermo Fisher Scientific, Loughborough, U.K.) before being transferred to liquid nitrogen for long-term storage

Cells were resuscitated from cryopreservation by thawing vials in a 37°C water bath and immediately transferring the suspension to a universal container with 5ml of complete growth medium. Cells were pelleted by centrifugation at 1500rpm for 5 minutes and the medium containing DMSO was removed. Cells were then resuspended in 5ml of complete growth medium and transferred to a 25cm^2 Corning cell culture flask and cultured as detailed in Section 2.3.2.

2.3.2 Maintenance of Established Cell Lines

Cells were routinely passaged at approximately 80% confluence. Medium was removed and the cells rinsed with an appropriate volume of phosphate buffered saline (PBS) solution (Invitrogen, Paisley, U.K.), depending on the volume of flask (typically 6-10ml). Up to 5ml of 0.25% Trypsin-EDTA solution (Sigma, Missouri, U.S.A.) was added to the flask of cells and, after incubation at 37°C for 2-4 minutes, the cells were detached from the flask. The Trypsin-EDTA solution was then inactivated by adding an equal volume of complete growth medium. Cells were transferred to a universal container and pelleted by centrifugation at 1500rpm for 5 minutes. The supernatant was discarded and the cell pellet resuspended in an appropriate volume of fresh complete growth medium, depending on the desired sub-cultivation ratio. Typically, complete growth medium was replenished every 2-3 days, with a 150cm^2 flask of H295R cells being sub-cultured into 2 or 3 flasks and HeLa cells into 5 flasks.

2.3.3 Counting Cells

Cell number was calculated using a Bright Line Haemocytometer (Sigma-Aldrich, Poole, U.K.). Cells were detached from the flask, pelleted as described in Section 2.2.2 and resuspended in 10ml of complete growth medium. 20 μ l of cell suspension was applied across the chamber beneath a coverslip. With the aid of a light microscope, cells in each 1mm corner square were counted and an average number taken. Each corner square on the haemocytometer represents a volume of 10⁴cm³ and, since 1cm³ is approximately equal to 1ml, the concentration of cells per ml were calculated:

$$\text{Cell number/ml} = \text{average cell count per square} \times 10,000$$

Knowing the number of cells per ml in the cell suspension enabled cells to be plated at the desired density.

2.3.4 Stimulation of H295R Cells

Cell steroidogenesis was stimulated 24 hours after sub-culturing. Normal growth medium was removed from the cells before rinsing with PBS, and replaced with normal growth medium supplemented with the desired trophin (1mM dibutyryl cAMP). A more specific and detailed account of the stimulation of cells for particular experiments can be found in the methods section of the appropriate results chapter.

2.4 RNA Isolation & DNase Digestion

The miRNeasy mini-kit (QIAGEN, Crawley, U.K.) was used for efficient purification and isolation of mRNA and miRNA from cells cultured in 6-well plates. The direct lysis method from the manual supplied with the kit was followed (dated October 2007). The cell medium was removed and the cells rinsed with PBS before adding 700 μ l of QIAzol lysis reagent. The plates were then incubated at -80°C for at least 15 minutes to ensure efficient lysis and then thawed at room temperature. Each sample was then transferred to an RNase-free Eppendorf tube and kept at room temperature for 5 minutes; this promotes dissociation of nucleoprotein complexes. After the addition of 140 μ l of chloroform, each tube was thoroughly mixed by vigorous shaking for 15 seconds.

Samples were then centrifuged at 12,000g for 15 minutes at 4°C. After centrifugation, the upper colourless aqueous phase was separated from the white interphase and the lower, red, organic phase using a pipette and transferred to a fresh Eppendorf tube. 1.5 volumes of 100% ethanol were added to each sample and mixed by pipetting. The sample was then passed through an RNeasy mini-spin column by brief centrifugation at 8,000g to allow RNA molecules to bind to the silica membrane. Flow-through was discarded before performing on-column DNase digestion to eliminate residual genomic DNA contamination. The spin column membrane was washed by adding 350µl of Buffer RWT and centrifuging for 15 seconds at 8,000g, with the flow-through discarded immediately. 10µl of DNase I stock solution was added to 70µl of Buffer RDD for each sample, both provided by the RNase-free DNase Set kit (QIAGEN, Crawley, U.K.), and the resulting 80µl was dispensed directly on to the spin column membrane. The column then remained at room temperature for 15 minutes. The wash step with Buffer RWT was then repeated and the flow-through discarded. The column was further washed twice with 500µl of buffer RPE, with flow-through discarded, first, after brief centrifugation, and second, after 2 minutes of centrifuging at 8,000g. The spin column was then placed in a fresh collection tube and centrifuged at full speed for 1 minute to prevent carryover of wash buffers. Finally, the spin column was transferred to a 1.5ml Eppendorf tube; 50µl RNase-free water was dispensed directly onto the spin column membrane and centrifuged for 1 minute at 8,000g to elute the RNA. RNA quantity and quality was assessed using the method described in Section 2.2.2 and stored at -80°C.

2.5 Reverse Transcription

The miScript II Reverse Transcription kit (QIAGEN, Crawley, U.K.) was used to produce cDNA (first strand complementary DNA) from RNA. This allowed quantification of both microRNA and messenger RNA by qRT-PCR using a two-step protocol. Each reaction mixture was assembled following the manual provided with the kit (dated August 2011). They comprised the following components:

Reagent	Volume
5x miScript HiFlex Buffer	4 μ l
10x Nucleics Mix	2 μ l
miScript Reverse Transcriptase Mix	2 μ l
200ng of DNase-treated RNA	Variable
RNase-free water	Up to total volume of 20 μ l

Reactions were loaded on to a standard 96-well PCR plate and run on the Multi Block System Satellite 0.2 Thermo Cooler (Thermo Fisher Scientific, Loughborough, U.K.) with the following conditions:

Step	Time	Temperature
Reverse Transcription	120 mins	37°C
Inactivation of RT Mix	5 mins	95°C

For each RNA sample, a control reaction omitting reverse transcriptase was also set up. Blank controls omitting RNA were also used. 80 μ l of RNase-free water was added to each sample, which was then stored at -20°C

2.6 Quantitative Real-Time Polymerase Chain Reaction

Quantitative real-time PCR (qRT-PCR) assays were carried out using cDNA template to assess the quantities of mRNA and miRNA in a sample. All reactions were performed in ThermoFast® 384-well PCR plates (Thermo Fisher Scientific, Loughborough U.K.) on an ABI PRISM 7900HT PCR System. Measurements of samples, positive controls and water blanks were performed in triplicate.

2.6.1 Universal ProbeLibrary

The human Universal ProbeLibrary (UPL) system (Roche Diagnostics Ltd, Burgess Hill, U.K.) currently consists of 165 pre-validated real-time PCR probes, labelled at the 5' end with fluorescein (FAM) and with a dark quencher dye at the 3' end. Each probe binds to around 7000 transcripts although only one specific transcript is detected at a time in a given PCR assay, as defined by the set of chosen PCR primers. Primers were designed using the Roche online UPL assay design centre (<http://www.roche-applied-science.com/sis/rtpcr/upl/index.jsp?id=UP030000>)

and obtained from Eurofins MWG Operon (Germany), details of which are shown in Table 2-1:

Table 2-1 Primer sequences for gene expression assays.

Gene	Primer Sequence	Probe
CYP17A1	(F) CTATGCTCATCCCCACAG (R) TTGTCCACAGCAAACCTCACC	#67
ACTB	(F) CCAACCGCGAGAAGATGA (R) CCAGAGGCGTACAGGGATAG	#64

As well as primers, reagents required for each reaction included Absolute™ QPCR ROX mix (ABgene, Epsom, U.K.) and the appropriate UPL probe (Roche Diagnostics Ltd, Burgess Hill, UK). Master mixes were created to provide each reaction mixture with the following components:

Reagent	Volume (µl)	Final Concentration
Absolute™ QPCR ROX mix	5.0	1x
Forward Primer (10µM)	0.4	400nM
Reverse Primer (10µM)	0.4	400nM
UPL Probe (10µM)	0.1	100nM
Nuclease-free water	2.1	

8µl of master mix was added to 2µl of cDNA (prepared from miScript Reverse Transcription kit, Section 2.3) in a 384-well plate which was then sealed with an optical QPCR Absolute seal (ABgene Ltd, Epsom, U.K.). The reactions were run on the ABI PRISM 7900HT cycler using SDS v2.3 software under the following conditions:

Step	Time	Temperature	Cycles
Enzyme Activation	15 mins	95° C	1
Denaturation	15 secs	95° C	60
Annealing & Extension	1 min	60° C	

2.6.2 miScript qRT-PCR System

The miScript SYBR Green PCR kit (QIAGEN, Crawley, U.K.) was used to detect and quantify mature microRNA. 10x miScript Primer Assays, detailed in Table 2-2, (QIAGEN, Crawley, U.K.) were reconstituted in 550µl of TE (pH 8.0) and stored at -20°C.

Table 2-2 Primer assay molecules.

Primer Assay	miRNA Sequence	Product Code
hsa-miR-320a	AAAAGCUGGGUUGAGAGGGCGA	MS00014707
hsa-miR-34c-3p	AAUCACUAACCACACGGCCAGG	MS00009548

Master mixes were created to provide each reaction with the following components:

Reagent	Volume
QuantiTect SYBR Green PCR Master Mix (2x)	10 µl
10x miScript Universal Primer	2 µl
10x miScript Primer Assay	2 µl
Nuclease-free water	4 µl

18µl of master mix was added to 2µl of cDNA (Section 2.3) in a 384-well plate which was then sealed with an optical Absolute seal (ABgene Ltd, Epsom, U.K.). The reactions were run on the ABI PRISM 7900HT cycler using SDS v2.3 software under the following conditions:

Step	Time	Temperature	Cycles
Enzyme Activation	15 mins	95°C	1
Denaturation	15 secs	94°C	
Annealing	30 secs	55°C	40
Extension	30 secs	70°C	
	15 secs	95°C	
Melt Curve	15 secs	60°C	1
	15 secs	95°C (slow ramp)	

A melt curve was performed immediately following the cycling conditions to verify the specificity of the PCR products. Data were collected during the ramp phase between 60°C to 95°C. A single and unique PCR product was confirmed by observing a single peak in the melting curve for each primer assay.

2.6.3 qRT-PCR Data Analysis

Results of qRT-PCR were analysed using the relative method of comparative C_t ($2^{-\Delta\Delta C_t}$) (Livak and Schmittgen 2001), with β -actin and small nucleolar RNU48 utilised as an endogenous controls. This permits the standardisation of the amount of cDNA added to the reaction, acting as a normalising control to correct for sampling discrepancies. The extension phase of the PCR reaction induces fluorescence from the respective qRT-PCR probe that is proportional to the amount of product generated in each cycle. This is measured directly by the ABI PRISM 7900HT thermo cycler. A threshold of fluorescence is set during the exponential phase of amplification. The cycle number at which the fluorescence signal crosses this threshold is called the cycle threshold (C_t). The housekeeping gene expression was used to calculate the ΔC_t for the gene of interest as follows:

$$\Delta C_t = C_t (\text{sample}) - C_t (\beta\text{-actin})$$

All experiments were then compared to a reference control (e.g. non-transfected cells or scrambled control cells), details of which can be found in the appropriate results chapter methods section. This allowed the calculation of $\Delta\Delta C_t$

$$\Delta\Delta C_t = \Delta C_t (\text{sample}) - \Delta C_t (\text{reference})$$

The relative quantity (RQ) value for the messenger RNA or microRNA was then calculated:

$$RQ = 2^{-\Delta\Delta C_t}$$

2.7 Reporter Constructs

2.7.1 pEZX - 3'UTR Reporter Construct

To assess miRNA binding to the 3'UTR, a reporter construct containing the *CYP17A1* 3'UTR (pEZX-17) was purchased from LabOmics (Nivelles, Belgium). A negative control empty vector (pEZX-Con) was also purchased. Each construct contains a pEZX-reporter backbone, which consists of a renilla reporter gene coupled to a SV40 (Simian virus 40) viral promoter; a firefly experimental gene coupled to a CMV (Cytomegalovirus) promoter; a multiple cloning site located at the 3'end of the gene; and a Kanamycin resistance gene for antibiotic selection. Constructs were transformed and grown as described in Section 2.7.3.

2.7.2 pGL3 - 5' Regulatory Region Reporter Construct

The pGL3 Basic vector containing the *CYP17A1* 5' region (2898bp) was a generous gift from Professor Neil Hanley (University of Manchester, Manchester, U.K.) and was used to investigate the effect of polymorphic variation on promoter activity. Vectors used as controls were purchased from Promega (Wisconsin, U.S.A.). Controls included a negative control empty pGL3 Basic vector, pGL4.13 containing only the firefly (*Photinus pyralis*) luciferase gene and pGL4.73 containing only the coding region for renilla (*Renilla reniformis*) luciferase which was used to control for transfection efficiency. All constructs contained an Ampicillin resistance gene for antibiotic selection.

2.7.2.1 Site-Directed Mutagenesis

To investigate the effect of polymorphic variation on *CYP17A1* promoter activity, each SNP of interest was mutated to its alternative allele using the QuikChange Site-Directed Mutagenesis kit (Agilent Technologies U.K. Ltd, Berkshire, U.K.). The *CYP17A1* 5' construct (pGL3-17) was transformed and grown as described in Sections 2.7.3 - 2.7.5. Mutagenic primers required to alter each SNP of interest were designed using the online Quikchange Primer Design Program (www.agilent.com/genomics/qcpd) and ordered from Eurofins MWG Operon (Germany); primer sequences can be found in Appendix 1. The Mutant Strand Synthesis Reaction section of the kit protocol (Revision C, 2010) was followed, with each reaction mixture comprising the following components:

Reagent	Volume
10x Reaction Buffer	5 μ l
50ng of dsDNA Template	Variable
125ng of Primer 1	Variable
125ng of Primer 2	Variable
dNTP Mix	1 μ l
Double-distilled water	Up to volume of 49 μ l

Then...	

<i>Pfu Turbo</i> DNA polymerase (2.5U/ μ l)	1 μ l

The control reaction mixture recommended by the protocol was also followed but was of limited diagnostic value as it required vastly different cycling conditions. Cycling conditions for the main reactions, however, were as follows:

Step	Time	Temperature	Cycles
Enzyme Activation	30 secs	95 °C	1

Denaturation	30 secs	95 °C	
Annealing	1 min	55 °C	12
Extension	7.5 mins	68 °C	

Following thermal cycling, reaction mixtures were cooled to $\leq 37^\circ\text{C}$. The DpnI endonuclease (target sequence: 5'-Gm⁶ATC-3') is specific for methylated DNA and is used to digest the parental DNA template, thus selecting for mutation-containing DNA. 10U of the DpnI restriction enzyme was added directly to each reaction mixture and gently mixed by pipetting, before being incubated at 37 °C for 1 hour. The kit protocol suggests a transformation method using competent cells provided within the kit and 1 μ l of PCR product. However, this proved unsuccessful so transformations were performed using the JM109 competent cells instead (Promega, Wisconsin, U.S.A.). These were successful using the method described in Section 2.7.3.

2.7.3 Transformation of Competent Cells

100ng of the pGL3 promoter reporter construct plasmid DNA, or its associated control plasmids, was used to transform 100 μ l of JM109 *E. Coli* competent cells (efficiency $>10^8$ cfu/ μ g, Promega, Wisconsin, U.S.A.). 50ng of either pEZX-17 or

pEZX-Con was used to transform 50µl of MAX Efficiency[®] DH5α competent cells (efficiency >10⁹ cfu/µg, Invitrogen, Paisley, U.K.). Cells were transformed in parallel with a positive control and a DNA-free control. Competent cells were thawed on ice before being gently mixed with the appropriate volume of plasmid DNA in a prechilled 14ml BD Falcon polypropylene round-bottom tube (BD Biosciences, Oxford, U.K.), as recommended by the QuikChange Site-Directed Mutagenesis Kit (Section 2.7.2.1). All transformation reactions were incubated on ice for 10 minutes before being subjected to heat-shock treatment (42°C for 45 seconds). The cells were returned to ice for 2 minutes before 950µl of room temperature SOC (Super Optimal broth with Catabolite repression) medium was added (Invitrogen, Paisley, U.K.). Tubes were then incubated at 37°C whilst shaking at 225rpm for 1 hour in an Innova[®] 44 incubator shaker (New Brunswick Scientific, St. Albans, U.K.). 250µl of each transformation reaction was plated onto LB (Luria Broth) agar plates with either kanamycin (25mg/ml) or ampicillin (100mg/ml) as appropriate and incubated overnight at 37°C. Single colonies were picked and added to 10mls of LB supplemented with kanamycin (25mg/ml) or ampicillin (100mg/ml) as appropriate and shaken overnight at 225rpm and 37°C.

2.7.4 Small Scale DNA Purification

The QIAprep Spin Miniprep kit (QIAGEN, Crawley, U.K.) was used to purify DNA after overnight incubation. 2ml of the incubated solution was transferred to a 2ml Eppendorf tube and cells pelleted by centrifugation at 6000g for 10 minutes. Instructions provided with the kit (December 2006) were followed. Briefly, cells were resuspended and lysed in 250µl of Buffer P1 (50mM 2-amino-2-hydroxymethyl-1,3-propanediol, pH 8.0; 10mM EDTA, 10µg/ml RNase A) followed by the addition of 250µl Buffer P2 (200mM NaOH; 1% sodium dodecyl sulphate) and mixed by inversion. 350µl of Buffer N3 (3M potassium acetate pH5.5) was added to neutralise the reaction and, again, mixed by inversion. Samples were then centrifuged at 13,000g for 10 minutes and the resulting supernatants transferred to a QIAprep spin column. Columns were centrifuged at 13,000g for 1 minute to bind the DNA onto the silica membrane. The column was then washed twice, first with 500µl of Buffer PB, and secondly with 750µl of Buffer PE, with brief centrifugation and discarding of the eluate each time. The spin column was then subjected to a final spin at maximum speed for 1 minute to remove residual

wash buffer. The column was then placed in a fresh 1.5ml Eppendorf tube and the DNA eluted by adding 50µl of nuclease-free water to the spin column. This was allowed to stand for 1 minute prior to being centrifuged at 13,000g for 1 minute. Plasmid DNA was then quantified as described in Section 2.2.2 and sequenced to confirm the identity of the product (Sections 2.2.6 - 2.2.8). Primers used for each construct at this stage can be found in Appendix 1. Cycling conditions of BIGSEQ60 were utilised for all reactions (Section 2.2.6).

2.7.5 Large Scale DNA Purification

Large scale plasmid preparations were obtained using the QIAGEN[®] Plasmid Purification Kit (Maxi) (QIAGEN, Crawley, U.K.). 5ml of starter culture (Section 2.7.3) was added to 500ml of LB (Luria Broth), supplemented with kanamycin (25mg/ml) or ampicillin (100mg/ml) as appropriate, and shaken overnight at 225rpm and 37°C.

The manufacturer's protocol provided with the kit (November 2005 version) was adapted to the following method: cells were pelleted by centrifugation at 6000g for 15 minutes at 4°C and then resuspended in 10ml of Buffer P1. Cells were then lysed with 10ml of Buffer P2 and mixed by inversion. 10ml of chilled Buffer P3 was then added and mixed by vigorous inversion before being incubated on ice for 20 minutes. The solution was then centrifuged at 20,000g for 30 minutes at 4°C and the supernatant applied to a QIAGEN-tip 500, which had been equilibrated with 10ml of Buffer QBT. The sample was allowed to enter the resin by gravity flow. The QIAGEN-tip was washed twice with 15ml of Buffer QC before the DNA was eluted with 15ml of Buffer QF, and precipitated with 0.7 volumes of room temperature isopropanol. DNA was pelleted by centrifugation at 15,000g for 30 minutes at 4°C. The DNA pellet was resuspended in 5ml of 70% ethanol and centrifuged at 15,000g for 10 minutes in 1.5ml Eppendorf tubes. The supernatant was discarded and the pellets air-dried for 10 minutes before being redissolved in 50µl of nuclease-free water. Contents of each Eppendorf tube were combined and the DNA quantified (Section 2.2.2) and stored at -20°C. The identity of all products was confirmed by both restriction endonuclease digestion and sequencing (Section 2.7.6).

2.7.6 Verification of Plasmids

Following large scale DNA purification (Section 2.7.5) all plasmids were subjected to restriction endonuclease digestion to confirm their molecular size and circularisation. Sequencing confirmed the presence of the insert in its correct orientation.

2.7.6.1 Restriction Endonuclease Digestion

Restriction digests were performed using the following enzymes (Promega, Wisconsin, U.S.A):

Enzyme	Buffer	Target Backbone
Sma I	J	pGL3
EcoRI	H	pGL3
Bgl I	D	pGL3
Bgl II	D	pEZX
Pst I	H	pEZX

The following components were assembled in an Eppendorf tube in order:

Component	Volume per reaction (μ l)
Restriction enzyme 10x buffer	2.0
Acetylated BSA (10 μ g/ μ l)	0.2
Plasmid DNA (0.5 - 1 μ g)	variable
Restriction enzyme (10u/ μ l)	0.5
Nuclease-free water	Up to final volume of 20 μ l

The mixture was then incubated at 37°C for 2 hours. Restriction digests were visualised by agarose gel electrophoresis as described in Section 2.2.4.

2.7.6.2 Plasmid Sequencing

Sequencing of all constructs was conducted using the methods described in Section 2.2.6 to Section 2.2.8. Promoter constructs were sequenced using several primers to span the entire insert; other primers annealed to the pGL3 Basic backbone, details of which can be found in Appendix 1. The pEZX-17 and

pEZX-Con plasmids were sequenced across the insert using primers which lay in the flanking regions of the insert, thus confirming some backbone sequence and the 3'UTR sequence. Again, primers can be found in Appendix 1. Cycling conditions of BIGSEQ60 were utilised for all reactions (Section 2.2.6).

2.8 Transient Cell Line Transfection

H295R cells and HeLa cells were grown as described in Section 2.3.2. For transfection, H295R cells were subcultured onto 6-well or 24-well cell culture plates at a density of 5×10^5 cells/well or 2×10^5 cells/well respectively (Section 2.3.3). HeLa cells were subcultured at a density of 8×10^4 cells/well into 24-well cell culture plates.

2.8.1 5' Regulatory Region Reporter Construct Transfection

H295R cells were transfected in 24-well cell culture plates with original (Section 2.7.2) or mutated plasmids (Section 2.7.2.1) using siPORT™ NeoFX™ Transfection Agent (Applied Biosystems, Warrington, U.K.). The manufacturer's protocol was followed and utilised the reverse transfection method. A solution containing 1.5µl of transfection agent combined with 48.5µl Opti-MEM® reduced serum medium (Invitrogen, Paisley, U.K.) was allowed to equilibrate for 10 minutes. Achieving a 50:1 ratio, 1000ng of the plasmid of interest was combined with 20ng of pGL4.73 and made up to a total volume of 50µl with Opti-MEM®. The transfection agent/Opti-MEM® solution was added to the DNA/Opti-MEM® solution creating a final volume of 100µl and again was allowed to equilibrate for 10 minutes. This volume was then dispensed into each well before adding 400µl of cell solution. The plate was rocked to ensure even coverage.

Positive controls reactions utilised 500ng of pGL4.13 and pGL4.73, both described in Section 2.7.2. Negative controls included pGL3-Basic plus pGL4.73 (50:1 ratio) as well as cells with no DNA transfected. Reactions were performed in quadruplicate.

The cell culture plates were incubated at 37°C and, after 24 hours, the transfectant was removed and replaced with serum-free medium or medium containing dibutyryl cAMP (1mM). Cells were again incubated for 24 hours before

being rinsed with PBS and lysed with 1x Passive Lysis Buffer (1xPLB). 25µl of each sample was assessed in duplicate using the Dual Reporter Luciferase Assay, as described in Section 2.9

2.8.2 3'UTR Reporter Construct Transfection

2.8.2.1 Preparation of Small Molecules

To test the effects of specific miRNAs on *CYP17A1 in vitro*, various small molecules were utilised. In order to artificially increase or decrease the levels of specific miRNAs, mimics (Pre-miR™) or inhibitors (Anti-miR™) were purchased (Applied Biosystems, Warrington, U.K.). Scrambled control molecules were also purchased. Details of these molecules can be found in Table 2-3. Each lyophilised Pre-miR™ or Anti-miR™ was reconstituted to a stock concentration of 6.25µmoles and stored at -20°C.

Table 2-3 Pre-miR™ and Anti-miR™ molecules.

miRNA	Pre-miR™ Product Code	Anti-miR™ Product Code
Negative Control #1	AM17110	AM17010
hsa-miR-320a	PM11621	PM11621
hsa-miR-34c-3p	PM12342	AM12342

A siRNA targeting the *CYP17A1* 3'UTR was designed to provide a positive control and confirm knockdown of firefly luciferase expression (Table 2.4). The lyophilised siRNA molecules were reconstituted to a final concentration of 10µM and stored at -20°C.

Table 2-4 siRNA targeted to *CYP17A1* 3'UTR.

siRNA Name	Sequence
17_3UTR_si	UGC CAG UGA UGU GCA UAA A

2.8.2.2 3'UTR Reporter Construct Co-transfection

The pEZX-17 reporter construct (Section 2.7.1) was co-transfected with either Pre-miR™ or Anti-miR™ molecules, described in Section 2.8.2.1, into HeLa cells. For use in 24-well cell culture plates, 1.5µl of siPORT™ NeoFX™ Transfection Agent and 48.5µl of Opti-MEM® reduced serum medium were mixed and allowed

to equilibrate for 10 minutes. The pEZX-17 construct (100ng) was mixed with 4µl of Pre-miR™ or Anti-miR™, as appropriate (final concentration 50nM) and made up to a final volume of 50µl with Opti-MEM®. The transfection agent/Opti-MEM® solution was added to the DNA/small molecule/Opti-MEM® solution creating a final volume of 100µl and again was allowed to equilibrate for 10 minutes. This volume was then dispensed into each well before adding 400µl of cell solution. The plate was then rocked to ensure even coverage.

Positive controls included 500ng of pGL4.13 and pGL4.73, both described in Section 2.7.2, which confirmed the specificity of the luminometer (Section 2.9). Co-transfection with pEZX-17 and the specific siRNA molecule (Section 2.8.2.1) was also performed. Negative controls included pEZX empty vector (pEZX-Con) as well as cells with no DNA transfected. Reactions were performed in quadruplicate.

The cell culture plates were incubated at 37°C and, after 24 hours, the transfectant was removed and replaced with complete growth medium. Cells were again incubated for 24 hours before being rinsed with PBS and lysed with 1x Passive Lysis Buffer (1xPLB). 10µl of each sample was assessed in duplicate using the Dual Reporter Luciferase Assay described in Section 2.9.

2.8.2.3 Small Molecule Transient Transfection

Small molecules (Pre-miR™ or Anti-miR™) were transfected into H295R cells. Reactions were performed in triplicate and in 6-well cell culture plates. A similar transfection protocol to those described in Section 2.8.1 and Section 2.8.2.2 was followed, with the volumes of reagents increased accordingly. For each reaction, 9µl of siPORT™ NeoFX™ Transfection Agent and 291µl of Opti-MEM® reduced serum medium were mixed and allowed to equilibrate for 10 minutes. To achieve a final concentration of 50nM, 24µl of Pre-miR™ or Anti-miR™ stock solution was mixed with 276µl of Opti-MEM®. Both mixtures were then combined, creating a final volume of 600µl per reaction, and allowed to equilibrate for 10 minutes. This volume was then dispensed into each well before adding 2.4ml of cell solution. The plate was rocked to ensure even coverage. The cell culture plates were incubated at 37°C and, after 24 hours, the transfectant was removed and replaced with 3ml serum-free medium or medium containing dibutyryl cAMP

(1mM). Cells were again incubated for 24 hours before being rinsed with PBS and lysed with 700µl of QIAzol lysis reagent in preparation for RNA extraction (Section 2.4).

2.9 Dual Reporter Luciferase Assay

The Dual Luciferase Reporter Assay (Promega, Wisconsin, U.S.A.) was used to measure Renilla and Firefly luciferase activity in cells, and performed on a Lumat LB 9507 tube luminometer (Berthold Technologies, Herts, U.K.). Injection lines were rinsed with distilled water and 70% ethanol before and after use. Reagents were thawed at room temperature then prepared by reconstituting the lyophilised luciferase assay substrate in 10ml of luciferase assay buffer II (LAR II), and by adding 200µl of Stop & Glo substrate to 10ml of Stop & Glo Buffer. The tubing of the luminometer was primed immediately prior to samples being loaded. A suitable volume (detail provided in methods section of the appropriate results chapter) was dispensed into the bottom of a 5ml round-bottomed polypropylene tube (75 x 12mm) (Sarstedt, Leicester, U.K.). The luminometer was programmed to inject 50µl of LAR II into the tube (firefly measurement) followed by 50µl of Stop & Glo reagent (renilla measurement), with a 2-second pre-measurement delay, followed by a 10-second measurement period for each reporter assay. Samples were each measured twice by this method. The ratio of firefly luciferase activity to renilla luciferase activity, as measured in Relative Light Units (RLU), was taken, controlling for transfection efficiency.

2.10 Statistical Analysis

Statistical analysis was performed using Microsoft Excel 2007, Minitab v15 and Prism 4.0 Graph Pad software. All results are expressed as mean \pm SEM (standard error of the mean) unless otherwise stated. *In vitro* experiments were performed in at least three technical replicates, on at least three independent occasions. *In vitro* results were analysed by either unpaired Student's t-test or one-sample t-test as stated. Analyses of results for multiple groups were performed by one-way analysis of variance (ANOVA). Associations of genotype with corticosteroid intermediate phenotype were assessed by the non-parametric Mann-Whitney U test. Confidence intervals of 95% were used, with a p-value of <0.05 being considered significant.

3 Characterisation of Genetic Variation at the Human *CYP17A1* Locus

3.1 Introduction

Variants within the *CYP17A1* gene have been studied for association with various disorders including PCOS, cancer and premature male baldness (Section 1.3.3.2). However, these studies have failed to define any molecular mechanism linking such variants to the development of these disorders. In 2009, two genome-wide association studies (GWAS) investigating hypertension were published linking variants in *CYP17A1* to increased systolic blood pressure (Section 1.1.3.2). One variant was located in intron 3 of the gene and the other 250,000 bp upstream of the *CYP17A1* locus. These GWAS reported both polymorphisms to be in LD with each other and therefore, it could be hypothesised that these SNPs are also in LD with other as yet unidentified functional polymorphisms. Mutations in *CYP17A1* are already known to cause a rare form of congenital adrenal hyperplasia (Section 1.3.3.1) where patients develop hypertension due to excess mineralocorticoid. The hypothesis tested in this thesis proposes that more common variations within this gene cause subtle increases in blood pressure. Such investigations require detailed knowledge of variations across this locus.

There are publically available repositories where genotyping information can be accessed e.g. Hapmap (Gibbs *et al.*, 2003) (<http://hapmap.ncbi.nlm.nih.gov/>) and the 1000 Genomes Project (Via *et al.*, 2010) (<http://www.1000genomes.org>). At the time the work presented in this chapter was conducted, the patterns of LD at the *CYP17A1* locus were not described by Hapmap in sufficient detail, and genotyping data from just four individuals was available from the 1000 Genomes Project. Therefore, in order to investigate the patterns of LD at this locus present in a Caucasian population, a detailed examination of *CYP17A1* was conducted.

3.2 Aims

The aim of this study was to analyse genetic variation across the *CYP17A1* locus, determining haplotype structure and identifying any patterns of LD that may be present. The most interesting and informative regions could then be assessed in a hypertensive population.

3.3 Methods

3.3.1 Subjects

3.3.1.1 SNP Discovery Phase

Normal volunteers living in the West of Scotland had previously been recruited to participate in the Adrenal Function Study conducted by Dr. Frances McManus at the University of Glasgow. Full details of recruitment and study protocol are described by Dr. McManus (2012). Participants were aged 18-70 at the time of recruitment, in good health and were not on any antihypertensive medication. Genomic DNA was available from 60 participants (27 males, 33 females), extracted as described in Section 2.2.1.1. Demographic characteristics are displayed below.

Demographic Characteristics	N=60 (median & IQ range)
Age (years)	51 (32-67)
Weight (kg)	70 (61-76)
SBP (mmHg)	126 (116-136)
DBP (mmHg)	77 (70-84)

3.3.1.2 Hypertensive Population

A subset of the MRC BRitish Genetics of HyperTension (BRIGHT) cohort was selected for a detailed examination of variation within the promoter region of the *CYP17A1* gene (see Section 2.2.1.2). Corticosteroid and androgen profiles were available for 511 unrelated individuals but DNA for only 232 participants could be obtained for this study. Demographic characteristics of this cohort are displayed in Table 4-2.

3.3.2 Sequencing

The entire *CYP17A1* locus was sequenced directly in each AFS subject. This encompassed a region approximately 2.4 kb upstream of the transcription start site and included all exons, introns and the 3'UTR. Sections of the locus were first amplified by PCR and verified by gel electrophoresis before sequencing. Full

details of the PCR and sequencing reactions are provided in Section 2.2 and Appendix 1.

3.3.3 Statistical Analysis

Sequencing results were visualised using SeqScape v. 2.1.1 software. Data were collated on a Microsoft Excel spreadsheet before export to Haploview v. 4.2 (Section 2.2.9). This software was used to analyse genotype frequencies, calculate genotype distribution using the Hardy Weinberg equilibrium, and to assess LD at the locus, as well as interpreting haplotype structure.

3.4 Results

The variation at *CYP17A1* was first examined by direct sequencing of the locus in a cohort of normotensive participants from the Adrenal Function Study (AFS). This stage was named the SNP Discovery Phase. After identification of potential functional polymorphisms, these were then analysed in a hypertensive population. The results from each stage are presented below.

3.4.1 SNP Discovery Phase

3.4.1.1 PCR of *CYP17A1*

The *CYP17A1* gene was amplified in several sections prior to sequencing. Each PCR was initially optimised by analysing a gradient of annealing temperatures, as outlined in Section 2.2.3. In the first instance, approximately 2.4kb of promoter region was amplified and verified by gel electrophoresis (Figure 3-1). Thereafter, numerous PCRs were performed using primer pairs (described in Appendix 1) designed to amplify individual exons, introns and the 3'UTR. Successful PCR was verified by fragment size on gel electrophoresis.

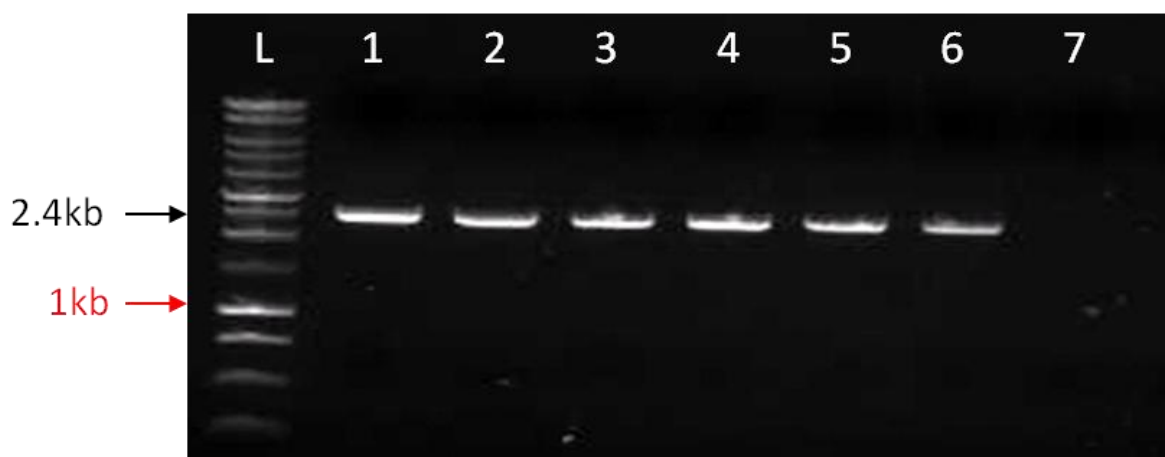


Figure 3-1 PCR fragments from 6 different AFS samples.

25ng of DNA was amplified by PCR then resolved on a 1% agarose gel. Promega 1 kb ladder was used for size determination (L). Lanes 1-6 show a single band 2.4kb in size for AFS samples 1-6, respectively. Lane 7 contains a negative control reaction, with no visible band indicating no sample contamination.

3.4.1.2 Polymorphism Identification

Sequence reads for each participant were collated using the SeqScape software enabling the entire locus to be scanned for polymorphisms. The reads were then aligned to the reference sequence, provided in Appendix 2. An example of electropherograms of the sequencing around the polymorphism at position -34 of the promoter region is shown in Figure 3-2.

A total of 36 polymorphisms were identified across the *CYP17A1* locus. The characteristics of each are described in Table 3-1. 35 were single base changes, while rs139275291 consists of a 35 bp region within intron seven which is present in the major allele but deleted from the minor allele (+/- CCATAATAAGGCTACATCCTCAGATCAGGGTCCCC). A schematic diagram of the variants' locations is provided in Figure 3-3. 14 variants were identified in the 5'UTR and 2.4kb upstream promoter region. 3 synonymous SNPs were located in exon 1, meaning that variants did not change the resulting amino acid (rs61754263: Arg21Arg; rs6162: His46His; rs6163: Ser65Ser). No variation was discovered in the other seven exons. The remaining 19 SNPs were spread across the intronic regions. No variation was found in the 3'UTR.

None of the variants departed significantly from Hardy-Weinberg equilibrium ($p < 0.001$) and were therefore eligible to be included in further analysis. The Hardy-Weinberg equilibrium is a principle which states that allele and genotype frequencies will remain constant through generations in the absence of other evolutionary influencing factors. These factors may include non-random mating, mutations and genetic drift. Genetic drift can arise through changes to allele frequencies when studying small populations, although this was not evident in the AFS cohort.

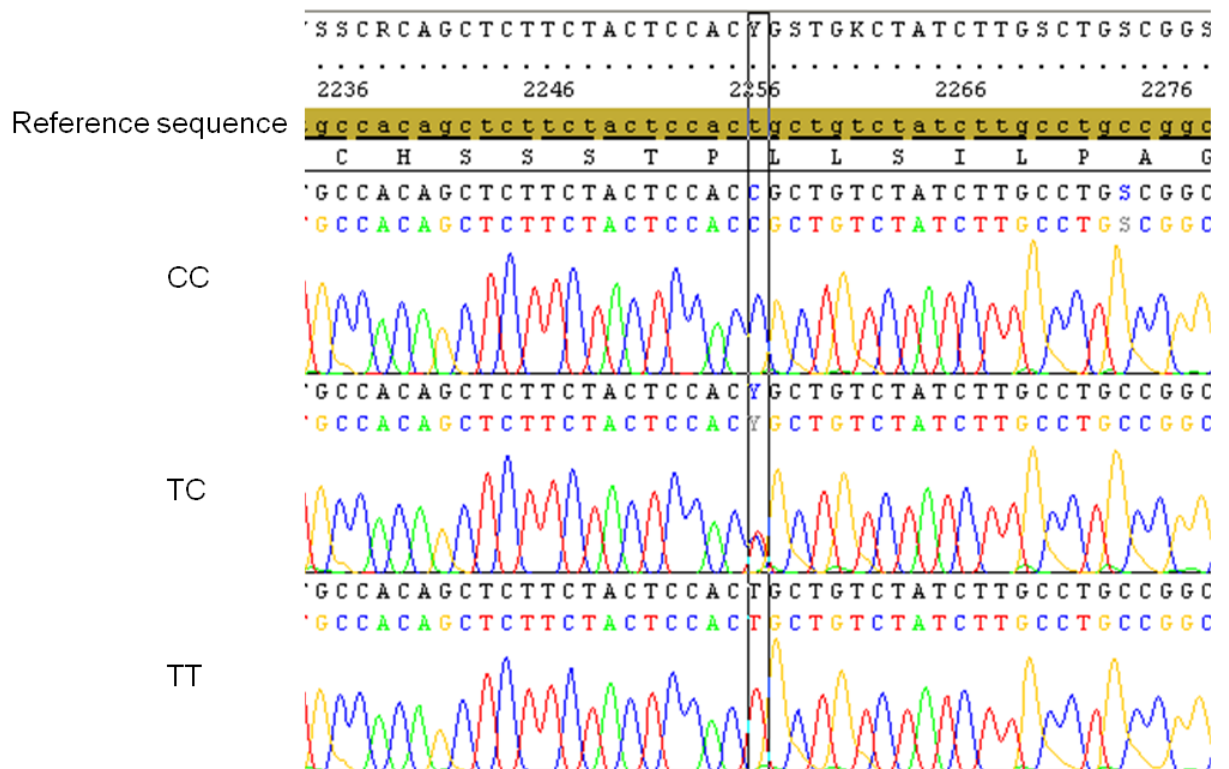


Figure 3-2 Sequence analysis of the human *CYP17A1* gene.

An example of the electropherogram reads from three different samples of the AFS cohort, one from each genotype group. This example shows the T/C SNP at position -34 in the *CYP17A1* promoter (rs743572).

Table 3-1 Characteristics of polymorphisms identified by sequencing across the human *CYP17A1* locus in subjects from the Adrenal Function Study population.

SNP: single nucleotide polymorphism; ID: Haploview identification number; Position: chromosomal location from ENSEMBL Homo sapiens version 72.37 (GRCh37); MAF: minor allele frequency; HWE: Hardy-Weinberg equilibrium p-value; % Geno: % of samples successfully genotyped.

SNP	ID	Location	Position	Alleles	MAF	HWE (p)	% Geno
rs2150927	36	-2205	10:104599323	C/T	0.306	0.0973	100
rs117574307	35	-1933	10:104599051	C/T	0.032	1.0000	100
rs138009835	34	-1877	10:104598995	C/T	0.089	1.0000	100
rs183906459	33	-1722	10:104598840	T/A	0.008	1.0000	100
rs10786714	32	-1488	10:104598606	C/G	0.210	0.1584	100
-1366	31	-1366	10:104598484	C/T	0.008	1.0000	100
rs10786713	30	-1204	10:104598322	T/C	0.306	0.2835	100
-1077	29	-1077	10:104598195	C/T	0.008	1.0000	100
rs10883784	28	-804	10:104597922	G/A	0.210	0.1584	100
rs190440742	27	-734	10:104597852	G/A	0.016	1.0000	100
-638	26	-638	10:104597756	C/T	0.016	0.0163	100
rs61752856	25	-626	10:104597744	C/T	0.016	1.0000	100
rs2486758	24	-362	10:104597480	A/G	0.242	0.9939	100
rs743572	23	-34	10:104597152	T/C	0.282	0.0973	100
rs61754263	22	Exon 1	10:104597057	G/A	0.008	1.0000	100
rs6162	21	Exon 1	10:104596981	C/T	0.315	0.1449	100
rs6163	20	Exon 1	10:104596924	G/T	0.306	0.0249	100
rs10786712	19	Intron 1	10:104596396	G/A	0.293	0.0232	93.5
rs45463800	18	Intron 1	10:104596356	G/A	0.017	1.0000	95.2
INT1+811	17	Intron 1	10:104596011	G/A	0.008	1.0000	95.2
rs3824755	16	Intron 1	10:104595849	C/G	0.052	1.0000	93.5
rs284847	15	Intron 1	10:104595828	C/T	0.068	0.4480	95.2
rs3781286	14	Intron 1	10:104595719	G/A	0.302	0.0396	93.5
rs3781287	13	Intron 1	10:104595420	A/C	0.322	0.1374	95.2
rs4919687	12	Intron 1	10:104595240	C/T	0.241	0.0247	93.5
rs743575	11	Intron 2	10:104594906	A/C	0.208	0.4270	96.8
rs1004467	10	Intron 3	10:104594507	T/C	0.083	1.0000	96.8
INT4 +599	9	Intron 4	10:104593194	G/A	0.008	1.0000	95.2
rs3740397	8	Intron 5	10:104592675	C/G	0.292	0.1196	96.8
rs4919686	7	Intron 6	10:104592249	T/G	0.220	0.0448	95.2
rs284848	6	Intron 6	10:104592125	C/T	0.212	1.0000	95.2
rs45609333	5	Intron 6	10:104591639	C/T	0.025	1.0000	95.2
rs17115100	4	Intron 6	10:104591393	C/A	0.085	1.0000	95.2
rs284849	3	Intron 7	10:104591182	C/A	0.234	0.3853	100
rs10883783	2	Intron 7	10:104591152	A/T	0.218	0.2194	100
rs139275291	1	Intron 7	10:104590871	+/-35bp	0.218	0.2194	100

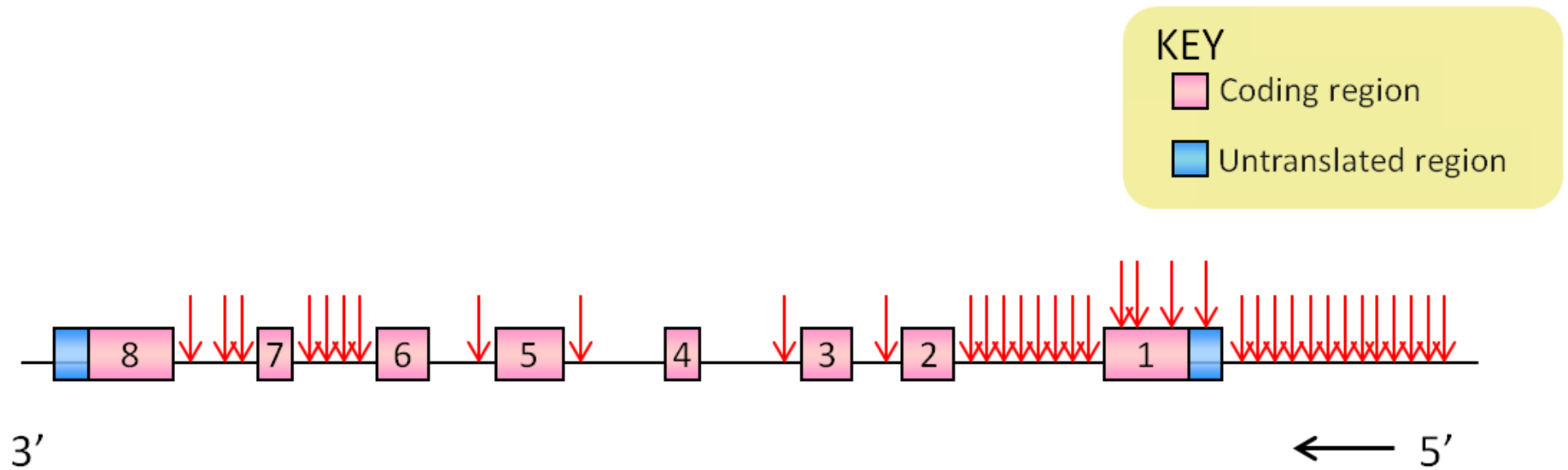


Figure 3-3 Positions of the 36 variations identified across the human *CYP17A1* locus.

Red arrows indicate positions of polymorphisms identified through direct sequencing of 62 individuals from the Adrenal Function Study.

3.4.1.3 Linkage Disequilibrium

The most informative regions across the *CYP17A1* locus were identified by generating LD plots. The simplest measure of LD is D , first proposed by Lewontin and Kojima (1960), D quantifies disequilibrium as the difference between the observed frequency of a haplotype and the expected frequency if the alleles were segregating at random. However, it is not a particularly useful measure of the strength or comparative levels of LD. The two more commonly used metrics for such measurements are D' and r^2 . $D'=1$ (100%) denotes complete LD, whereby the SNPs in question are not separated by recombination. $r^2=1$ denotes perfect LD whereby, in addition to the absence of a recombination event between the two markers, the alleles of each SNP also have the same frequencies. The complex equations to generate both D' and r^2 values have been previously explained by Mueller (2004).

Sequencing data were converted to the appropriate file format for analysis by Haploview v4.2 software. In the first instance, an LD plot was generated with all sequencing data (Figure 3-4). Regions in red are indicative of a D' value close to or equal to 1, denoting a strong association between the SNPs, scaling down to white, which represents a D' close or equal to 0 i.e. little or no association between SNPs. Lilac squares indicate insufficient data to interpret the LD between two markers. The plot in Figure 3-4 has a considerable percentage of lilac colour and, since the hypothesis of this thesis was to assess the association of common genetic variation with hypertension, the SNPs with a MAF of <0.05 (5%) were removed and the corresponding LD plot examined (Figure 3-5). This figure shows association between many of the common polymorphisms.

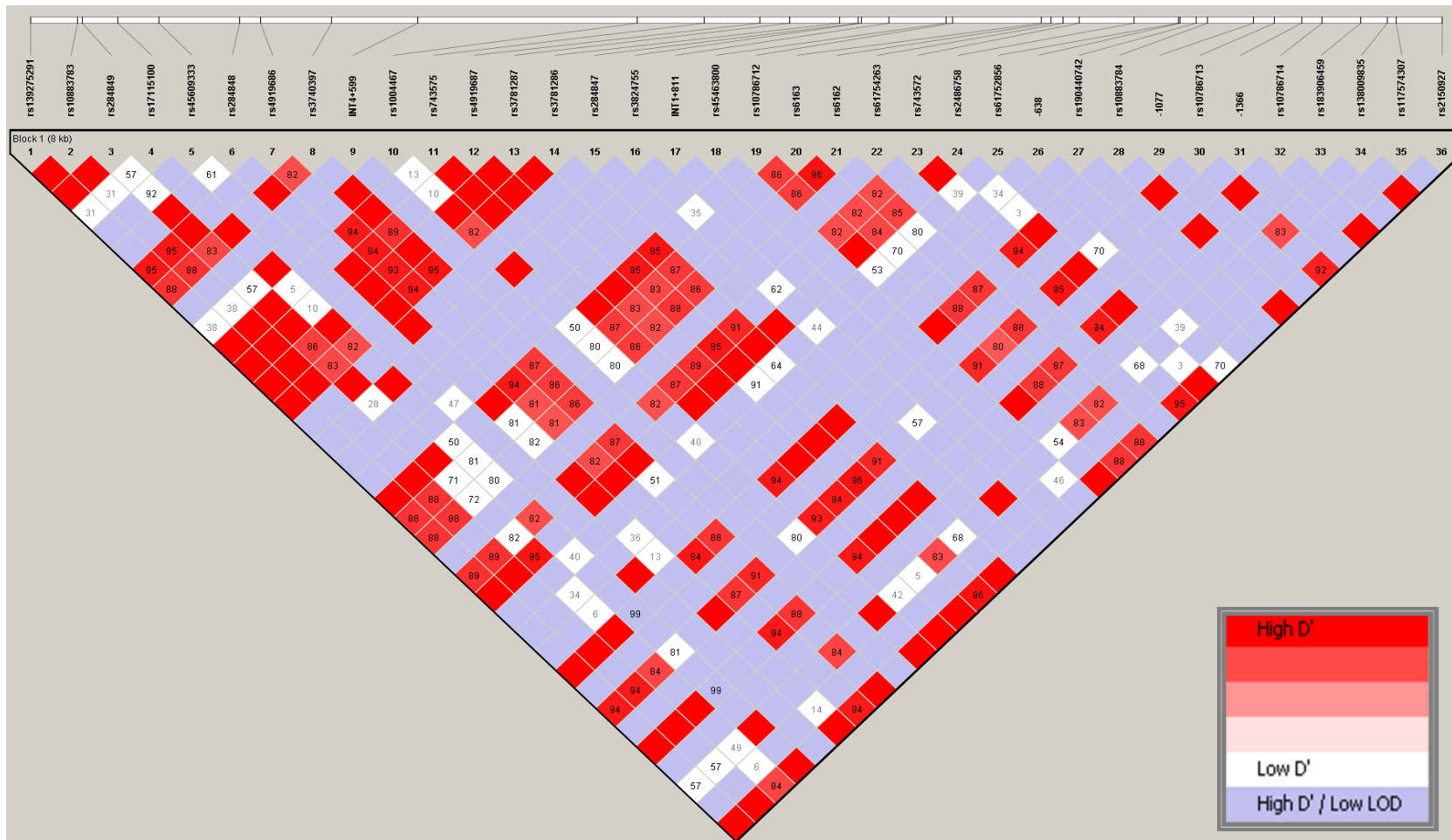


Figure 3-4 Linkage disequilibrium plot of all polymorphisms identified in the human *CYP17A1* gene.

The LD plot of all 36 variants found across the human *CYP17A1* gene in the Adrenal Function Study cohort. The LD plot displays D' values (%) for each pair of SNPs in the box at the intersection of the diagonals from each SNP.

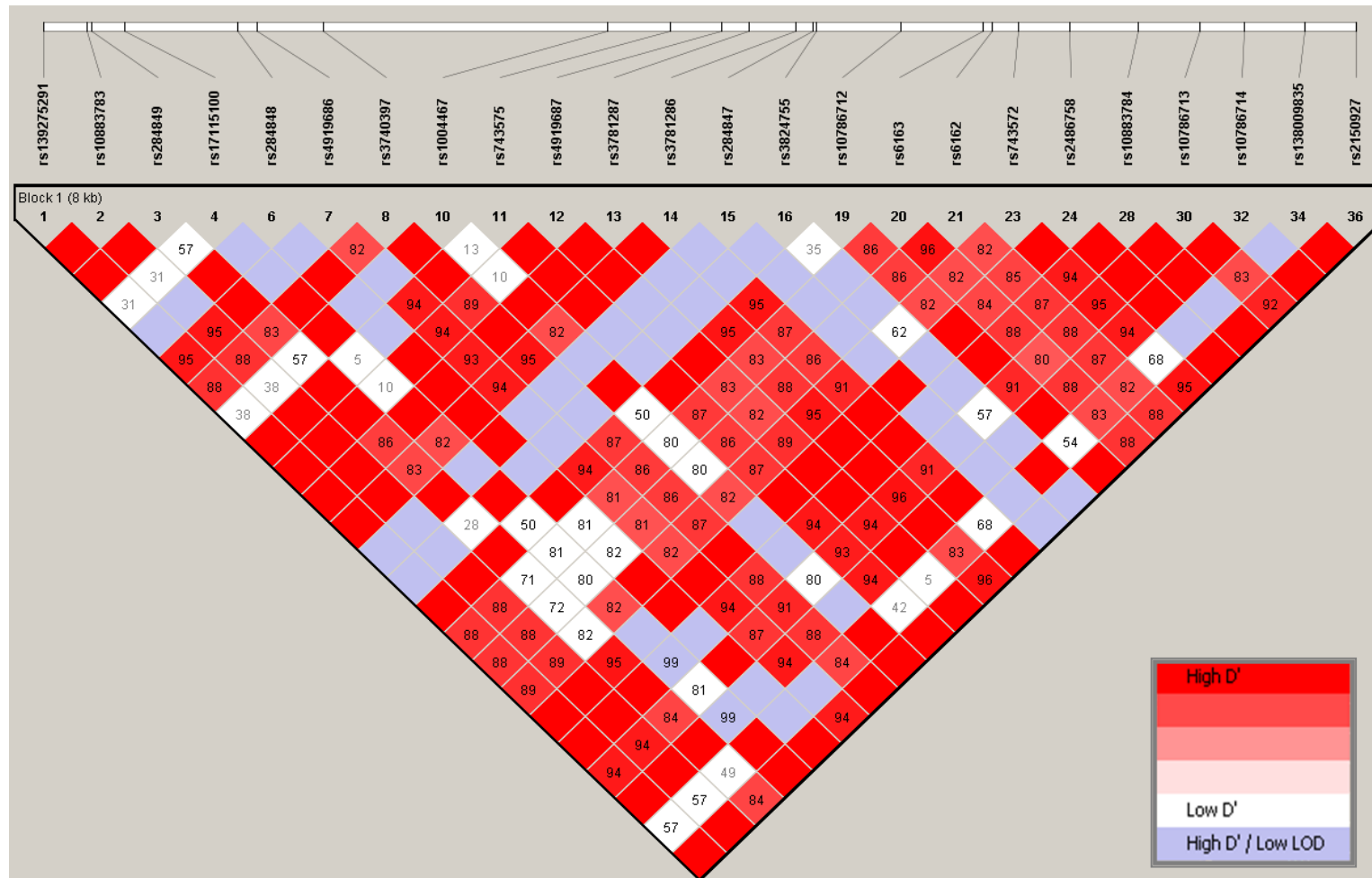


Figure 3-5 Linkage disequilibrium plot of polymorphisms with minor allele frequency >0.05 identified in the human *CYP17A1* gene.
 The LD plot of the variants found across the human *CYP17A1* gene in the Adrenal Function Study cohort with MAF >0.05. The LD plot displays D' values (%) for each pair of SNPs in the box at the intersection of the diagonals from each SNP.

Once the assessment of association across the entire *CYP17A1* locus was complete, a detailed examination of the SNPs present in the promoter region was undertaken. Since variations found within exons and introns were not predicted to alter amino acids and resulting protein structure, regulatory control of gene expression was the focus of further inspection. The LD plot for all variations found in the 2.4kb of the promoter region generated with the D' method is displayed in Figure 3-6. A similar plot containing r^2 values is shown in Figure 3-7. Similar to the LD plots generated with D' values, colour intensity denotes the strength of association in the r^2 LD plots. It can be seen from both measurements that approximately half of the variation found in this region is uninformative. Therefore the polymorphisms with $MAF < 0.05$ were removed and D' (Figure 3-8) and r^2 (Figure 3-9) values reassessed. Examination of these plots reveals an association between six of the seven polymorphisms. Data for the unassociated rs138009835 was therefore removed and the LD plots in Figure 3-10 and Figure 3-11 generated. Figure 3-10 shows D' values and, as the region is entirely red in colour, it can be concluded that high LD exists across these polymorphisms. The plot displaying r^2 values also shows association between these SNPs although the LD is weaker, particularly for rs2486758. This was expected as the measurement of r^2 is a more stringent test than D' as it also assesses allele frequencies.

Around the same time that the work in this chapter was undertaken, a research article was published which analysed the association between SNPs at this region of chromosome 10 (Gomez-Rubio *et al.*, 2010). This paper reported three intronic SNPs in *CYP17A1* (rs3824755, rs1004467, rs17115100) to be part of a larger cluster of SNPs in LD across this region. Closer inspection of the LD plots generated from the AFS cohort found the same three SNPs to be in high LD with a variant at position -1877 upstream from the transcription start site. This SNP has since been officially designated as rs138009835. D' and r^2 value plots of these four polymorphisms are displayed in Figure 3-12 and Figure 3-13, respectively. Interestingly, rs138009835 was the SNP removed from analysis in Figures 3-10 and 3-11 due to lack of association with the other six SNPs in the promoter region with $MAF > 0.05$. This indicates the presence of two unrelated blocks of polymorphisms in high LD across this locus.

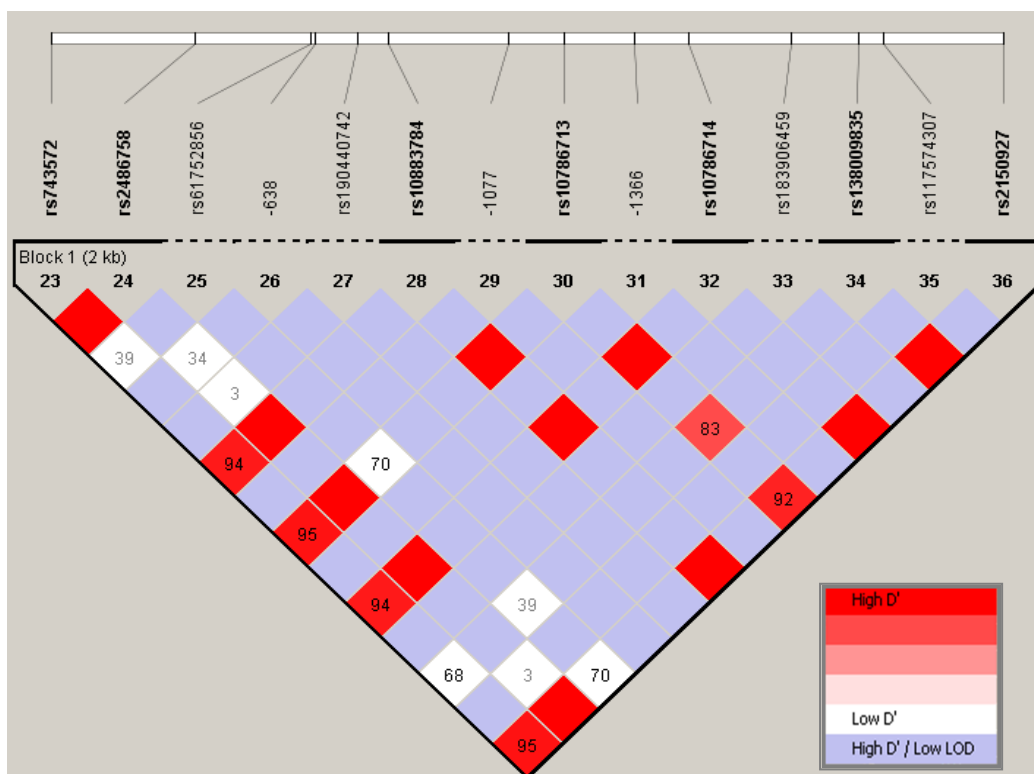


Figure 3-6 Linkage disequilibrium plot of *CYP17A1* promoter polymorphisms (D' values). LD plot of all 14 variants found across the 2.4 kb of human *CYP17A1* promoter region in the Adrenal Function Study cohort. The LD plot displays D' values (%) for each pair of SNPs in the box at the intersection of the diagonals from each SNP.

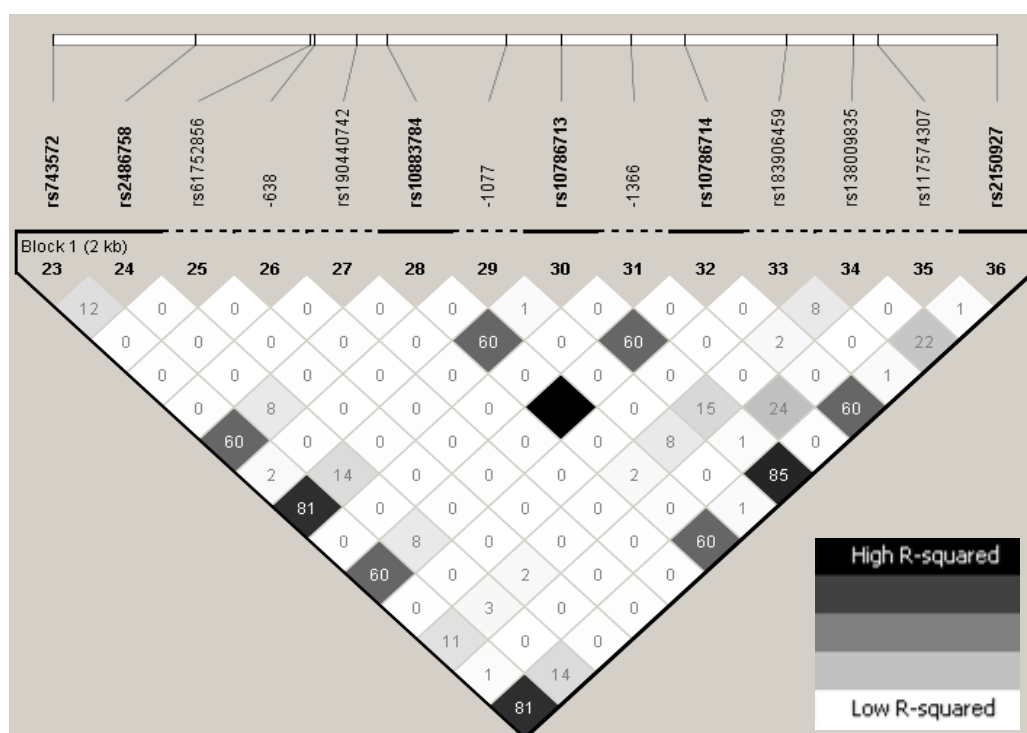


Figure 3-7 Linkage disequilibrium plot of *CYP17A1* promoter polymorphisms (r^2 values). LD plot of all 14 variants found across the 2.4 kb of human *CYP17A1* promoter region in the Adrenal Function study cohort. The LD plot displays r^2 values (%) for each pair of SNPs in the box at the intersection of the diagonals from each SNP.

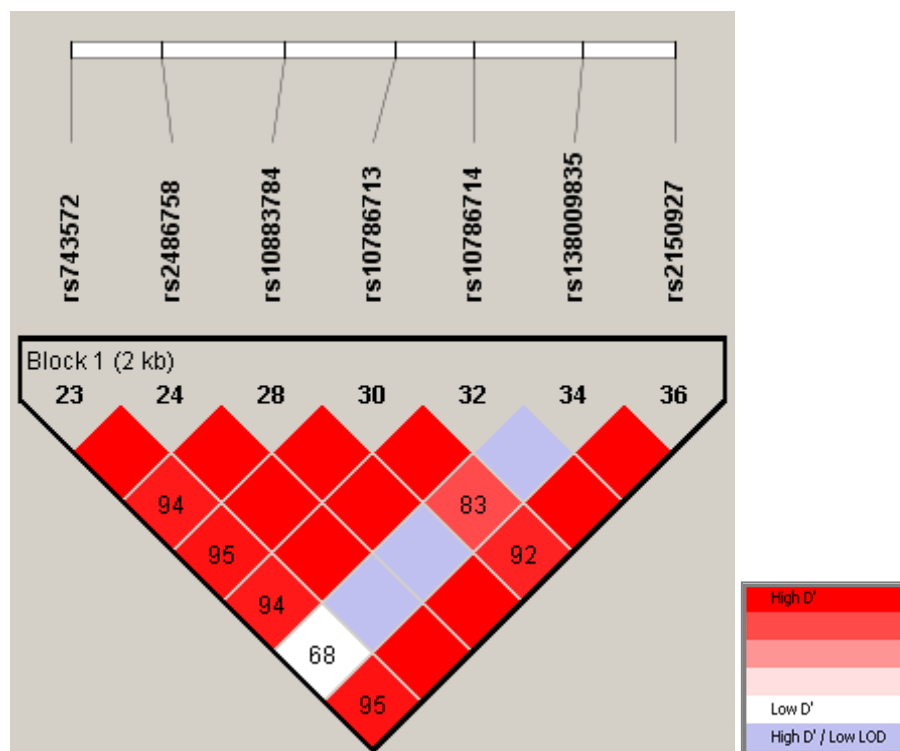


Figure 3-8 Linkage disequilibrium plot of *CYP17A1* promoter polymorphisms with MAF >0.05 (D' values).

LD plot of variants with minor allele frequency <0.05 found across the 2.4kb of human *CYP17A1* promoter region in the Adrenal Function Study cohort. The LD plot displays D' values (%) for each pair of SNPs in the box at the intersection of the diagonals from each SNP.

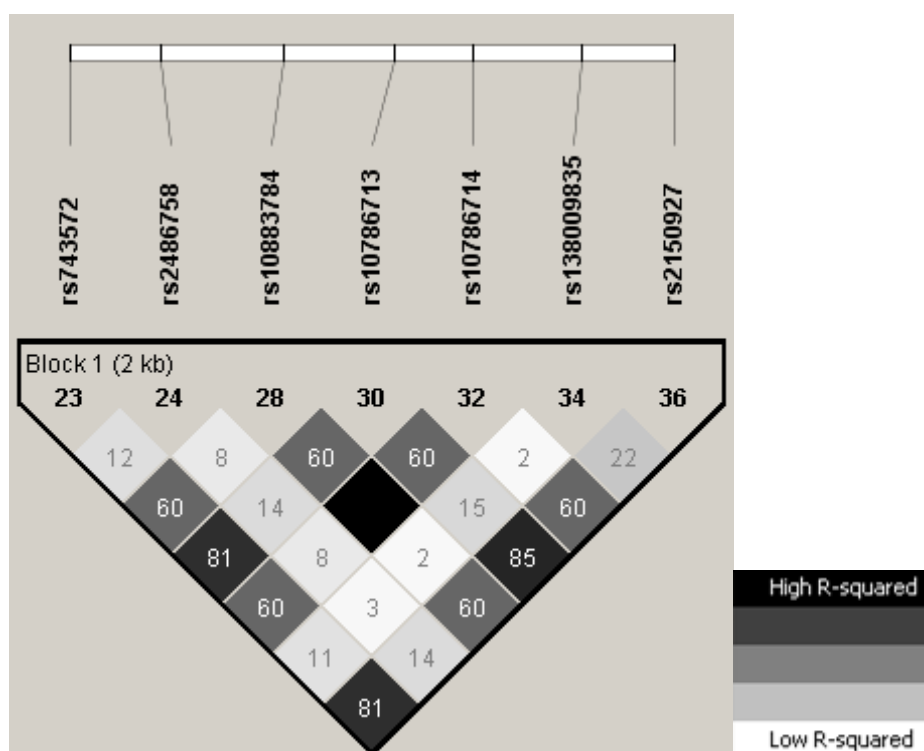


Figure 3-9 Linkage disequilibrium plot of *CYP17A1* promoter polymorphisms with MAF >0.05 (r^2 values).

LD plot of variants with minor allele frequency <0.05 found across the 2.4kb of human *CYP17A1* promoter region in the Adrenal Function Study cohort. The LD plot displays r^2 values (%) for each pair of SNPs in the box at the intersection of the diagonals from each SNP.

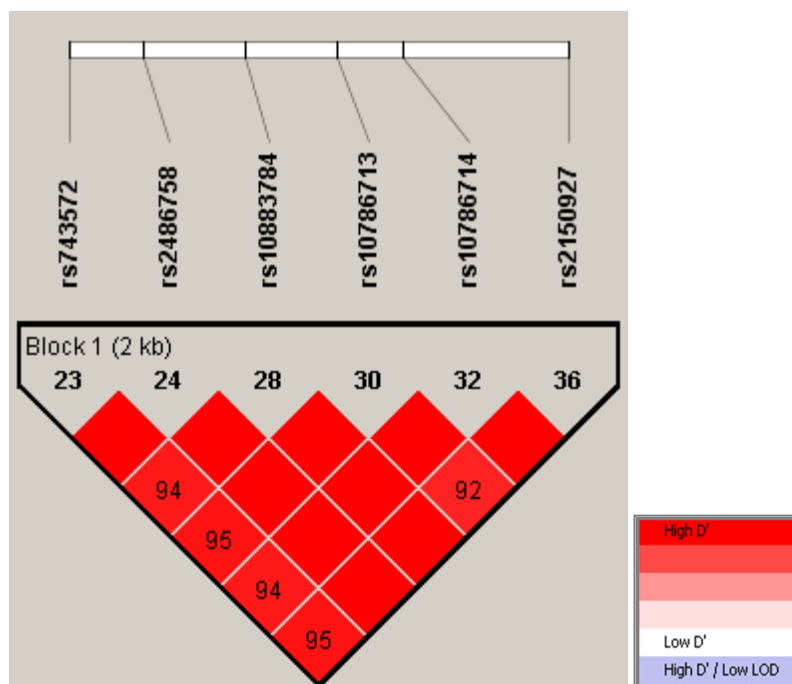


Figure 3-10 Linkage disequilibrium plot of six *CYP17A1* promoter polymorphisms (D' values).

LD plot of six variants in high LD found across the 2.4kb of human *CYP17A1* promoter region in the Adrenal Function Study cohort. The LD plot displays D' values (%) for each pair of SNPs in the box at the intersection of the diagonals from each SNP.

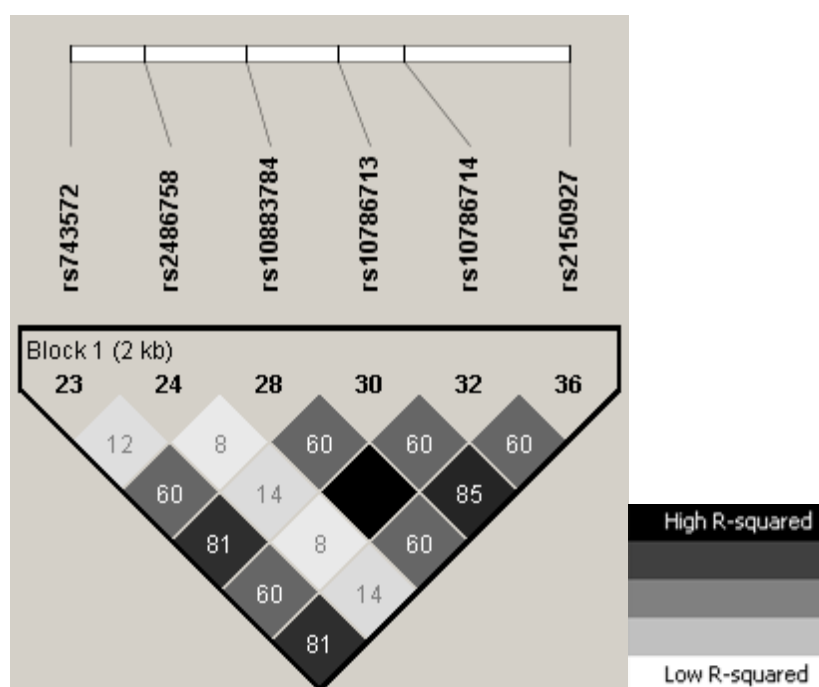


Figure 3-11 Linkage disequilibrium plot of six *CYP17A1* promoter polymorphisms (r^2 values).

LD plot of six variants in high LD found across the 2.4kb of human *CYP17A1* promoter region in the Adrenal Function Study cohort. The LD plot displays r^2 values (%) for each pair of SNPs in the box at the intersection of the diagonals from each SNP.

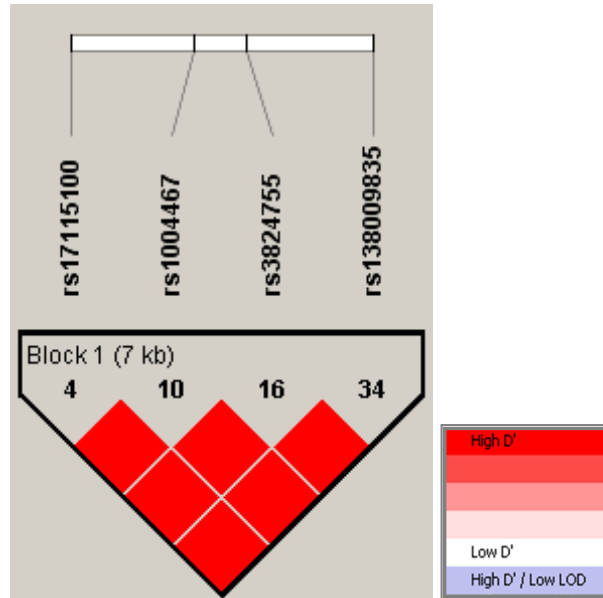


Figure 3-12 Linkage disequilibrium plot of four variants found across the *CYP17A1* locus (D' values).

LD plot of four variants found across the human *CYP17A1* locus in high LD in the Adrenal Function Study cohort. The LD plot displays D' values (%) for each pair of SNPs in the box at the intersection of the diagonals from each SNP.

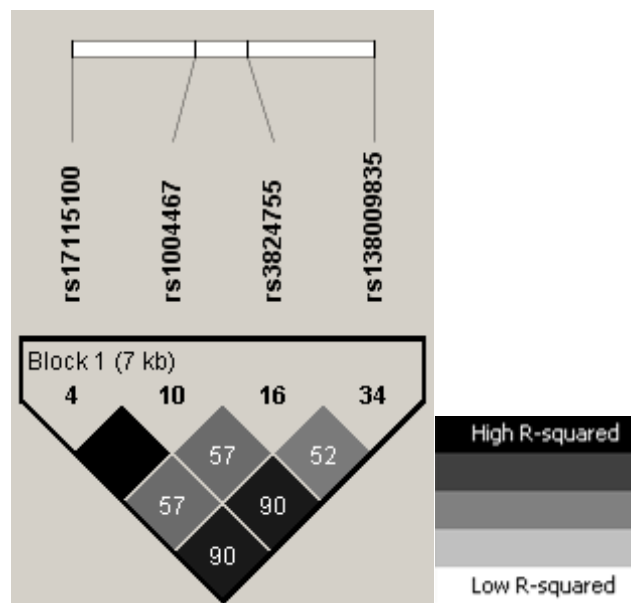


Figure 3-13 Linkage disequilibrium plot of four variants found across the *CYP17A1* locus (r^2 values).

LD plot of four variants found across the human *CYP17A1* locus in the Adrenal Function Study cohort. The LD plot displays r^2 values (%) for each pair of SNPs in the box at the intersection of the diagonals from each SNP.

3.4.1.4 Haplotype Analysis

As there is significant LD across the *CYP17A1* locus, it is possible to generate haplotypes, i.e. a combination of alleles that are inherited together. Section 3.4.1.3 identified two interesting unrelated blocks of SNPs in LD across the locus, the first encompassing six polymorphisms located within a 2.4kb region immediately upstream of the transcription start site (LD Block 1), and the second with four variants, one in the promoter and three located intronically (LD Block 2). Haploview v4.2 software generates haplotypes on the basis of inputted genotype data.

The six haplotypes generated from LD Block 1 polymorphisms (Figure 3-14) cover 97.7% of the normotensive AFS population. Haplotypes 1-4 can be considered common (i.e. >5%). Haplotype 1 (44.4%) and Haplotype 2 (22.6%) are the most frequent and therefore it is not surprising that they mostly include the major form of each SNP. In fact, each haplotype varies only by the allele at position -362 (rs2486758) which had lower r^2 values than the other five polymorphisms when LD was assessed (Figure 3-11). Haplotype 3 contains mostly minor allele forms and is present in 20.2% of individuals. Haplotype 4 consists of a combination of major and minor alleles and is present in 7.3% of the AFS population.

The three haplotypes generated from LD Block 2 polymorphisms (Figure 3-15) cover 99.1% of the normotensive AFS population. The most common haplotype is present in 90.8% of individuals, with the major allele present at each SNP. 5% of individuals have the minor allele at each SNP, and only 3.3% have a combination of major and minor alleles.

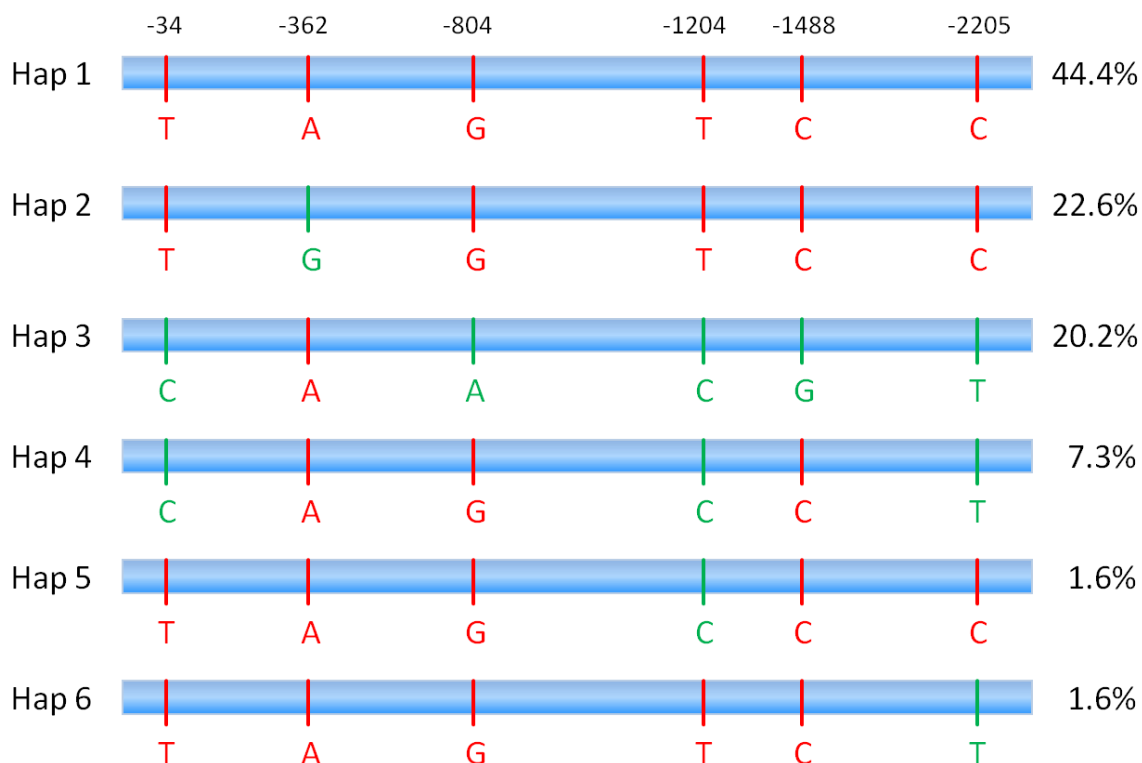


Figure 3-14 Schematic representation of haplotypes generated from LD Block 1 polymorphisms.

Frequencies of each haplotype within the Adrenal Function Study cohort are indicated on the right. Major alleles are depicted in red and minor alleles in green.

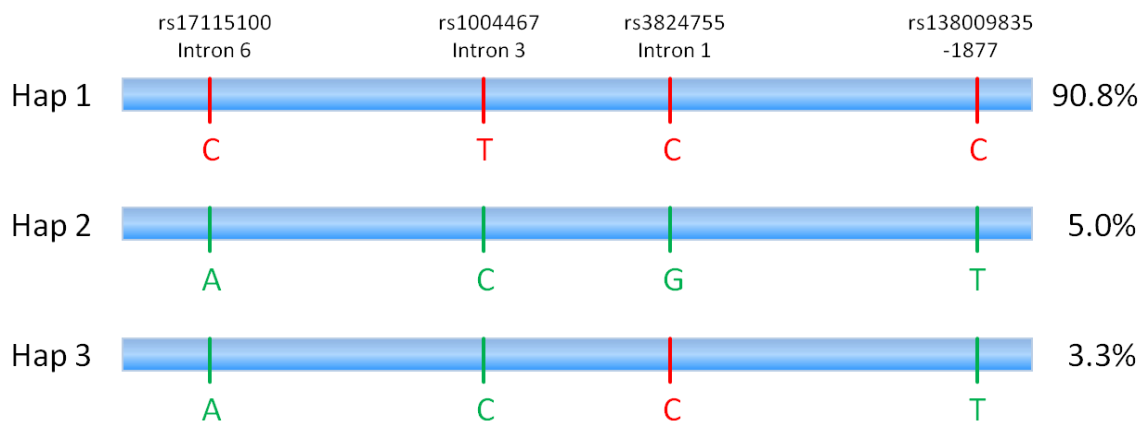


Figure 3-15 Schematic representation of haplotypes generated from LD Block 2 polymorphisms.

Frequencies of each haplotype within the Adrenal Function Study cohort are indicated on the right. Major alleles are depicted in red and minor alleles in green.

3.4.2 Hypertensive Population

The SNP Discovery Phase identified common polymorphisms in a small cohort of normotensive Caucasians. An interesting variant was detected -1877 bases upstream of the transcription start site (rs138009835), which is in high LD with variants implicated in recent GWAS (Levy *et al.*, 2009; Newton-Cheh *et al.*, 2009). Furthermore, an additional unrelated block of SNPs in high LD was also found in the promoter region. Variation in the promoter has the potential to affect transcriptional regulation of the *CYP17A1* gene through altered transcription factor binding. Therefore this region was selected for inspection within a larger cohort of 232 unrelated hypertensive individuals drawn from the BRIGHT cohort for whom both DNA and steroid profiles were available.

3.4.2.1 Promoter Region Variation in the *CYP17A1* Gene

2.4kb of *CYP17A1* promoter region was amplified by PCR (with fragment size verified by gel electrophoresis) using identical methods to those in the SNP Discovery Phase. Subsequent sequencing enabled genotyping each SNP of interest. Characteristics of this genotyping are provided in Table 3-2. Although the DNA was extracted approximately ten years prior to this analysis, the percentage of successful genotyping at each SNP was consistently high. Furthermore, none of the variants departed significantly from Hardy-Weinberg equilibrium ($p < 0.001$) and were therefore eligible to be included in further analysis.

Table 3-2 Characteristics of polymorphisms genotyped across the human *CYP17A1* locus in a subset of the BRIGHT cohort.

SNP: single nucleotide polymorphism; ID: Haploview identification number; Position: chromosomal location from ENSEMBL Homo sapiens version 72.37 (GRCh37); MAF: minor allele frequency; HWE: Hardy-Weinberg equilibrium p-value; % Geno: % of samples successfully genotyped.

SNP	ID	Location	Position	Alleles	MAF	HWE (p)	% Geno
rs2150927	7	-2205	10:104599323	C/T	0.413	0.9276	99.1
rs138009835	6	-1877	10:104598995	C/T	0.109	0.9940	100
rs10786714	5	-1488	10:104598606	C/G	0.304	0.7485	99.6
rs10786713	4	-1204	10:104598322	T/C	0.417	0.9121	99.6
rs10883784	3	-804	10:104597922	G/A	0.304	0.6991	100
rs2486758	2	-362	10:104597480	A/G	0.183	1.0000	96.9
rs743572	1	-34	10:104597152	T/C	0.420	0.8284	96.9

3.4.2.2 Linkage Disequilibrium and Haplotype Analysis

Following sequencing, genotype data from all 232 hypertensive individuals were collated and a LD plot of D' values generated (Figure 3-16). The red squares indicate a D' value close or equal to 1 meaning that the seven common SNPs identified in the AFS cohort show a strong association in this hypertensive population. The lilac square signifies a lack of sufficient information to determine the association between the SNPs at positions -362 and -1877, probably due to the low minor allele frequency of the -1877 variant.

An LD plot of r^2 values was also generated and is displayed in Figure 3-17. Similar to the plots produced from sequencing of the AFS cohort, the r^2 values here typically show weaker association between the SNPs. Most of the SNPs here exhibit fairly high LD although those at -362 and -1877 exhibit weak association with the other polymorphisms.

These data were used to derive haplotypes. Since the D' values indicated association between the -1877 SNP and the other polymorphisms, which was not the case in the AFS cohort, it was not removed from this analysis. Four possible haplotypes were found to be present, accounting for 99.5% of this hypertensive population (Figure 3-18). Haplotype 1 contains the major alleles at each site and is present in 39.7% of this population. Haplotypes 2, 3 and 4 contain a combination of major and minor alleles and are present in 18.5%, 30.4% and 10.9% of the population, respectively.

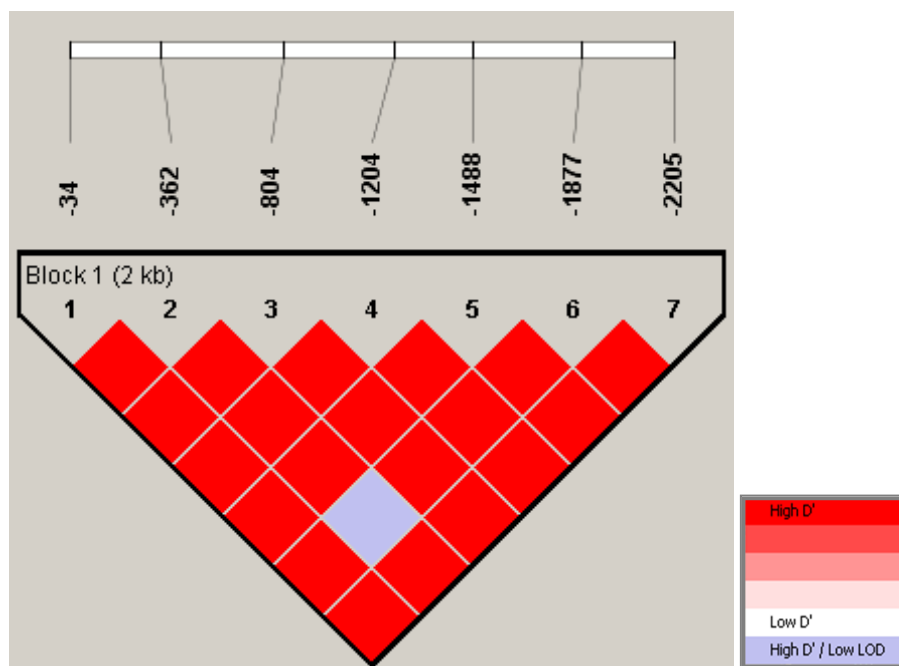


Figure 3-16 Linkage disequilibrium plot of common promoter polymorphisms genotyped in a subset of the BRIGHT cohort (D' values).

LD plot of variants genotyped within 2.4kb of the human *CYP17A1* promoter region in a subset of the BRIGHT cohort. The LD plot displays D' values (%) for each pair of SNPs in the box at the intersection of the diagonals from each SNP.

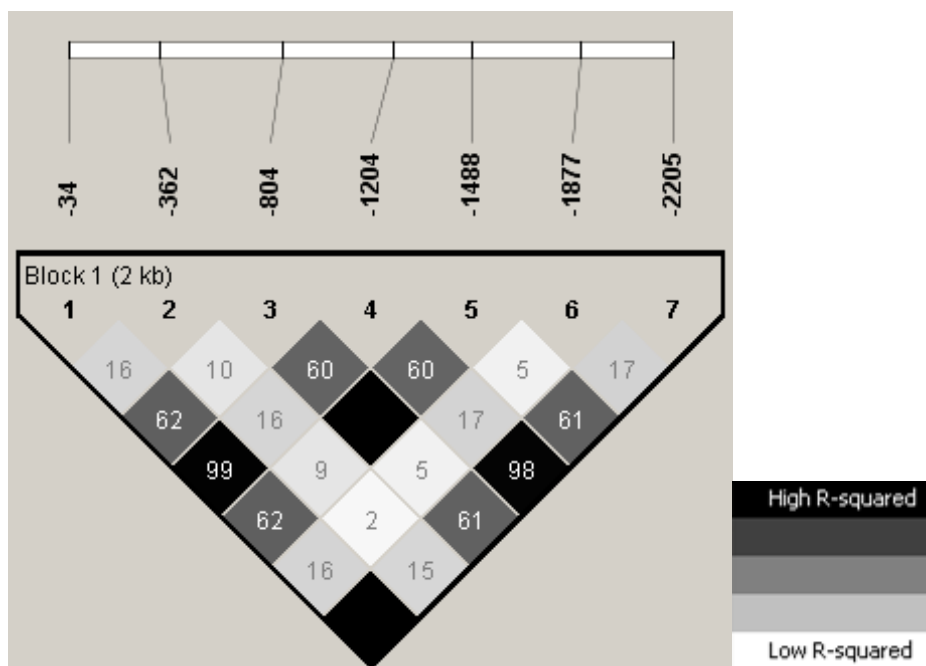


Figure 3-17 Linkage disequilibrium plot of common promoter polymorphisms genotyped in a subset of the BRIGHT cohort (r^2 values).

LD plot of variants genotyped within 2.4kb of the human *CYP17A1* promoter region in a subset of the BRIGHT cohort. The LD plot displays r^2 values (%) for each pair of SNPs in the box at the intersection of the diagonals from each SNP.

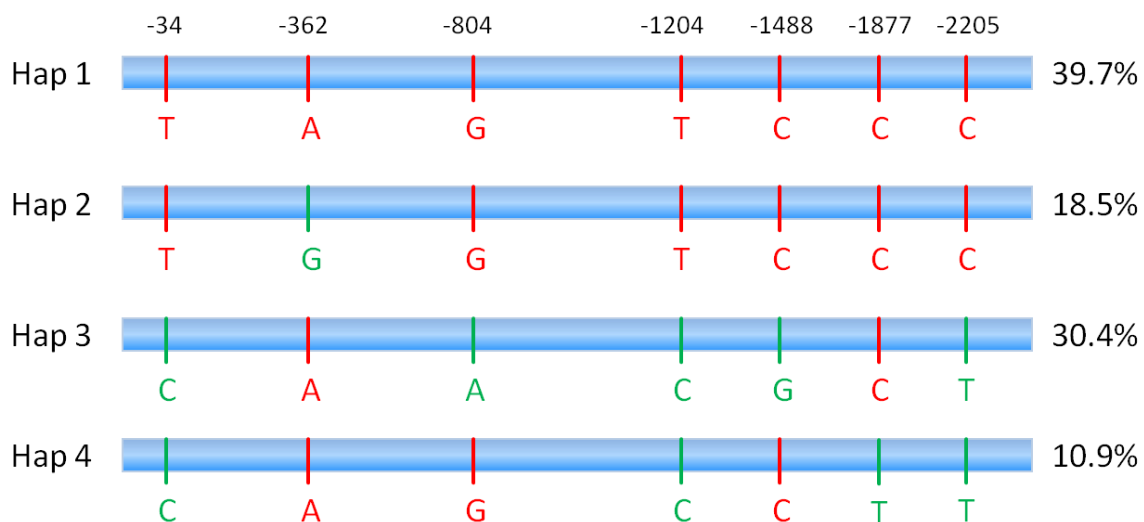


Figure 3-18 Schematic representation of haplotypes present in 2.4kb of the *CYP17A1* promoter region in a subset of the BRIGHT cohort.

Frequencies of each haplotype within the subset of the BRIGHT cohort are indicated on the right. The major allele are depicted in red, minor alleles in green.

3.5 Discussion

This study has provided a detailed examination of sequence variation across the *CYP17A1* locus. The SNP discovery phase was conducted in a group of 62 unrelated normotensive individuals who had previously participated in the Adrenal Function Study. The size of this cohort was judged sufficient for the detection of common variants, as previous studies with sample sizes of 23 and 24 had provided >99% chance of detecting SNPs with a frequency of 5% and >87% chance for SNPs of 1% frequency (Crawford *et al.*, 2004).

AFS DNA quality was good and enabled successful call rates of >93% for each SNP across the locus. Three synonymous SNPs were reported in exon 1, therefore resulting in no change to the corresponding amino acids. Several further polymorphisms were located within introns. These could potentially alter splicing of the *CYP17A1* transcript and affect protein structure. Although none were located directly within splice sites at the exon/intron junctions, they may disrupt the intronic branch site, which facilitates intronic splicing (Madhani and Guthrie 1994). It would be possible to examine the functional effects on splicing *in vitro* using a minigene system, whereby the complete exonic and intronic regions are cloned into a vector and transfected into a suitable cell line. Total RNA could then be isolated and qRT-PCR performed to compare wild-type and mutant constructs.

No variation was found in the 3'UTR. Polymorphisms in this region may affect RNA stability, thus the lack of variation may signify the importance of this region in the translation of RNA to protein. Variants in this region may also affect post-transcriptional regulation through altered binding of miRNAs. Little is currently known about the regulation of *CYP17A1* expression by miRNA and is explored in Chapter 6.

A total of 14 polymorphisms were identified in the 2.4kb region immediately upstream of the transcription start site. Half of these had a minor allele frequency above 5% and were therefore considered to be common genetic variant. The SNPs identified in this region were of considerable interest as previous research on other steroidogenic genes has shown alteration in transcriptional activity to occur in an allele-dependent manner (Section 1.3.3.2).

It is entirely possible that any of the 14 SNPs could alter the transcriptional regulation of the gene; however, in keeping with the hypothesis of this thesis, the 7 common variants were prioritised for further examination. Association between the SNPs was assessed through the generation of LD plots. LD is a useful concept in the analysis of SNPs and statistical genetics. LD should remain relatively stable assuming breeding occurs within those with similar ancestries; however LD between alleles may decline over generations due to recombination and mutation events. Both D' and r^2 are measurements of LD and both are displayed in the LD plots presented above. $D'=1$ indicates complete linkage disequilibrium and is useful for assessing historical recombination at the locus. For the data presented here, D' values were high for the SNPs comprising both LD Block 1 and LD Block 2 in the *CYP17A1* promoter region, suggesting little historical recombination between these loci. In contrast, r^2 is a useful concept to measure the correlation between alleles i.e. when $r^2=1$, the allele present at one SNP will perfectly predict the allele at the other SNP. These values are of particular use when selecting 'tag' SNPs. A 'tag' SNP is a polymorphism selected for its ability to represent a particular haplotype depending on the allele present. This enables high-throughput and efficient genotyping of a locus on the basis of a single SNP and is commonly used in large population studies. Selection of a 'tag' SNP requires detailed information on LD present at the locus. The r^2 values of associations comparing each SNP to rs2486758 (-362) indicate weak LD (Figure 3-11). This contradicts the high D' values seen in Figure 3-10, and is likely to be due to differences in the frequencies of major and minor alleles relative to the other SNPs. It therefore may not be the most suitable variant for the prediction of alleles present elsewhere in the haplotype.

The SNP Discovery Phase of this study has identified two distinct blocks of SNPs which exhibit high LD. LD Block 1 contains six SNPs located in the promoter region and LD Block 2 contains one SNP in the promoter region and three in the introns. When the genotypes at all seven promoter SNPs were examined in the hypertensive population, D' values suggested strong association between all the variants (Figure 3-16). This was surprising as the polymorphism at position -1877 (rs138009835) is clearly unrelated to the others in the smaller normotensive cohort. It is not appropriate to compare fully the results between the normotensive and hypertensive cohorts as this would require a specific case-

control matched study. However, examination of r^2 values suggests very weak association between -1877 and the other six SNPs (Figure 3-17). An observation from the haplotypes derived from this cohort is that the minor T allele at -1877 is present only in Haplotype 4, which occurs in 10.9% of this population. Since this minor allele is so rare compared to those of the other six SNPs (Table 3-2), it is plausible to suggest that the presence of the major C allele in approximately 90% of subjects is the reason for the high D' values. Interestingly, a study investigating the association of genotype with PCOS reported similar findings. Four 'tag' SNPs were selected for genotyping in the case-control PCOS cohort, which included rs1004467 and rs743572 (Chua *et al.*, 2012). Variant rs1004467 is located in intron 3 and is part of LD Block 2 while rs743572 is located at position -34 and is in LD Block 1. The authors report $D'=1$ between these two SNPs, although the minor allele frequencies are 0.096 and 0.420 respectively. Again, the presence of the major allele at rs1004467 nearly 90% of the time may allow it to appear that rs1004467 is in the same LD block as the others. It may be useful to genotype the BRIGHT hypertensive cohort for the three intronic LD Block 2 SNPs and generate LD plots. In addition, genotyping a suitable case-control study would enable allele, genotype and haplotype frequencies to be compared and perhaps identify a particular risk haplotype for the development of hypertension.

Recent GWAS has identified two SNPs around the *CYP17A1* locus in which the major allele raises systolic blood pressure (see Section 1.1.3.2). One is located within intron 3 of *CYP17A1*, the other approximately 250 kb upstream, although the two are in LD. A follow-up study performed an additional conditional regression analysis with both SNPs in the one model and suggested that neither variant was likely to be the causal SNP driving the association with hypertension (Liu *et al.*, 2011). It is possible that the causal variant lies within any of the six genes spanned by this particular LD block, although *CYP17A1* is the most obvious candidate for blood pressure regulation (Section 1.1.3.2). Therefore, since polymorphisms in the promoter region have the potential to alter expression through changes in transcriptional properties, this region of *CYP17A1* was considered the ideal place to search for the causal variant(s).

3.6 Conclusions

This study has examined the genetic variation within the *CYP17A1* gene in great detail and identified a range of common and less frequent polymorphisms. Patterns of linkage disequilibrium were established and common haplotypes derived. An interesting polymorphism at position -1877 (rs138009835) has been identified which has high D' and r^2 values in relation to rs1004467, a SNP implicated in recent hypertension GWAS. It also associates with six other promoter SNPs in a hypertensive population. These seven promoter variations will be investigated further to establish any phenotypic consequences for each allele (Chapter 4), as well as their functional effects *in vitro* (Chapter 5).

**4 Investigation of the Phenotypic Consequences
of *CYP17A1* Promoter Region Polymorphisms
on Corticosteroid Production in a Hypertensive
Population.**

4.1 Introduction

The adrenal cortex synthesises and secretes a number of biologically active steroid hormones or corticosteroids that are crucial to the efficient function of many of the body's systems (Section 1.2.1.1). Therefore, the ability to monitor the level of adrenocortical activity and to locate precisely any clinically relevant malfunction is essential. The corticosteroids are synthesised from cholesterol via a small number of pathways, each comprising a series of consecutive enzyme-catalysed reactions (Figure 1-7). In addition to the end products, a proportion of intermediate compounds are also secreted. Changes in the efficiency of any constituent enzyme will alter the pattern of secretion, with possible metabolic and pathological consequences. The location, size, structure and vascularisation of the adrenal gland make direct and specific access to the tissue or to venous effluent blood difficult in patients and ethically unacceptable in normal human subjects. Detailed direct monitoring of function is therefore rarely possible; information on the internal status of the adrenal cortex must be obtained 'externally'. There are two principal approaches. Firstly, short term changes in the rate of secretion of each compound are reflected in their plasma concentration. Secondly, each of these circulating compounds is metabolised, principally in the liver, to one or more unique metabolites and excreted as conjugates in the urine (Table 1-6). Again, the relative concentrations of these urinary metabolites reflect those of their parent compounds within the adrenal cortex and can act as surrogate markers of activity. Analysis of an accurate 24-hour collection provides an average activity over that period and is ideal for comparing effects of genetic variation on steroid secretion. In addition to measuring the excretion rates of the principal end products, careful scrutiny of the overall pattern of metabolites may reveal variations in the efficiency of the individual enzyme-catalysed reactions; as efficiency decreases, enzyme kinetics dictate that, to maintain optimum conversion, the concentration of precursor must increase. Thus, for example, a relatively inefficient 11 β -hydroxylase will require higher levels of its precursor, 11-deoxycortisol, in order to maintain cortisol levels and this will be reflected in the ratio of 11-deoxycortisol to cortisol metabolites in the urine. This principle can also be applied to the more complex 17 α -hydroxylase/lyase enzyme, which catalyses two key transformations (Figure 1-8). Thus, altered efficiency will affect not only the

relative balance of the 17-hydroxy and 17-deoxy pathways but also the relationship between these and adrenal androgen synthesis. A decrease in the efficiency of the 17 α -hydroxylase/lyase enzyme would be expected to result in lower androgen and cortisol levels, with accumulation of the precursors pregnenolone and progesterone and an accentuation of the 17-deoxycorticosteroid pathway producing 11-deoxycorticosterone and corticosterone. This has been reported in case studies of CAH due to 17 α -hydroxylase deficiency (Section 1.3.3.1). Alternatively, a more efficient 17 α -hydroxylase/lyase enzyme would be expected to have an inverse effect, tending to increase the production of cortisol and androgens but the negative feedback loop (Figure 1-6) between ACTH and cortisol ensures maintenance of normal end product levels. Nevertheless, the ratios of levels of intermediates to end products would still be affected.

The use of a specific *CYP17A1* inhibitor has recently been introduced clinically as an effective treatment for men with castration-resistant prostate cancer. The consequent effects on the steroidogenic profile of these individuals provides an extreme example of what one might expect as a consequence of altered transcriptional activity arising from allelic changes in the *CYP17A1* promoter. In the Phase I clinical trial of the *CYP17A1* inhibitor abiraterone acetate, secondary mineralocorticoid excess (hypertension, hypokalaemia and fluid retention) was a common side effect (Attard *et al.*, 2008). Inhibition of both the 17 α -hydroxylase and the 17,20 lyase enzymatic functions reduces cortisol and androgen production (Figure 4-1). In the absence of cortisol, ACTH drive is increased and results in increased levels of 11-deoxycortisosterone and corticosterone, hence mineralocorticoid excess. In clinical trials, administration of synthetic glucocorticoids (e.g. prednisone or dexamethasone) concurrently with abiraterone acetate significantly reduced these side effects (Danila *et al.*, 2010; Fizazi *et al.*, 2012). It is therefore reasonable to hypothesise that less severe changes to the expression of *CYP17A1*, possibly as a result of single base changes in the promoter region, may result in smaller but similar changes to patterns of corticosteroid production.

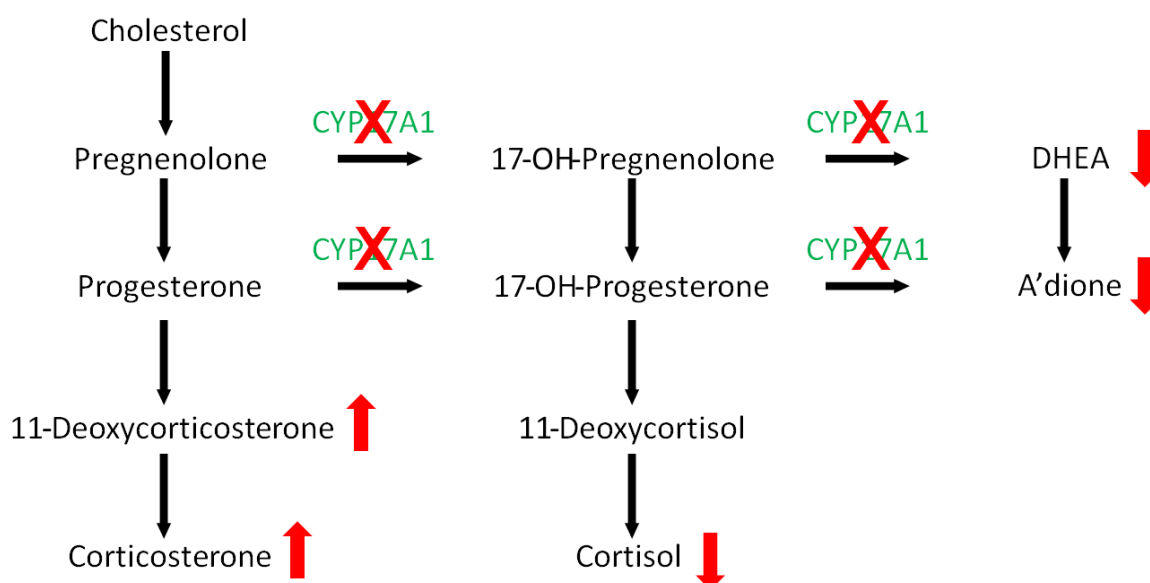


Figure 4-1 Physiological consequences of treatment with a selective *CYP17A1* inhibitor e.g. abiraterone acetate.

Data from a comprehensive urinary steroid analysis of a subset of 511 unrelated hypertensive patients from the BRIGHT cohort presented an ideal opportunity to compare differences in *CYP17A1* genotype with corticosteroid intermediate phenotypes. Chapter 3 describes the genotyping of seven common polymorphisms located in the promoter region of *CYP17A1*. These variants have the potential to affect enzymatic function through altered gene transcription. Genomic DNA was available for only 232 individuals in this BRIGHT subset.

4.2 Aims

This study aimed to examine the influence of genotype on the efficiency of the 17 α -hydroxylase/17,20 lyase enzyme. The association of specific variants in the promoter region of *CYP17A1* with corticosteroid metabolite excretion rates and their inter-relationships in a hypertensive cohort was assessed.

4.3 Methods

4.3.1 Study Subjects

Details of recruitment of subjects for the BRIGHT population have been outlined in Section 2.2.1.2. In brief, hypertensive subjects with a mean pre-treatment blood pressure of >145/95 mmHg were recruited from primary care. All had

onset of hypertension before 60 years of age. Subjects underwent medical assessment and details of sex, height, weight and anthropometric measurements such as waist-hip ratio (WHR) and body mass index (BMI) were recorded. Those with BMI >30 were excluded from the study. Caucasian and British ancestry was confirmed for all participants of the BRIGHT study to grand-parental level. Ethical approval for the study was granted by the local ethics committees of the participating centres and fully informed written consent of the subjects was obtained.

4.3.2 Urinary Corticosteroid Metabolite Measurements

For the present investigation, urinary corticosteroid metabolite measurements were available for a random group of 511 unrelated subjects. Precise details of measurement by gas chromatography/mass spectrometry (GC/MS) have been described previously (Barr *et al.*, 2007; Freel *et al.*, 2007). Excretion rate data were analysed for the 232 members of this BRIGHT subgroup that had been successfully genotyped (Chapter 3).

4.3.3 Data Analysis

Demographic and steroid excretion data were not normally distributed and were therefore analysed by non-parametric methods (Mann-Whitney tests) unless otherwise stated. Comparisons of genotype with steroid excretion were conducted by adopting the dominant model whereby heterozygotes and minor allele homozygotes are grouped and compared with major allele homozygotes. Statistical analyses were conducted using Minitab software v15.

4.4 Results

Genomic DNA and steroid excretion data were available for a subset of the BRIGHT cohort comprising 232 hypertensive individuals. Sequencing of the *CYP17A1* promoter region was performed on the genomic DNA of these individuals and genotypes at the seven common polymorphic locations recorded. (These data have been presented in Chapter 3.) Table 4-1 summarises the number of individuals of each genotype at each SNP of interest. In order to assess the association of genotype with steroid excretion, it would be desirable to compare the major homozygote group with the minor homozygote group, but

the number of individuals with the minor homozygote genotype at positions -1877 and -362 was too low to permit this. Therefore the dominant model approach was used. Heterozygotes and minor allele homozygotes were grouped together and compared with major allele homozygotes. The merits and assumptions of this model are discussed in Section 4-5.

Table 4-1 Number of individuals with each genotype at the seven *CYP17A1* promoter SNPs.

SNP	Major Homozygotes	Heterozygotes	Minor Homozygotes
-34 (rs743572)	72	109	37
-362 (rs2486758)	145	66	7
-804 (rs10883784)	107	99	19
-1204 (rs10786713)	75	111	38
-1488 (rs10786714)	107	98	19
-1877 (rs138009835)	178	45	2
-2205 (rs2150927)	76	110	37

4.4.1 Demographics

Blood pressure and other relevant demographic characteristics of the BRIGHT cohort sub-group are displayed in Table 4-2. Age, blood pressure and BMI were not significantly different between males and females although, as expected, waist-hip ratio was significantly higher in males ($p < 0.001$).

Similar demographic characteristics of the groups stratified according to their genotype at each SNP are shown in Table 4-3 to Table 4-9. The numbers of males and females within each genotype group were approximately equal. Age, blood pressure, BMI and WHR were not statistically different between the genotyped groups.

Table 4-2 Demographic data on the BRIGHT study subgroup.

Demographic data (median and interquartile ranges) of the BRIGHT study subgroup. Demographic characteristics of males and females were compared by the non-parametric Mann-Whitney test. SBP: systolic blood pressure; DBP: diastolic blood pressure; BMI: body mass index; WHR: waist-hip ratio.

	All Subjects N=232	Males N=106	Females N=126	p-value (Male vs. Female)
Age (Years)	63 (56-69)	63 (56-68)	64 (56-69)	0.47
SBP (mm/Hg)	157 (153-190)	157 (151.25-187)	181.5 (153-191)	0.07
DBP (mm/Hg)	103 (98-110)	103 (98-110)	102 (98-109.5)	0.43
BMI (kg/m ²)	27 (25-30)	28 (25-30.75)	27 (25-30)	0.26
WHR	0.88 (0.81-0.93)	0.93 (0.90-0.97)	0.82 (0.78-0.86)	<0.001

Table 4-3 Demographic data on the BRIGHT study subgroup stratified by -34 genotype.

Demographic data (median and interquartile ranges) of the BRIGHT study subgroup stratified by -34 genotype. Demographic characteristics were compared by the non-parametric Mann-Whitney test using the dominant model. SBP: systolic blood pressure; DBP: diastolic blood pressure; BMI: body mass index; WHR: waist-hip ratio.

	-34 TT N=72	-34 CT N=109	-34 CC N=37	p-value (TT vs. CT+CC)
Age (Years)	63 (58-67)	62 (55-70)	64 (58-68)	0.99
SBP (mm/Hg)	157 (153-187)	183 (153-190)	155 (152-191)	0.53
DBP (mm/Hg)	102 (98-107)	103 (99-110)	103 (98-110)	0.51
BMI (kg/m ²)	27 (24-30)	27.5 (25-30)	27 (25-31)	0.47
WHR	0.86 (0.83-0.92)	0.88 (0.81-0.93)	0.91 (0.83-0.94)	0.49

Table 4-4 Demographic data on the BRIGHT study subgroup stratified by -362 genotype.

Demographic data (median and interquartile ranges) of the BRIGHT study subgroup stratified by -362 genotype. Demographic characteristics were compared by the non-parametric Mann-Whitney test using the dominant model. SBP: systolic blood pressure; DBP: diastolic blood pressure; BMI: body mass index; WHR: waist-hip ratio.

	-362 AA N=145	-362 AG N=66	-362 GG N=7	p-value AA vs. AG+GG
Age (Years)	63 (56-67.25)	63 (56-70)	63 (60.5-65)	0.52
SBP (mm/Hg)	157 (153-190)	181.5 (152-190)	186 (169-189.5)	0.42
DBP (mm/Hg)	103 (99-108)	103 (98-110.75)	99 (98-103)	0.94
BMI (kg/m ²)	27 (24-30)	27 (25-29)	30 (27-30)	0.81
WHR	0.89 (0.81-0.93)	0.89 (0.81-0.93)	0.79 (0.76-0.85)	0.44

Table 4-5 Demographic data on the BRIGHT study subgroup stratified by -804 genotype.

Demographic data (median and interquartile ranges) of the BRIGHT study subgroup stratified by -804 genotype. Demographic characteristics were compared by the non-parametric Mann-Whitney test using the dominant model. SBP: systolic blood pressure; DBP: diastolic blood pressure; BMI: body mass index; WHR: waist-hip ratio.

	-804 GG N=107	-804 GA N=99	-804 AA N=19	p-value GG vs. GA+AA
Age (Years)	63.5 (58.25-68)	62 (54.5-70)	63 (60.5-67)	0.43
SBP (mm/Hg)	157 (153-190)	157 (153-190)	153 (152-186.5)	0.76
DBP (mm/Hg)	103 (98-108)	103 (98-110)	102 (98-110)	0.97
BMI (kg/m ²)	27 (24-30)	27 (25-30)	28 (26-31)	0.38
WHR	0.86 (0.80-0.92)	0.88 (0.81-0.93)	0.92 (0.89-0.94)	0.30

Table 4-6 Demographic data on the BRIGHT study subgroup stratified by -1204 genotype.

Demographic data (median and interquartile ranges) of the BRIGHT study subgroup stratified by -1204 genotype. Demographic characteristics were compared by the non-parametric Mann-Whitney test using the dominant model. SBP: systolic blood pressure; DBP: diastolic blood pressure; BMI: body mass index; WHR: waist-hip ratio.

	-1204 TT N=75	-1204 TC N=111	-1204 CC N=38	p-value TT vs. TC+CC
Age (Years)	63 (58-67)	63 (55-70)	64.5 (58.5-68)	0.94
SBP (mm/Hg)	157 (153-187)	183 (153-190)	156 (152-191)	0.76
DBP (mm/Hg)	102 (98-107)	103 (99-110)	103 (98.25-109)	0.58
BMI (kg/m ²)	27 (24-29.75)	28 (25-30)	27 (24.25-30.75)	0.36
WHR	0.86 (0.81-0.91)	0.88 (0.81-0.93)	0.91 (0.82-0.94)	0.34

Table 4-7 Demographic data on the BRIGHT study subgroup stratified by -1488 genotype.

Demographic data (median and interquartile ranges) of the BRIGHT study subgroup stratified by -1488 genotype. Demographic characteristics were compared by the non-parametric Mann-Whitney test using the dominant model. SBP: systolic blood pressure; DBP: diastolic blood pressure; BMI: body mass index; WHR: waist-hip ratio.

	-1488 CC N=107	-1488 CG N=98	-1488 GG N=19	p-value CC vs. CG+GG
Age (Years)	63.5 (58.25-68)	62.5 (55-70)	63 (60.5-67)	0.49
SBP (mm/Hg)	157 (153-190)	169 (153-190)	153 (152-186.5)	0.81
DBP (mm/Hg)	103 (98-108)	103 (98-110)	102(98-110)	0.98
BMI (kg/m ²)	27 (24-30)	27 (25-30)	28 (26-31)	0.39
WHR	0.86 (0.80-0.92)	0.88 (0.81-0.93)	0.92 (0.89-0.94)	0.26

Table 4-8 Demographic data on the BRIGHT study subgroup stratified by -1877 genotype.

Demographic data (median and interquartile ranges) of the BRIGHT study subgroup stratified by -1877 genotype. Demographic characteristics were compared by the non-parametric Mann-Whitney test using the dominant model. SBP: systolic blood pressure; DBP: diastolic blood pressure; BMI: body mass index; WHR: waist-hip ratio.

	-1877 CC N=178	-1877 CT N=45	-1877 TT N=2	p-value CC vs. CT+TT
Age (Years)	63 (56-68)	65 (58-70)	67 (66-68)	0.29
SBP (mm/Hg)	157 (153-190)	183 (153-197)	156 (155.5-156.5)	0.61
DBP (mm/Hg)	102.5 (98-110)	103 (100-110)	106 (103-109)	0.72
BMI (kg/m ²)	27 (25-30)	27 (24-30)	25.5 (25-26)	0.51
WHR	0.88 (0.81-0.93)	0.87 (0.79-0.92)	0.99 (0.96-1.01)	0.66

Table 4-9 Demographic data on the BRIGHT study subgroup stratified by -2205 genotype.

Demographic data (median and interquartile ranges) of the BRIGHT study subgroup stratified by -2205 genotype. Demographic characteristics were compared by the non-parametric Mann-Whitney test using the dominant model. SBP: systolic blood pressure; DBP: diastolic blood pressure; BMI: body mass index; WHR: waist-hip ratio.

	-2205 CC N=76	-2205 CT N=110	-2205 TT N=37	p-value CC vs. CT+TT
Age (Years)	63 (58-67)	63 (55-70)	64 (58-68)	0.94
SBP (mm/Hg)	157 (153-187)	182 (153-190)	155 (152-191)	0.90
DBP (mm/Hg)	102.5 (98-107)	103 (99-110)	103 (98-110)	0.64
BMI (kg/m ²)	27 (24-30)	28 (25-30)	27 (25-31)	0.42
WHR	0.86 (0.81-0.91)	0.88 (0.80-0.93)	0.91 (0.83-0.94)	0.30

4.4.2 Association of Genotype with Urinary Corticosteroid Metabolite Excretion Rates and Patterns

The *CYP17A1* gene is expressed in the zona fasciculata and zona reticularis; the excretion rates of major urinary corticosteroid metabolites derived from products of these regions in the BRIGHT study subgroup are listed in Table 4-10. Corticosterone, cortisol and androgen metabolite excretion rates were significantly less in females than in males ($p < 0.001$).

Spearman correlation coefficients representing the relationships between the major urinary corticosteroid metabolite excretion rates are displayed in Figure 4-2 to Figure 4-4. These results reflect a common regulatory factor: ACTH. There was a strong correlation between metabolite excretion rates of total corticosterone and total cortisol ($r = 0.7035$, $p < 0.0001$), total corticosterone and total androgen excretion rates ($r = 0.5464$, $p < 0.0001$) and total cortisol and total androgens ($r = 0.6569$, $p < 0.0001$). These relationships were also analysed separately for males and females because gender-dependent effects were obvious from Table 4-10. Positive correlations were seen in both sexes for all three relationships, although the correlation between total cortisol and total androgens was stronger in males ($r = 0.7267$, $p < 0.0001$) than in females ($r = 0.4974$, $p < 0.0001$).

Table 4-10 Urinary corticosteroid excretion rates of the BRIGHT study subgroup.

Urinary corticosteroid excretion rates (median and interquartile ranges) of the BRIGHT study subgroup. Metabolite excretion of males and females were compared by the non-parametric Mann-Whitney test. THB: tetrahydrocorticosterone; aTHB: allotetrahydrocorticosterone; THA: tetrahydro-11-dehydrocorticosterone; THF: tetrahydrocortisol; aTHF: allotetrahydrocortisol; THE: tetrahydrocortisone; DHEA: dehydroepiandrosterone; Aetio: aetiocholanolone; Andro: androsterone.

Urinary Steroid Metabolite ($\mu\text{g}/24\text{h}$)	All Subjects N=232	Males N=106	Females N=126	p-value (Male vs. Female)
Corticosterone metabolites (Total B: THB + aTHB + THA)	103 (61-188)	140 (79-228)	86.5 (54-156)	<0.001
Cortisol metabolites (Total F: THF + aTHF + THE)	1467 (759-2559)	2081 (1130-3526)	1118 (661-1989)	<0.001
Androgen metabolites (Total Androgens: DHEA + Aetio + Andro)	613 (322-1227)	1008 (503-1852)	447 (225-815)	<0.001

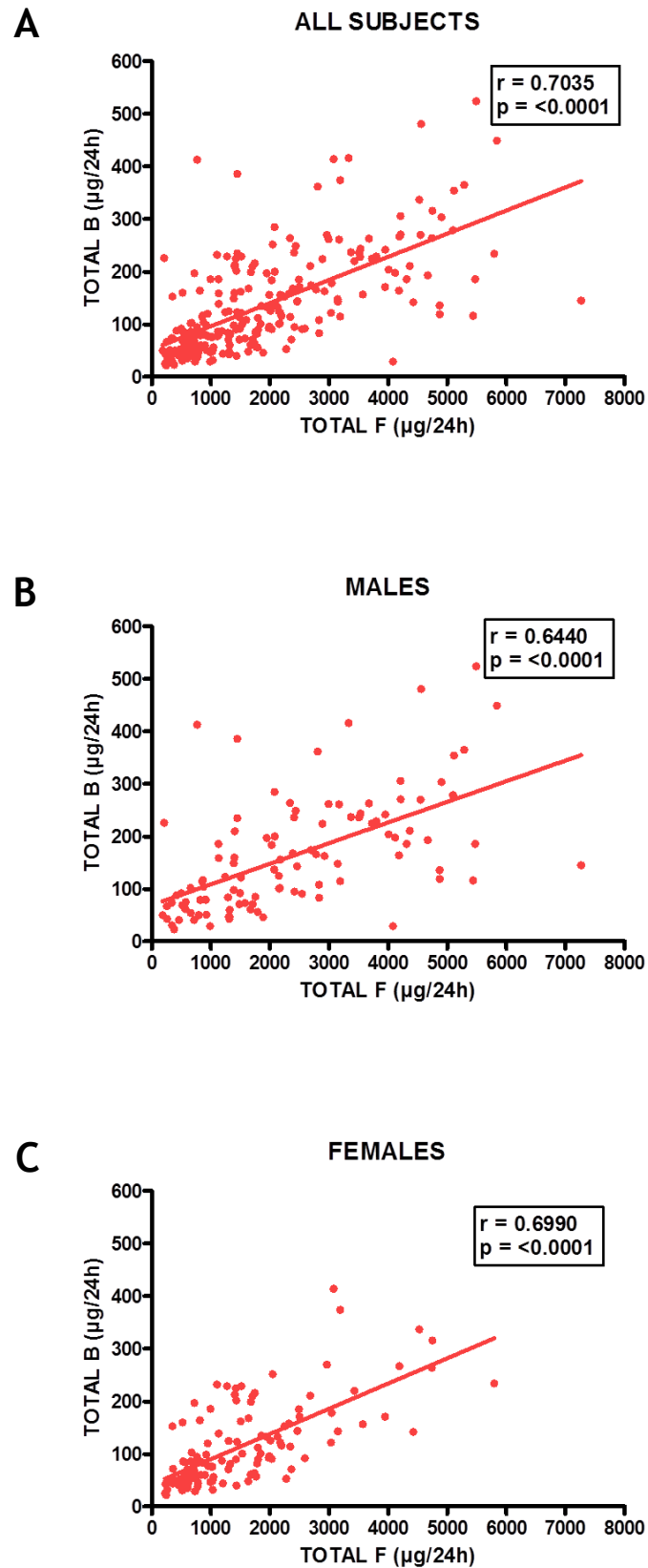


Figure 4-2 Correlation between excretion rates of total cortisol and total corticosterone metabolites.

Correlation between excretion of total cortisol (THF + (a)THF + THE) urinary metabolites and total corticosterone (THB + aTHB + THA) urinary metabolites in A) all subjects B) males only and C) females only. Spearman correlation coefficients are displayed.

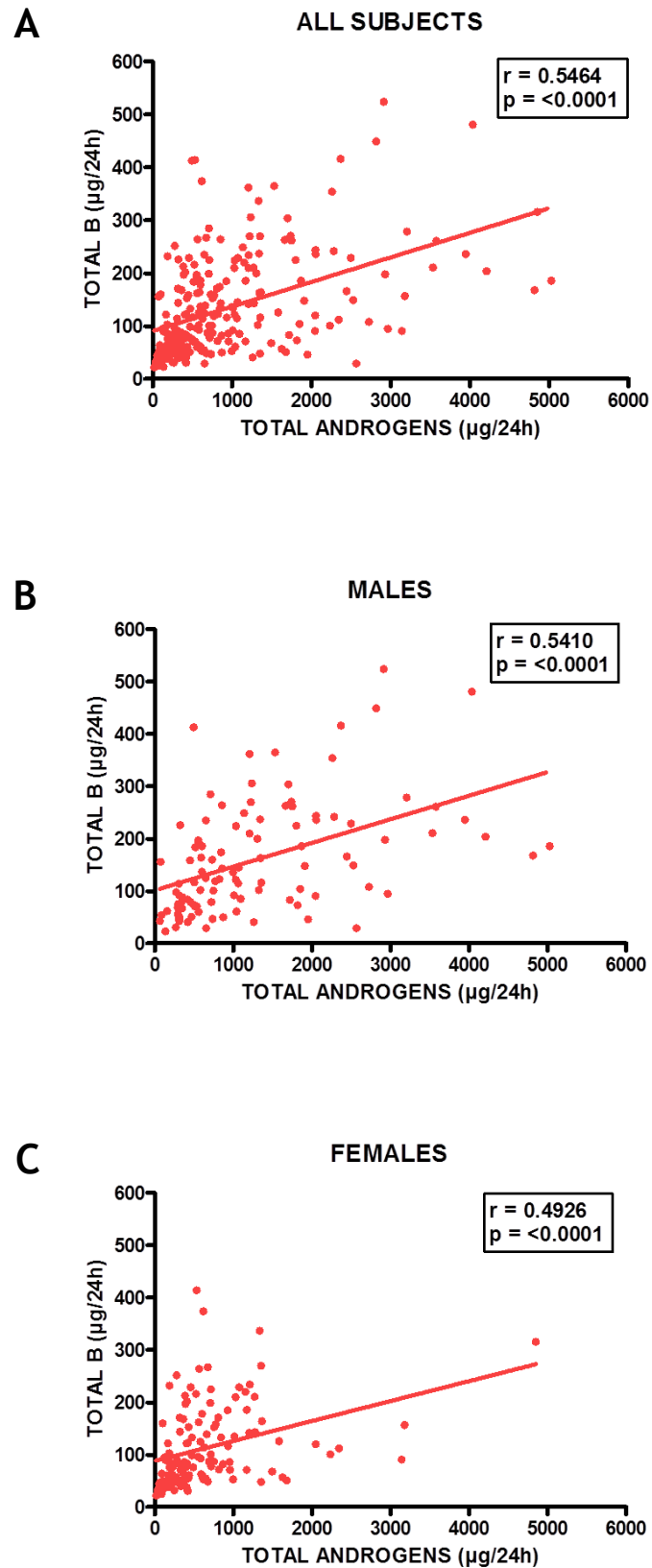


Figure 4-3 Correlation between excretion rates of total androgen and total corticosterone metabolites.

Correlation between excretion of total androgen (DHEA + andro + aetio) urinary metabolites and total corticosterone (THB + aTHB + THA) urinary metabolites in A) all subjects B) males only and C) females only. Spearman correlation coefficients are displayed.

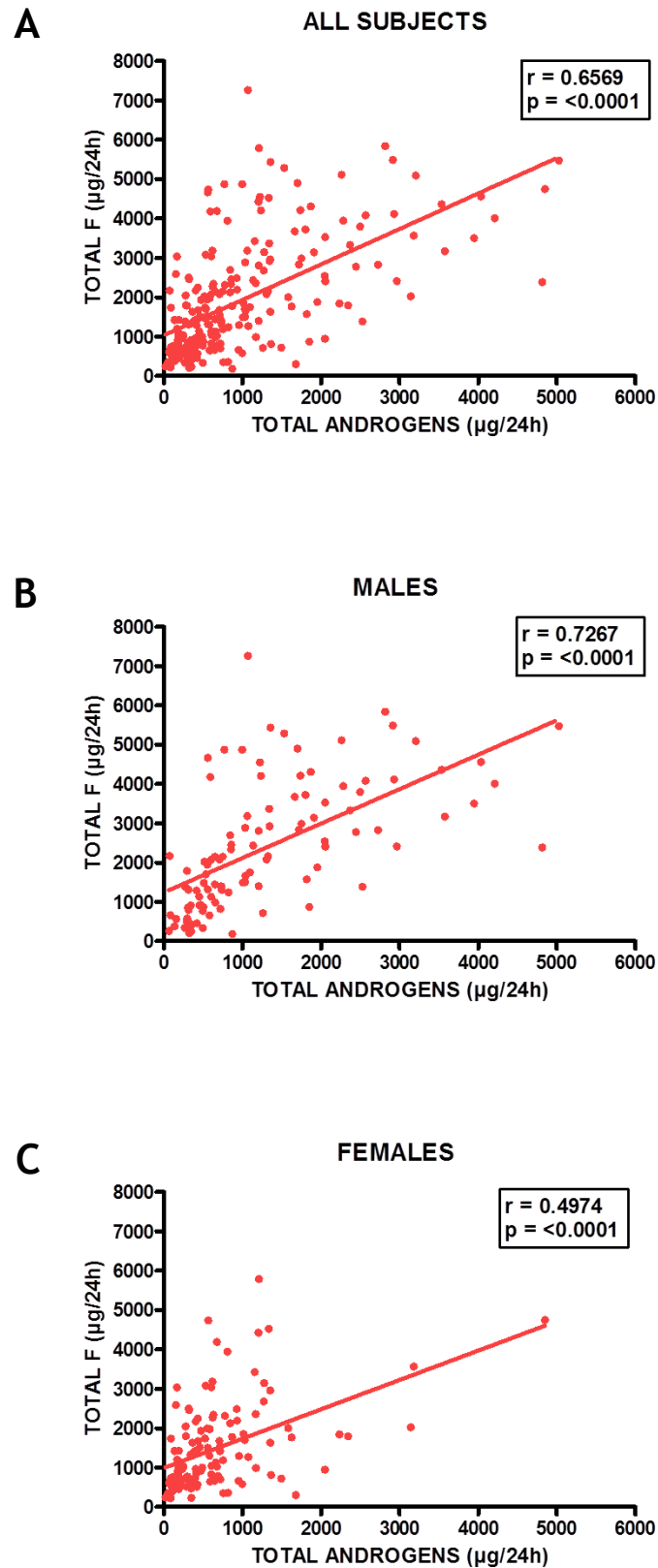


Figure 4-4 Correlation between excretion rates of total cortisol and total androgen metabolites.

Correlation between excretion of total cortisol (THF + aTHF + THE) urinary metabolites and total androgen (DHEA + andro + aetio) urinary metabolites in A) all subjects B) males only and C) females only. Spearman correlation coefficients are displayed.

Corticosterone, cortisol and androgen metabolite excretion rates were stratified by genotype for each polymorphism and compared by the non-parametric Mann-Whitney test using the dominant model. Corticosterone, cortisol and androgen metabolite excretion rates did not differ significantly between individuals with the major homozygote genotype and those with the heterozygote and minor homozygote genotype at positions -34, -804, -1488 and -1877. This was also the case when assessed separately by gender (Table 4-11, Table 4-13, Table 4-15, and Table 4-16 respectively).

Corticosterone and androgen metabolite excretion rates were not significantly different when stratified by genotype at position -362. Cortisol metabolite excretion rates, however, were significantly higher in males with the AG genotype compared to those with the AA genotype ($p=0.05$). There were no males with the GG genotype. This effect was not replicated in females, nor in the cohort as a whole (Table 4-12).

In females, cortisol metabolite excretion rates were significantly higher in the heterozygote and minor homozygote genotype group when compared to the major homozygote group at position -1204 ($p=0.04$). This effect was not seen in males, or in the combined group (Table 4-14). Corticosterone and androgen metabolite excretion rates were not significantly altered when stratified by genotype and gender at this polymorphic site.

Cortisol metabolite excretion rates were significantly higher in females in the heterozygote and minor homozygote genotype group at position -2205 compared to the major homozygote group ($p=0.04$). Again, this effect was not seen in males or in the combined group. No difference was observed in corticosterone and androgen metabolite excretion rates between genotype groups when assessed as a whole or by gender (Table 4-17).

Table 4-11 Urinary corticosteroid excretion rates of the BRIGHT study subgroup stratified by -34 genotype.

Urinary corticosteroid excretion rates (median and interquartile ranges) of the BRIGHT study subgroup stratified by -34 genotype. Metabolite excretion rates were compared by the non-parametric Mann-Whitney test. THB: tetrahydrocorticosterone; aTHB: allotetrahydrocorticosterone; THA: tetrahydro-11-dehydrocorticosterone; THF: tetrahydrocortisol; aTHF: allotetrahydrocortisol; THE: tetrahydrocortisone; DHEA: dehydroepiandrosterone; Aetio: aetiocholanolone; Andro: androsterone.

Urinary Steroid Metabolite ($\mu\text{g}/24\text{h}$)		-34 TT	-34 CT	-34 CC	p-value TT vs. CT+CC
Corticosterone metabolites (THB + aTHB + THA)	Total	101.5 (59-180)	112 (69-204)	99 (75-186)	0.58
	Males	163 (90-219)	156 (77-236)	123 (86-177)	0.69
	Females	81 (53-146)	90 (55-140)	87 (56-149)	0.57
Cortisol metabolites (THF + aTHF + THE)	Total	1354 (671-2435)	1704 (823-2888)	1388 (769-2149)	0.21
	Males	2116 (1375-3381)	2407 (951-3875)	1478 (888-2833)	0.79
	Females	904 (530-1789)	1366 (746-2103)	995 (755-1523)	0.08
Androgen metabolites (DHEA + Aetio + Andro)	Total	614 (317-1182)	688 (342-1342)	599 (310-1031)	0.57
	Males	850 (550-1727)	1234 (511-1866)	737 (439-1581)	0.76
	Females	504 (233-953)	483 (216-912)	435 (205-682)	0.91

Table 4-12 Urinary corticosteroid excretion rates of the BRIGHT study subgroup stratified by -362 genotype.

Urinary corticosteroid excretion rates (median and interquartile ranges) of the BRIGHT study subgroup stratified by -362 genotype. Metabolite excretion rates were compared by the non-parametric Mann-Whitney test. THB: tetrahydrocorticosterone; aTHB: allotetrahydrocorticosterone; THA: tetrahydro-11-dehydrocorticosterone; THF: tetrahydrocortisol; aTHF: allotetrahydrocortisol; THE: tetrahydrocortisone; DHEA: dehydroepiandrosterone; Aetio: aetiocholanolone; Andro: androsterone.

Urinary Steroid Metabolite ($\mu\text{g}/24\text{h}$)		-362 AA	-362 AG	-362 GG	p-value AA vs. AG+GG
Corticosterone metabolites (THB + aTHB + THA)	Total	96 (60-168)	123.5 (65-203)	171 (120-216)	0.08
	Males	121 (76-221)	167 (101-241)	-	0.09
	Females	84 (54-125)	77 (52-158)	171 (120-216)	0.27
Cortisol metabolites (THF + aTHF + THE)	Total	1388 (765-2342)	1786 (289-3177)	1104 (674-2089)	0.21
	Males	1711 (918-3284)	2619 (1546-3992)	-	0.05
	Females	1026 (715-1798)	1251 (547-2296)	1104 (674-2089)	0.94
Androgen metabolites (DHEA + Aetio + Andro)	Total	599 (331-1208)	747 (327-1340)	376 (252-692)	0.56
	Males	933 (475-1844)	1062 (582-1804)	-	0.48
	Females	423 (262-701)	593 (183-1169)	376 (252-692)	0.64

Table 4-13 Urinary corticosteroid excretion rates of the BRIGHT study subgroup stratified by -804 genotype.

Urinary corticosteroid excretion rates (median and interquartile ranges) of the BRIGHT study subgroup stratified by -804 genotype. Metabolite excretion rates were compared by the non-parametric Mann-Whitney test. THB: tetrahydrocorticosterone; aTHB: allotetrahydrocorticosterone; THA: tetrahydro-11-dehydrocorticosterone; THF: tetrahydrocortisol; aTHF: allotetrahydrocortisol; THE: tetrahydrocortisone; DHEA: dehydroepiandrosterone; Aetio: aetiocholanolone; Andro: androsterone.

Urinary Steroid Metabolite ($\mu\text{g}/24\text{h}$)		-804 GG	-804 GA	-804 AA	p-value GG vs. GA+AA
Corticosterone metabolites (THB + aTHB + THA)	Total	102 (59-173)	96 (69-202)	123 (85-198)	0.44
	Males	147 (80-211)	156 (78-237)	123 (83-149)	0.61
	Females	86 (53-153)	83 (55-133)	149 (91-218)	0.94
Cortisol metabolites (THF + aTHF + THE)	Total	1316 (694-2457)	1704 (770-2700)	1388 (891-1800)	0.24
	Males	2053 (1170-3526)	2407 (2496-4045)	1388 (1245-2149)	0.96
	Females	992 (601-1843)	1300 (730-2054)	1209 (838-1493)	0.20
Androgen metabolites (DHEA + Aetio + Andro)	Total	604 (323-1082)	649 (313-1334)	648 (439-927)	0.46
	Males	758 (511-1586)	1242 (1224-1866)	648 (494-1700)	0.41
	Females	423 (247-934)	429 (190-824)	574 (408-707)	0.61

Table 4-14 Urinary corticosteroid excretion rates of the BRIGHT study subgroup stratified by -1204 genotype.

Urinary corticosteroid excretion rates (median and interquartile ranges) of the BRIGHT study subgroup stratified by -1204 genotype. Metabolite excretion rates were compared by the non-parametric Mann-Whitney test. THB: tetrahydrocorticosterone; aTHB: allotetrahydrocorticosterone; THA: tetrahydro-11-dehydrocorticosterone; THF: tetrahydrocortisol; aTHF: allotetrahydrocortisol; THE: tetrahydrocortisone; DHEA: dehydroepiandrosterone; Aetio: aetiocholanolone; Andro: androsterone.

Urinary Steroid Metabolite (µg/24h)		-1204 TT	-1204 TC	-1204 CC	p-value TT vs. TC+CC
Corticosterone metabolites (THB + aTHB + THA)	Total	101 (57-181)	112 (68-193)	98.5 (76-177)	0.55
	Males	163 (90-219)	186 (74-233)	123 (86-177)	0.59
	Females	78 (52-148)	91 (55-146)	86 (58-125)	0.44
Cortisol metabolites (THF + aTHF + THE)	Total	1312 (660-2376)	1704 (819-2676)	1388 (735-2129)	0.16
	Males	2116 (1375-3381)	2384 (914-3875)	1478 (888-2833)	0.68
	Females	863 (520-1754)	1414 (759-2139)	976 (692-1519)	0.04
Androgen metabolites (DHEA + Aetio + Andro)	Total	606 (316-1122)	638 (341-1321)	580 (300-1022)	0.54
	Males	850 (550-1727)	1173 (497-1866)	737 (439-1581)	0.87
	Females	413 (223-854)	483 (266-883)	413 (191-678)	0.99

Table 4-15 Urinary corticosteroid excretion rates of the BRIGHT study subgroup stratified by -1488 genotype.

Urinary corticosteroid excretion rates (median and interquartile ranges) of the BRIGHT study subgroup stratified by -1488 genotype. Metabolite excretion rates were compared by the non-parametric Mann-Whitney test. THB: tetrahydrocorticosterone; aTHB: allotetrahydrocorticosterone; THA: tetrahydro-11-dehydrocorticosterone; THF: tetrahydrocortisol; aTHF: allotetrahydrocortisol; THE: tetrahydrocortisone; DHEA: dehydroepiandrosterone; Aetio: aetiocholanolone; Andro: androsterone.

Urinary Steroid Metabolite (µg/24h)		-1488 CC	-1488 CG	-1488 GG	p-value CC vs. CG+GG
Corticosterone metabolites (THB + aTHB + THA)	Total	102 (59-173)	97.5 (68-203)	123 (85-198)	0.43
	Males	147 (80-211)	156 (78-237)	123 (83-149)	0.61
	Females	86 (53-153)	82 (54-133)	149 (91-218)	0.95
Cortisol metabolites (THF + aTHF + THE)	Total	1316 (694-2457)	1704 (768-2755)	1388 (891-1800)	0.25
	Males	2053 (1170-3526)	2407 (1023-4045)	1388 (1245-2149)	0.96
	Females	992 (601-1843)	1272 (727-2060)	1209 (838-1493)	0.23
Androgen metabolites (DHEA + Aetio + Andro)	Total	604 (323-1082)	646 (310-1326)	648 (439-927)	0.53
	Males	758 (511-1586)	1242 (511-1866)	648 (484-1700)	0.41
	Females	423 (247-934)	427 (189-797)	574 (408-707)	0.50

Table 4-16 Urinary corticosteroid excretion rates of the BRIGHT study subgroup stratified by -1877 genotype.

Urinary corticosteroid excretion rates (median and interquartile ranges) of the BRIGHT study subgroup stratified by -1877 genotype. Metabolite excretion rates were compared by the non-parametric Mann-Whitney test. THB: tetrahydrocorticosterone; aTHB: allotetrahydrocorticosterone; THA: tetrahydro-11-dehydrocorticosterone; THF: tetrahydrocortisol; aTHF: allotetrahydrocortisol; THE: tetrahydrocortisone; DHEA: dehydroepiandrosterone; Aetio: aetiocholanolone; Andro: androsterone.

Urinary Steroid Metabolite (µg/24h)		-1877 CC	-1877 CT	-1877 TT	p-value CC vs. CT+TT
Corticosterone metabolites (THB + aTHB + THA)	Total	102 (61-191)	108 (61-164)	86.5 (86-87)	0.79
	Males	147 (76-234)	128 (82-218)	86.5 (86-87)	0.50
	Females	86 (53-153)	92 (57-134)	-	0.84
Cortisol metabolites (THF + aTHF + THE)	Total	1467 (734-2452)	1404 (823-3188)	1086 (752-1419)	0.71
	Males	2116 (1257-3361)	2877 (933-4124)	1086 (752-1419)	0.84
	Females	1037 (658-1946)	1188 (718-2010)	-	0.51
Androgen metabolites (DHEA + Aetio + Andro)	Total	629 (327-1260)	580 (308-998)	725 (540-909)	0.53
	Males	1034 (509-1820)	746 (490-2050)	725 (540-909)	0.66
	Females	429 (233-824)	435 (205-714)	-	0.81

Table 4-17 Urinary corticosteroid excretion rates of the BRIGHT study subgroup stratified by -2205 genotype.

Urinary corticosteroid excretion rates (median and interquartile ranges) of the BRIGHT study subgroup stratified by -2205 genotype. Metabolite excretion rates were compared by the non-parametric Mann-Whitney test. THB: tetrahydrocorticosterone; aTHB: allotetrahydrocorticosterone; THA: tetrahydro-11-dehydrocorticosterone; THF: tetrahydrocortisol; aTHF: allotetrahydrocortisol; THE: tetrahydrocortisone; DHEA: dehydroepiandrosterone; Aetio: aetiocolanalone; Andro: androsterone.

Urinary Steroid Metabolite ($\mu\text{g}/24\text{h}$)		-2205 CC	-2205 CT	-2205 TT	p-value CC vs. CT+TT
Corticosterone metabolites (THB + aTHB + THA)	Total	98 (57-180)	108 (68-186)	99 (75-186)	0.49
	Males	160 (84-211)	143 (74-236)	123 (86-177)	0.74
	Females	78 (52-148)	90 (55-144)	87 (56-149)	0.44
Cortisol metabolites (THF + aTHF + THE)	Total	1306 (660-2358)	1671 (816-2529)	1388 (769-2149)	0.15
	Males	2079 (1312-3331)	2384 (915-3725)	1478 (888-2833)	0.79
	Females	863 (520-1749)	1404 (740-2127)	995 (755-1523)	0.04
Androgen metabolites (DHEA + Aetio + Andro)	Total	605 (315-1096)	629 (340-1307)	599 (310-1031)	0.53
	Males	845 (517-1666)	1173 (501-1828)	737 (439-1581)	0.76
	Females	413 (223-806)	475 (223-868)	435 (205-682)	0.99

In addition to assessing the end products of the three major arms of the steroidogenic pathway in the zona fasciculata and zone reticularis, stratified by genotype at each of the seven polymorphisms of interest, ratios of components from the 17-deoxycorticosteroid pathway to 17-hydroxycorticosteroid pathway and of the 17-hydroxycorticosteroid pathway to the androgen arm of the pathway were used as indices of 17 α -hydroxylase activity and 17,20 lyase activity, respectively.

It would be most beneficial to assess the ratios of immediate precursor metabolites to immediate product metabolites for 17 α -hydroxylase/17,20 lyase in order to ascertain enzymatic efficiency but measurements of these metabolite excretion rates were not available. Instead, ratios of the urinary metabolite rates of deoxycorticosterone (DOC) to 11-deoxycortisol (S) and of corticosterone (B) to cortisol (F) were used as indices of 17 α -hydroxylase activity, while ratios of 11-deoxycortisol (S) to dehydroepiandrosterone (DHEA) and of cortisol (F) to total available androgen metabolites (DHEA + aetiocholanolone + androsterone) were used as indices of 17,20 lyase activity.

These four ratios were first analysed for the total cohort and then separately by gender (Table 4-18). The ratios of the urinary metabolite excretion rates of DOC:S ($p=0.110$) and B:F ($p=0.130$) were not significantly different between males and females, although examination of the mean ratio values indicated a trend to higher values for both ratios in females. The ratio of S:DHEA rates approached significance between males and females, with higher ratios again evident in females when looking at the mean values (0.066). The ratio of F/androgen metabolite was significantly higher in females ($p=0.002$).

The cohort was then stratified by genotype for each polymorphism and the same four ratios compared. Ratios between genotype groups were compared by the non-parametric Mann-Whitney test using the dominant model. Ratios were also assessed separately by gender. None of the four ratios differed significantly between the genotype groups for the polymorphisms at positions -362 (Table 4-20) and -1877 (Table 4-24).

The ratio of THDOC:THS was significantly lower in females from the heterozygote and minor homozygote group at positions -34 ($p=0.004$), -1204

($p=0.005$) and -2205 ($p=0.005$) compared to the corresponding major homozygote groups (Table 4-19, Table 4-22 and Table 4-25, respectively). While no significant differences were observed in males at any of these polymorphic sites, analysis of the cohort as a whole overall reflected the observed effect in females, albeit with slightly reduced significance. Similar trends were observed at positions -804 (Table 4-21) and -1488 (Table 4-23), although statistical significance was not attained. These effects were not so clear when examining ratios of the urinary metabolite of B:F. Significantly lower ratios were observed in females from the heterozygote and minor homozygote group at positions -1204 ($p=0.034$) and -2205 ($p=0.034$) when compared to the major homozygote group of each. Similar trends, though not significant, were observed at positions -34, -804 and -1488. Ratios of B:F were not significantly different when analysing the whole cohort or males alone.

Ratios of THS:DHEA and F:total androgen metabolite did not change significantly when stratified by genotype and/or gender. However, in the female group, higher ratios of F:total androgen metabolite were apparent in the heterozygote and minor homozygote group at positions -34 ($p=0.077$), -1204 ($p=0.054$), -1488 (0.076) and -2205 ($p=0.054$) when compared to their respective major homozygote groups, although not reaching statistical significance.

Table 4-18 Ratios of urinary corticosteroid excretion rates of the BRIGHT study subgroup stratified by -34 genotype.

Ratios of urinary corticosteroid excretion rates (median and interquartile ranges) of the BRIGHT study subgroup stratified by -34 genotype. Ratios were compared by the non-parametric Mann-Whitney test. THDOC: tetrahydrodeoxycorticosterone; THS: tetrahydrodeoxycortisol; THB: tetrahydrocorticosterone; aTHB: allotetrahydrocorticosterone; THA: tetrahydro-11-dehydrocorticosterone; THF: tetrahydrocortisol; aTHF: allotetrahydrocortisol; THE: tetrahydrocortisone; DHEA: dehydroepiandrosterone; Aetio: aetiocholanolone; Andro: androsterone.

Urinary Steroid Metabolite ($\mu\text{g}/24\text{h}$)	All Subjects N=232	Males N=106	Females N=126	p-value (Male vs. Female)
THDOC:THS	0.57 (0.31-1.10)	0.50 (0.29-1.00)	0.64 (0.35-1.17)	0.110
Total B:Total F (Total B: THB + aTHB + THA) (Total F: THF + aTHF + THE)	0.07 (0.05-0.11)	0.07 (0.05-0.11)	0.08 (0.06-0.12)	0.130
THS:DHEA	0.71 (0.27-2.00)	0.62 (0.25-1.49)	1.00 (0.35-2.29)	0.066
Total F:Total Androgens (Total F: THF + aTHF + THE) (Total Androgens: DHEA + Aetio + Andro)	2.26 (1.41-3.68)	1.91 (1.28-2.92)	2.68 (1.56-4.52)	0.002

Table 4-19 Ratios of urinary corticosteroid excretion rates of the BRIGHT study subgroup stratified by -34 genotype.

Ratios of urinary corticosteroid excretion rates (median and interquartile ranges) of the BRIGHT study subgroup stratified by -34 genotype. Ratios were compared by the non-parametric Mann-Whitney test. THDOC: tetrahydrodeoxycorticosterone; THS: tetrahydrodeoxycortisol; THB: tetrahydrocorticosterone; aTHB: allotetrahydrocorticosterone; THA: tetrahydro-11-dehydrocorticosterone; THF: tetrahydrocortisol; aTHF: allotetrahydrocortisol; THE: tetrahydrocortisone; DHEA: dehydroepiandrosterone; Aetio: aetiocholanolone; Andro: androsterone.

Urinary Steroid Metabolites (µg/24h)		-34 TT	-34 CT	-34 CC	p-value TT vs. CT+CC
THDOC:THS	Total	0.70 (0.44-1.67)	0.50 (0.28-0.88)	0.67 (0.35-1.07)	0.014
	Males	0.50 (0.40-0.78)	0.40 (0.28-1.00)	0.69 (0.26-1.15)	0.575
	Females	1.00 (0.44-2.00)	0.54 (0.29-0.84)	0.67 (0.37-0.93)	0.004
Total B:Total F (Total B: THB + aTHB + THA) (Total F: THF + aTHF + THE)	Total	0.08 (0.05-0.12)	0.07 (0.05-0.10)	0.07 (0.05-0.11)	0.250
	Males	0.06 (0.05-0.11)	0.07 (0.05-0.10)	0.09 (0.05-0.11)	0.674
	Females	0.10 (0.06-0.12)	0.07 (0.06-0.09)	0.08 (0.05-0.12)	0.052
THS:DHEA	Total	0.81 (0.31-2.12)	0.83 (0.29-2.00)	0.63 (0.30-1.89)	0.795
	Males	0.70 (0.38-1.85)	0.46 (0.21-1.26)	0.62 (0.26-1.36)	0.364
	Females	1.00 (0.31-2.79)	1.35 (0.43-2.25)	0.90 (0.44-2.92)	0.608
Total F:Total Androgens (Total F: THF + aTHF + THE) (Total Androgens: DHEA + Aetio + Andro)	Total	2.03 (1.33-3.67)	2.37 (1.52-4.02)	1.99 (1.51-3.46)	0.570
	Males	2.09 (1.56-3.12)	1.95 (1.19-2.76)	1.61 (1.31-2.75)	0.204
	Females	2.00 (1.23-4.24)	3.18 (1.71-5.19)	3.31 (1.97-3.96)	0.077

Table 4-20 Ratios of urinary corticosteroid excretion rates of the BRIGHT study subgroup stratified by -362 genotype.

Ratios of urinary corticosteroid excretion rates (median and interquartile ranges) of the BRIGHT study subgroup stratified by -362 genotype. Ratios were compared by the non-parametric Mann-Whitney test. THDOC: tetrahydrodeoxycorticosterone; THS: tetrahydrodeoxycortisol; THB: tetrahydrocorticosterone; aTHB: allotetrahydrocorticosterone; THA: tetrahydro-11-dehydrocorticosterone; THF: tetrahydrocortisol; aTHF: allotetrahydrocortisol; THE: tetrahydrocortisone; DHEA: dehydroepiandrosterone; Aetio: aetiocholanolone; Andro: androsterone.

Urinary Steroid Metabolites (µg/24h)		-362 AA	-362 AG	-362 GG	p-value AA vs. AG+GG
THDOC:THS	Total	0.63 (0.33-1.00)	0.57 (0.29-1.67)	0.56 (0.35-1.33)	0.780
	Males	0.50 (0.31-1.00)	0.43 (0.29-1.04)	-	0.797
	Females	0.67 (0.36-1.10)	0.73 (0.36-2.00)	0.56 (0.35-1.33)	0.564
Total B:Total F (Total B: THB + aTHB + THA) (Total F: THF + aTHF + THE)	Total	0.07 (0.05-0.11)	0.07 (0.05-0.11)	0.12 (0.09-0.19)	0.620
	Males	0.07 (0.05-0.11)	0.07 (0.05-0.10)	-	0.665
	Females	0.08 (0.06-0.11)	0.09 (0.05-0.12)	0.12 (0.09-0.19)	0.259
THS:DHEA	Total	0.68 (0.30-2.00)	0.77 (0.28-1.57)	4.00 (3.00-7.33)	0.900
	Males	0.58 (0.22-1.38)	0.64 (0.27-1.50)	-	0.993
	Females	1.00 (0.35-2.00)	0.89 (0.29-2.00)	4.00 (3.00-7.33)	0.886
Total F:Total Androgens (Total F: THF + aTHF + THE) (Total Androgens: DHEA + Aetio + Andro)	Total	2.17 (1.41-3.60)	2.33 (1.37-4.07)	4.45 (1.89-6.07)	0.389
	Males	1.75 (1.25-2.77)	2.07 (1.59-3.45)	-	0.145
	Females	2.91 (1.64-4.32)	2.44 (1.36-4.88)	4.45 (1.89-6.07)	0.902

Table 4-21 Ratios of urinary corticosteroid excretion rates of the BRIGHT study subgroup stratified by -804 genotype.

Ratios of urinary corticosteroid excretion rates (median and interquartile ranges) of the BRIGHT study subgroup stratified by -804 genotype. Ratios were compared by the non-parametric Mann-Whitney test. THDOC: tetrahydrodeoxycorticosterone; THS: tetrahydrodeoxycortisol; THB: tetrahydrocorticosterone; aTHB: allotetrahydrocorticosterone; THA: tetrahydro-11-dehydrocorticosterone; THF: tetrahydrocortisol; aTHF: allotetrahydrocortisol; THE: tetrahydrocortisone; DHEA: dehydroepiandrosterone; Aetio: aetiocholanolone; Andro: androsterone.

Urinary Steroid Metabolites (µg/24h)		-804 GG	-804 GA	-804 AA	p-value GG vs. GA+AA
THDOC:THS	Total	0.64 (0.38-1.33)	0.50 (0.27-1.00)	0.63 (0.36-1.11)	0.064
	Males	0.50 (0.38-0.83)	0.40 (0.23-1.00)	0.61 (0.30-1.23)	0.503
	Females	0.76 (0.42-1.67)	0.57 (0.29-0.86)	0.63 (0.41-0.94)	0.056
Total B:Total F (Total B: THB + aTHB + THA) (Total F: THF + aTHF + THE)	Total	0.07 (0.05-0.12)	0.07 (0.05-0.10)	0.08 (0.06-0.11)	0.610
	Males	0.06 (0.05-0.10)	0.07 (0.05-0.12)	0.07 (0.06-0.09)	0.235
	Females	0.09 (0.06-0.12)	0.07 (0.05-0.09)	0.13 (0.08-0.16)	0.086
THS:DHEA	Total	0.75 (0.30-1.82)	0.89 (0.29-2.09)	0.63 (0.33-1.00)	0.836
	Males	0.55 (0.22-1.58)	0.60 (0.23-1.34)	0.63 (0.30-1.36)	0.921
	Females	1.00 (0.35-2.08)	1.55 (0.40-3.00)	0.75 (0.54-0.97)	0.495
Total F:Total Androgens (Total F: THF + aTHF + THE) (Total Androgens: DHEA + Aetio + Andro)	Total	2.21 (1.38-3.68)	2.47 (1.59-3.89)	1.85 (1.43-3.10)	0.800
	Males	1.99 (1.51-3.05)	1.91 (1.14-2.62)	1.56 (1.41-2.88)	0.201
	Females	2.37 (1.36-4.18)	3.39 (2.00-5.28)	2.07 (1.88-3.02)	0.107

Table 4-22 Ratios of urinary corticosteroid excretion rates of the BRIGHT study subgroup stratified by -1204 genotype.

Ratios of urinary corticosteroid excretion rates (median and interquartile ranges) of the BRIGHT study subgroup stratified by -1204 genotype. Ratios were compared by the non-parametric Mann-Whitney test. THDOC: tetrahydrodeoxycorticosterone; THS: tetrahydrodeoxycortisol; THB: tetrahydrocorticosterone; aTHB: allotetrahydrocorticosterone; THA: tetrahydro-11-dehydrocorticosterone; THF: tetrahydrocortisol; aTHF: allotetrahydrocortisol; THE: tetrahydrocortisone; DHEA: dehydroepiandrosterone; Aetio: aetiocholanolone; Andro: androsterone.

Urinary Steroid Metabolites (µg/24h)		-1204 TT	-1204 TC	-1204 CC	p-value TT vs. TC+CC
THDOC:THS	Total	0.71 (0.44-1.63)	0.50 (0.29-1.00)	0.70 (0.35-1.04)	0.019
	Males	0.50 (0.40-0.78)	0.46 (0.29-1.00)	0.69 (0.26-1.15)	0.682
	Females	1.00 (0.44-2.00)	0.54 (0.29-0.88)	0.70 (0.28-0.89)	0.005
Total B:Total F (Total B: THB + aTHB + THA) (Total F: THF + aTHF + THE)	Total	0.08 (0.05-0.12)	0.07 (0.05-0.10)	0.08 (0.05-0.12)	0.190
	Males	0.06 (0.05-0.11)	0.07 (0.05-0.10)	0.07 (0.05-0.11)	0.690
	Females	0.10 (0.06-0.13)	0.07 (0.06-0.09)	0.09 (0.06-0.13)	0.034
THS:DHEA	Total	0.77 (0.30-2.00)	0.88 (0.30-2.00)	0.63 (0.30-1.67)	0.946
	Males	0.70 (0.38-1.85)	0.50 (0.21-1.26)	0.62 (0.26-1.36)	0.407
	Females	1.00 (0.30-2.15)	1.35 (0.43-2.49)	0.89 (0.48-2.63)	0.479
Total F:Total Androgens (Total F: THF + aTHF + THE) (Total Androgens: DHEA + Aetio + Andro)	Total	2.09 (1.36-3.63)	2.41 (1.53-4.06)	2.07 (1.52-3.44)	0.513
	Males	2.09 (1.56-3.12)	1.95 (1.19-2.76)	1.61 (1.31-2.75)	0.204
	Females	2.09 (1.25-4.02)	3.18 (1.80-5.20)	3.22 (1.98-3.91)	0.054

Table 4-23 Ratios of urinary corticosteroid excretion rates of the BRIGHT study subgroup stratified by -1488 genotype.

Ratios of urinary corticosteroid excretion rates (median and interquartile ranges) of the BRIGHT study subgroup stratified by -1488 genotype. Ratios were compared by the non-parametric Mann-Whitney test. THDOC: tetrahydrodeoxycorticosterone; THS: tetrahydrodeoxycortisol; THB: tetrahydrocorticosterone; aTHB: allotetrahydrocorticosterone; THA: tetrahydro-11-dehydrocorticosterone; THF: tetrahydrocortisol; aTHF: allotetrahydrocortisol; THE: tetrahydrocortisone; DHEA: dehydroepiandrosterone; Aetio: aetiocholanolone; Andro: androsterone.

Urinary Steroid Metabolites (µg/24h)		-1488 CC	-1488 CG	-1488 GG	p-value CC vs. CG+GG
THDOC:THS	Total	0.64 (0.38-1.33)	0.50 (0.27-1.00)	0.63 (0.36-1.11)	0.060
	Males	0.50 (0.38-0.83)	0.40 (0.23-1.00)	0.61 (0.30-1.23)	0.503
	Females	0.76 (0.42-1.67)	0.57 (0.29-0.87)	0.63 (0.41-0.94)	0.052
Total B:Total F (Total B: THB + aTHB + THA) (Total F: THF + aTHF + THE)	Total	0.07 (0.05-0.12)	0.07 (0.05-0.10)	0.08 (0.06-0.11)	0.660
	Males	0.06 (0.05-0.10)	0.07 (0.05-0.12)	0.07 (0.06-0.09)	0.235
	Females	0.09 (0.06-0.12)	0.07 (0.05-0.09)	0.13 (0.08-0.16)	0.107
THS:DHEA	Total	0.75 (0.30-1.82)	0.90 (0.28-2.13)	0.63 (0.33-1.00)	0.829
	Males	0.55 (0.22-1.58)	0.60 (0.23-1.34)	0.63 (0.31-1.36)	0.921
	Females	1.00 (0.35-2.08)	1.55 (0.38-3.08)	0.75 (0.54-0.97)	0.477
Total F:Total Androgens (Total F: THF + aTHF + THE) (Total Androgens: DHEA + Aetio + Andro)	Total	2.21 (1.38-3.68)	2.52 (1.59-3.90)	1.85 (1.43-3.10)	0.722
	Males	1.99 (1.52-3.05)	1.91 (1.14-2.62)	1.56 (1.41-2.88)	0.201
	Females	2.37 (1.36-4.18)	3.39 (2.03-5.33)	2.07 (1.88-3.02)	0.076

Table 4-24 Ratios of urinary corticosteroid excretion rates of the BRIGHT study subgroup stratified by -1877 genotype.

Ratios of urinary corticosteroid excretion rates (median and interquartile ranges) of the BRIGHT study subgroup stratified by -1877 genotype. Ratios were compared by the non-parametric Mann-Whitney test. THDOC: tetrahydrodeoxycorticosterone; THS: tetrahydrodeoxycortisol; THB: tetrahydrocorticosterone; aTHB: allotetrahydrocorticosterone; THA: tetrahydro-11-dehydrocorticosterone; THF: tetrahydrocortisol; aTHF: allotetrahydrocortisol; THE: tetrahydrocortisone; DHEA: dehydroepiandrosterone; Aetio: aetiocholanolone; Andro: androsterone.

Urinary Steroid Metabolites (µg/24h)		-1877 CC	-1877 CT	-1877 TT	p-value CC vs. CT+TT
THDOC:THS	Total	0.57 (0.32-1.16)	0.57 (0.32-1.00)	0.92 (n=1)	0.500
	Males	0.50 (0.29-1.00)	0.53 (0.30-0.96)	0.92 (n=1)	0.996
	Females	0.73 (0.35-1.38)	0.63 (0.34-0.93)	-	0.325
Total B:Total F (Total B: THB + aTHB + THA) (Total F: THF + aTHF + THE)	Total	0.07 (0.05-0.11)	0.07 (0.05-0.10)	0.13 (0.09-0.17)	0.210
	Males	0.07 (0.05-0.10)	0.06 (0.04-0.09)	0.13 (0.09-0.17)	0.268
	Females	0.08 (0.06-0.12)	0.07 (0.06-0.10)	-	0.351
THS:DHEA	Total	0.83 (0.30-2.00)	0.71 (0.32-2.33)	0.16 (n=1)	0.960
	Males	0.66 (0.28-1.46)	0.38 (0.17-1.25)	0.16 (n=1)	0.286
	Females	1.00 (0.36-2.15)	1.00 (0.40-3.46)	-	0.574
Total F:Total Androgens (Total F: THF + aTHF + THE) (Total Androgens: DHEA + Aetio + Andro)	Total	2.21 (1.37-3.61)	2.79 (1.58-4.18)	1.39 (1.28-1.50)	0.257
	Males	1.91 (1.41-2.88)	1.98 (1.51-3.49)	1.39 (1.28-1.50)	0.963
	Females	2.53 (1.37-4.50)	3.41 (2.10-4.67)	-	0.278

Table 4-25 Ratios of urinary corticosteroid excretion rates of the BRIGHT study subgroup stratified by -2205 genotype.

Ratios of urinary corticosteroid excretion rates (median and interquartile ranges) of the BRIGHT study subgroup stratified by -2205 genotype. Ratios were compared by the non-parametric Mann-Whitney test. THDOC: tetrahydrodeoxycorticosterone; THS: tetrahydrodeoxycortisol; THB: tetrahydrocorticosterone; aTHB: allottetrahydrocorticosterone; THA: tetrahydro-11-dehydrocorticosterone; THF: tetrahydrocortisol; aTHF: allottetrahydrocortisol; THE: tetrahydrocortisone; DHEA: dehydroepiandrosterone; Aetio: aetiocholanolone; Andro: androsterone.

Urinary Steroid Metabolites (µg/24h)		-2205 CC	-2205 CT	-2205 TT	p-value CC vs. CT+TT
THDOC:THS	Total	0.73 (0.44-1.58)	0.50 (0.28-0.91)	0.67 (0.35-1.07)	0.015
	Males	0.50 (0.41-0.82)	0.40 (0.28-1.00)	0.69 (0.26-1.15)	0.536
	Females	1.00 (0.44-2.00)	0.57 (0.29-0.88)	0.67 (0.37-0.93)	0.005
Total B:Total F (Total B: THB + aTHB + THA) (Total F: THF + aTHF + THE)	Total	0.08 (0.05-0.12)	0.07 (0.05-0.10)	0.07 (0.05-0.11)	0.220
	Males	0.06 (0.05-0.11)	0.07 (0.05-0.10)	0.07 (0.05-0.11)	0.643
	Females	0.10 (0.06-0.13)	0.07 (0.06-0.09)	0.08 (0.05-0.12)	0.034
THS:DHEA	Total	0.81 (0.31-1.95)	0.86 (0.33-2.00)	0.63 (0.30-1.89)	0.985
	Males	0.71 (0.42-1.80)	0.50 (0.25-1.31)	0.62 (0.26-1.36)	0.410
	Females	1.00 (0.30-2.15)	1.17 (0.44-2.37)	0.90 (0.44-2.92)	0.479
Total F:Total Androgens (Total F: THF + aTHF + THE) (Total Androgens: DHEA + Aetio + Andro)	Total	2.14 (1.36-3.62)	2.52 (1.55-4.07)	1.99 (1.51-3.46)	0.478
	Males	2.21 (1.59-3.09)	1.95 (1.22-2.79)	1.61 (1.31-2.75)	0.198
	Females	2.09 (1.25-4.02)	2.98 (1.86-5.20)	3.31 (1.97-3.96)	0.054

Aldosterone is a major steroid product and is synthesised in the zona glomerulosa. Its production is largely controlled by angiotensin II (ang II) and potassium although there is also evidence of ACTH-dependence (Section 4.5). In the hypertensive BRIGHT study subgroup, the urinary excretion rate of the metabolite of aldosterone (THAldo) was significantly higher in males than females ($p=0.002$) (Table 4-26).

When stratified by genotype, the major homozygote group (CC) at position -1877 had significantly higher aldosterone production than the heterozygote and minor homozygote group (CT+TT) (4.44 ± 0.41 vs. 3.36 ± 0.69 µg/24h, $p=0.049$). This effect did not appear to be associated with either gender. No significant changes were observed for any other polymorphism (Table 4-27 to Table 4-33).

Table 4-26 THAldo excretion of the BRIGHT study subgroup.

Tetrahydroaldosterone (THAldo) excretion rates (median and interquartile ranges) of the BRIGHT study subgroup. Metabolite excretion was compared by the non-parametric Mann-Whitney test.

Steroid Metabolite ($\mu\text{g}/24\text{h}$)	All Subjects N=232	Males N=106	Females N=126	p-value (Male vs. Female)
Aldosterone (THAldo)	3 (1-5)	3 (2-6)	2 (1-4)	0.002

Table 4-27 THAldo excretion of the BRIGHT study subgroup stratified by -34 genotype.

Tetrahydroaldosterone (THAldo) excretion rates (median and interquartile ranges) of the BRIGHT study subgroup stratified by -34 genotype. Metabolite excretion was compared by the non-parametric Mann-Whitney test.

Steroid Metabolite ($\mu\text{g}/24\text{h}$)		-34 TT	-34 CT	-34 CC	p-value TT vs. CT+CC
Aldosterone (THAldo)	Total	3 (1-5)	3 (2-4)	2 (1-4.75)	0.72
	Males	3 (2-4.75)	3 (2-5)	3 (2-6.5)	0.57
	Females	2 (1-5)	2 (1.25-3)	2 (1-2)	0.94

Table 4-28 THAldo excretion of the BRIGHT study subgroup stratified by -362 genotype.

Tetrahydroaldosterone (THAldo) excretion rates (median and interquartile ranges) of the BRIGHT study subgroup stratified by -362 genotype. Metabolite was excretion compared by the non-parametric Mann-Whitney test.

Steroid Metabolite ($\mu\text{g}/24\text{h}$)		-362 AA	-362 AG	-362 GG	p-value AA vs. AG+GG
Aldosterone (THAldo)	Total	2 (1.25-4)	3 (1-6)	2(1-3)	0.71
	Males	3 (2-5)	3 (2-8.25)	-	0.88
	Females	2(1-3)	2(1-5)	2(1-3)	0.37

Table 4-29 THAldo excretion of the BRIGHT study subgroup stratified by -804 genotype.

Tetrahydroaldosterone (THAldo) excretion rates (median and interquartile ranges) of the BRIGHT study subgroup stratified by -804 genotype. Metabolite excretion was compared by the non-parametric Mann-Whitney test.

Steroid Metabolite ($\mu\text{g}/24\text{h}$)		-804 GG	-804 GA	-804 AA	p-value GG vs. GA+AA
Aldosterone (THAldo)	Total	2 (1-4)	1 (1.25-5)	3 (2-4)	0.54
	Males	3 (2-4.5)	3 (3-6)	3 (2.5-10.5)	0.67
	Females	2 (1-4)	2 (1-3)	2 (2-2.75)	0.91

Table 4-30 THAldo excretion of the BRIGHT study subgroup stratified by -1204 genotype.

Tetrahydroaldosterone (THAldo) excretion rates (median and interquartile ranges) of the BRIGHT study subgroup stratified by -1204 genotype. Metabolite excretion was compared by the non-parametric Mann-Whitney test.

Steroid Metabolite ($\mu\text{g}/24\text{h}$)		-1204 TT	-1204 TC	-1204 CC	p-value TT vs. TC+CC
Aldosterone (THAldo)	Total	2 (1-5)	3 (2-4)	2 (1-4.5)	0.98
	Males	3 (2-4.75)	3 (2-4.75)	3 (2-6.5)	0.48
	Females	2 (1-4.5)	2 (1.75-3.25)	2 (1-2)	0.66

Table 4-31 THAldo excretion of the BRIGHT study subgroup stratified by -1488 genotype.

Tetrahydroaldosterone (THAldo) excretion rates (median and interquartile ranges) of the BRIGHT study subgroup stratified by -1488 genotype. Metabolite excretion was compared by the non-parametric Mann-Whitney test.

Steroid Metabolite ($\mu\text{g}/24\text{h}$)		-1488 CC	-1488 CG	-1488 GG	p-value CC vs. CG+GG
Aldosterone (THAldo)	Total	2 (1-4)	2 (1-5)	2 (3-4)	0.52
	Males	3 (2-4.5)	3 (2-6)	3 (2.5-10.5)	0.67
	Females	2 (1-4)	2 (1-3)	2 (2-2.75)	0.90

Table 4-32 THAldo excretion of the BRIGHT study subgroup stratified by -1877 genotype.

Tetrahydroaldosterone (THAldo) excretion rates (median and interquartile ranges) of the BRIGHT study subgroup stratified by -1877 genotype. Metabolite excretion was compared by the non-parametric Mann-Whitney test.

Steroid Metabolite ($\mu\text{g}/24\text{h}$)		-1877 CC	-1877 CT	-1877 TT	p-value CC vs. CT+TT
Aldosterone (THAldo)	Total	3 (2-5)	2 (1-3)	5.5 (5.25-5.75)	0.05
	Males	3 (2-5.75)	2 (1-3.25)	5.5 (5.25-5.75)	0.14
	Females	2 (1-4)	2 (1-3)	-	0.34

Table 4-33 THAldo excretion of the BRIGHT study subgroup stratified by -2205 genotype.

Tetrahydroaldosterone (THAldo) excretion rates (median and interquartile ranges) of the BRIGHT study subgroup stratified by -2205 genotype. Metabolite excretion was compared by the non-parametric Mann-Whitney test.

Steroid Metabolite ($\mu\text{g}/24\text{h}$)		-2205 CC N=76	-2205 CT N=110	-2205 TT N=37	p-value CC vs. CT+TT
Aldosterone (THAldo)	Total	2 (1-4.75)	3 (2-4)	2 (1-4.75)	0.93
	Males	3 (2-4.5)	3 (2-5)	3 (2-6.5)	0.67
	Females	2 (1-5)	2 (2-3)	2 (1-2)	0.66

As described in Chapter 3, the alleles of the studied SNPs exist in various, but not random, combinations (Figure 3-18). Here, the association between groups of specific genotypes and demographic and corticosteroid excretion rate data was compared. Upon examination of Figure 3-18 and data presented in Table 4-19 to Table 4-23, SNPs at positions -34, -804, -1204, -1488 and -2205 appear to exhibit strong linkage disequilibrium. Data from individuals within the BRIGHT subgroup who were major homozygote, minor homozygote or heterozygote at all five positions (shown below) were extracted and analysed.

SNP	-34	-804	-1204	-1488	-2205
Group 1	CC	GG	TT	CC	CC
Group 2	TT	AA	CC	GG	TT
Group 3	CT	GA	TC	CG	CT

Demographic variables were assessed by comparing the major homozygotes group (Group 1) with the minor homozygotes group (Group 2). Age, SBP, DBP and BMI were not significantly different between groups, nor when further stratified by gender (Table 4-35). WHR was significantly higher in Group 2 compared with Group 1, but this effect was not replicated when males and females were assessed independently. This difference may be partly explained by the presence of considerably more males (n=13) in Group 2 than females (n=6) since the gender-specific effects of WHR are well-documented. Corticosteroid excretion rates were not significantly different between the two groups, nor when assessed separately by gender (Table 4-36). It is likely that these comparisons are underpowered to detect small changes. Therefore, the dominant model was adopted whereby the major homozygotes (Group 1) were compared to the combination of minor homozygotes (Group 2) and those heterozygote at all five positions (Group 3). Age, SBP, DBP, BMI and WHR were not significantly different between groups (Table 4-37). Similar to when assessed singly, the heterozygote and minor homozygote group had significantly lower THDOC:THS ratios compared with the major homozygote group, indicative of increased 17 α -hydroxylase activity (Table 4-37). When stratified by gender, this effect is evident only in females. This ratio was then further examined to investigate a possible 'heterozygote effect' (effect is seen only in heterozygotes) where Group 1 and Group 3 were compared and similar significant alterations observed (Table 4-38).

Table 4-34 Demographic data on the BRIGHT study subgroup stratified by combinations of alleles (Group 1 vs. Group 2).

Demographic data (median and interquartile ranges) of the BRIGHT study subgroup stratified by combinations of alleles at positions -34, -804, -1204, -1488 and -2205 of the *CYP17A1* gene. Demographic characteristics were compared by the non-parametric Mann-Whitney test. SBP: systolic blood pressure; DBP: diastolic blood pressure; BMI: body mass index; WHR: waist-hip ratio.

	Whole Cohort n=91			Males n=41			Females n=50		
	Group 1 n=72	Group 2 n=19	p-value 1 vs. 2	Group 1 n=28	Group 2 n=13	p-value 1 vs. 2	Group 1 n=44	Group 2 n=6	p-value 1 vs. 2
Age (Years)	63 (58-67)	63 (61-67)	0.84	62 (58-66)	63 (61-68)	0.33	64 (59-69)	65 (56-66)	0.69
SBP (mm/Hg)	157 (153-187)	153 (152-187)	0.43	157 (149-186)	153 (151-183)	0.67	169 (156-187)	173 (153-195)	0.96
DBP (mm/Hg)	102 (98-107)	102 (98-110)	0.89	105 (98-108)	105 (98-110)	0.89	101 (98-106)	101 (96-105)	0.74
BMI (kg/m ²)	27 (24-30)	28 (27-31)	0.36	27 (24-30)	28 (27-31)	0.15	27 (25-30)	26 (24-30)	0.77
WHR	0.86 (0.83-0.92)	0.92 (0.89-0.94)	0.04	0.94 (0.90-0.95)	0.92 (0.91-0.94)	0.68	0.84 (0.80-0.86)	0.84 (0.80-0.91)	0.56

Table 4-35 Urinary corticosteroid excretion rates of the BRIGHT study subgroup stratified by combinations of alleles (Group 1 vs. Group 2).

Ratios of urinary corticosteroid excretion rates (median and interquartile ranges) of the BRIGHT study subgroup stratified by combinations of alleles at positions -34, -804, -1204, -1488 and -2205 of the *CYP17A1* gene. Ratios were compared by the non-parametric Mann-Whitney test. THB: tetrahydrocorticosterone; aTHB: allotetrahydrocorticosterone; THA: tetrahydro-11-dehydrocorticosterone; THF: tetrahydrocortisol; aTHF: allotetrahydrocortisol; THE: tetrahydrocortisone; DHEA: dehydroepiandrosterone; Aetio: aetiocholanolone; Andro: androsterone; THAldo: tetrahydroaldosterone; THDOC: tetrahydrodeoxycorticosterone; THS: tetrahydrodeoxycortisol.

Urinary Steroid Metabolites (µg/24h)		Group 1	Group 2	p-value Group 1 vs. Group 2
Corticosterone metabolites (THB + (a)THB + THA)	Total	102 (59-180)	123 (85-198)	0.49
	Males	163 (90-219)	123 (83-149)	0.36
	Females	81 (53-146)	149 (91-218)	0.16
Cortisol metabolites (THF + (a)THF + THE)	Total	1354 (670-2435)	1388 (891-1800)	0.90
	Males	2116 (1375-3381)	1388 (1245-2149)	0.20
	Females	904 (530-1789)	1209 (838-1493)	0.64
Androgen metabolites (DHEA + Aetio + Andro)	Total	614 (317-1182)	648 (439-927)	0.73
	Males	850 (550-1727)	648 (494-1700)	0.55
	Females	504 (233-953)	574 (408-707)	0.78
Aldosterone (THAldo)	Total	3 (1-5)	3 (2-4)	0.64
	Males	3 (2-4.75)	3 (2.5-10.5)	0.79
	Females	2 (1-5)	2 (2-2.75)	1.00
THDOC:THS	Total	0.70 (0.44-1.67)	0.63 (0.36-1.11)	0.48
	Males	0.50 (0.40-0.78)	0.61 (0.30-1.23)	1.00
	Females	1.00 (0.44-2.00)	0.63 (0.41-0.94)	0.49
Total B:Total F (Total B: THB + (a)THB + THA) (Total F: THF + (a)THF + THE)	Total	0.08 (0.05-0.12)	0.08 (0.06-0.11)	0.89
	Males	0.06 (0.05-0.11)	0.07 (0.06-0.09)	0.68
	Females	0.10 (0.06-0.12)	0.13 (0.08-0.16)	0.39
THS:DHEA	Total	0.77 (0.29-2.08)	0.63 (0.33-1.00)	0.53
	Males	0.70 (0.38-1.85)	0.63 (0.30-1.36)	0.71
	Females	1.00 (0.29-2.58)	0.75 (0.54-0.97)	0.55
Total F:Total Androgens (Total F: THF + (a)THF + THE) (Total Androgens: DHEA + Aetio + Andro)	Total	2.03 (1.33-3.67)	1.85 (1.43-3.10)	0.54
	Males	2.09 (1.56-3.12)	1.56 (1.41-2.88)	0.31
	Females	2.00 (1.23-4.24)	2.07 (1.88-3.02)	0.89

Table 4-36 Demographic data on the BRIGHT study subgroup stratified by combinations of alleles (Group 1 vs. Group 2+3).

Demographic data (median and interquartile ranges) of the BRIGHT study subgroup stratified combinations of alleles at positions -34, -804, -1204, -1488 and -2205 of the *CYP17A1* gene. Demographic characteristics were compared by the non-parametric Mann-Whitney test using the dominant model. SBP: systolic blood pressure; DBP: diastolic blood pressure; BMI: body mass index; WHR: waist-hip ratio.

	Whole Cohort n=167			Males n=78			Females n=89		
	Group 1 n=72	Group 2+3 n=95	p- value 1 vs. 2+3	Group 1 n=28	Group 2+3 n=50	p- value 1 vs. 2+3	Group 1 n=44	Group 2+3 n=45	p- value 1 vs. 2+3
Age (Years)	63 (58-67)	63 (55-69)	0.73	62 (58-66)	63 (55-68)	0.67	64 (59-69)	63 (55-69)	0.50
SBP (mm/Hg)	157 (153-187)	157 (153-190)	0.70	157 (149-186)	157 (152-188)	0.52	169 (156-187)	183 (153-190)	0.80
DBP (mm/Hg)	102 (98-107)	102 (98-110)	0.71	105 (98-108)	103 (98-110)	0.59	101 (98-106)	102 (98-110)	0.41
BMI (kg/m ²)	27 (24-30)	28 (25-31)	0.25	27 (24-30)	28 (26-31)	0.09	27 (25-30)	27 (25-29)	0.92
WHR	0.86 (0.83-0.92)	0.90 (0.82-0.93)	0.27	0.94 (0.90-0.95)	0.93 (0.91-0.96)	0.95	0.84 (0.80-0.86)	0.81 (0.79-0.87)	0.30

Table 4-37 Urinary corticosteroid excretion rates of the BRIGHT study subgroup stratified by combinations of alleles (Group 1 vs. Group 2+3).

Ratios of urinary corticosteroid excretion rates (median and interquartile ranges) of the BRIGHT study subgroup stratified by combinations of alleles at positions -34, -804, -1204, -1488 and -2205 of the *CYP17A1* gene. Ratios were compared by the non-parametric Mann-Whitney test. THB: tetrahydrocorticosterone; aTHB: allotetrahydrocorticosterone; THA: tetrahydro-11-dehydrocorticosterone; THF: tetrahydrocortisol; aTHF: allotetrahydrocortisol; THE: tetrahydrocortisone; DHEA: dehydroepiandrosterone; Aetio: aetiocholanolone; Andro: androsterone; THAldo: tetrahydroaldosterone; THDOC: tetrahydrodeoxycorticosterone; THS: tetrahydrodeoxycortisol.

Urinary Steroid Metabolites (µg/24h)		Group 1	Group 2 + 3	p-value Group 1 vs. Group 2+3
Corticosterone metabolites (THB + (a)THB + THA)	Total	102 (59-180)	102 (69-199)	0.62
	Males	163 (90-219)	124 (73-226)	0.68
	Females	81 (53-146)	87 (55-226)	0.63
Cortisol metabolites (THF + (a)THF + THE)	Total	1354 (670-2435)	1516 (776-2447)	0.35
	Males	2116 (1375-3381)	2076 (967-2964)	0.52
	Females	904 (530-1789)	1327 (740-1935)	0.13
Androgen metabolites (DHEA + Aetio + Andro)	Total	614 (317-1182)	647 (341-1295)	0.59
	Males	850 (550-1727)	1062 (495-1804)	0.84
	Females	504 (233-953)	458 (244-817)	0.86
Aldosterone (THAldo)	Total	3 (1-5)	3 (2-5)	0.69
	Males	3 (2-4.75)	3 (2-5.25)	0.85
	Females	2 (1-5)	2 (2-3)	0.65
THDOC:THS	Total	0.70 (0.44-1.67)	0.50 (0.29-1.00)	0.03
	Males	0.50 (0.40-0.78)	0.40 (0.26-1.07)	0.58
	Females	1.00 (0.44-2.00)	0.57 (0.33-0.88)	0.01
Total B:Total F (Total B: THB + (a)THB + THA) (Total F: THF + (a)THF + THE)	Total	0.08 (0.05-0.12)	0.07 (0.05-0.10)	0.49
	Males	0.06 (0.05-0.11)	0.07 (0.05-0.10)	0.42
	Females	0.10 (0.06-0.12)	0.07 (0.05-0.10)	0.10
THS:DHEA	Total	0.77 (0.29-2.08)	0.88 (0.30-1.90)	0.94
	Males	0.70 (0.38-1.85)	0.67 (0.28-1.38)	0.71
	Females	1.00 (0.29-2.58)	1.00 (0.42-2.06)	0.64
Total F:Total Androgens (Total F: THF + (a)THF + THE) (Total Androgens: DHEA + Aetio + Andro)	Total	2.03 (1.33-3.67)	2.28 (1.47-3.57)	0.76
	Males	2.09 (1.56-3.12)	1.77 (1.24-2.79)	0.18
	Females	2.00 (1.23-4.24)	2.97 (1.85-4.79)	0.10

Table 4-38 Ratios of THDOC:THS of the BRIGHT study subgroup stratified by combinations of alleles (Group 1 vs. Group 3).

Ratios of THDOC:THS (median and interquartile ranges) of the BRIGHT study subgroup stratified by combinations of alleles at positions -34, -804, -1204, -1488 and -2205 of the *CYP17A1* gene. Ratios were compared by the non-parametric Mann-Whitney test. THDOC: tetrahydrodeoxycorticosterone; THS: tetrahydrodeoxycortisol.

Urinary Steroid Metabolites ($\mu\text{g}/24\text{h}$)		Group 1	Group 3	p-value Group 1 vs. Group 3
THDOC:THS	Total	0.70 (0.44-1.67)	0.49 (0.29-1.00)	0.02
	Males	0.50 (0.40-0.78)	0.40 (0.25-1.00)	0.49
	Females	1.00 (0.44-2.00)	0.57 (0.29-0.88)	0.01

4.5 Discussion

This is the first study to provide a detailed and extensive examination of the association between polymorphic variation in the human *CYP17A1* gene and intermediate steroidogenic phenotype in a hypertensive cohort. Seven common polymorphisms located in the promoter region immediately upstream of the gene transcriptional start site were selected for investigation. A subset of the BRIGHT study cohort (n=511) had previously been analysed in a similar study looking at associations between corticosteroid excretion and polymorphisms in the *CYP11B1* and *CYP11B2* genes (Barr *et al.*, 2007; Freel *et al.*, 2007). In the current study, however, the remaining DNA was available for just 232 of these subjects. The genotype distribution of each polymorphism in this group was presented in Chapter 3. The association of the alleles at these polymorphic locations in *CYP17A1* with corticosteroid metabolite excretion has been assessed and the findings will now be discussed.

Power & Data Analysis

The earlier studies had calculated that 180 homozygous subjects from this cohort would be required in order to achieve 80% power to detect a difference in THS/Total F ratio of 0.004 with an α level of 0.05 (Barr *et al.*, 2007; Freel *et al.*, 2007). The size of the effect of each allele of SNPs in *CYP17A1* on corticosteroid excretion was not known however, rendering accurate power calculations for the current study difficult. In addition, the number of subjects available in this study was approximately half that of previous studies. Although this remains a relatively large study, the analysis proceeded in the knowledge that a larger number of participants may be required in order to detect excretion rate differences at similar levels of significance.

Choosing a suitable method of analysis was partly dictated by the fact that the cohort contained only two individuals with the minor homozygote genotype at position -1877 (Table 4-1). The dominant model was therefore adopted, whereby the major homozygote group is compared to a group combining heterozygotes and minor homozygotes (DD vs. Dd & dd). This model specifically tests the association of having at least one minor allele versus none at all i.e. testing whether the presence of the minor allele, whether it be one copy or two, is

associated with altered corticosteroid excretion. The dominant model is suitable for this study as it includes the data from all individuals. Previous studies of this cohort examined the allelic effect (i.e. DD vs. dd), ignoring heterozygote data, or the genotype effect (DD vs. Dd vs. dd) which addresses possible additive or 'dose-dependent' effects of alleles (e.g. do individuals with dd genotype exhibit a greater phenotypic effect than those with Dd genotype when compared to DD individuals?). The dominant model does not allow this comparison. Nonetheless, the dominant model is more appropriate for genotype groups with low numbers. Therefore, it was used to assess association of excretion rates with all seven polymorphisms in order to ensure that associations were derived in the same way and could be compared without bias. In future, it would be interesting to test the data using different models of analysis, wherever the number of individuals is sufficient to permit this.

Urinary corticosteroid excretion data were not normally distributed and non-parametric testing was employed. Various transformations, including log, inverse and square root, were performed on the data in an attempt to achieve a normal distribution pattern that would enable increased statistical power through parametric testing, but THAldo, THS, THDOC and the combination of cortisol (F) metabolites all failed to conform. Therefore non-parametric analysis was conducted on all metabolite excretion rate data. The two main methods of analysis in this dataset were the Mann-Whitney U-test and the Spearman coefficient of variation. Had the data been normally distributed, linear regression analyses might have been utilised allowing adjustment for covariates, such as gender. Instead, gender effects were assessed separately.

Demographic Variables & Steroid Excretion

The mean BMI of this hypertensive population was 27.5, and therefore not grossly over weight. Waist:hip ratio was significantly higher in males compared to females due to gender-dependent differences in fat distribution (Table 4-2). There were no genotype-dependent effects on blood pressure, BMI or WHR (Table 4-3 to Table 4-9). Interestingly, comparison of systolic blood pressure between genotype groups showed no significant differences. Recent GWAS associated the major allele of a SNP in strong LD with -1877 in the human *CYP17A1* gene with an increase in systolic blood pressure of 1.16 mmHg (Levy *et*

al., 2009; Newton-Cheh *et al.*, 2009). In fact, the BRIGHT cohort from which this subgroup was obtained was part of one of those GWAS (Newton-Cheh *et al.*, 2009). For a better understanding of the postulated contribution of corticosteroids to this systolic blood pressure increase, a comparison of -1877 CC vs. TT genotype groups would have been ideal. Furthermore, to assess whether the presence of the C allele contributed to increased blood pressure, the recessive model of analysis could have been adopted (CC+CT vs. TT). Given that the minor allele frequency is approximately 9%, urinary corticosteroid excretion data would be required for thousands of hypertensive individuals in order to attain a large enough TT genotype group for valid statistical comparison. This would be a large and expensive study. A smaller, detailed analysis of intermediary and end-product metabolites such as that described here may better provide a guide to new lines of investigation that can be pursued further using *in vitro* systems.

Highly significant correlations between the three major zona fasciculata and zona reticularis corticosteroid sub-groups were seen in this cohort. The explanation is that corticosterone, cortisol and androgen production rates are all ACTH-dependent. In addition, all three were found to be significantly different in males compared with females (Table 4-10). When corticosterone, cortisol and androgen excretion rates were stratified by genotype for the whole cohort, no significant differences were observed between genotypes at any locus. When further split by gender, a significantly higher cortisol metabolite excretion rate was noted for males of AG genotype at position -362, compared to the AA genotype (there were no males of GG genotype). Similarly, cortisol metabolite excretion was higher in the female heterozygote and minor homozygote group at positions -1204 and -2205 when compared with the major homozygote group. Interestingly, corticosterone and androgen excretion was not altered. Based on observations when using an inhibitor of *CYP17A1* clinically (Section 4.1), it would be expected that alterations in corticosterone and androgen excretion rates would occur in tandem with changes in cortisol excretion rates, due to a disturbance in the flow of the system. These results indicate a gender-dependent effect of these alleles on cortisol production alone. It should be borne in mind that the urinary androgen metabolite excretion rates in males are likely to contain a significant contribution from the testes, hence are not solely

representative of adrenal production (Auchus and Arlt 2013). The gender-specific differences in plasma cortisol levels and urinary excretion rates have previously been reported (Van Cauter *et al.*, 1996; Fraser *et al.*, 1999) but the additional genotype-dependent effects seen here are less-well explained. A recent study reported an association between increased systolic blood pressure and a variant located near *CYP17A1* (rs11191548) in female but not male children (Wu *et al.*, 2012). In isolation, theory suggests the negative feedback inhibition resulting in reduced ACTH drive, would preserve normal physiological levels (Section 1.2.1.1). The reality is more complex. For example, the presence of the minor allele at a SNP might alter transcription factor binding to the region, increasing enzyme production. An increased supply of cortisol precursors in the 17 α -hydroxy-pathway would increase cortisol production, so long as *CYP11B1* is not a limiting factor. This theory implies that increased 17 α -OH-pregnenolone and 17 α -OH-progesterone would result, providing additional substrate for 17,20 lyase. However, insufficient quantities of, for example, the cytochrome b₅ co-factor may be a limiting factor preventing an increase in this arm of the pathway and explaining the lack of increased androgen production.

Ratios of 17 α -Hydroxylase/17, 20 Lyase Activity

Ratios of levels of substrate to product can provide an index of enzymatic activity (Section 4-1). For the respective conversions of pregnenolone and progesterone to DHEA and androstenedione, such ratios would have been an ideal indicator of 17 α -hydroxylase/17,20 lyase efficiency, utilising measurements of the intermediary compounds 17 α -OH-pregnenolone and 17 α -OH-progesterone to provide insight into the individual hydroxylase and lyase reactions (Figure 1-7). These measurements were not made in this cohort. Instead, ratios of the urinary metabolites of DOC:S and B:F were used as indices of 17 α -hydroxylase activity, with DOC and B representing the 17-deoxysteroid pathway and S and F the 17 α -hydroxysteroid pathway. S:DHEA and F:total androgen metabolites (DHEA + aetiocholanolone + androsterone) acted as indices of 17,20 lyase activity. A disadvantage is that the ratios may also be affected by other enzymes in the pathway (e.g. *CYP11B1*, *3BHSDII* and *CYP21A1*) if these are rate-limiting and so cannot serve solely as indications of *CYP17A1* enzymatic activity. Ratios of DOC:S and B:F did not differ significantly between males and females. However, it is interesting to observe an apparent gender effect when further stratified by

genotype at positions -34, -1204, -2205, and (less convincingly) -804 and -1488. In females, ratios of THDOC:THS were lower in the presence of the minor allele at these polymorphic locations and may suggest increased activity of 17 α -hydroxylase. This is particularly interesting as increased cortisol excretion rates were observed in females carrying the minor allele at positions -1204 and -2205. A slightly higher ACTH drive, or greater sensitivity to ACTH by the adrenal cortex has previously been postulated in females and may contribute to the effects seen here (Horrocks *et al.*, 1990). These five SNPs exhibit high LD (Chapter 3) and therefore it is not surprising that similar changes in ratios were observed. Further *in vitro* analysis is required to separate those SNPs serving merely as markers co-inherited alongside the causative SNP/SNPs.

Theoretically, similar significant genotype-dependent ratios may be expected for DOC:S and B:F, since the former are precursors of the latter compounds. The data presented here do not comply with this prediction (Table 4-18 to Table 4-25). There are several possible explanations. Firstly the 11 β -hydroxylase (*CYP11B1*) enzyme converts DOC to B and S to F. It is possible that this enzyme step is at or near capacity, which has previously been suggested (McManus 2012). This would be reflected in ratios of the urinary metabolite excretion rates of DOC:B and S:F. 11 β -hydroxylase has previously been implicated in the development of hypertension (Section 1.1.3.1 and Section 1.3.3.2) and may also be separately impaired in these subjects. In fact, previous studies on this cohort have suggested altered 11 β -hydroxylase activity in the presence of a particular allele (Freel *et al.*, 2007). Secondly increased levels of DOC (and corticosterone) and decreased levels of 11-deoxycortisol (and cortisol) are evident in individuals with 17 α -hydroxylase deficiency and mineralocorticoid hypertension (Dhir *et al.*, 2009; Neres *et al.*, 2010). Future work might include collating the data from past and present studies and examining the combined effects of polymorphic variation in candidate genes.

In general, ratios of S:DHEA and F:(DHEA + aetiocholanolone + androsterone) levels were not significantly different when stratified by genotype. The F:DHEAS ratio has previously been shown to be higher in men with the metabolic syndrome (MetS) than in normal men (Phillips *et al.*, 2010). MetS is a collection of symptoms that increase cardiovascular risk (NCEP 2002). Phillips *et al.* utilised

measurements from blood samples which, given the diurnal rhythm of cortisol, may not be directly comparable to 24-hour urinary measurements.

Aldosterone

Aldosterone excretion rates of the group carrying the CC genotype at position -1877 were significantly higher than those of CT+TT group (Table 4-32). This is intriguing, as the zonation and direction of blood flow within the adrenal cortex, renders it very unlikely that *CYP17A1* could have a direct effect on aldosterone production. However, an indirect effect of ACTH has previously been proposed following the identification of significant correlation between excretion rates and levels of cortisol and androgen metabolites in hypertensive individuals with TT genotype at position -344 of the *CYP11B2* gene (Freel *et al.*, 2007). In addition, several genes required for the production of aldosterone are ACTH responsive (Miller 1988). It could be postulated that the CC genotype at position -1877 of *CYP17A1* is associated with increased ACTH drive which may, in the long term, enhance the response of aldosterone to its trophins. Long term, small increases may enhance responsiveness whereas massive increases, as seen in 17 α -hydroxylase deficiency, inhibit it completely.

SNPs in Combination

The effects of some of the polymorphisms as they exist in combination in man have been briefly explored. Investigations here have revealed SNPs at positions -34, -804, -1204, -1488 and -2205 exhibit strong linkage disequilibrium. The individual analysis of urinary corticosteroid excretion rates stratified by genotype at each of these locations displayed similar trends strengthening the notion that certain combinations of alleles are inherited together (Table 4-36, Table 4-38 and Table 4-39). It was possible that examination of SNPs in combination might produce a more pronounced effect or even a neutralising one; however, the results presented here give credence to the hypothesis that one or more of the SNPs may be functional and the rest are merely markers inherited alongside. It is unclear from these analyses whether the comparison of major and minor homozygote groups is underpowered or whether the heterozygote allelic combination is solely responsible for the effect seen on

THDOC:THS ratios. It would be necessary to examine this further in a larger population.

Overall review

There are limitations to this study imposed by the nature and quantity of the experimental material available. A comparable control group with urine measurements is lacking but this study, as a comparison of genotypes, is internally-controlled. However it would be interesting to observe whether differences observed also exist in normotensives. In addition, as described in Chapter 3, the polymorphisms of interest exist in haplotype blocks and the overall effects of these SNPs in combination have only been briefly explored here. Nonetheless, clear and convincing genotype-dependent changes in corticosteroid excretion rates were observed, despite using a smaller, albeit still large, cohort than had been employed in previous similar studies. These data provide an excellent basis both for an expanded genotype/intermediate phenotype analysis and for molecular characterisation studies to elucidate the underlying mechanisms.

4.6 Conclusions

This is the first study to explore the underlying genetic basis and consequences of polymorphic variation across the *CYP17A1* locus in a hypertensive population. Evidence is presented that genetic variation within the *CYP17A1* promoter region is related to alterations in corticosteroid levels which may contribute to the phenotype of hypertension. Further investigation into the molecular mechanisms behind these genotype-dependent corticosteroid alterations is warranted.

5 *In Vitro* Studies of CYP17A1 Transcription.

5.1 Introduction

Since there is minimal storage of steroid hormones in the adrenal cortex, an increase in the levels of circulating hormones is principally determined by the conversion of cholesterol in response to trophins that initiates in the steroidogenic pathway. The trophin of interest in this thesis is ACTH. The transcriptional regulation of steroidogenic enzymes upon ACTH stimulation is therefore a crucial factor in steroid homeostasis. This chapter will examine the functional effects of polymorphic variations in the *CYP17A1* promoter region on gene transcription.

As reviewed in Section 1.4.2, there have been numerous investigations into the transcriptional regulation of *CYP17A1*. The majority of these studies were undertaken around a decade before the work contained in this thesis. Early investigations revealed that the first 227 base pairs immediately upstream of the transcriptional start site are responsible for 60-80% of the transcriptional activity at this locus (Lin *et al.*, 2001). Transcription factors regulating adrenally-expressed *CYP17A1* are summarised in Figure 5-1, which also shows the location of their binding sites.

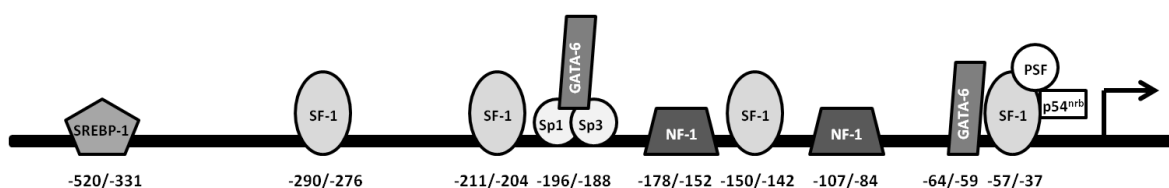


Figure 5-1 Transcription factor binding sites characterised in the human adrenally-expressed *CYP17A1* promoter region.

Locations of DNA binding regions relative to the transcription start site are provided beneath each transcription factor. SREBP-1: sterol regulatory element binding protein 1; SF-1: steroidogenic factor 1; Sp1/3: specificity protein-1/3; GATA-6: family member 6 of GATA transcription factor family; NF-1: nuclear factor 1.

The currently favoured human cell model of adrenal steroidogenesis is the NCI-H295 cell line. It is derived from an adrenocortical carcinoma that was surgically removed from a 48-year-old black female. An adherent cell line, H295R, was generated which has the ability to synthesise and secrete most adrenal steroids (Gazdar *et al.*, 1990; Rainey *et al.*, 1994). Several modified

strains of this cell line are now available, overcoming the requirement for the bovine-derived serum substitute Ultrosor G which is in limited supply. Steroid-producing capabilities are, however, greatest using Ultrosor G, so this particular strain was selected for this study. H295R cells are deemed to combine the characteristics of cells from the three zones of the adrenal cortex, hence expressing enzymes required for the biosynthesis of mineralocorticoids, glucocorticoids and androgens. The cells are responsive to the trophins AngII and potassium (K^+) but do not express the ACTH receptor and therefore do not respond to ACTH stimulation (Bird *et al.*, 1993; Mountjoy *et al.*, 1994). To overcome this issue, cells are routinely stimulated with either dibutyryl cyclic adenosine monophosphate ((Bu)₂cAMP), or Forskolin, as a substitute to mimic the intracellular activation of cAMP, which normally occurs upon stimulation by ACTH.

The data presented in Chapter 3 of this thesis identified a total of 14 polymorphisms in the region upstream from the transcriptional start site of *CYP17A1*. Of the 14, 7 SNPs had a minor allele frequency above 5% and are therefore considered a common polymorphism in the studied cohort of 60 Caucasian normotensive volunteers from the west of Scotland. The same 7 SNPs had a minor allele frequency above 5% in the hypertensive subset of the BRIGHT cohort (Table 3-2). These 7 polymorphisms were therefore chosen for further *in vitro* investigation of the hypothesis that common genetic variation can lead to subtle changes in blood pressure through effects on steroidogenesis.

5.2 Aims

The aims of this study were to investigate functional effects of common polymorphic variation in the promoter region of *CYP17A1*. By firstly using bioinformatic databases, putative transcription factor binding at the sites of polymorphic variation were identified. The polymorphic sites were then assessed and prioritised for further *in vitro* study based on these bioinformatic predictions. An *in vitro* reporter gene system was then used to determine the effects of SNP variation on *CYP17A1* basal promoter activity and in response to stimuli.

5.3 Bioinformatics

5.3.1 Methods

To investigate whether polymorphisms of interest reside within putative transcription factor binding sites, the DNA sequences flanking the SNPs were assessed using three databases. The sequences entered into each database are displayed in Table 5-1. The Transcription Element Search System (TESS) is an internet-based tool for predicting transcription factor binding sites within DNA sequences (<http://www.cbil.upenn.edu/tess>). Searches were performed on 24/09/10 using default settings; however, this resource has since been removed from service. Similar searches were performed using MatInspector software within the Genomatrix Software Suite v2.7. This software is previously described elsewhere (Quandt *et al.*, 1995; Cartharius *et al.*, 2005). In addition, polymorphic sites of interest were evaluated for putative transcription factor binding using TRANSFAC® Professional v10.1 database. This database allows DNA sequences to be compared to transcription factor binding sequences verified experimentally and published in peer-reviewed journals. The database contains an internet-based program called Match which assesses putative transcription factor binding using matrices. Matrices combine both experimentally validated transcription factor binding sequences and data extracted from published studies. Match then assigns a score of the relative likelihood of the DNA sequence binding to a particular transcription factor. The five most highly conserved bases within the sequence are termed the 'core'. Thresholds were set to the suggested value of 0.75 for core binding and 0.70 for matrix binding, with 1.0 corresponding to 100% similarity. The option to analyse only vertebrate matrices was selected. These results were obtained during a free trial of this subscription-only database.

Table 5-1 Sequences entered into bioinformatic searches for putative transcription factor binding around sites of polymorphic variation.

TSS: transcriptional start site; MAF: minor allele frequency

SNP	SNP Position Relative to TSS	MAF in AFS	MAF in BRIGHT	Sequence
rs743572 T/C	-34	0.282	0.420	tactccacTgctgtcta tactccacCgctgtcta
rs2486758 A/G	-362	0.242	0.183	ttttgcaAcatggaa ttttgcaGcatggaa
rs10883784 G/A	-804	0.210	0.304	ctcagccGgctgacac ctcagccAgctgacac
rs10786713 T/C	-1204	0.306	0.417	agacagtaTgtgcacc agacagtaCgtgcacc
rs10786714 C/G	-1488	0.210	0.304	ataaatggaCatgcaagta ataaatggaGatgcaagta
rs138009835 C/T	-1877	0.177	0.109	gagatgttGgggaagtc gagatgttTgggaagtc
rs2150927 C/T	-2205	0.306	0.413	ggtcaaaggaCaccttctggg ggtcaaaggaTcaccttctggg

Output files from all three searches were compiled within Microsoft Excel and duplicates removed. The results for each site of polymorphic variation were then compared.

5.3.2 Results

After the removal of duplicate results, in excess of 1,000 individual transcription factors were predicted to bind to the seven polymorphic sites of interest within the *CYP17A1* promoter region. Output from each search varied, as may be expected, with the freely-accessible databases providing substantially fewer matches compared to the subscription-only database. The number of individual transcription factors predicted to bind to the DNA sequences containing the flanking regions of each SNP can be found in Table 5-2.

Table 5-2 Number of transcription factor binding sites predicted by each database for the flanking sequence of each polymorphism.

TSS: transcriptional start site; TESS: Transcription Element Search System

SNP (Position relative to TSS)	Allele	TESS	MatInspector	TRANSFAC®
rs743572	T	3	0	48
(-34)	C	4	2	57
rs2486758	A	5	7	59
(-362)	G	1	3	29
rs10883784	G	2	4	34
(-804)	A	6	6	60
rs10786713	T	2	1	48
(-1204)	C	2	3	45
rs10786714	C	3	2	108
(-1488)	G	4	2	90
rs138009835	C	4	3	112
(-1877)	T	5	2	91
rs2150927	C	9	3	117
(-2205)	T	7	1	97

Opposing alleles were predicted to alter transcription factor binding for all seven SNPs of interest. Many of the predictions saw the same transcription factor bind to each site, independent of the allele at the polymorphic site, presumably with altered binding affinity. These transcription factors are not presented in this thesis, although a selection of those previously reported to regulate *CYP17A1* are presented in Table 5-3 and discussed below (Section 5.3.3). The remainder of transcription factor binding site predictions either introduced an alternative transcription factor or abolished a putative site when comparing alleles at each site. The results for each SNP are shown in Table 5-4 to Table 5-10. A literature search was then conducted to identify any previously reported transcription factors implicated in the regulation of adrenal *CYP17A1*. These are highlighted in red.

Table 5-3 Transcription factors predicted to bind to each polymorphism irrespective of allele.

SNP	SNP Position Relative to TSS	Transcription Factor	Summary	Reference
rs2486758 A/G	-362	NF-1	Nuclear Factor 1, a transcription factor shown to interact with the Sp1:Sp3 complex and regulate the basal transcription of <i>CYP17A1</i>	Lin <i>et al.</i> , 2001
rs138009835 C/T	-1877	GATA-6	GATA binding protein 6, a transcription factor expressed in the zona reticularis of the adrenal cortex and shown to regulate both <i>CYP17A1</i> and <i>CYP5A</i>	Jimenez <i>et al.</i> , 2003, Flück and Miller 2004
rs2150927 C/T	-2205	SF-1 (NR5A1)	Nuclear receptor subfamily 5 group A member 1, a transcription factor with known involvement in steroidogenesis and <i>CYP17A1</i> transcription	Sewer <i>et al.</i> , 2002, Hanley <i>et al.</i> , 2001

Table 5-4 Transcription factors predicted to bind only the T allele or the C allele at position -34 of *CYP17A1*.

Transcription factors previously implicated in the literature as being transcriptional regulators of *CYP17A1* are highlighted.

-34 (rs743572)			
T allele		C allele	
BRN1 (POU3F3)	POU class 3 homeobox 3	AP-2	Transcription factor AP-2 family
c-Myb	Homolog of v-myb myeloblastosis viral oncogene	deltaEF1 (ZEB1/ AREB6)	Zinc finger E-box binding homeobox 1
HIC1	Hypermethylated in cancer 1	BTEB3 (KLF 13)	Kruppel-like factor 13,
Kid3 (ZNF354C)	Protein with high similarity to zinc finger protein 354c	CAC binding protein	CAC binding protein
LTF	Lactoferrin	CBF	Core binding factor
NF-Y	Nuclear transcription factor Y family	CNOT3	CCR4-NOT transcription complex subunit 3
Nkx-2.5 (CSX)	NK2 homeobox 5	deltaEF1 (ZEB1/ AREB6)	Zinc finger E-box binding homeobox 1
NKX3A	NK3 homeobox 1	E2F	E2F transcription factor family
SMAD5	SMAD family member 5	Egr	Early growth response 1/family
Sox4	SRY-box 4	EKLF (KLF1)	Kruppel-like factor 1 erythroid
TTF-1 (Nkx2-1)	NK2 homeobox 1	ETF	EGFR-specific transcription factor
		FKLF (KLF 11)	Kruppel-like factor 11
		FPM315 (ZNF263)	Zinc finger protein 263
		GKLF (KLF4)	Kruppel-like factor 4
		GLI3	GLI family zinc finger 3
		INSM1	Insulinoma-associated 1
		LRF	Zinc finger and BTB domain containing 7A
		NF-E4	Transcription factor NF-E4
		Pbx-1	Pre-B-cell leukaemia transcription factor 1
		PEBP (AML1 / RUNX1)	Runt-related transcription factor 1, a transcriptional coactivator
		SNA (SNAI1)	Snail homolog 1, a transcriptional repressor
		Sp1	Sp1 transcription factor
		Sp1:Sp3	Sp1:Sp3 transcription factor complex
		Sp2	Sp2 transcription factor
		Sp4	Sp4 transcription factor
		T3RALPHA (THRA)	Thyroid hormone receptor alpha
		ZABC1 (ZNF217)	Zinc finger protein 217
		ZBP89	Zinc finger protein 148

Table 5-5 Transcription factors predicted to bind only the A allele or the G allele at position -362 of *CYP17A1*.

Transcription factors previously implicated in the literature as being transcriptional regulators of *CYP17A1* are highlighted.

-362 (rs2486758)			
A allele		G allele	
Dec1	Basic helix-loop-helix family member e40	AhR	Aryl hydrocarbon receptor
PEBP (AML1 / RUNX1)	Runt-related transcription factor 1	BEN (GTF2IRD1)	GTF2I repeat domain-containing 1
deltaEF1 (ZEB1/AREB6)	Zinc finger E-box binding homeobox 1	KAISO (ZBTB33)	Zinc finger and BTB domain containing 33
BRCA1:USF2	Breast cancer 1 early onset: Upstream transcription factor 2 complex	MafA	V-maf musculoaponeurotic fibrosarcoma oncogene homolog A
c-Myb	Homolog of v-myb myeloblastosis viral oncogene	SAP-1a (ELK4)	ELK4 ETS-domain protein
Ebox	Enhancer box	SMAD1	SMAD family member 1
Evi-1 (MECOM)	MDS1 and EVI1 complex locus	SMAD5	SMAD family member 5
FAC1 (BPTF)	Bromodomain PHD finger transcription factor		
FOXO4	Forkhead box O4		
HIF-1alpha	Hypoxia inducible factor 1 alpha		
HIF-2alpha (EPAS1)	Endothelial PAS domain protein 1		
HMG1Y (HMGA1)	High mobility group AT-hook 1		
HNF-3alpha (FOXA1)	Forkhead box A1		
HNF-3beta (FOXA2)	Forkhead box A2		
MITF	Microphthalmia-associated transcription factor		
MRF-2 (ARID5B)	AT rich interactive domain 5B (MRF1-like)		
MYB	Homolog of v-myb myeloblastosis viral oncogene family		
N-MYC	V-myc myelocytomatosis viral related oncogene neuroblastoma derived		
POU5F1 (Oct3)	POU class 5 homeobox 1		
Prx2	Paired related homeobox 2		
Sox17	SRY (sex determining region Y)-box 17		
Sox18	SRY (sex determining region Y)-box 18,		
Sox4	SRY (sex determining region Y)-box 4,		
Sox5	SRY (sex determining region Y)-box 5		
TFE (TFEA/TFE3)	Transcription factor E3		

Table 5-6 Transcription factors predicted to bind only the G allele or the A allele at position -804 of *CYP17A1*.

Transcription factors previously implicated in the literature as being transcriptional regulators of *CYP17A1* are highlighted.

-804 (rs10883784)			
	G allele		A allele
AP-2beta	Transcription factor AP-2 beta	AP1	Activating enhancer binding protein 1
BTEB3 (KLF 13)	Kruppel-like factor 13	CCAAT box	CCAAT box
E2F	E2F transcription factor family	c-MAF	v-maf musculoaponeurotic fibrosarcoma oncogene homolog
ELK-1	ELK1 member of ETS oncogene family	Dec	Basic helix-loop-helix family members
Erm (ETV5)	ETS variant 5	deltaEF1 (ZEB1)	Zinc finger E-box binding homeobox 1
FKLF (KLF 11)	Kruppel-like factor 11	E12 (TCF3)	Transcription factor 3 (also E2A/E47)
MECP2	Methyl CpG binding protein-2	Ebox	Enhancer box
Sp1	Sp1 transcription factor	Fra-1 (FOSL1)	FOS like antigen 1
		GCMa	Glial cells missing homolog 1
		HTF4 (TCF12)	Transcription factor 12
		JunB	Jun B proto-oncogene
		Kid3 (ZNF354C)	Similarity to zinc finger protein 354c
		Lmo2 (RBTN2)	LIM domain only 2
		MEIS1A:HOXA9	Meis homeobox 1: Homeobox A9
		MITF	Microphthalmia-associated TF
		MRF4 (myf6)	Myogenic factor 6
		MyoD	Myogenic differentiation 1
		N-Myc	V-myc myelocytomatosis derived
		p53 (TP53)	Tumour protein p53
		REX1 (ZFP42)	Zinc finger protein 42 homolog
		RP58 (ZBTB18)	Zinc finger protein 238, C2H2-type
		slug (SNAI2)	Snail homolog-2
		SMAD2	SMAD family member 2
		SNA (SNAI1)	Snail homolog 1
		SREBP1 (SREBF1)	Sterol regulatory element binding 1
		TTF-1 (Nkx2-1)	NK2 homeobox 1
		TWIST	Twist homolog 1
		USF	Upstream transcription factor 1
		USF2	Upstream transcription factor 2
		YY1	YY1 transcription factor
		ZF5 (ZPB161)	Zinc finger protein 161 homolog

Table 5-7 Transcription factors predicted to bind only the T allele or the C allele at position -1204 of *CYP17A1*.

Transcription factors previously implicated in the literature as being transcriptional regulators of *CYP17A1* are highlighted.

-1204 (rs10786713)			
T allele		C allele	
Oct1 (POU2F)	POU class 2 homeobox 1	Dec1 (BHLHE40)	Basic helix-loop-helix family member e40
PEBP (AML1 / RUNX1)	Runt-related transcription factor 1	ChREBP (MLXIPL)	MLX interacting protein-like, a bHLH transcription factor
GR (NR3C1)	Nuclear receptor subfamily 3 group C member 1/ glucocorticoid receptor	HSF2	Heat shock transcription factor 2
MafA	V-maf musculoaponeurotic fibrosarcoma oncogene homolog A	MITF	Microphthalmia-associated transcription factor
mef2A	Myocyte enhancer factor 2A	MyoD	Myogenic differentiation 1
MEF-2C	Myocyte enhancer factor 2C	p53 (TP53)	Tumour protein p53
MEF-2D	Myocyte enhancer factor 2D	TR4 (NR2C2)	Nuclear receptor subfamily 2 group C member 2
MRF4 (myf6)	Myogenic factor 6	TTF-1 (Nkx2-1)	NK2 homeobox 1
Osf2 (AML3/ RUNX2)	Runt-related transcription factor 2	USF2	Upstream transcription factor 2
SNA (SNAI1)	Snail homolog 1	ZF5 (ZBTB14/ZPB161)	Zinc finger protein 161 homolog
Sox5	SRY (sex determining region Y)-box 5		
SREBP1 (SREBF1)	Sterol regulatory element binding transcription factor 1		
TBP	TATA box binding protein		
YY1	YY1 transcription factor		
ZNF333	Zinc finger protein 333		

Table 5-8 Transcription factors predicted to bind only the C allele or the G allele at position -1488 of CYP17A1.

Transcription factors previously implicated in the literature as being transcriptional regulators of CYP17A1 are highlighted.

-1488 (rs10786714)			
	C allele		G allele
Dec1	Basic helix-loop-helix family member e40	AP-3	Activating enhancer binding protein 3
AhR	Aryl hydrocarbon receptor	AP-4	Activating enhancer binding protein 4
AR	Androgen receptor	ATF5	Activating transcription factor 5
Arnt	Aryl hydrocarbon receptor nuclear translocator	CDP CR3+HD	Cut-like homeobox 1
COUP-TF1	Chicken ovalbumin upstream promoter transcription factor 1	deltaEF1 (ZEB1)	Zinc finger E-box binding homeobox 1
ER-alpha (ESR1)	Estrogen receptor 1	E12 (TCF3/ E2A/ E47)	Transcription factor 3
ER-beta (ESR2)	Estrogen receptor 2	Gfi1b	Growth factor independent 1B
ERR1 (ESRRA)	Estrogen-related receptor alpha	HTF4 (TCF12)	Transcription factor 12
Evi-1 (MECOM)	MDS1 and EVI1 complex locus	ING4	Inhibitor of growth family member 4
FXR (NR1H4)	Nuclear receptor subfamily 1 group H member 4	MafA	V-maf musculoaponeurotic fibrosarcoma oncogene homolog A
HIC1	Hypermethylated in cancer 1	MATH1 (ATOH1)	Atonal homolog 1
HIF-1alpha	Hypoxia inducible factor 1 alpha	MRF4 (Myf6)	Myogenic factor 6,
HIF1A:ARNT	Aryl hydrocarbon receptor nuclear translocator:Hypoxia inducible factor 1 alpha complex	MyoD	Myogenic differentiation 1
HIF-2alpha (EPAS1)	Endothelial PAS domain protein 1	MZF1	Myeloid zinc finger 1
KAISO (ZBTB33)	Zinc finger and BTB domain containing 33	NeuroD	Neuronal differentiation 1
LTF	Lactoferrin	NF-E2	Nuclear factor erythroid derived 2
MEIS1	Meis homeobox 1	PAX5	Paired box 5
MITF	Microphthalmia-associated transcription factor	POU6F1	POU class 6 homeobox 1
MIZF	Histone H4 transcription factor	RFX	Regulatory factor X 1
Msx-1	Msh homeobox 1	Smad2	SMAD family member 2ator
Nanog	Nanog homeobox	Smad3	SMAD family member 3
NR1B1 (RARA)	Retinoic acid receptor alpha	Sp2	Sp2 transcription factor
NR1B2 (RARB)	Retinoic acid receptor beta	Tal-1	T-cell acute lymphocytic leukemia 1
NR4A2 (NURR1)	Nuclear receptor subfamily 4 group A member 2	Whn (FOXN1)	Forkhead box N1
p53 (TP53)	Tumor protein p53	WT1	Wilms tumor 1
Pbx	Pre-B-cell leukemia transcription factor 1		
RAR-gamma	Retinoic acid receptor gamma		
SMAD	SMAD family member		
Sox17	SRY (sex determining region Y)-box 17		
Sox5	SRY (sex determining region Y)-box 5		
TFE	Transcription factor E3		
TGIF	TGFB-induced factor homeobox-1		
TR4 (NR2C2)	Nuclear receptor subfamily 2 group C member 2		
XBP-1	X-box binding protein 1		
ZF5 (ZBTB14/ZPB161)	Zinc finger protein 161 homolog		

Table 5-9 Transcription factors predicted to bind only the C allele or the T allele at position -1877 of CYP17A1.

Transcription factors previously implicated in the literature as being transcriptional regulators of CYP17A1 are highlighted.

-1877 (rs138009835)			
	C allele		T allele
AhR	Aryl hydrocarbon receptor	Evi-1 (MECOM)	MDS1 and EVI1 complex locus
AP-2alpha	Transcription factor AP-2 alpha	FOXD3 (HFH2)	Forkhead box D3
AP-4	Activating enhancer binding protein 4	GLI1	GLI family zinc finger 1
CEBPepsilon	CCAAT enhancer binding protein epsilon	HES1	Hairy and enhancer of split 1
DMRT4 (DMRTA1)	DMRT-like family A1	Kid3 (ZNF354C)	Protein with high similarity to zinc finger protein 354c
E2F-1	E2F transcription factor 1	KROX (Egr-1)	Early growth response 1
E2F-3	E2F transcription factor 3	NF-1A	Nuclear factor IA,
HIC1	Hypermethylated in cancer 1	p300 (EP300)	E1A binding protein p300
HSF1	Heat shock transcription factor 1	Pax-4	Paired box gene 4
HSF2	Heat shock transcription factor 2	PEBP (AML1 / RUNX1)	Runt-related transcription factor 1
KAISO (ZBTB33)	Zinc finger and BTB domain containing 33	RREB-1	Ras responsive element binding protein 1
RNF96 (TRIM28)	Tripartite motif-containing 28	Sox9	SRY (sex determining region Y)-box 9
SAP-1a (ELK4)	ELK4 ETS-domain protein	SREBP1 (SREBF1)	Sterol regulatory element binding transcription factor 1
SMAD5	SMAD family member 5	TBP	TATA box binding protein
STAT3	Signal transducer and activator of transcription 3	TBR2 (EOMES)	Eomesodermin
VBP (TEF)	Thyrotrophic embryonic factor	TBX5	T-box 5,
XBP1	X-box binding protein 1	USF	Upstream transcription factor 1
		YB-1	Y-box binding protein 1
		Zscan4	Similar to zinc finger and SCAN domain containing 4

Table 5-10 Transcription factors predicted to bind only the C allele or the T allele at position -2205 of CYP17A1.

Transcription factors previously implicated in the literature as being transcriptional regulators of CYP17A1 are highlighted.

-2205 (rs2150927)			
	C allele		T allele
Dec1	Basic helix-loop-helix family member e40	Oct1 (POU2F1)	POU class 2 homeobox 1,
AhR, Arnt, HIF-1	Aryl hydrocarbon receptor, Aryl hydrocarbon receptor nuclear translocator, Hypoxia inducible factor 1 alpha	CDP (CUX1)	Cut-like homeobox 1
AP-4	Activating enhancer binding protein 4	DMRT1	Doublesex and mab-3 related transcription factor 1
AR	Androgen receptor	DMRT2	Doublesex and mab-3 related transcription factor 2
Arnt	Aryl hydrocarbon receptor nuclear translocator	DMRT3	Protein has low similarity to mouse Dmrt2
BTEB2 (KLF5)	Kruppel-like factor 5	DMRT4 (DMRTA1)	DMRT-like family A1
COUP-TF1 (NR2F1)	Nuclear receptor subfamily 2 group F member 1	Evi-1 (MECOM)	MDS1 and EVI1 complex locus
COUP-TF2 (NR2F2)	Nuclear receptor subfamily 2 group F member 2	GATA-1	GATA binding protein 1
E12 (TCF3/ E2A/ E47)	Transcription factor 3	GATA-2	GATA binding protein 2
Ebox	Enhancer box	GATA-3	GATA-binding protein 3
ER-alpha (ESR1)	Estrogen receptor 1	GATA-4	GATA binding protein 4
ER-beta (ESR2)	Estrogen receptor 2	GATA-5	GATA binding protein 5
ERR2 (ESRRB)	Estrogen-related receptor beta	GATA-6	GATA binding protein 6
FXR (NR1H4)	Nuclear receptor subfamily 1 group H member 4	HMGYI (HMGA1)	High mobility group AT-hook 1
GCNF (NR6A1)	Nuclear receptor subfamily 6 group A member 1	Lmo2 (RBTN2) complex	LIM domain only 2
Gm397	Similar to zinc finger and SCAN domain containing 4	TEF-1 (TEAD1)	TEA domain family member 1
HES1	Hairy and enhancer of split 1		
HIF-1alpha	Hypoxia inducible factor 1 alpha		
HIF-2alpha (EPAS1)	Endothelial PAS domain protein 1		
HTF4 (TCF12)	Transcription factor 12		
Kid3 (ZNF354C)	Protein with high similarity to zinc finger protein 354c		
MATH1 (ATOH1)	Atonal homolog 1		
MEIS1	Meis homeobox 1		
MEIS1B:HOXA9	Meis homeobox 1: Homeo box A9 complex		
MRF4 (myf6)	Myogenic factor 6		
Myc (c-myc)	V-myc myelocytomatosis viral oncogene homolog		
MyoD	Myogenic differentiation 1		
Neuro D	Neuronal differentiation 1		
Nkx-2.5 (CSX)	NK2 homeobox 5		
NKX2B	NK2 homeobox 2 (NKX 2-2)		
N-Myc	V-myc myelocytomatosis viral related oncogene neuroblastoma derived		
NR1B1 (RARA)	Retinoic acid receptor alpha		
NR1B2 (RARB)	Retinoic acid receptor beta		
p300 (EP300)	E1A binding protein p300		
Pax-4	Paired box gene 4		
RAR-gamma	Retinoic acid receptor gamma		
RFX	Regulatory factor X 1		
RORalpha1	RAR-related orphan receptor A		
slug (SNAI2)	Snail homolog-2		
SMAD	SMAD family member		
Sox5	SRY (sex determining region Y)-box 5		
Sp1	Sp1 transcription factor		
SREBP1 (SREBF1)	Sterol regulatory element binding transcription factor 1		
SREBP-2 (SREBF2)	Sterol regulatory element binding transcription factor 2		
TGIF	TGFB-induced factor homeobox-1		
TR4 (NR2C2)	Nuclear receptor subfamily 2 group C member 2,		
TWIST	Twist homolog 1		
USF	Upstream transcription factor 1		
Whn (FOXP1)	Forkhead box N1		
WT1	Wilms tumor 1		
Zscan4	Similar to zinc finger and SCAN domain containing 4		

5.3.3 Discussion

Bioinformatic searches yielded numerous putative transcription factor binding sites for each polymorphic site of interest in the *CYP17A1* promoter. Furthermore, several transcription factor binding sites are introduced or eliminated by single nucleotide substitutions. In an attempt to prioritise polymorphic sites for further *in vitro* investigation, a literature search was conducted to identify any predicted transcription factors already known to be involved in the regulation of *CYP17A1* or steroidogenesis. All seven SNP sites yielded at least one potentially interesting putative transcription factor binding site, summarised in Table 5-11.

Table 5-11 Transcription factors implicated in the regulation of *CYP17A1*.

TSS: transcription start site

SNP (Position relative to TSS)	Transcription Factor	Bind to Major allele	Bind to Minor allele	Reference
rs743572 (-34)	Sp1		✓	Flück and Miller 2004
	Sp1:Sp3		✓	Lin <i>et al.</i> , 2001
rs2486758 (-362)	NF-1	✓	✓	Lin <i>et al.</i> , 2001
rs10883784 (-804)	Sp1	✓		Flück and Miller 2004
	SREBP1 (SREBF1)		✓	Ozbay <i>et al.</i> , 2006
rs10786713 (-1204)	SREBP1 (SREBF1)	✓		Ozbay <i>et al.</i> , 2006
rs10786714 (-1488)	COUP-TF1	✓		Wang <i>et al.</i> , 1989, Shibata <i>et al.</i> , 2003
rs138009835 (-1877)	GATA-6	✓	✓	Jimenez <i>et al.</i> , 2003, Flück and Miller 2004
	SREBP1 (SREBF1)		✓	Ozbay <i>et al.</i> , 2006
rs2150927 (-2205)	COUP-TF1	✓		Wang <i>et al.</i> , 1989, Shibata <i>et al.</i> , 2003
	COUP-TF2	✓		Wang <i>et al.</i> , 1989, Shibata <i>et al.</i> , 2003
	SF-1 (NR5A1)	✓	✓	Sewer <i>et al.</i> , 2002, Hanley <i>et al.</i> , 2001
	Sp1	✓		Flück and Miller 2004
	SREBP1 (SREBF1)	✓		Ozbay <i>et al.</i> , 2006
	GATA-6		✓	Jimenez <i>et al.</i> , 2003, Flück and Miller 2004

The literature regarding the transcription factors displayed in Table 5-11 has been presented and discussed in Section 1.4.2. The transcription factor SREBP-1 has been shown to bind a region 520 to 331 bases upstream of the *CYP17A1* transcriptional start site, but bioinformatic analysis does not predict the binding

location to include the polymorphic site at position -362. Therefore, none of the transcription factors already known to regulate *CYP17A1* expression in the adrenal gland bind the polymorphic regions of interest.

The vast majority of published literature focuses on the initial 227 base pairs of the promoter region as this is believed to account for 60-80% of basal transcription of *CYP17A1* (Lin *et al.*, 2001). Therefore a considerable amount of basal transcription, and cAMP-dependent transcription too, has yet to be accounted for. The promoter region of human *CYP17A1* is not precisely defined. Studies of other steroidogenic genes have identified functional polymorphisms that alter transcription factor binding 1500 to 2000 bases upstream of the transcriptional start site (Barr *et al.*, 2007; McManus *et al.*, 2012). The results presented here predict that polymorphisms have the potential to alter transcription factor binding.

The majority of transcription factors displayed in Table 5-11 are expressed in the human adrenal gland and known to regulate *CYP17A1*. The COUP-TF family are predicted to bind to sites which encompass polymorphisms at position -1488 and -2205 of the human *CYP17A1* promoter region. Thus far, COUP-TFs have been implicated in the regulation of the bovine *CYP17* gene, but evidence is lacking for a direct role in the human equivalent. Both COUP-TFI and COUP-TFII are expressed in the normal human adrenal gland and correlate inversely with increased *CYP17A1* expression in cortisol-producing adenomas (Shibata *et al.*, 2001). A study over-expressing COUP-TF *in vitro* has shown that it influences promoter activity of the human *CYP11B1* and *CYP11B2* genes involved in the latter stages of cortisol and aldosterone production (Cheng and Li 2012). Therefore a role for COUP-TF in the regulation of *CYP17A1*, either direct or indirect, is entirely plausible. Of course, Table 5-11 does not provide an exhaustive list of transcription factors that may bind to these regions, but they represent the most likely candidates given their established role in the regulation of steroidogenic gene transcription.

The volume of results generated from the freely accessible databases differed vastly from that of the subscription database. The parameters were deliberately relaxed to include candidate transcription factors with weak binding to the sequence of interest. This is likely to have generated a significant proportion of

false positive results in Table 5-4 to Table 5-10. The databases make various assumptions in order to compile their search results, which may be an additional source of error. For example, as described in Section 5.3.1, the five most highly conserved bases within the sequence are termed the 'core' binding site of the transcription factor. The user can define the threshold level at which alignment between promoter sequence and transcription factor sequence is identified. However, not all transcription factors have a core binding sequence of five nucleotides, so in some cases this may not accurately reflect a real biological binding event. Furthermore, the three-dimensional structure of both the transcription factor and target DNA strand are crucial to the specificity of binding, and may be affected by adjacent protein:DNA interactions (Sarai and Kono 2005). The results should therefore be interpreted with caution. Although *in silico* analysis must be followed by suitable laboratory investigation in order to determine definitive biological interactions, it is nonetheless a valuable tool for generating new research leads.

In summary, *in silico* analysis identified putative transcription factor binding sites at all polymorphic regions of interest. Some of the predicted transcription factors have previously been reported as being to be important in the regulation of *CYP17A1*. As *in silico* analysis failed to prioritise the polymorphic regions, all were deemed worthy of further analysis *in vitro*.

5.4 Reporter Gene Assays

Reporter construct assays are a useful tool for assessing the transcriptional activity of the promoter regions in genes of interest. The desired promoter region is cloned into a plasmid immediately upstream of a 'reporter gene', e.g. firefly luciferase. Plasmids are then transfected into a suitable cell line, which should contain the necessary signal transduction pathways and transcription factors to induce transcription. In this case, the widely-used adrenocortical carcinoma cell line, H295R, was considered the best available model for assessment of the *CYP17A1* promoter. In theory, the promoter should induce transcription of luciferase mRNA, which is, in turn, translated into protein that can be detected by a basic luciferase assay.

5.4.1 Methods

Based on the results of bioinformatic searches and those presented in Chapter 4, the decision was taken to further assess all the variants classed as 'common' polymorphic variations, i.e. those with a minor allele frequency above 5%. This is in keeping with the hypothesis of this thesis that common genetic variants are associated with small changes in blood pressure through changes in steroidogenesis.

A reporter construct (Section 2.7.2) containing 2,898 base pairs upstream from the transcriptional start site of *CYP17A1* (Figure 5-2) was a kind gift from Professor Neil Hanley, and its construction is previously described elsewhere (Hanley *et al.*, 2001). Upon arrival, the construct was verified using methods described in Section 2.7.6. This construct was then used as a template for site-directed mutagenesis to generate seven new constructs, each varying from the original by a single base at each site of interest (Section 2.7.2.1). All plasmids were prepared and verified as described in Sections 2.7.3 - 2.7.6. Transient transfection was conducted in H295R cells in cell culture dishes using appropriate controls (Section 2.8). Transfection efficiency was assessed through the co-transfection of control plasmid containing the reporter gene renilla luciferase pGL4.73 (Promega, Wisconsin, U.S.A.) at a ratio of 50:1. 24 Hours post-transfection, H295R cells were incubated under either basal conditions or following stimulation with (Bu)₂cAMP (1mM). Cells were lysed after a further 24

hours and luminescence measured by Dual-Luciferase Reporter Assay (Section 2.9).

A similar protocol was adopted to generate reporter constructs which contained the six haplotypes previously described in Chapter 3. Site-directed mutagenesis converted each base in turn to its opposing allele, as required. A reminder of the haplotypes and their frequencies within each of the populations studied in this thesis are displayed in Table 5-12. Again, H295R cells were transfected with constructs containing the various haplotypes and transcriptional activity assessed under basal and stimulated conditions.

Table 5-12 Haplotypes found in the promoter region of *CYP17A1* and their frequencies in the Adrenal Function Study population and subset of the BRIGHT cohort.

	-34	-362	-804	-1204	-1488	-2205	Frequency in Adrenal Function Study Population	Frequency in subset of the BRIGHT cohort
Hap1	T	A	G	T	C	C	44.4%	39.7%
Hap2	T	G	G	T	C	C	22.6%	18.5%
Hap3	C	A	A	C	G	T	20.2%	30.4%
Hap4	C	A	G	C	C	T	7.3%	10.9%
Hap5	T	A	G	C	C	C	1.6%	unknown
Hap6	T	A	G	T	C	T	1.6%	unknown

H295R cells can be difficult to transfect and, as a result, the magnitude of the firefly/renilla ratio varied between experiments, although the direction of change between alleles was constant. As a consequence, changes in transcriptional activity between alleles at each polymorphic site were calculated by displaying one allele as a proportion of the other. When assessing the transcriptional activity of constructs containing the various haplotypes, each is displayed as the raw firefly luciferase value normalised to renilla luciferase value. Statistical analyses were conducted on mean firefly/renilla values, with the use of \log_{10} transformation. Results displayed are the mean of four experiments, each performed in quadruplicate, with statistical significance determined by one-sample t-test using Prism 4.0 Graph Pad software, unless otherwise described.

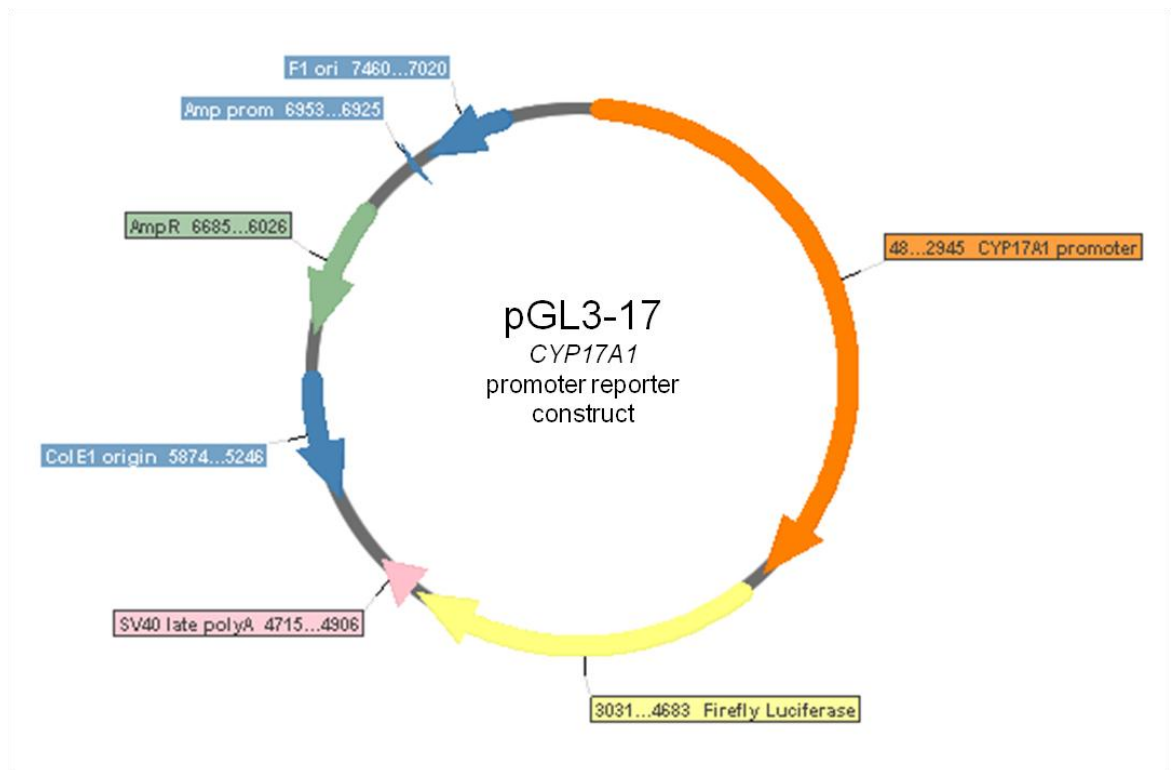


Figure 5-2 pGL3-17 - the *CYP17A1* promoter reporter construct.

2898 bp of the *CYP17A1* promoter region had been inserted into the pGL3 plasmid which contains a luciferase reporter gene. Col E1 origin: origin of replication for replication of plasmid in bacteria; SV40 late polyA: viral late polyadenylation signal; Firefly Luciferase: firefly luciferase gene; *CYP17A1* promoter: 2898 bp section of the *CYP17A1* promoter region; F1 ori: origin of replication.

5.4.2 Results – Assessment of Allele Transcriptional Activity

In order to assess the transcriptional activity of alleles at polymorphic sites of interest the pGL3-17 reporter construct was sequenced then specifically mutated at a single base to generate seven new constructs, varying from the original by a single nucleotide. This allowed comparison of the transcriptional activity of each allele at the seven polymorphic sites. Plasmids were digested before transfection to confirm their size and circular conformation (Section 5.4.2.1) and mutagenesis was verified by sequencing (Section 5.4.2.2).

5.4.2.1 Restriction Digestion of Plasmids

The pGL3-17 construct (7,761 bp) comprises approximately 2.9kb of *CYP17A1* promoter region and was previously described in Section 2.7.2. Restriction endonuclease digestion was performed on pGL3-17 and the seven mutant plasmids using the enzyme *Sma*I. *Sma*I cleaves each construct twice to create products 4841 bp and 2920 bp in size. One restriction site was located in the pGL3 backbone, the other within in the insert. Each digestion was performed alongside a negative control, or ‘uncut’ plasmid. Digestions were resolved on an agarose gel and confirm the size and circular conformation of the mutated and non-mutated experimental reporter constructs (Figure 5-3).

5.4.2.2 Confirmation of Mutations

All plasmids were directly sequenced to confirm the success of site-directed mutagenesis and the substitution of the correct allele. In addition, the entire insert and flanking regions of the construct were sequenced ensuring no nonspecific mutations had been introduced. Examples of electropherograms generated for each construct are displayed in Figure 5-4. These show that the site-directed mutagenesis procedure was successful in generating constructs with the opposing allele from that of the original pGL3-17 for each polymorphic site of interest.

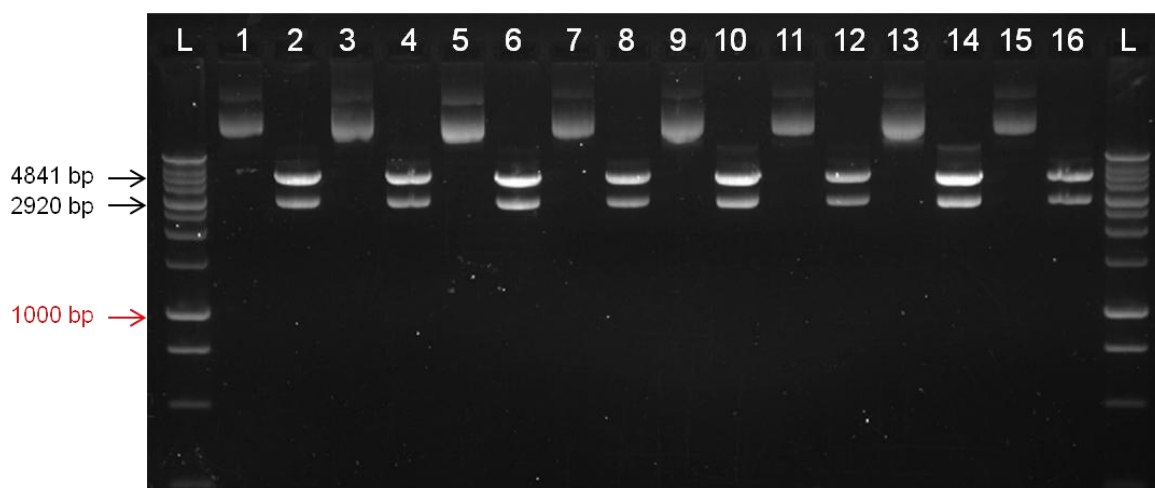


Figure 5-3 Restriction endonuclease digestion of pGL3-17 and seven mutated constructs.

1 μ g of plasmid was digested with SmaI restriction enzyme and resolved on 1% agarose gel. Promega 1 kb ladder was used for size determination (L). Lanes 1 and 2 show uncut and cut samples of the original pGL3-17 respectively. Lanes 4, 6, 8, 10, 12, 14 and 16 show cut constructs mutated at positions -34, -362, -804, -1204, -1488, -1877 and -2205 respectively. Lanes 3, 5, 7, 9, 11, 13 and 15 show uncut constructs mutated at positions -34, -362, -804, -1204, -1488, -1877 and -2205, respectively.

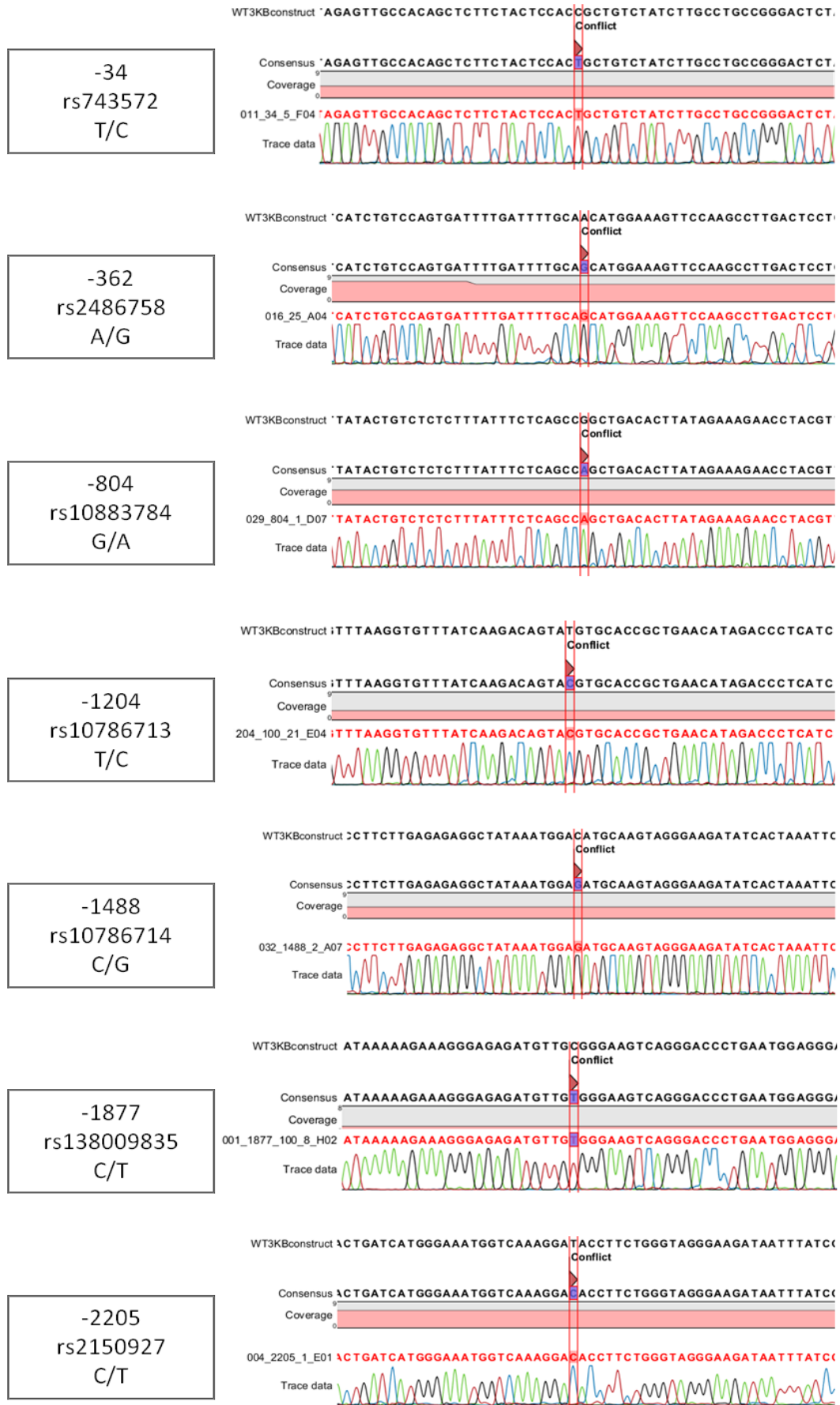


Figure 5-4 Sequence analysis of pGL3-17 mutated plasmids.

Electropherogram reads from sequence analysis of mutated constructs showing the successful incorporation of the desired mutation. Red lines show the base changed from the original pGL3-17 reporter construct. Sequencing was visualised using CLC Genomics Workbench v4.9 software.

5.4.2.3 Transcriptional Activity *in vitro*

In the first instance, the transcriptional activity of the original unmutated pGL3-17 was assessed under both basal and stimulated conditions in H295R cells, utilising the commercially available empty vector pGL3-Basic as a control. Figure 5-5 shows that the pGL3-17 plasmid increases the firefly/renilla ratio to 4.277 ± 0.314 relative to the empty vector pGL3-Basic under basal conditions ($p < 0.001$). When stimulated for 24 hours with $(\text{Bu})_2\text{cAMP}$, this effect is amplified to 10.080 ± 1.508 relative to pGL3-Basic ($p < 0.001$). The increase in transcriptional activity observed under stimulated conditions is also significant relative to basal ($p < 0.001$). This experiment successfully demonstrates that the transcriptional activity of the reporter construct arises from the insertion of approximately 2.9kb of the *CYP17A1* promoter, not from the backbone of the vector, and that this activity is further increased by stimulation with the trophin $(\text{Bu})_2\text{cAMP}$.

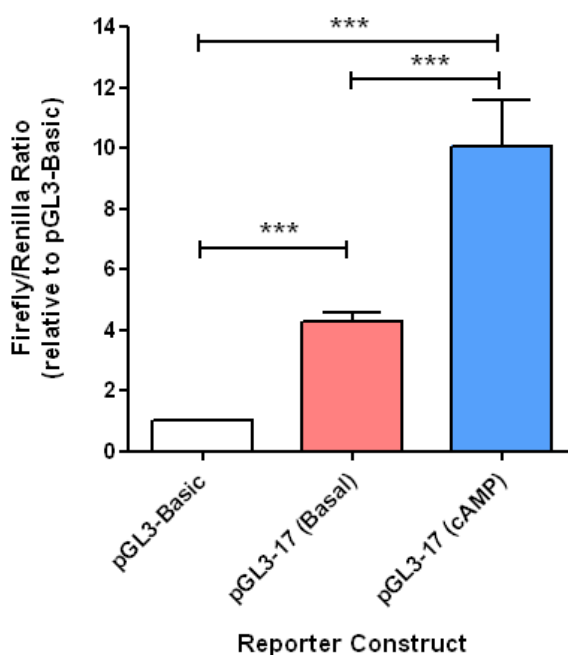


Figure 5-5 Assessment of relative levels of reporter construct activities.

H295R cells were transfected with pGL3-Basic or pGL3-17 and grown under basal or stimulated conditions. The transcriptional activity of each plasmid is displayed as a proportion of pGL3-Basic for comparison purposes, with data expressed as the mean of four independent experiments, each performed in quadruplicate; error bars represent standard error of the mean (SEM). Statistical differences were analysed by a one-way analysis of variance (ANOVA) and Bonferroni's post-hoc tests on log transformed values. *** $p < 0.001$.

Under basal conditions, H295R cells were transfected with pGL3-17 or one of the seven mutated plasmids. Cells were lysed 24 hours post-transfection and transcriptional activity assessed by measurement of firefly and renilla luciferase luminescence. Results are displayed in Figure 5-6. Transcriptional activity resulting from the plasmid with a T allele at position -34 (rs743572) was not significantly different from that with the C allele. Calculated as a proportion of the activity of the C allele construct, the mean activity of the T allele construct was 0.936 ± 0.175 ($p=0.581$). A G allele at position -362 (rs248658) however, yielded a significant increase in transcriptional activity compared to its counterpart containing an A allele (1.683 ± 0.097 , $p=0.003$). An A allele at position -804 (rs10883784) did not produce a significant change in luciferase luminescence compared to the G allele (1.015 ± 0.165 , $p=0.869$). Similarly, alternative alleles at positions -1204 (rs10786713) and -1488 (rs10786714) did not differ significantly: the C allele at -1204 measured 0.993 ± 0.186 as a proportion of its opposing T allele ($p=0.768$); the G allele at position -1488 yielded expression 0.995 ± 0.076 of the C allele ($p=0.865$). Transcriptional activity with the T allele at position -1877 (rs138009835) was significantly lower compared to the C allele at the same site (0.734 ± 0.078 , $p=0.048$). A significant change was also observed after transfection with the reporter construct containing the C allele at position -2205 (rs2150927), displaying lower activity compared to constructs containing the T allele at the same position (0.865 ± 0.032 , $p=0.031$).

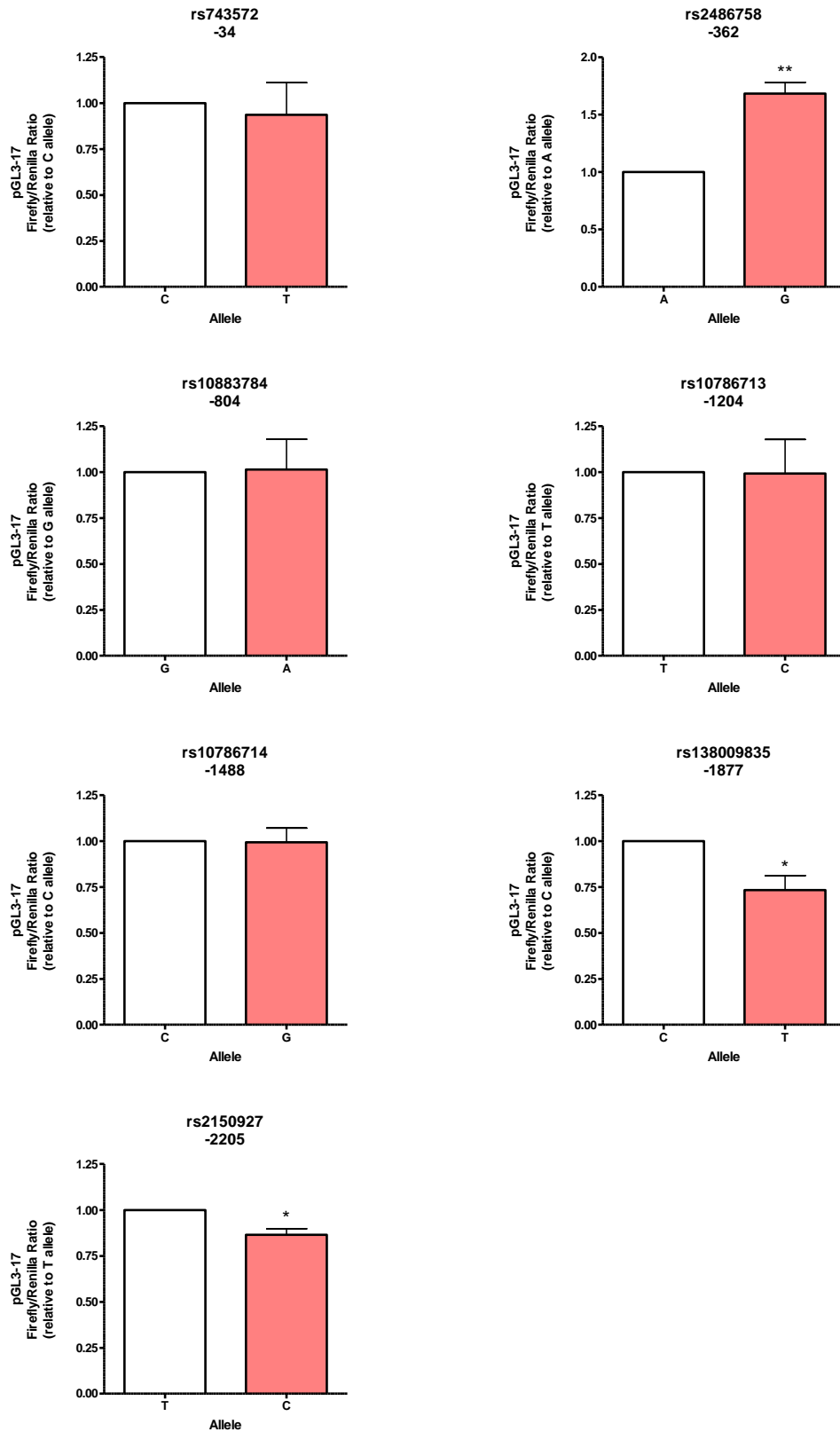


Figure 5-6 Basal expression of mutated reporter constructs relative to opposing allele.

H295R cells were transfected with identical reporter constructs varying only at the base indicated. The transcriptional activity of the base pair change induced by mutation is displayed as a proportion of its opposing allele, with data expressed as the mean of four independent experiments, each performed in quadruplicate; error bars represent standard error of the mean (SEM). Statistical differences were analysed by one-sample t-test on log transformed values. * $p < 0.05$, ** $p < 0.01$.

The above assays were also performed in cells stimulated with (Bu)₂cAMP (a substitute for ACTH) and the response of the reporter constructs examined. Results are displayed in Figure 5-7. Significant changes similar to those seen under basal conditions were observed. Transcriptional activity with the T allele at position -34 (rs743572) was not significantly different from that with the C allele. Again, calculated as a proportion of the activity of the construct containing the C allele, the mean activity from the T allele construct was 0.693 ± 0.083 , $p=0.053$. The G allele at position -362 (rs248658) however, yielded a significant increase in transcriptional activity compared to its counterpart A allele (1.458 ± 0.089 , $p=0.009$). The A allele at position -804 (rs10883784) did not produce a significant change in luciferase luminescence compared to the G allele (1.046 ± 0.170 , $p=0.970$). Similarly, the alleles at positions -1204 (rs10786713) and -1488 (rs10786714) did not result in a significant difference. The luciferase luminescence of the construct containing the C allele at -1204 was 1.075 ± 0.126 as a proportion of its opposing T allele ($p=0.705$); the G allele at position -1488 yielded expression 1.075 ± 0.083 of the C allele at this site ($p=0.447$). Transcriptional activity of the T allele at position -1877 (rs138009835) was significantly lower compared to the C allele at the same site (0.840 ± 0.062 , $p=0.049$). A significant change was also observed after transfection with the reporter construct containing the C allele at position -2204 (rs2150927) displaying lower activity compared to constructs containing the T allele at the same locus (0.625 ± 0.036 , $p=0.004$). A visual comparison of the raw firefly/renilla luciferase ratios saw a 2-3 fold increase in transcriptional activity upon stimulation compared with basal in all experiments. This is consistent with the results presented in Figure 5-5.

In summary, transcriptional activity is significantly altered by base changes at three of the seven polymorphic sites investigated. At position -362, the minor G allele exhibits a greater level of transcriptional activity compared to the major A allele. The minor T allele at position -1877 confers significantly lower activity when compared to the major C allele at the same site. Finally, the major C allele at position -2205 produced lower expression compared to the minor T allele. These effects were seen when cells were grown under basal and stimulated conditions.

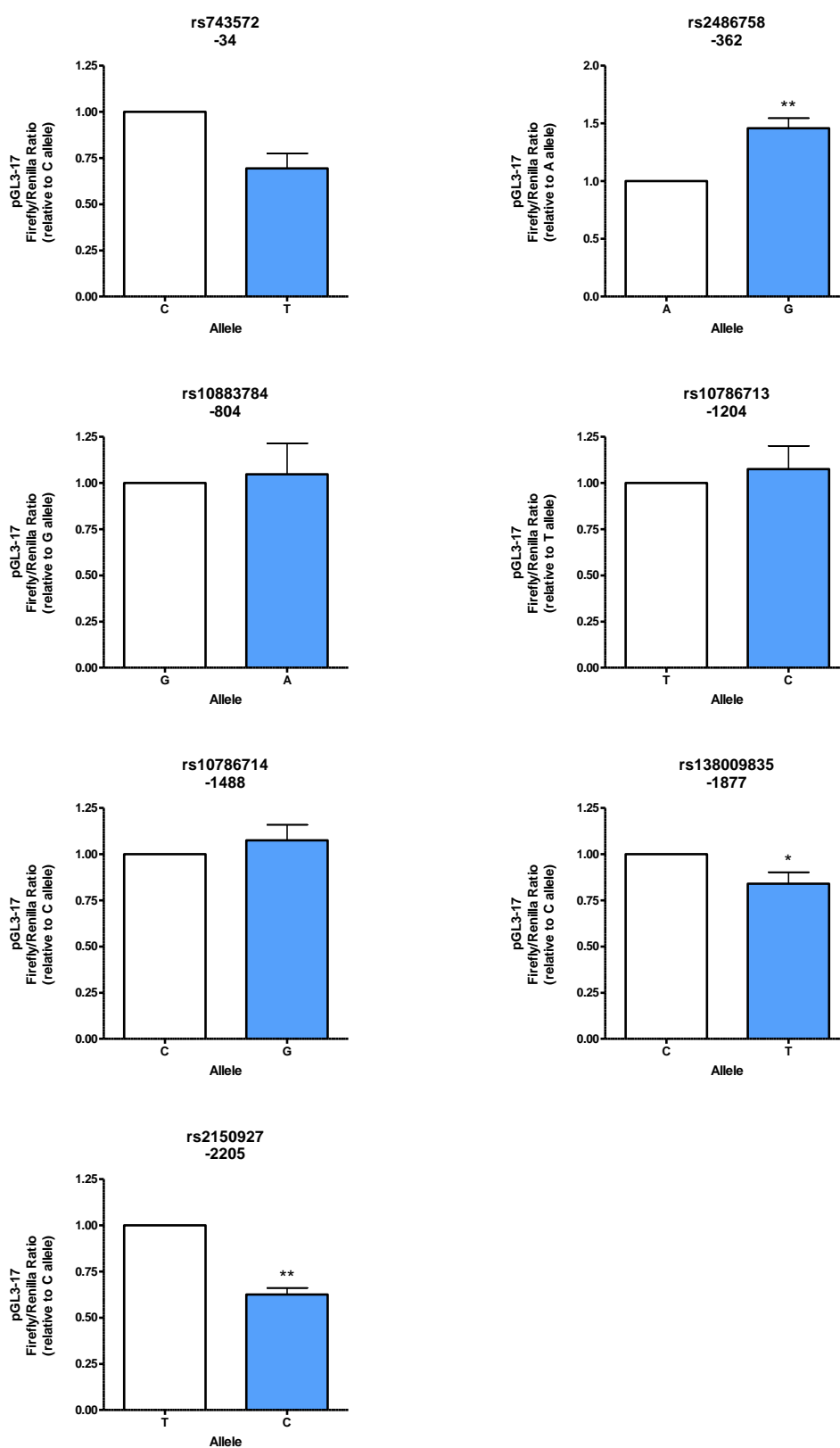


Figure 5-7 Stimulated expression of mutated reporter constructs relative to opposing allele. H295R cells were transfected with identical reporter constructs varying only at the base indicated. Cells were stimulated with 1mM (Bu)₂cAMP 24 hours post-transfection. The transcriptional activity of the base pair change induced by mutation is displayed as a proportion of its opposing allele, with data expressed as the mean of four independent experiments, each performed in quadruplicate; error bars represent standard error of the mean (SEM). Statistical differences were analysed by one-sample t-test on log transformed values. *p<0.05, **p<0.01.

5.4.3 Results – Assessment of Haplotype Transcriptional Activity

With some interesting results generated by studying the effect of single SNPs on transcriptional activity, further experiments were designed to study the effect of combinations of polymorphisms in the context of haplotypes. Site-directed mutagenesis was utilised to generate six reporter gene constructs varying only at selected polymorphic sites and encompassing the six different haplotypes (previously presented in Chapter 3).

5.4.3.1 Verification of Plasmids

Restriction endonuclease digestion was performed on each of the six reporter gene constructs containing the haplotypes of interest to assess their conformation. Plasmids were digested with the enzyme EcoRI to produce a linear product 7761 bp in size, and separately by the enzyme BglI to produce three products of sizes 5717 bp, 1268 bp and 776 bp. Products were viewed by gel electrophoresis, with uncut plasmid as a negative control (Figure 5-8).

The sequence of the plasmid insert and flanking regions were confirmed for each reporter construct. The six constructs varied only at the polymorphic sites of interest. A schematic representation of the mutations present in each plasmid to generate each haplotype reporter construct is displayed in Figure 5-9.

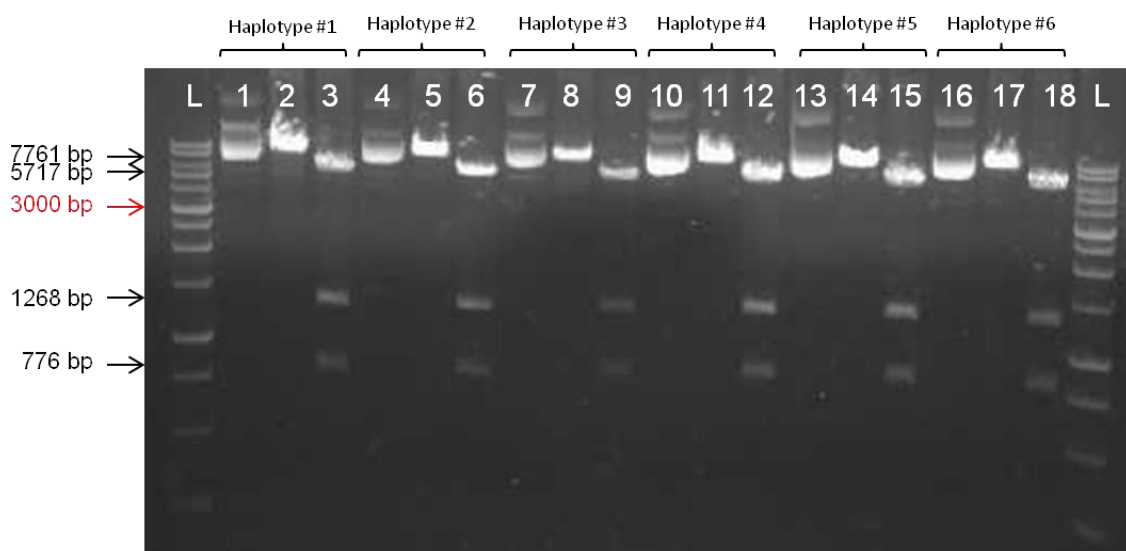


Figure 5-8 Restriction endonuclease digestion of pGL-17 haplotype reporter constructs.

1 μ g of plasmid was digested with either EcoRI or BglI restriction enzyme and resolved on 1% agarose gel. Promega 1 kb ladder was used for size determination (L). Lanes 1, 4, 7, 10, 13 and 16 show uncut plasmid for each haplotype construct. Reporter constructs in lanes 2, 5, 8, 11, 14, and 17 were linearised with EcoRI. Reporter constructs in lanes 3, 6, 9, 13, 15 and 18 were cleaved by BglI to produce three fragments.

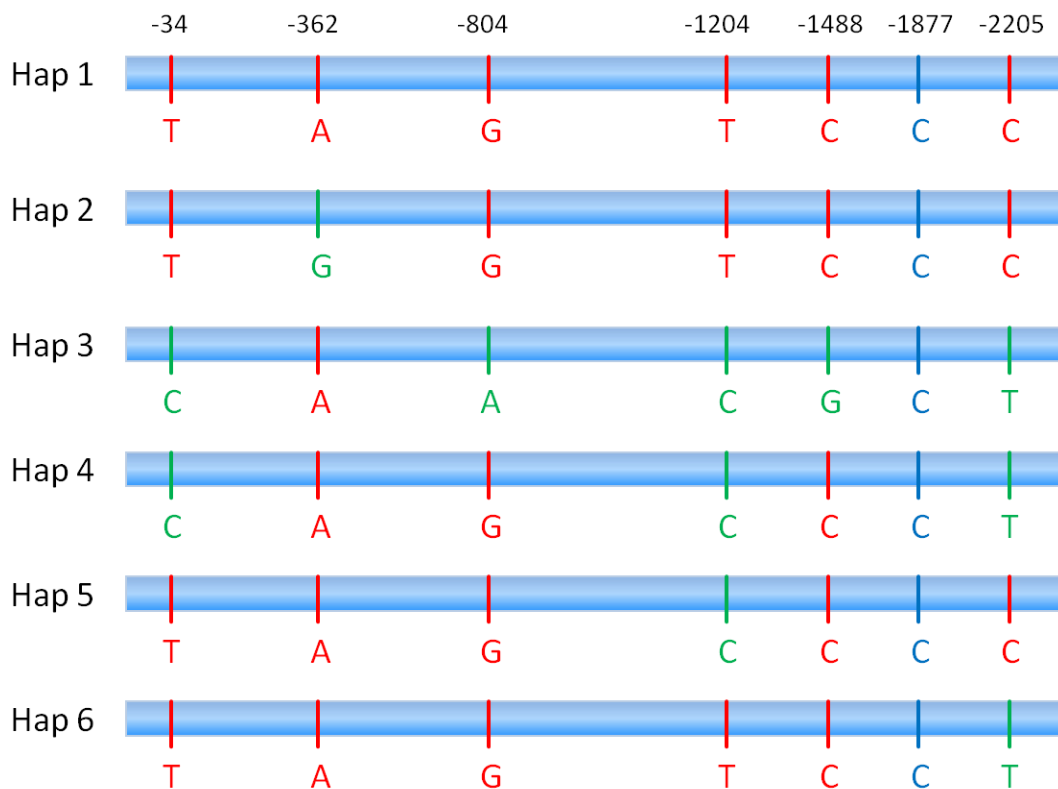


Figure 5-9 Schematic representation of alleles present in each haplotype reporter construct.

The major alleles are depicted in red, minor alleles in green. The SNP at position -1877 is not in the same LD block and was therefore the same within each haplotype construct, shown in blue.

5.4.3.2 Transcriptional Activity *in vitro*

Under basal conditions, H295R cells were separately transfected with each of the six haplotype reporter constructs. Cells were lysed 24 hours post-transfection and transcriptional activity assessed by measurement of luciferase luminescence. Results are displayed in Figure 5-10. Luciferase luminescence was not significantly different in any of the six haplotype reporter constructs.

The above assays were also performed in cells stimulated with (Bu)₂cAMP (a substitute for ACTH) and the response of the reporter constructs to stimulation examined. Results are displayed in Figure 5-11. Again, transcriptional activity was not significantly different in any of the constructs.

Luciferase luminescence produced by each construct under both basal and stimulated conditions was then compared to assess whether any was particularly responsive to stimulation. Results are displayed in Figure 5-12. Reporter constructs containing haplotype 1 transfected into cells grown under basal conditions had a mean of 0.028 ± 0.007 RLU compared to 0.085 ± 0.020 RLU under stimulated conditions; this difference was statistically significant ($p=0.03$). Haplotype 2 was not statistically different, giving means of 0.035 ± 0.103 RLU in basal conditions and 0.129 ± 0.047 RLU under stimulation ($p=0.08$). Haplotype 3 produced a significant increase in transcriptional activity under stimulation with (Bu)₂cAMP with an average of 0.136 ± 0.063 RLU compared to 0.029 ± 0.004 RLU under basal conditions ($p=0.02$). Luciferase luminescence from reporter constructs containing haplotype 4 was not significantly different in cells grown under basal and stimulated conditions (0.051 ± 0.015 RLU and 0.098 ± 0.051 RLU respectively, $p=0.39$). Similarly, the rarest haplotypes, 5 and 6, were also not significantly altered by stimulation when compared to activity under basal conditions. Basal conditions for haplotype 5 gave a mean of 0.060 ± 0.015 RLU, while stimulated conditions resulted in 0.093 ± 0.033 RLU, $p=0.48$. Haplotype 6 produced means of 0.050 ± 0.013 RLU and 0.071 ± 0.016 RLU for constructs transfected into basal and stimulated cells respectively ($p=0.32$).

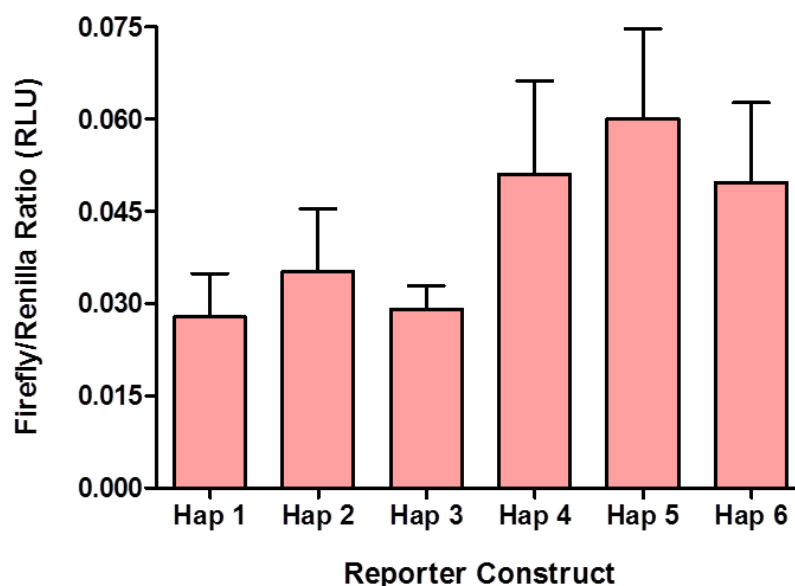


Figure 5-10 Basal expression of haplotype reporter constructs.

H295R cells were transfected with reporter constructs varying only at specific bases to reflect the indicated haplotype. The transcriptional activity of reporter constructs are displayed as raw firefly luciferase value normalised to renilla luciferase value (RLU: relative light units). Data displayed is the mean of four independent experiments, each performed in quadruplicate; error bars represent standard error of the mean (SEM). Statistical differences were analysed by one-way analysis of variance (ANOVA) and Bonferroni's post-hoc tests on log transformed values.

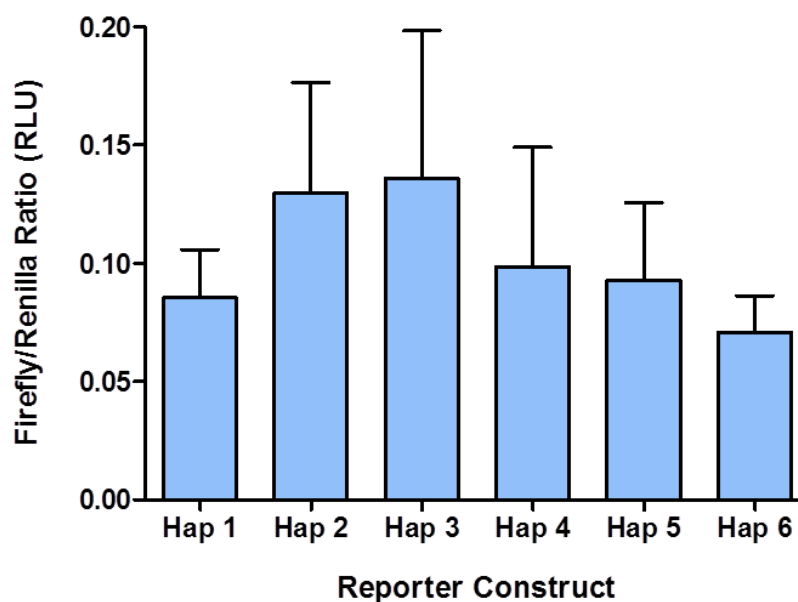


Figure 5-11 Stimulated expression of haplotype reporter constructs.

H295R cells were transfected with reporter constructs varying only at specific bases to reflect the indicated haplotype. Cells were stimulated with 1mM (Bu)₂cAMP 24 hours post-transfection. The transcriptional activity of reporter constructs are displayed as raw firefly luciferase value normalised to renilla luciferase value (RLU: relative light units). Data displayed is the mean of four independent experiments, each performed in quadruplicate; error bars represent standard error of the mean (SEM). Statistical differences were analysed by one-way analysis of variance (ANOVA) and Bonferroni's post-hoc tests on log transformed values.

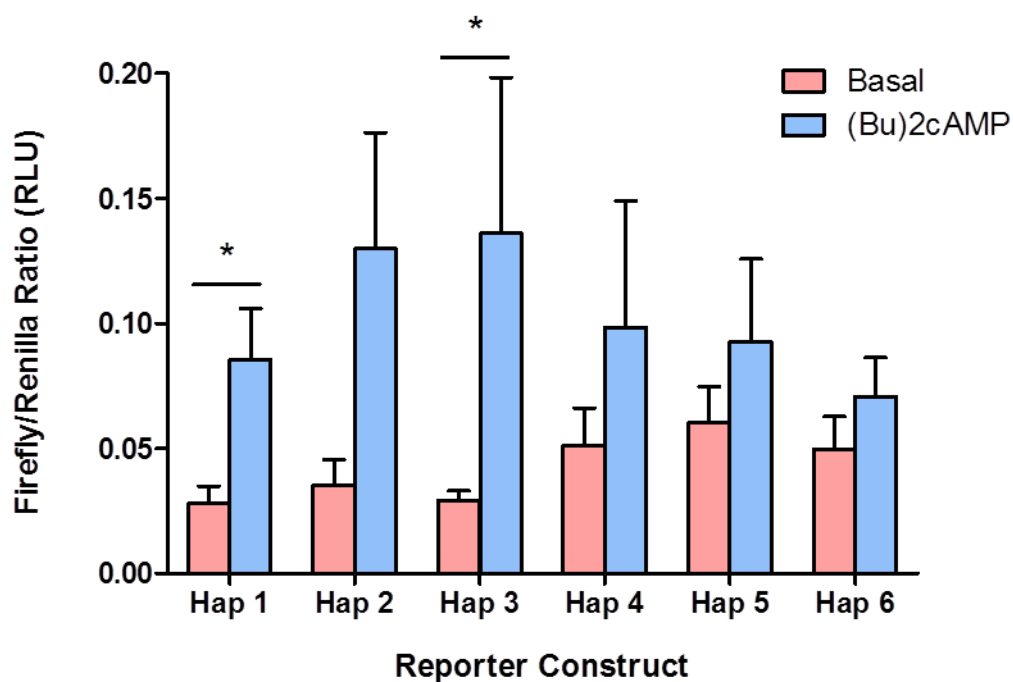


Figure 5-12 Basal versus stimulated expression of haplotype reporter constructs.

H295R cells were transfected with reporter constructs varying at specific bases to reflect the indicated haplotype. Cells were either stimulated with 1mM (Bu)₂cAMP 24 hours post-transfection or grown under basal conditions. The transcriptional activity of reporter constructs is displayed as raw firefly luciferase value normalised to renilla luciferase value (RLU: relative light units). Data displayed is the mean of four independent experiments, each performed in quadruplicate; error bars represent standard error of the mean (SEM). Statistical differences of basal vs. stimulated constructs were analysed by two-sample t-test on log transformed values. *p<0.05.

5.4.4 Discussion

The reporter gene assay utilised in the above experiments is a useful biological tool commonly used in research for assessing promoter activity. There are, however, certain limitations of this method which should be considered when interpreting the results. H295R cells proved difficult to transfect and extensive optimisation of the procedure was required. Toxicity from the transfectant solution was a key issue, although doubling the cell number and density, as recommended by the manufacturer of the transfection reagent did improve results. A plasmid expressing renilla luciferase was transfected alongside the experimental reporter constructs to control for transfection efficiency. While this is a particularly successful and robust method of controlling transfection efficiency, simultaneously transfecting two such reasonably large plasmids into cells may have hindered transfection success and cell viability. An ideal option would have been to use a reporter construct containing both firefly and renilla luciferase genes, similar to that described in Section 6.3.4.

The experiments described above made use of the Dual Luciferase Reporter Assay (DLRA) to quantify luciferase luminescence. The procedure benefits from this assay as both firefly and renilla luciferase luminescence can be measured from a single lysate, thereby simplifying the experimental procedure and reducing sample variation. This contributed to the production of reproducible and convincing results.

This is the first study to demonstrate a significant transcriptional effect of common polymorphic variation in the promoter region of *CYP17A1*. A previous study investigated the effect of the T/C polymorphism at position -34 and found no significant difference in transcriptional activity (Lin *et al.*, 2001). This is corroborated by the results presented above. To date, none of the other SNPs have been previously investigated in this way. These data show that transcriptional activity was significantly altered by the alleles present at sites -362, -1877 and -2205. The magnitude of change was similar at -362 and -1877 under basal and stimulated conditions, but, the reduction in activity from the C allele at -2205 relative to the T allele was exaggerated in response to the trophin. This suggests that the T allele at this site may be important to the regulation of the gene by ACTH and cAMP.

It is interesting that the T allele at position -1877 is associated with lower transcriptional activity than the C allele: the data presented in Chapter 3 of this thesis show this SNP to be in linkage disequilibrium with rs1004467, the SNP located in intron 3 of the gene, which was reported by the recent GWAS to have significant association with increased systolic blood pressure (Section 1.1.3.2). Therefore, it is entirely plausible that rs1004467 is simply a marker for another causative SNP within the same LD block. The major allele of rs1004467 was reported to associate with an increase in systolic blood pressure of around 1.05 mmHg, while the above data show that the major C allele at -1877 results in higher transcriptional activity than the minor T allele. The exact mechanism by which increased *CYP17A1* transcription results in increased systolic blood pressure, and what other factors may be involved, have yet to be elucidated. Nevertheless, the consistency of the results, together with data from the GWAS, justifies further investigation.

The above experiments tested variants at each locus individually and in combination. While the experiments assessing effects of single SNPs are fairly consistent, the constructs reflecting actual haplotypes produced considerably more variable results, particularly following stimulation, reflected in the wider error bars. No significant change in transcriptional activity was seen between haplotype constructs under basal or stimulated conditions. While greater variability may hide significant alterations in activity, it is also possible that a compensatory mechanism may be in place whereby the increase in activity as a result of one allele is masked by the decrease resulting from another. An increase in the number of both technical and biological replicates may reduce variability. In addition, each haplotype construct contained the C allele at position -1877. This site is not in LD with the other six polymorphisms in the normotensive cohort and the TT homozygote is particularly rare in the population. It would have been interesting to assess each haplotype construct with the T allele at -1877; if transcriptional activity had then been altered between haplotypes, it would have provided an insight into possible interactions between transcription factors at this locus.

Studying polymorphisms in combination is clearly more complex than examining each SNP individually. It is not known which, if any, transcription factors bind these regions or the exact effect that each base change has on transcription

factor binding. Useful future studies could focus on identifying the proteins binding to each site of interest, and assessing changes caused by the switch of allele, which may alter binding affinity or enable binding of an entirely different transcription factor.

In summary, reporter gene assays were used to assess the effect of polymorphisms on transcriptional activity at various sites of interest. Examining each SNP individually produced convincing results, with significant changes observed at positions -362, -1877 and -2205, under both basal and stimulated conditions. Reporter constructs were then generated to reflect haplotypes identified from the normotensive population described in Chapter 3. However, results from these experiments were considerably more variable and no significant changes were observed between the various haplotypes. The variability of the haplotype data may mask significant functional changes; this highlights the difficulty of studying transcriptional regulation of genes, where polymorphic regions provide an additional layer of complexity.

5.5 Conclusions

In conclusion, bioinformatic analysis has identified numerous putative transcription factor binding sites at seven polymorphic sites of interest. The transcriptional activities of various alleles differing at seven SNP sites were then assessed *in vitro*, both singly and in combination. Three polymorphisms showed significant allele-dependent variation in transcriptional activity. Further studies are necessary to definitively identify transcription factors binding at these polymorphic sites, with examination of sites at -362, -1877 and -2205 being a priority. This is the first study to show that allelic variation upstream of the transcriptional start site of the *CYP17A1* gene can have significant and reproducible effects on transcription. This work has opened up new avenues of investigation that may reveal a novel molecular mechanism to explain the association between genetic variation and increased blood pressure.

6 Investigating the Role of MicroRNAs in the Regulation of *CYP17A1* Expression.

6.1 Introduction

While the study of the transcriptional regulation of genes is important, research in recent years has identified post-transcriptional regulation as a new and exciting field of research. Post-transcriptional regulation by microRNA is a novel, negative regulator of mRNA abundance and protein expression (Section 1-5). Deletion of the RNase III enzyme Dicer, essential for miRNA maturation (Section 1.5.1.3), in SF-1 positive cells of mouse embryos inhibits the formation of the adrenal glands (Huang and Yao 2010), thus implying that miRNAs are of vital importance in their embryonic development. The exact role of miRNAs in the fully-formed adrenal gland is less clear. Recently published research in this field is summarised in Section 1.5.1.6, but many questions about the role of miRNAs in the regulation of steroidogenic genes remain. The question to be addressed in this chapter is whether *CYP17A1* expression in the adrenal cortex is modulated by miRNAs.

In the H295R adrenal carcinoma cell line, Wood *et al.* (2011) utilised a siRNA approach to knock down *Dicer1*, thus inhibiting the maturation of miRNAs. Two siRNAs (A and B) were designed, targeting different regions of *Dicer1* mRNA. Transfection of H295R cells with these siRNAs resulted in a significantly increased abundance of *CYP17A1* mRNA relative to control cells, consistent with canonical miRNA action (1.73 ± 0.22 fold vs 1.02 ± 0.07 fold; $p < 0.01$). 24-Hour steroid secretion was measured in the medium of transfected cells by liquid chromatography tandem mass spectrometry (LC:MS/MS) but found no significant change in cortisol production. Unfortunately, the compounds in the androgen arm of the steroidogenic pathway were not measured so it is not known whether the increase in *CYP17A1* mRNA levels translated into increased androgen production, while simultaneously leaving cortisol production unaltered. Regardless, these preliminary data imply that regulation of *CYP17A1* by miRNAs is worthy of further investigation.

6.2 Aims

The aim of this study was to assess the effect of miRNAs on the expression of adrenal *CYP17A1*. To achieve this, bioinformatic analysis was first combined with microarray expression data in order to predict which adrenal miRNAs are most likely to regulate *CYP17A1* expression. The expression of miRNAs of interest was then analysed in non-tumourous and in diseased adrenal tissue. The effect of these miRNAs on *CYP17A1* mRNA was also investigated by manipulating their levels in the adrenocortical cell line H295R, through transfection of small molecule mimics and inhibitors (i.e. Pre-miR™ and Anti-miR™). Finally, reporter construct analysis was used to assess targeting of the *CYP17A1* mRNA 3'UTR by selected miRNAs.

6.3 Materials and Methods

6.3.1 Bioinformatic Analysis

6.3.1.1 Identification of miRNA Genes Located Within *CYP17A1* Sequence

The genomic co-ordinates and sequence of *CYP17A1* were identified using the Ensembl Genome Browser (release 69 - October 2012) before being cross-referenced with known miRNA precursor sequences stored in the miRbase database, described previously in Section 1.4.1.2 (release 19 - August 2012). Default settings were used and sequences searched using the BLASTN option.

6.3.1.2 Investigation of the Evolutionary Sequence Conservation of *CYP17A1* 3'UTR

The 3'UTR of *CYP17A1* mRNA was analysed for evolutionary sequence conservation using the UCSC Genome Browser Gateway (February 2009 assembly). A graphical representation of conservation was generated for comparison using 3 primates (Chimpanzee, Gorilla and Rhesus monkey) and 5 mammals (Mouse, Rat, Rabbit, Cow and Dog).

6.3.1.3 Bioinformatic miRNA Target Prediction

To identify putative miRNA binding sites on the *CYP17A1* mRNA, a combinatorial *in silico* approach was utilised in which the results from 6 databases were collated and duplicates removed. Each program has its own unique algorithm and parameters with varying levels of stringency. Default settings were used, altering the search to include all miRNAs, not only those conserved, where possible and set to include all transcripts of the genes of interest unless otherwise stated. The miRWalk database uses a unique algorithm, which allows the selection of up to 8 independent prediction programs to be searched, while examining the entire target gene as opposed to only the 3'UTR. Areas up to 2500 bases upstream of the transcriptional start site were included in the search. It was necessary to independently examine three of the programs used by miRWalk in order to access the latest versions. The databases and versions used are summarised in Table 6-1.

Table 6-1 Bioinformatic databases used for miRNA target prediction.

Database	Version	Algorithm	Reference
MicroCosm Targets (formally miRbase)	5	miRanda	http://www.ebi.ac.uk/enright-srv/microcosm/htdocs/targets/v5/ (Griffiths-Jones 2006; Griffiths-Jones <i>et al.</i> , 2008))
TargetScan	6.2	TargetScanS	http://www.targetscan.org/vert_50/ (Lewis <i>et al.</i> , 2005; Grimson <i>et al.</i> , 2007; Friedman <i>et al.</i> , 2009)
microrna.org	August 2010 Release Last Update: 01/11/10	Target sites by miRanda, Scores by mirSVR (Support Vector Regression)	http://www.microrna.org/microrna/home.do (John <i>et al.</i> , 2004; Betel <i>et al.</i> , 2010)
miR-viewer	June 2005, ensembl 27.1 build	miRanda	http://cbio.mskcc.org/cgi-bin/mirnaviewer/mirnaviewer.pl
miRWalk	March 2011	'miRWalk'	http://www.umm.uni-heidelberg.de/apps/zmf/mirwalk/index.html (Dweep <i>et al.</i> , 2011)
TarBase	5c	Experimentally validated miRNAs and target genes	http://diana.cslab.ece.ntua.gr/tarbase/ (Papadopoulos <i>et al.</i> , 2009)

6.3.2 Assessment of miRNA Expression in Normal Adrenal Tissue and APA Tissue

MiRNA expression profiling of four non-tumorous adrenal glands and four aldosterone-producing adenoma (APA) samples was previously conducted using μ Paraflo technology microarray (Robertson *et al.*, 2013). Manufacturers' recommendations were followed and 500 arbitrary units (AU) was used as the cut-off point for background threshold levels; microRNAs expressed at levels greater than this value were deemed to be expressed in the particular tissue. Twenty miRNAs were further selected for validation by qRT-PCR, conducted by LC Sciences (Houston, U.S.A) and is fully described elsewhere (Wood 2011). A cross-array normalisation was performed between non-tumorous adrenal and APA microarray experiments before comparing the relative signal intensities.

6.3.3 Pre-miR™ or Anti-miR™ Transfection of H295R Cells

The Pre-miR™ and Anti-miR™ molecules used are listed in Table 2-3 and were prepared as described in Section 2.8.2.1. H295R cells were transfected in 6-well cell culture dishes as detailed in Section 2.8.2.3. The cell medium was replaced at 24 hours post-transfection with either basal or (Bu)₂cAMP supplemented medium. At 48 hours post-transfection, cell medium was removed. Total RNA was

then isolated from cell lysates (Section 2.4) before being prepared for qRT-PCR analysis as described in Sections 2.5 and 2.6. Data were analysed using the $\Delta\Delta C_t$ method (Section 2.6.3) and results expressed relative to the negative control-transfected cells.

6.3.4 Investigation of miRNA Binding to 3'UTR Reporter Construct

Reporter constructs utilising a pEZX backbone were prepared as outlined in Sections 2.7.1, 2.73 - 2.76. As described in Section 2.8.2, HeLa cells were co-transfected with pEZX reporter constructs and small molecules (Pre-miR™, Anti-miR™, or siRNA) in 24-well cell culture dishes. Cell lysates were prepared 48 hours post-transfection, diluted 1:10. Firefly and renilla luciferase activities were measured using Dual Reporter Luciferase Assays (DRLA, Section 2.9). Transfection efficiency was normalised by taking the ratio of firefly luciferase activity to renilla luciferase activity, each expressed in relative light units (RLU). This ratio was then compared to the appropriate negative control and expressed as a percentage.

6.3.5 Statistical Analysis

Comparisons of miRNA expression in non-tumourous and APA tissue were statistically analysed by Student's t-test using Prism 4.0 Graph Pad software.

All transfection experiments were performed at least in triplicate on at least three independent occasions. As described above, the effect of the miRNA by the addition of Pre-miR™ or Anti-miR™ molecules was normalised to cells transfected with scrambled Pre-miR™ or Anti-miR™ negative control molecules, as appropriate. The $\Delta\Delta C_t$ method, described in Section 2.6.3, was used for analyses, with the mean $\Delta\Delta C_t$ values of the biologically independent experiments taken and statistical analysis performed using a one-sample t-test using Minitab v15 software, imputing 0.00 as the reference level to which experimental values were compared. For experiments involving co-transfection of reporter constructs and small molecules, data is displayed as a percentage of the appropriate negative control, and statistical significance determined using a Student's t-test.

For all analyses, confidence intervals of 95 % were used and $p < 0.05$ was the threshold for statistical significance. Data are expressed as the mean \pm SEM.

6.4 Results

6.4.1 Identification of miRNAs Originating from *CYP17A1* Locus

In order to identify any miRNAs located genomically within the *CYP17A1* sequence, the genomic co-ordinates of *CYP17A1* were identified using the Ensembl Genome Browser (Table 6-3). These were then cross-referenced with miRbase. Since several miRNAs are synthesised from the introns of other genes, the intronic sequence of *CYP17A1* was entered directly; matches to numerous miRNA precursor stem-loop sequences were found, as summarised in Table 6-2. However, utilising the option to search for both mature and miRNA precursor sequences based on genomic location, no positive results were returned, meaning that no miRNAs are known to arise from this location (Table 6-3).

Table 6-2 Number of precursor and mature miRNA sequences found within *CYP17A1* introns.

<i>CYP17A1</i> Intron #	Size (bases)	Number of Precursor miRNA Sequences	Number of Mature miRNA Sequences
1	1,672	87	41
2	239	12	22
3	662	4	10
4	827	77	18
5	312	5	6
6	899	53	13
7	522	9	9

Table 6-3 Genomic location information required for miRNA sequence prediction.

Gene	Chromosome Location	Start Co-ordinates	End Co-ordinates	Size (bases)	Number of Mature/Precursor miRNA Sequences
<i>CYP17A1</i>	10	104,590,288	104,597,290	7,002	0

6.4.2 Analysis of the 3'UTR of the *CYP17A1* Gene

The evolutionary conservation of the *CYP17A1* 3'UTR sequence was assessed using the UCSC Genome Browser. Results are depicted in Figure 6-1. Figure 6-1a displays the 3'UTR between the red dashed lines, with the solid black bars indicating sequence conservation. Figure 6-1b shows the entire *CYP17A1* 3'UTR consensus sequence (171 bases), with the corresponding sequence from various mammals aligned beneath. The combined figure demonstrates that the sequence is well conserved across primates such as Chimpanzee, Gorilla and Rhesus monkey, but the degree of similarity is less so for other mammals including mouse, rat, rabbit, cow and dog.

6.4.3 Identification of Putative miRNA Binding Sites in *CYP17A1*

Since many of the available programs for miRNA bioinformatic predictions utilise different algorithms and levels of stringency when searching, it was necessary to collate data from various databases in order to identify putative binding sites. The most common method of post-transcriptional regulation by miRNA acts through binding to the 3'UTR. The *CYP17A1* 3'UTR is 171 bp and the number of miRNAs predicted by each program to bind to this region is shown in Table 6-4. The predicted miRNAs were collated and duplicate results removed, providing the list in Table 6-5; the miRWalk database allows for the prediction of miRNA target sites in other gene regions and these are also listed in Table 6-5.

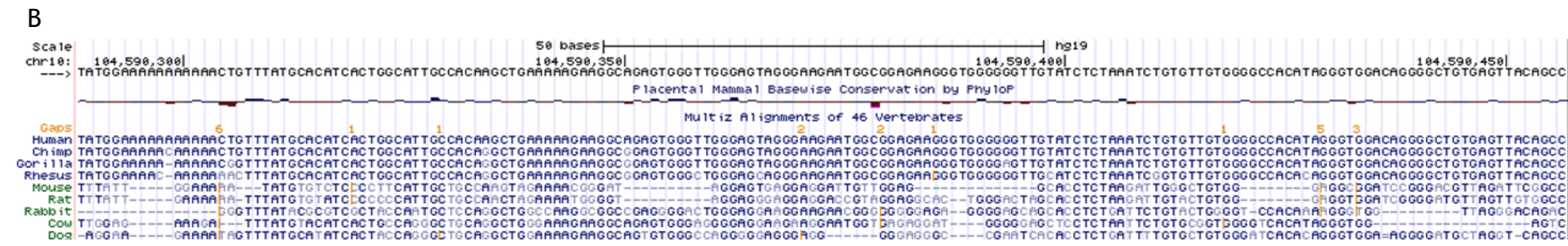
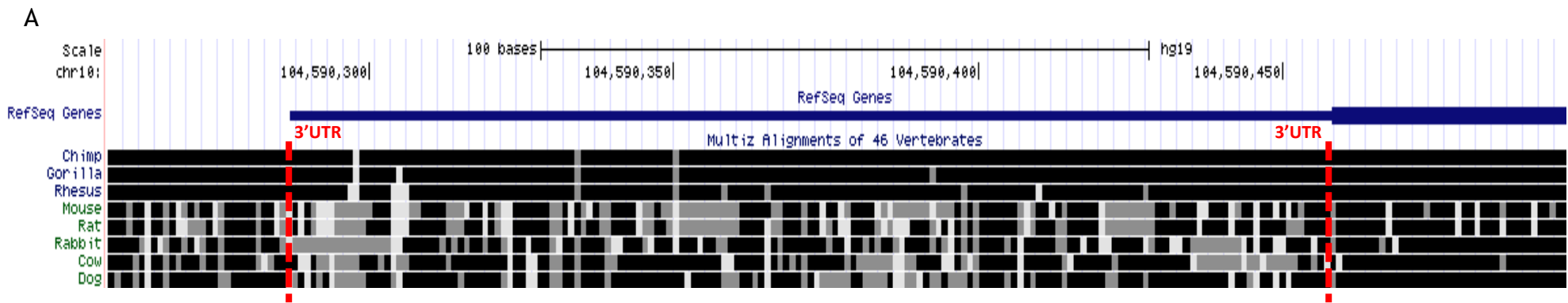


Figure 6-1 Mammalian evolutionary sequence conservation of *CYP17A1* 3'UTR.

The sequence conservation, generated by the UCSC Genome Browser Gateway for the *CYP17A1* 3'UTR across the species listed on the left-hand side. A) 3'UTR is shown by the blue bar and indicated by red dashed lines. Sequence similarity is illustrated by black bars. B) The entire human *CYP17A1* 3'UTR sequence is displayed with the 3'UTR sequence from the examined species aligned beneath.

Table 6-4 Bioinformatic miRNA target site predictions for *CYP17A1* 3'UTR.

Gene	3' UTR Length (bp)	MicroCosm	TargetScan	Microna.org	Mir-viewer	miRwalk	Tarbase	Total Unique miRNAs
<i>CYP17A1</i>	171	19	11	69	0	64	0	98

Table 6-5 Identities of miRNAs with putative binding sites in the *CYP17A1* 3'UTR, coding sequence and 5'UTR.

	3'UTR			Coding Sequence	5'UTR
hsa-let-7c*	hsa-miR-320a	hsa-miR-548x	hsa-miR-3128	hsa-miR-26a	hsa-miR-10a
hsa-miR-7	hsa-miR-320e	hsa-miR-581	hsa-miR-3133	hsa-miR-26b	hsa-miR-10b
hsa-miR-19b-2*	hsa-miR-323b-5p	hsa-miR-595	hsa-miR-3138	hsa-miR-34b	hsa-miR-31
hsa-miR-25*	hsa-miR-363*	hsa-miR-598	hsa-miR-3147	hsa-miR-138	hsa-miR-214
hsa-miR-30b*	hsa-miR-376c	hsa-miR-599	hsa-miR-3148	hsa-miR-143	hsa-miR-624
hsa-miR-30c-1*	hsa-miR-448	hsa-miR-602	hsa-miR-3149	hsa-miR-147b	hsa-miR-647
hsa-miR-30c-2*	hsa-miR-449c	hsa-miR-603	hsa-miR-3151	hsa-miR-188-3p	hsa-miR-650
hsa-miR-34b*	hsa-miR-452	hsa-miR-652	hsa-miR-3154	hsa-miR-338-3p	
hsa-miR-34c-3p	hsa-miR-491-3p	hsa-miR-654-5p	hsa-miR-3162	hsa-miR-377	
hsa-miR-92a-1*	hsa-miR-491-5p	hsa-miR-658	hsa-miR-3165	hsa-miR-382	
hsa-miR-92a-2*	hsa-miR-493	hsa-miR-744*	hsa-miR-3172	hsa-miR-453	
hsa-miR-124	hsa-miR-499-3p	hsa-miR-759	hsa-miR-3179	hsa-miR-555	
hsa-miR-125b-2*	hsa-miR-501-3p	hsa-miR-762	hsa-miR-3185	hsa-miR-556-5p	
hsa-miR-135a*	hsa-miR-502-3p	hsa-miR-875-3p	hsa-miR-4265	hsa-miR-646	
hsa-miR-185*	hsa-miR-506	hsa-miR-892b	hsa-miR-4283	hsa-miR-1231	
hsa-miR-186	hsa-miR-541	hsa-miR-940	hsa-miR-4296		
hsa-miR-187*	hsa-miR-548a-3p	hsa-miR-1253	hsa-miR-4317		
hsa-miR-193a-3p	hsa-miR-548d-3p	hsa-miR-1256	hsa-miR-4322		
hsa-miR-193b	hsa-miR-548e	hsa-miR-1275			
hsa-miR-193b*	hsa-miR-548f	hsa-miR-1293			
hsa-miR-296-3p	hsa-miR-548g	hsa-miR-3122			

6.4.4 Adrenally-Expressed miRNAs Predicted to Bind *CYP17A1* 3'UTR

MiRNA microarray analysis had previously been conducted on tissue from four non-tumorous ('normal') sections and four aldosterone-producing adenoma (APA) sections. These miRNA expression data were cross-referenced with miRNAs predicted from bioinformatic analyses to bind the 3'UTR of *CYP17A1*. This yielded three miRNAs expressed in the normal adrenal gland and three in APA tissue (Figure 6-2). Hsa-miR-376c expression was detected only in the normal adrenal tissue, whereas hsa-miR-34c-3p was detected only in APA tissue. Hsa-miR-7 and hsa-miR-320a expression was detected in both tissue types.

The microarray expression data had previously been normalised to allow comparisons between miRNA expression in the normal and diseased (APA) adrenal gland. Differentially-expressed miRNAs may indicate importance and assist in prioritising those to investigate further. Figure 6-3 shows that both miR-320a and miR-34c-3p expression are significantly different between the two tissue types. Although miR-320a is expressed in both tissues, it is significantly up-regulated in APA tissue. Similarly, miR-34c-3p expression is found to differ significantly between the tissue types, with detectable expression seen only in APA tissue. Expression of miR-7 was not found to be significantly different between normal and APA tissue. Similarly, expression of miR-376c is not significantly different between normal adrenal and APA tissue, despite only being expressed in normal tissue. This is due to the mean value in APA tissue falling just below the 500 AU cut-off for determination of expression.

Further details of the four adrenal miRNAs predicted to bind the 3'UTR of *CYP17A1* are provided in Table 6-6.

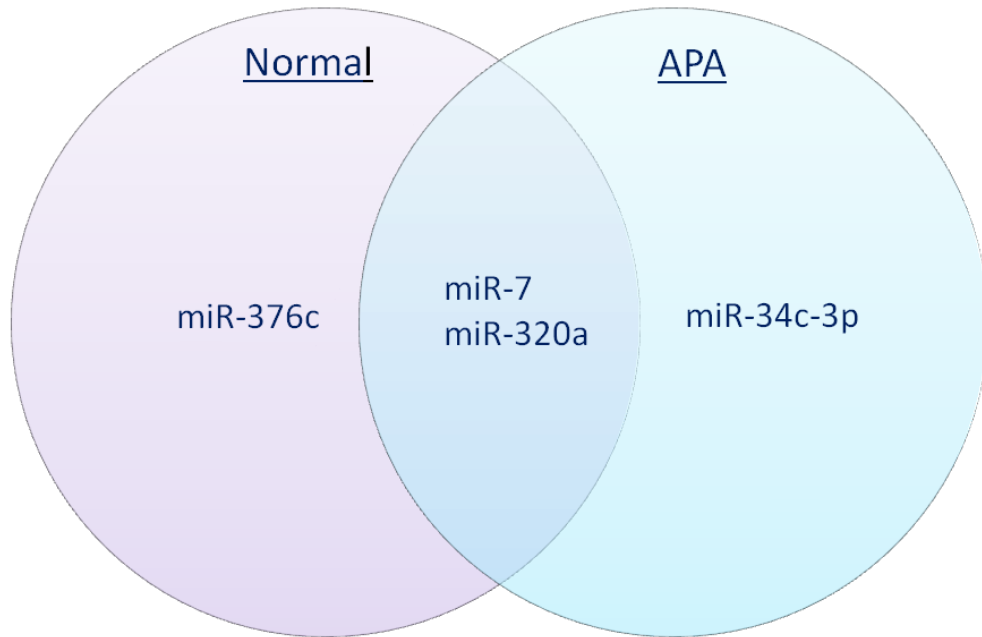


Figure 6-2 Venn diagram of miRNAs expressed in normal adrenal tissue and APA predicted to bind to the 3'UTR of *CYP17A1*.

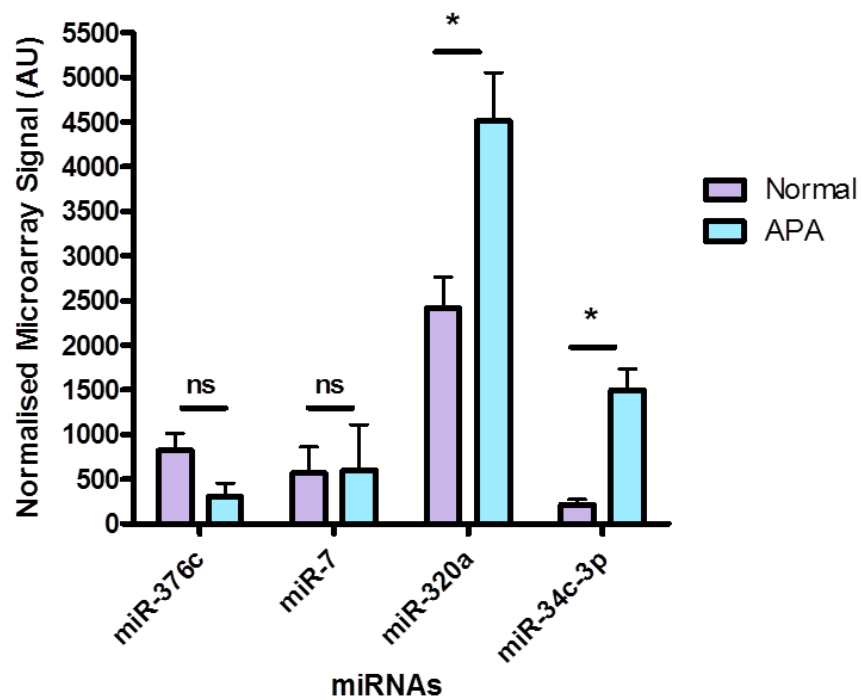


Figure 6-3 Expression analysis of miRNA predicted to bind to *CYP17A1* 3'UTR. Results show the relative expression levels of miRNAs predicted to bind to *CYP17A1* in normal adrenal (purple) or APA (blue) tissue. * $p < 0.05$

Table 6-6 Database prediction, sequence and genomic co-ordinates and base pair-matching for selected miRNAs.

miRNA	Database			miRNA Sequence & Genomic Co-ordinates	miRNA: mRNA Base Pair Match
	miRWalk	Microrna.org	microcosm		
hsa-miR-376c-3p	✓	✓		<p>aacauagaggaaauuccacgu</p> <p>14: 101,506,027 - 101,506,092 [+]</p>	<p>3' ugcaccuUaaagGaGAUACAa 5' miR-376c</p> <p style="text-align: center;">: </p> <p>5' agccccuGuccaCCUAUGUg 3' CYP17A1</p>
hsa-miR-7-5p	✓	✓		<p>uggaagacuagugauuuuguugu</p> <p>9: 86,584,663 - 86,584,772 [-]</p>	<p>3' uguuGuuuuaGUGAUCAGAAGGu 5' miR-7</p> <p style="text-align: center;"> : </p> <p>5' caccCuucucCGCCAUUCUUCc 3' CYP17A1</p>
hsa-miR-320a	✓		✓	<p>aaaagcuggguugagagggcga</p> <p>8: 22,102,475 - 22,102,556 [-]</p>	<p>3' AGcgGGAGaGuuGGGUCGAAaA 5' miR-320a</p> <p style="text-align: center;"> : : : </p> <p>5' UCUGCCUUCUUUUUCAGCUUgU 3' CYP17A1</p>
hsa-miR-34c-3p	✓	✓		<p>aaucacuaaccacacggccagg</p> <p>11: 111,384,164 - 111,384,240 [+]</p>	<p>3' gGAcCGgCacacCaaUCACUAa 5' miR-34c-3p</p> <p style="text-align: center;"> : </p> <p>5' gCUuGUgGcaauGccAGUGAUg 3' CYP17A1</p>

6.4.5 Assessment of miRNA Effect on *CYP17A1* mRNA Abundance

To investigate the actions of the miRNAs of interest on the full-length *CYP17A1* mRNA, Pre-miR™ and Anti-miR™ molecules were transfected into the H295R adrenocortical cell line, the best available model for *in vitro* investigations. Their effects were assessed by measuring the abundance of *CYP17A1* mRNA relative to transfected control cells. This procedure was previously optimised by Dr. Stacy Wood (Wood 2011) who concluded that transfection of Pre-miR™ molecules are capable of increasing the specific miRNA levels in H295R cells, while Anti-miR™ molecules are efficient at specifically decreasing the mature miRNA levels.

Based on the bioinformatic analysis cross-referenced with microarray data described earlier in this chapter, miRNAs expressed in the adrenal gland and predicted to bind to *CYP17A1* 3'UTR were identified. Both miR-320a and miR-34c-3p were found to be differentially expressed between non-tumourous and APA tissue, thus were initially selected for further investigation.

In the first instance, qRT-PCR was performed on untreated H295R cells to assess background levels of miR-320a and miR-34c-3p. The mean cycle threshold value for each miRNA is shown in Table 6-7, measured in technical triplicate on three independent occasions.

Table 6-7 qRT-PCR expression of selected miRNAs in H295R cells.

miRNA	Basal H295R Cells		H295R Cells + (Bu) ₂ cAMP	
	Ct value	Standard Error	Ct value	Standard Error
miR-320a	19.05	0.39	18.44	0.20
miR-34c-3p	22.49	0.99	23.40	1.19

Under basal conditions, cells were transfected with miR-320a-specific Pre-miR™, miR-34c-3p-specific Pre-miR™, or both Pre-miRs combined, in order to artificially increase the levels of those miRNAs in the cells. *CYP17A1* mRNA levels were measured and are displayed in Figure 6-4b relative to transfected-control cells. The relative abundance level ($RQ=2^{-\Delta\Delta Ct}$) of *CYP17A1* mRNA after transfection with miR-320a Pre-miR™ was 1.02 ± 0.12 and was not significantly different from

control cells ($p=0.959$). However, transfection with miR-34c-3p Pre-miR™ significantly reduced *CYP17A1* mRNA abundance (0.83 ± 0.02 , $p=0.012$). Transfection with both Pre-miRs™ did not significantly alter *CYP17A1* mRNA abundance (1.05 ± 0.03 , $p=0.184$). Levels of mature miR-320a and miR-34c-3p were measured post-transfection to confirm the successful transfection of the specific Pre-miRs™. Figure 6-4a shows that transfection with miR-320a Pre-miR™ significantly induced the levels of mature miR-320a in the cells with relative expression of 599 ± 86.4 , $p<0.001$; while levels of miR-34c-3p remained unaltered, as predicted (0.98 ± 0.06 , $p = 0.715$). Transfection with miR-34c-3p Pre-miR™ also had the predicted effect, increasing relative mature miR-34c-3p expression (137001 ± 52227 , $p=0.002$), with miR-320a levels unaffected (0.93 ± 0.06 , $p=0.366$). Transfection with both Pre-miRs™ simultaneously induced expression levels of a similar magnitude to the individual transfections with expression relative to control-transfected cells of 408.7 ± 86 ($p=0.002$) for miR-320a and 131726 ± 53156 ($p=0.003$) for miR-34c-3p.

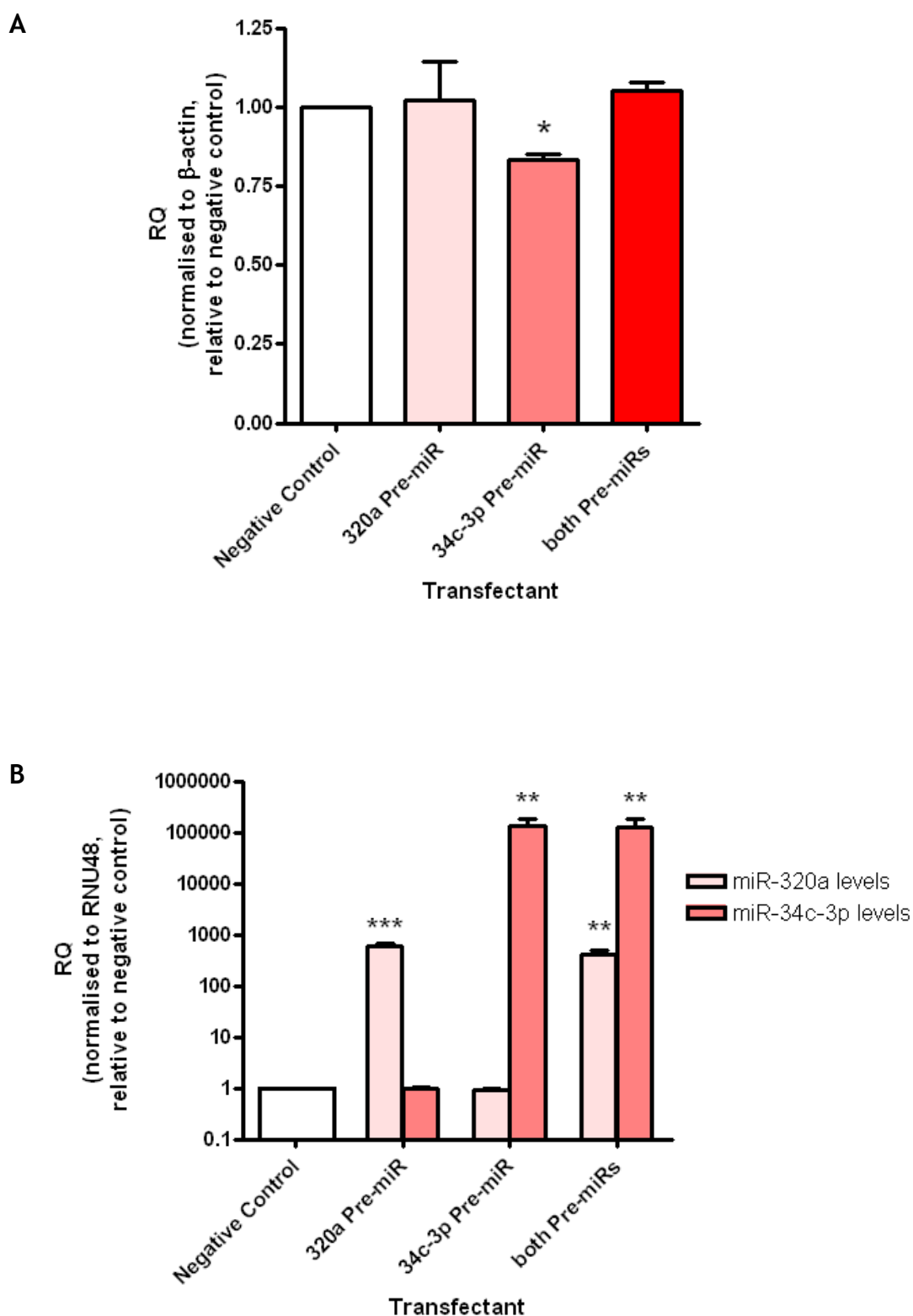


Figure 6-4 Assessment of A) *CYP17A1* mRNA abundance and B) mature miRNA levels post-transfection with specific pre-miRs™ in H295R cells grown in basal conditions.

H295R cells were transfected with miR-320a, miR-34c-3p Pre-miRs™, either singly or combined, and a scrambled negative control (final concentration 50nM). *CYP17A1* mRNA abundance and mature miRNA levels were measured 48 hours post-transfection by qRT-PCR. Cycle threshold values were normalised to β -actin or RNU48 mRNA, as stated on the y-axis, and expressed relative to negative control-transfected cells. Results represent the relative quantification ($RQ=2^{-\Delta\Delta Ct}$) of the mean of three independent biological experiments performed in triplicate; error bars represent standard error of the mean (SEM). Statistical differences were analysed by one-sample t-test on $\Delta\Delta Ct$ values. * $p < 0.05$, ** $p < 0.01$, *** $p < 0.001$.

Cells were transfected, again under basal conditions, with miR-320a-specific Anti-miR™, miR-34c-3p-specific Anti-miR™, or both Anti-miRs combined, in order to artificially reduce the levels of those miRNAs in the cells. *CYP17A1* mRNA levels were measured and are displayed, relative to transfected-control cell results, in Figure 6-5b. The relative abundance level ($RQ=2^{-\Delta\Delta Ct}$) of *CYP17A1* mRNA after transfection with miR-320a Anti-miR™ was 1.53 ± 0.09 , which was significantly increased compared to control cells ($p=0.016$). Transfection with miR-34c-3p Anti-miR™, however, did not significantly affect *CYP17A1* mRNA abundance (1.03 ± 0.03 , $p=0.473$). Transfection with both Anti-miRs™ significantly increased *CYP17A1* mRNA abundance (1.13 ± 0.03 , $p=0.042$), albeit to a lesser degree than transfection with miR-320a alone. Levels of mature miR-320a and miR-34c-3p were measured post-transfection to confirm the successful transfection of the specific Anti-miRs™. Figure 6-5a shows that transfection with miR-320a Anti-miR™ significantly reduced levels of mature miR-320a in the cells, with relative expression of 0.15 ± 0.02 ($p=0.005$), while levels of miR-34c-3p remained unaltered, as predicted (0.97 ± 0.15 , $p=0.739$). Transfection with miR-34c-3p Anti-miR™, however, did not significantly reduce levels of mature miR-34c-3p in the H295R cells (1.07 ± 0.17 , $p=0.838$). Mature miR-320a levels were unaffected, as expected (0.93 ± 0.11 , $p=0.222$). Simultaneous transfection with both Anti-miRs™ saw similar expression levels to those transfected individually, with expression relative to control-transfected cells of 0.15 ± 0.03 , $p=0.010$ for miR-320a and 1.19 ± 0.10 , $p=0.167$ for miR-34c-3p.

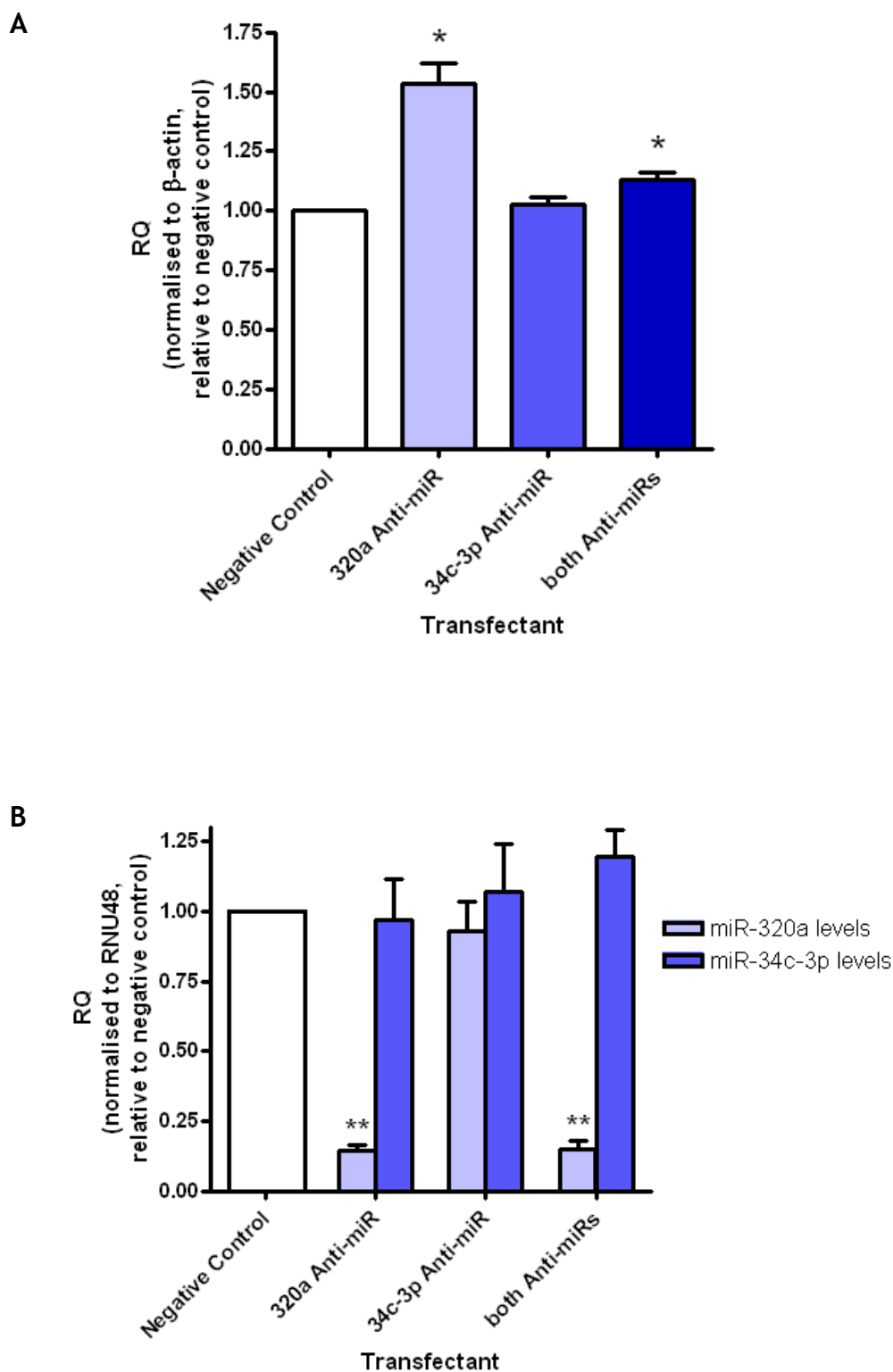


Figure 6-5 Assessment of A) *CYP17A1* mRNA abundance and B) mature miRNA levels post-transfection with specific anti-miRs™ in H295R cells grown in basal conditions.

H295R cells were transfected with miR-320a and miR-34c-3p Anti-miRs™, either singly or combined, and a scrambled negative control (final concentration 50nM). *CYP17A1* mRNA abundance and mature miRNA levels were measured 48 hours post-transfection by qRT-PCR. Cycle threshold values were normalised to β -actin or RNU48 mRNA, as stated on the y-axis, and expressed relative to negative control-transfected cells. Results represent the relative quantification ($RQ=2^{-\Delta\Delta C_t}$) of the mean of three independent biological experiments performed in triplicate; error bars represent standard error of the mean (SEM). Statistical differences were analysed by one-sample t-test on $\Delta\Delta C_t$ values. * $p < 0.05$, ** $p < 0.01$

CYP17A1 is expressed in the zona fasciculata, which is responsive to ACTH stimulation. Unfortunately, H295R cells do not express the ACTH receptor so $(\text{Bu})_2\text{cAMP}$ stimulation is commonly used to mimic the intracellular effects of ACTH. In H295R cells, upon stimulation with 1mM of $(\text{Bu})_2\text{cAMP}$, *CYP17A1* mRNA production is significantly increased relative to basal conditions (5.68 ± 0.41 , $p=0.008$), as displayed in Figure 6-6.

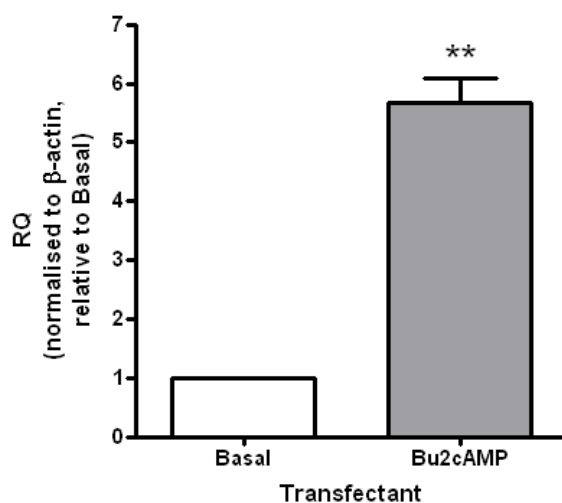


Figure 6-6 Assessment of *CYP17A1* mRNA abundance in H295R cells grown under basal conditions or stimulated with 1mM $(\text{Bu})_2\text{cAMP}$.

CYP17A1 mRNA abundance was measured 48 hours post-transfection by qRT-PCR. Cycle threshold values were normalised to β -actin and expressed relative to basal cells. Results represent the relative quantification ($\text{RQ}=2^{-\Delta\Delta\text{Ct}}$) of the mean of three independent biological experiments performed in triplicate; error bars represent standard error of the mean (SEM). Statistical differences were analysed by one-sample t-test on $\Delta\Delta\text{Ct}$ values. $**p<0.01$.

Cells were transfected with miR-320a specific Pre-miRTM, miR-34c-3p specific Pre-miRTM, or both Pre-miRs combined, and stimulated with $(\text{Bu})_2\text{cAMP}$ for 24 hours post-transfection. Transfections under basal and stimulated conditions were carried out simultaneously. *CYP17A1* mRNA levels were measured 48 hours post-transfection and are displayed in Figure 6-7b. The relative abundance ($\text{RQ}=2^{-\Delta\Delta\text{Ct}}$) of *CYP17A1* mRNA after transfection with miR-320a Pre-miRTM was 0.89 ± 0.01 , which was significantly increased relative to control cells ($p=0.003$), although transfection with miR-34c-3p Pre-miRTM had no significant effect on *CYP17A1* mRNA abundance (1.00 ± 0.05 , $p=0.965$). Transfection with both Pre-

miRs™ did significantly reduce *CYP17A1* mRNA abundance (0.79 ± 0.04 , $p=0.042$). Again, levels of mature miR-320a and miR-34c-3p were measured post-transfection to confirm successful transfection of the Pre-miRs™. Figure 6-7a shows that transfection with miR-320a Pre-miR™ significantly induced mature miR-320a in the cells, with relative expression of 4029 ± 2676 , $p=0.010$; levels of miR34c-3p remained unaltered (1.12 ± 0.25 , $p=0.783$). Transfection with miR-34c-3p Pre-miR™ increased relative mature miR-34c-3p expression (21781 ± 12663 , $p=0.004$), with miR-320a levels unaffected (1.08 ± 0.13 , $p=0.664$). Simultaneous transfection with both Pre-miRs™ induced expression to a similar degree as the individual transfections, with expression relative to control-transfected cells of 3568 ± 2174 , $p=0.006$ for miR-320a and 10609 ± 1611 , $p<0.001$ for miR-34c-3p.

Cells stimulated with $(\text{Bu})_2\text{cAMP}$ were also transfected with miR-320a-specific Anti-miR™, miR-34c-3p-specific Anti-miR™, or both Anti-miRs combined. *CYP17A1* mRNA levels were measured and the results are displayed in Figure 6-8b. The relative abundance level ($\text{RQ}=2^{-\Delta\Delta\text{Ct}}$) of *CYP17A1* mRNA after transfection with miR-320a Anti-miR™ was 1.15 ± 0.03 , which was significantly increased compared to control cells ($p=0.044$). However, transfection with miR-34c-3p Anti-miR™ did not significantly affect *CYP17A1* mRNA abundance (0.95 ± 0.11 , $p=0.628$). Transfection with both Anti-miRs™ failed to alter *CYP17A1* mRNA abundance significantly (1.16 ± 0.197 , $p=0.534$). Levels of mature miR-320a and miR-34c-3p were measured post-transfection to confirm the successful transfection of each Anti-miR™. Figure 6-8a shows that transfection with miR-320a Anti-miR™ significantly reduced the levels of mature miR-320a in the cells with relative expression of 0.28 ± 0.01 , $p=0.001$; while levels of miR34c-3p remained unaltered (1.00 ± 0.06 , $p=0.963$). Transfection with miR-34c-3p Anti-miR™, similar to the transfection experiments performed under basal conditions, did not significantly reduce levels of mature miR-34c-3p in the H295R cells (1.05 ± 0.25 , $p=0.964$); mature miR-320a levels were unaffected (0.99 ± 0.06 , $p=0.781$). Simultaneous transfection with both Anti-miRs™ saw similar results to individual transfections, with expression relative to control-transfected cells of 0.16 ± 0.05 , $p=0.044$ for miR-320a and 1.03 ± 0.28 , $p=0.976$ for miR-34c-3p.

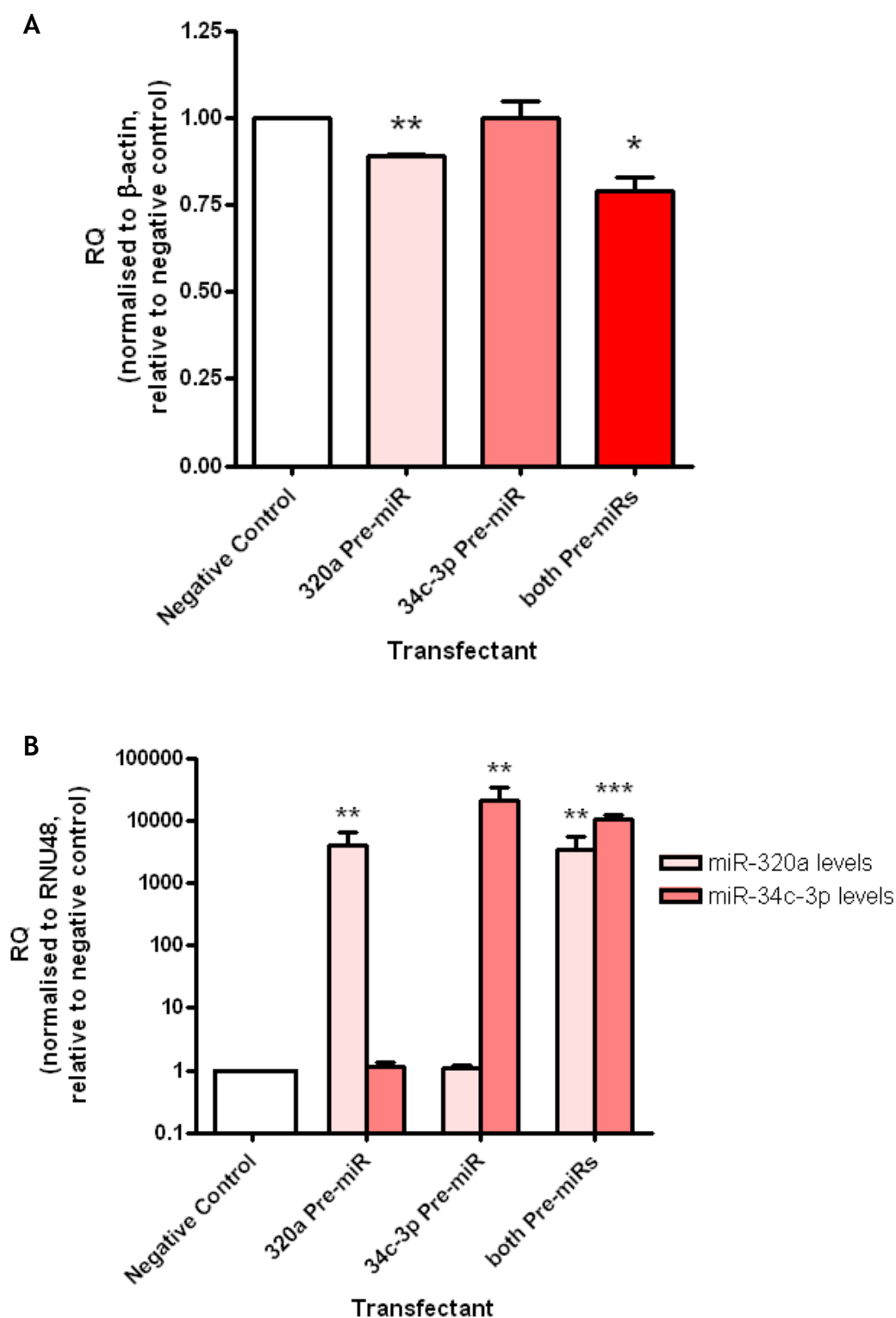


Figure 6-7 Assessment of A) *CYP17A1* mRNA abundance and B) mature miRNA levels post-transfection with specific pre-miRs™ in H295R cells stimulated with (Bu)₂cAMP.

H295R cells were transfected with miR-320a and miR-34c-3p Pre-miRs™, either singly or combined, and a scrambled negative control (final concentration 50nM). Cells were stimulated with 1mM (Bu)₂cAMP 24 hours post-transfection. *CYP17A1* mRNA abundance and mature miRNA levels were measured 48 hours post-transfection by qRT-PCR. Cycle threshold values were normalised to β -actin or RNU48 mRNA, as stated on the y-axis, and expressed relative to negative control-transfected cells. Results represent the relative quantification ($RQ=2^{-\Delta\Delta C_t}$) of the mean of three independent biological experiments performed in triplicate; error bars represent standard error of the mean (SEM). Statistical differences were analysed by one-sample t-test on $\Delta\Delta C_t$ values. * $p < 0.05$, ** $p < 0.01$, *** $p < 0.001$.

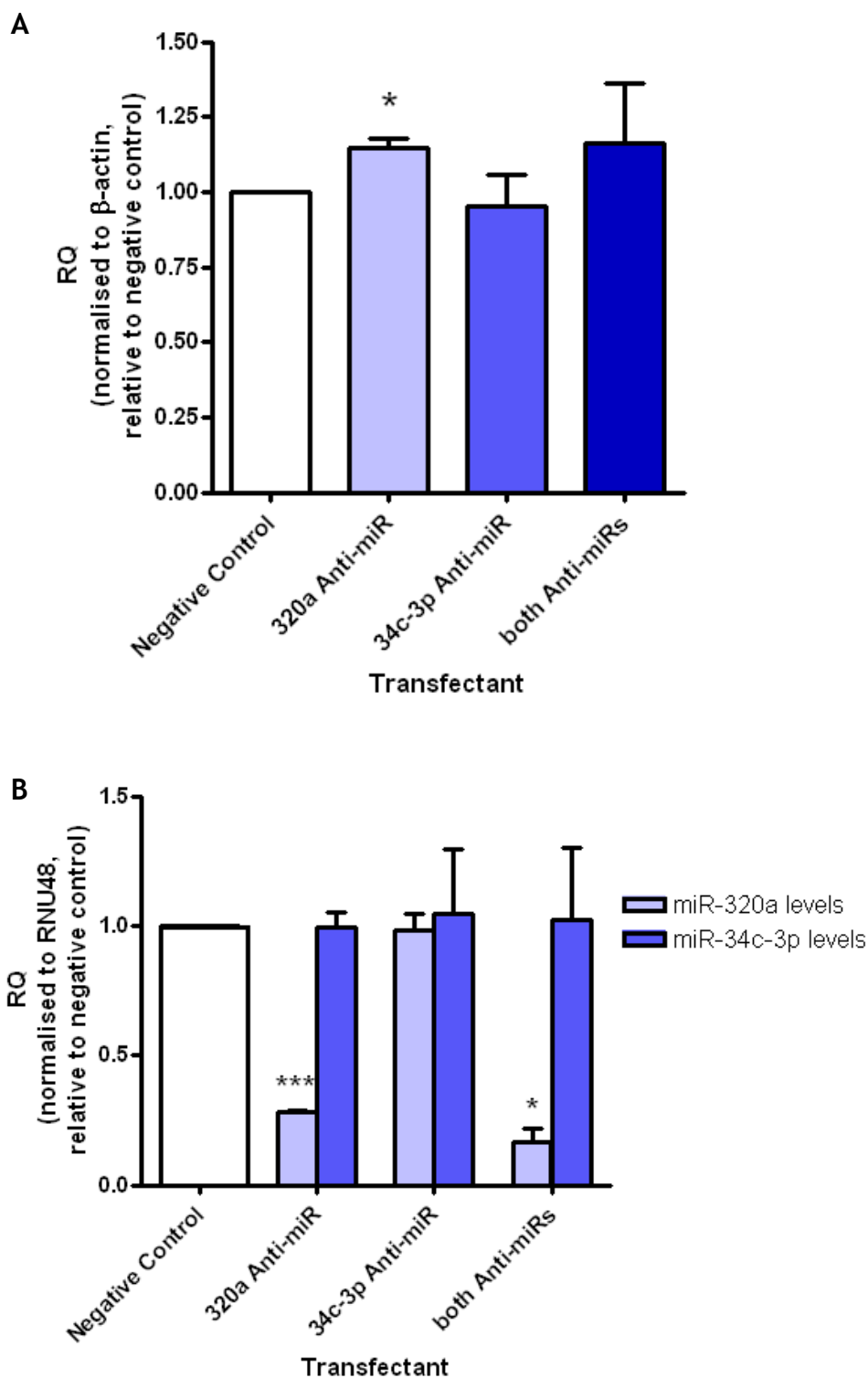


Figure 6-8 Assessment of A) *CYP17A1* mRNA abundance and B) mature miRNA levels post-transfection with specific anti-miRs™ in H295R cells stimulated with (Bu)₂cAMP.

H295R cells were transfected with miR-320a, miR-34c-3p Anti-miRs™, either singly or combined, and a scrambled negative control (final concentration 50nM). Cells were stimulated with 1mM (Bu)₂cAMP 24 hours post-transfection. *CYP17A1* mRNA abundance and mature miRNA levels were measured 48 hours post-transfection by qRT-PCR. Cycle threshold values were normalised to β -actin or RNU48 mRNA, as stated on the y-axis, and expressed relative to negative control-transfected cells. Results represent the relative quantification ($RQ=2^{-\Delta\Delta C_t}$) of the mean of three independent biological experiments performed in triplicate; error bars represent standard error of the mean (SEM). Statistical differences were analysed by one-sample t-test on $\Delta\Delta C_t$ values. * $p < 0.05$, *** $p < 0.001$.

6.4.6 Assessment of pEZX Reporter Construct as an Experimental Tool

To assess the suitability of the *CYP17A1* 3'UTR reporter construct as an experimental tool, a siRNA molecule was designed with perfect complementarity to a region of the 3'UTR (Table 2-4). The experimental siRNA or a control siRNA were then co-transfected into HeLa cells alongside the pEZX-17 reporter construct. The ratio of firefly luciferase to renilla luciferase was calculated, and the values from the experimental siRNA normalised to those of the control siRNA transfections. The *CYP17A1* 3'UTR-specific siRNA significantly decreased the normalised ratio from its 100% control level to $6.58\% \pm 0.69$, $p < 0.0001$ (Figure 6-9). The results offer experimental proof of concept that miRNAs targeting the 3'UTR of *CYP17A1* mRNA can induce significant changes in luciferase activity that can be measured experimentally.

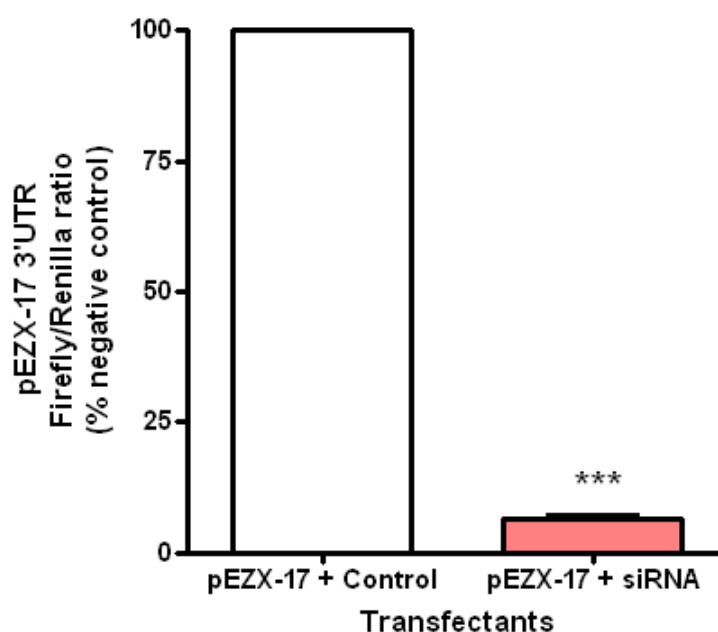


Figure 6-9 siRNA verification of the pEZX-17 reporter construct.

HeLa cells were co-transfected with pEZX-17 reporter construct and *CYP17A1* 3'UTR siRNA. Firefly and renilla luciferase were measured 48 hours post-transfections using the Dual-Luciferase Reporter Assay (DLRA). The ratio of firefly to renilla was calculated to normalise for transfection efficiency then expressed as a percentage of the negative siRNA control value. Results represent the mean of four independent biological experiments, performed in quadruplicate; error bars represent standard error of the mean (SEM). *** $p < 0.001$ compared to negative control.

6.4.7 miRNA Targeting to the 3'UTR of *CYP17A1* mRNA

In order to establish whether miR-320a and miR-34c-3p exerted their effects by acting directly on the 3'UTR of *CYP17A1*, pEZXR-reporter constructs containing the entire 3'UTR were subjected to analysis. These were co-transfected with specific miRNA mimics or inhibitors. For the co-transfection of reporter constructs with a specific miRNA inhibitor/Anti-miR™ to have an effect, the miRNA of interest must be expressed by the cell type of choice. To confirm this was the case, qRT-PCR was performed on untreated HeLa cells to assess the background levels of miR-320a and miR-34c-3p. The mean cycle threshold value for hsa-miR-320a was 19.25 ± 0.06 . For hsa-miR-34a-3p, the mean cycle threshold value was 20.95 ± 0.15 . Both miRNAs were measured in technical triplicate on three independent occasions.

The presence of both miRNAs of interest at moderate to high levels in HeLa cells allowed them to be used to assess targeting of the miR-320a and miR-34c-3p to the 3'UTR of *CYP17A1* mRNA. The effects of manipulating miR-320a and miR-34c-3p levels were assessed by calculating the ratio of firefly luciferase to firefly renilla, expressed as a percentage of the appropriate negative control. As shown in Figure 6-10, co-transfection with miR-320a Pre-miR™ did not significantly alter luciferase luminescence ($118.6 \pm 9.38\%$, $p=0.19$); similarly, inhibition with miR-320a Anti-miR™ failed to produce a significant change in luciferase luminescence ($114.3 \pm 27.81\%$, $p=0.64$). The miR-34c-3p Anti-miR™ was utilised in these experiments to test suspicions of a faulty design over a cell-line specific issue. Although inhibition of miR-34c-3p caused no significant change in luciferase activity in cells co-transfected with miR-34c-3p-specific Anti-miR™ (97.1 ± 2.62 , $p=0.34$), supplementation with Pre-miR™ increased it to 110.2 ± 2.50 , $p=0.03$ (Figure 6-11). While this result does not confirm the existence of a miRNA target site, nor is it consistent with canonical miRNA action, it may suggest some other form of regulation.

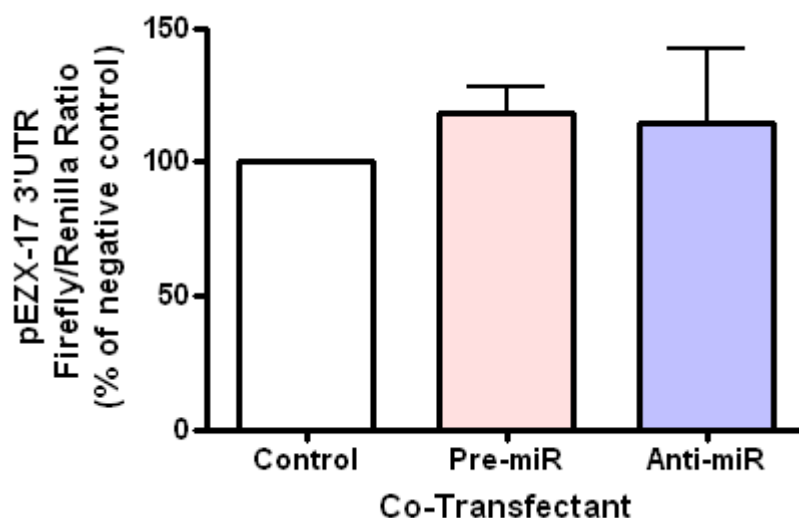


Figure 6-10 Effect of miR-320a targeting on the luciferase activity of the pEZX-17 reporter construct.

HeLa cells were co-transfected with the pEZX-17 reporter construct and Pre-miR™ or Anti-miR™ molecules specific for hsa-miR-320a. Firefly and renilla luciferase were measured 48 hours post-transfections using the DLRA kit. The ratio of firefly to renilla was calculated to normalise for transfection efficiency then expressed as a percentage of the appropriate negative control value. Results represent the mean of three (Pre-miR™) or four (Anti-miR™) independent biological experiments, each performed in quadruplicate; error bars represent standard error of the mean (SEM).

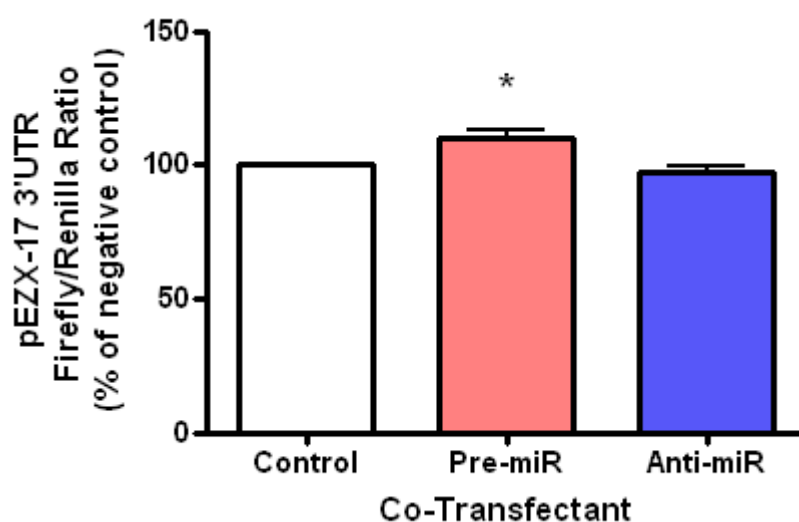


Figure 6-11 Effect of miR-34c-3p targeting on the luciferase activity of the pEZX-17 reporter construct.

HeLa cells were co-transfected with the pEZX-17 reporter construct and Pre-miR™ or Anti-miR™ molecules specific for hsa-miR-34c-3p. Firefly and renilla luciferase were measured 48 hours post-transfections using the DLRA kit. The ratio of firefly to renilla was calculated to normalise for transfection efficiency then expressed as a percentage of the appropriate negative control value. Results represent the mean of four independent biological experiments, each performed in quadruplicate; error bars represent standard error of the mean (SEM). * $p < 0.05$.

6.4.8 Further Investigation of miR-320a in Steroidogenesis

Section 6.4.5 describes the significant effects of miR-320a on *CYP17A1* mRNA abundance after artificially decreasing and increasing its levels in H295R cells. However, the results displayed in Section 6.4.7 imply that this effect is not caused through direct binding of miR-320a to the 3'UTR of *CYP17A1* mRNA. Therefore, similar bioinformatic analyses to that described in Section 6.4.3 were performed to investigate whether miR-320a is predicted to bind and possibly modulate other genes acting upstream from *CYP17A1* in the steroidogenic pathway. This analysis predicted miR-320a to bind mRNA encoding the side-chain cleavage enzyme, *CYP11A1*, which performs the initial conversion of cholesterol to pregnenolone in the steroidogenic pathway.

To investigate this further, H295R cells were transfected under basal conditions with miR-320a-specific Pre-miR™ or Anti-miR™ in order to artificially increase and decrease levels of the miRNA in the cells. *CYP11A1* mRNA levels were measured and are displayed in Figure 6-12a. The relative abundance level ($RQ=2^{-\Delta\Delta C_t}$) of *CYP11A1* mRNA after transfection with miR-320a Pre-miR™ was 0.81 ± 0.02 , significantly lower than that of control cells ($p=0.011$). Transfection with miR-320 Anti-miR™ significantly increased *CYP11A1* mRNA abundance (1.40 ± 0.03 , $p=0.003$). These results are consistent with canonical miRNA action. Levels of mature miR-320a were also measured post-transfection to confirm successful transfection of Pre-miR™ and Anti-miR™. Figure 6-12b shows that transfection with miR-320a Pre-miR™ significantly increased levels of mature miR-320a in the cells, with relative expression of 602 ± 89.6 , $p<0.001$, while it was reduced to 0.14 ± 0.02 ($p=0.005$ relative to control-transfected cells) in the presence of miR-320a Anti-miR™.

As with *CYP17A1*, these data are consistent with the modulation of *CYP11A1* mRNA abundance by miR-320a through canonical inhibitory miRNA action. However, due to time-constraints, confirmation that this is due to direct binding of *CYP11A1* mRNA was not performed at this stage.

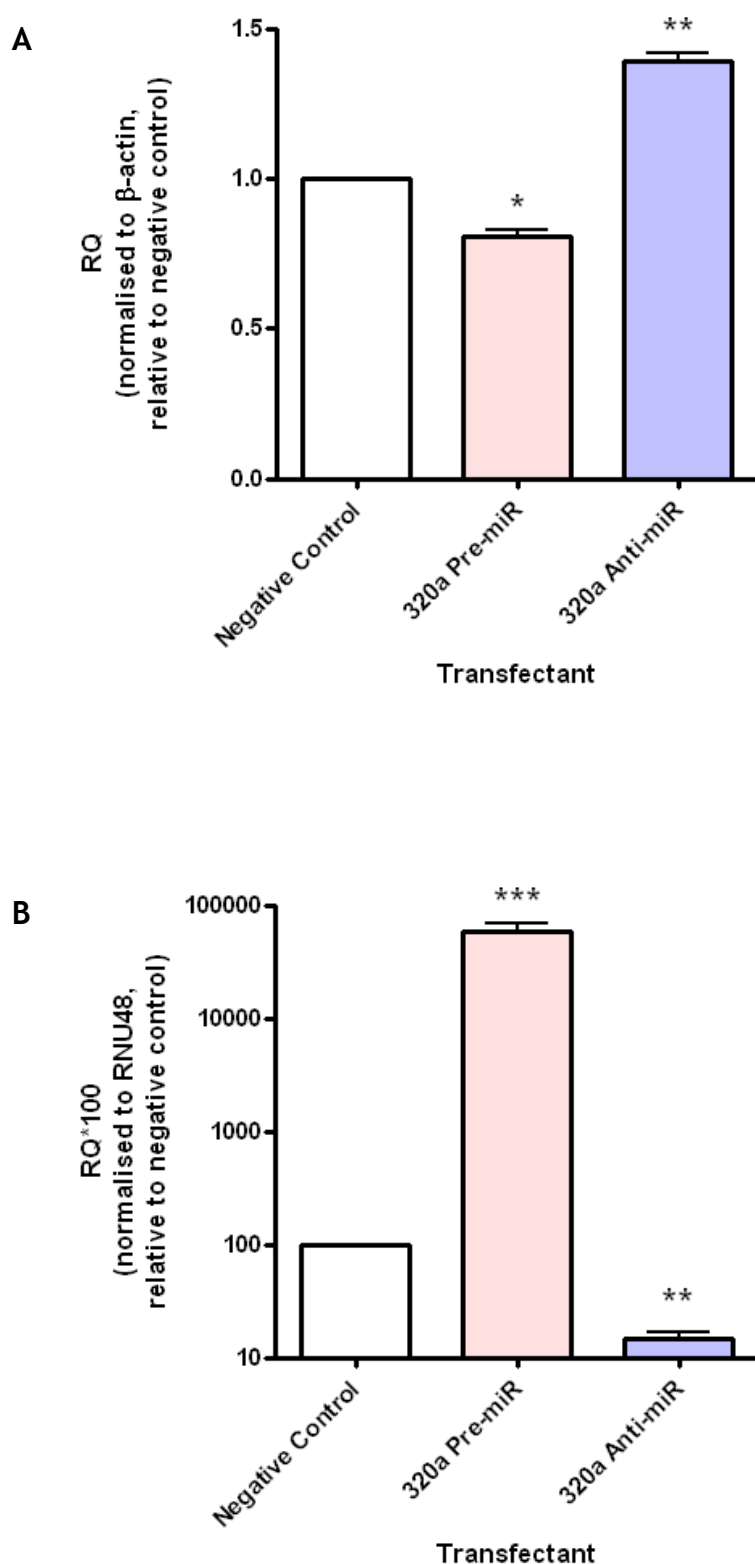


Figure 6-12 Assessment of A) *CYP11A1* mRNA abundance and B) mature miRNA levels post-transfection in H295R cells grown in basal conditions.

H295R cells were transfected with miR-320a Pre-miR™, Anti-miR™ and a scrambled negative control (final concentration 50nM). *CYP11A1* mRNA abundance and mature miRNA levels were measured 48 hours post-transfection by qRT-PCR. Cycle threshold values were normalised to β -actin or RNU48 mRNA, as stated on the y-axis, and expressed relative to negative control-transfected cells. Results represent the relative quantification ($RQ=2^{-\Delta\Delta Ct}$) of the mean of three independent biological experiments performed in triplicate; error bars represent standard error of the mean (SEM). Statistical differences were analysed by one-sample t-test on $\Delta\Delta Ct$ values. * $p < 0.05$, ** $p < 0.01$, *** $p < 0.001$.

6.4.9 Bioinformatic Analysis to Identify Putative miRNA Binding Sites in the 3'UTRs of *POR* and *CYB5A*

As previously described in Section 1.3.1, the selective action of *CYP17A1* in the adrenal cortex zones relies heavily upon the presence of the co-factors *POR* and *CYB5A*. It is entirely plausible to hypothesise that miRNAs may modulate the expression of these co-factors and affect the action of *CYP17A1* in the adrenal gland. To this end, similar bioinformatic analyses to those described in Section 6.4.3 were conducted to identify putative miRNA binding sites in the 3'UTRs of *POR* and *CYB5A*. Table 6-8 summarises the number of target sites predicted by each database within the 3'UTR of each gene, with a total of 264 unique miRNAs predicted to bind *POR* and 203 to bind *CYB5A*.

The miRNA expression data from the four normal samples and four aldosterone-producing adenoma (APA) samples were again cross-referenced with predicted miRNAs from bioinformatic analyses. Figure 6-13 lists those microRNAs expressed in normal adrenal tissue and APA tissue that were also predicted to bind the 3'UTRs of *POR* and *CYB5A*. Of particular interest are miR-24 and miR-21, which are predicted to bind *POR* and *CYB5A*, respectively. As reviewed in Section 1.5.1.6, both miRNAs have been shown to exhibit regulatory effects in adrenal steroidogenesis.

Table 6-8 Bioinformatic miRNA target site predictions for *CYB5A* and *POR* 3'UTRs.

Gene	3' UTR Length (bp)	MicroCosm	TargetScan	Microna.org	Mir-viewer	miRwalk	Tarbase	Total Unique miRNAs
<i>POR</i>	374	58	30	131	6	214	0	264
<i>CYB5A</i>	288	66	2	14	0	182	0	203

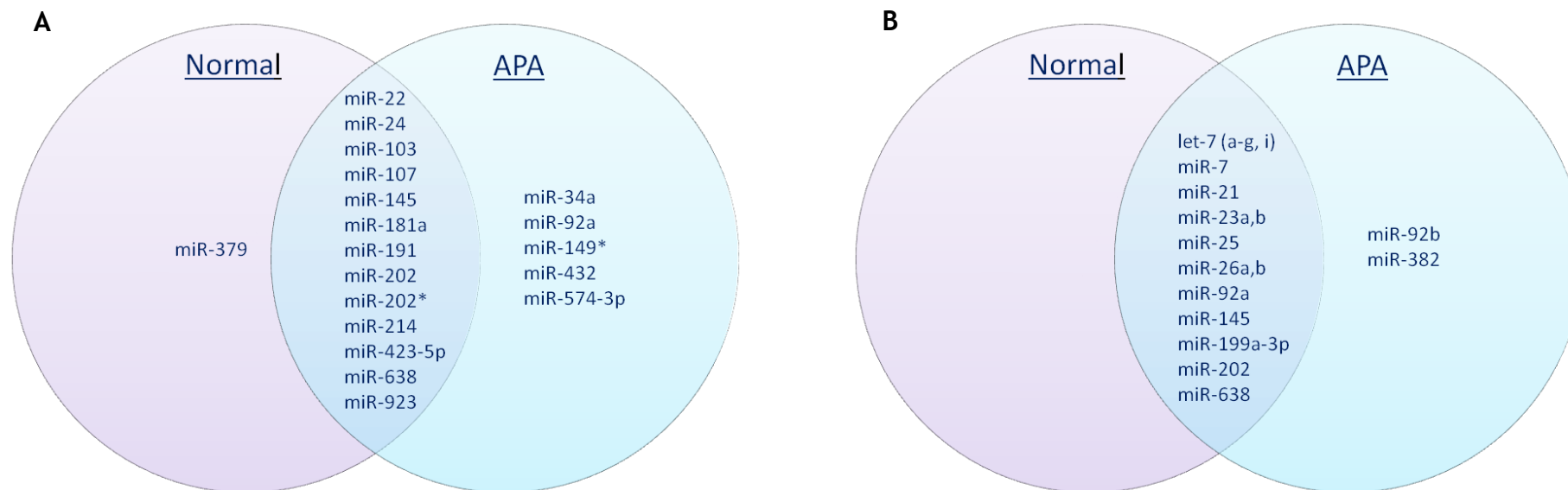


Figure 6-13 Venn diagrams showing microRNAs expressed in normal adrenal tissue and APA tissue that are predicted to bind the 3'UTRs of A) *POR* and B) *CYB5A*.

6.5 Discussion

The experiments presented in this chapter investigate the role of microRNA in the modulation of adrenal *CYP17A1* expression. To achieve this, *in silico* analysis identified miRNAs with putative binding sites in the *CYP17A1* mRNA, focussing primarily on the 3'UTR. These were then cross-referenced with microarray expression data in order to construct a list of miRNAs with the potential to regulate adrenal *CYP17A1*. Based on differential expression patterns between non-diseased and APA tissue, two miRNAs were selected for further study. Two primary methods were employed to analyse these:

- i) Assessment of specific miRNA effects on *CYP17A1* mRNA abundance through miRNA supplementation or inhibition in an adrenocortical cell line.
- ii) Assessment of direct mRNA:miRNA interactions through 3'UTR reporter construct studies.

The merits of these *in silico* and *in vitro* methods, and the findings of each, will be discussed below.

Bioinformatic Analysis

The first stage of *in silico* analysis investigated whether any miRNAs were produced from within the *CYP17A1* sequence. Many miRNAs arise from intronic locations but, despite many precursor and mature miRNA sequences matching sections of the *CYP17A1* introns, no miRNAs registered within the miRBase repository (2042 human miRNAs) have, to date, been mapped to these regions. Hence, SNPs located in these regions or splicing variants are not likely to affect the transcription of any miRNA. Therefore, any miRNA found to regulate adrenal *CYP17A1* would be subject to independent transcriptional regulation.

Comparison of *CYP17A1* 3'UTR sequence between species revealed high degrees of conservation between primates, and moderate conservation between mammals. A conserved 3'UTR sequence and, in particular, conserved putative miRNA binding sites, has been suggested as being an indicator of miRNA regulation (Friedman *et al.*, 2009). On the other hand, studies of basic cell homeostasis show that genes with short 3'UTRs are more resistant to miRNA-mediated repression (Stark *et al.*, 2005) and the *CYP17A1* 3'UTR is relatively

short at just 171 bases. In comparison, the 3'UTR of *CYP11B1*, for example, has 2015 bases and is known to be modulated by miRNA (Robertson *et al.*, 2013).

Several databases were used for bioinformatic prediction of putative miRNA binding sites in *CYP17A1*, *POR* and *CYB5A* mRNA. Each program has its own unique algorithm and parameters with varying levels of stringency, and so collating results from a variety of databases was deemed to be more reliable than simply relying on a single source. It is useful to be aware of the limitations of each database and to apply caution when analysing their output; bioinformatic databases are useful tools but are not definitive proof of mRNA:miRNA interaction. For example, the Tarbase program did not yield any predictions. This was to be expected since only experimentally validated interactions are stored in this database. The miRwalk database is evolving into a useful tool as it utilises up to eight different algorithms but, at present, it is necessary to search some of the individual databases it uses directly in order to obtain the most up-to-date information. Furthermore, the majority of programs employed in these searches are preset to only assess the 3'UTR of genes of interest, although experimental evidence is now emerging that miRNAs can act on other gene regions (Duursma *et al.*, 2008; Orom *et al.*, 2008); miRwalk results relate to putative miRNA binding sites in the coding regions and 5'UTR of genes. The precise details of mRNA:miRNA interactions are still emerging and therefore a combinatorial approach, selecting the lowest levels of stringency where necessary was considered advantageous. The degree of variation observed between databases highlights the need to improve understanding of miRNA-target binding, and is consistent with previous studies (Bartel 2009; Saito and Saetrom 2010).

Of the miRNAs predicted to bind to the 3'UTR of *CYP17A1*, a high proportion are miRNA*, derived from the passenger strand of the hairpin structure, which was originally believed to be non-functional. The currently favoured nomenclature assigns a -3p or -5p suffix to the derivatives of each strand, depending on its origin within the hairpin, as recent evidence suggests that either strand may be processed as the functional strand (see Section 1.5.1.3). Consequently, miRNA* predictions should not be disregarded as potential regulators of gene expression at this stage. It may also be useful to perform further *in silico* analyses: programs such as RNAFold or RNAHybrid can respectively predict the secondary

structure of the unbound 3'UTR and identify interesting mRNA:miRNA interactions (Kruger and Rehmsmeier 2006). Such assessment of the unbound 3'UTR secondary structure could reveal complex folds that inhibit putative miRNA interactions. While such programs are simply predictive tools, they may aid in prioritising miRNAs for further study.

Microarray data from expression profiling studies was available from both human non-tumourous adrenal (termed 'normal') and aldosterone producing adenoma (APA) tissue. The adrenal tissue sections used had not been laser dissected and were therefore likely to contain small amounts of adrenal medulla as well as cortex, although efforts were made to use blocks that were predominantly cortex. Across each sample type, miRNA levels were consistent suggesting the original starting material was not particularly variable in terms of its composition. The samples were deemed to be of good quality at the time of microarray and subsequent qRT-PCR validation. However, although probes covered 100% of known human miRNAs when the microarray was performed, there are currently 2042 human mature miRNAs listed on miRBase (v.19, August 2012), compared to the 723 included in the microarray data. This means that the work presented in this chapter is limited to the analysis of those 723 miRNAs and does not include over half of the currently known miRNAs. It would be useful, particularly for the study of the regulation of *CYP17A1* by miRNA, to obtain zone-specific expression profiles within the adrenal cortex, in order to identify if miRNAs modulate *CYP17A1* mRNA differently in the zona fasciculata compared to the zona reticularis. To date, it has proved difficult to obtain sufficient non-diseased adrenal tissue for this purpose.

Cross-referencing miRNAs predicted to bind to the 3'UTR of *CYP17A1* with those expressed in normal adrenal tissue or APA identified four unique miRNAs. Known previously in the literature as miR-368, miR-376c was found only to be expressed in normal adrenal tissue although, despite a clear trend, expression levels were not significantly different between tissue types. This may be caused by sample variation and significance could be altered by increasing the number of samples in each category. Hsa-miR-376c is transcribed from chromosome 14q32 as part of a large miRNA cluster. This cluster of miRNAs was previously shown to be dysregulated in ovarian cancer and gastro-intestinal tumour expression profiling studies (Zhang *et al.*, 2008; Haller *et al.*, 2010). Furthermore, eight miRNAs from

this cluster have been identified as potential tumour suppressor genes, including miR-376c (miR-368), and - of similar sequence and from the same family - miR-376a and miR-376b (Zhang *et al.*, 2008). Moreover, manipulation of miR-376c levels *in vitro* has recently been shown to affect expression of the insulin growth factor 1 receptor (IGF1R) (Zehavi *et al.*, 2012). Despite no published link between miR-376c and hypertension, its tumour suppressor role may indicate a role in the development and pathology of APA. In the production of this thesis, time constraints did not allow this miRNA to be investigated further although, as with all four miRNAs of interest, miRNA expression in both normal and APA tissue types would need to be validated by qRT-PCR, firstly to confirm the accuracy of the microarray and, secondly, to enable more precise quantitative measurement of expression changes between tissue types.

Arising from the 5' arm of the precursor hairpin, miR-7 was found to be expressed at similar levels in both normal adrenal and APA tissue. This miRNA can be transcribed from three different genomic locations on chromosomes 9, 15 and 19, with current nomenclature rules adding the suffixes -1,-2 and-3, respectively. In comparison to many other miRNAs, miR-7 is relatively well-studied. Studies have indicated that it is tightly regulated by the transcription factor Homeobox D10 (HoxD10) and its expression is dysregulated in many types of cancers, including aggressive breast cancer and glioblastomas (Foekens *et al.*, 2008; Kefas *et al.*, 2008; Reddy *et al.*, 2008). Furthermore, expression profiling studies and subsequent qRT-PCR validation on adrenocortical carcinomas (ACC) and adenomas (ACA) show miR-7 expression to be significantly reduced compared to normal adrenal tissue (Soon *et al.*, 2009; Singh *et al.*, 2012). This may suggest that, in addition to regulating processes surrounding adrenal pathology, this miRNA has wider roles in cell-cycle progression and tumourogenesis (Foekens *et al.*, 2008).

In Vitro Investigations

The subset of four adrenal miRNAs predicted to bind the *CYP17A1* 3'UTR was derived by bioinformatic analysis alone; experimental validation is required to confirm a functional effect on *CYP17A1* expression. Time constraints meant that investigation of miRNAs differentially expressed between normal and APA tissue was given priority, as these were deemed more likely to have an important role

in adrenal pathology. Initial *in vitro* experiments utilised miRNA mimics and inhibitors (Pre-miR[™] and Anti-miR[™]), which respectively increase or decrease levels of specific endogenous mature miRNAs in cells and are an established experimental tool in research (Cheng *et al.*, 2005). As the sequence of some miRNAs can vary by only one or two bases, it is important for these molecules to be highly specific and to avoid off-target effects. Successful transfection and expression of these molecules can be assessed by direct measurement of the mature miRNA level post-transfection. The results described in this chapter reveal that both miR-320a Pre-miR[™] and Anti-miR[™] were highly effective at modulating the levels of mature miR-320a in H295R cells. However, the Anti-miR[™] supposedly specific for inhibition of miR-34c-3p did not appear to be effective. Successful use of a miRNA inhibitor molecule depends upon its target miRNA being present within the chosen cell type. The presence of miR-34c-3p was assessed by qRT-PCR and confirmed to be present in both H295R and HeLa cells. Therefore, the failure of the miR-34c-3p may be due to faults in its preparation or design by the manufacturer, although the actual reason was not determined. The miR-34c-3p Pre-miR[™] did successfully increase levels of the mature miRNA in cells although the degree of change differed considerably from that of the miR-320a Pre-miR[™]. From previously conducted optimisation experiments, this variation appears typical of these synthetic molecules and, in both cases, the increase in miRNA was sufficient for significant changes to be detected. The changes in miRNA levels were very large and, particularly for Pre-miR[™] transfections, unlikely to be physiologically representative. However, as is often the case when using an *in vitro* model, supraphysiological changes are regularly required to investigate a pathway. Nevertheless, caution must be applied when interpreting such data as, for example, false positives may result from off-target effects or activation of other pathways due to overloading of the natural system.

The results from miR-34c-3p Pre-miR[™] and Anti-miR[™] transfections are variable. *CYP17A1* mRNA abundance was significantly reduced when basal H295R cells were transfected with Pre-miR[™] but not when stimulated with (Bu)₂CAMP, a substitute for ACTH. Taken together with reporter construct experiments, which were designed to assess whether miR-34c-3p binds the 3'UTR of *CYP17A1* directly, these results suggest a non-canonical form of miRNA action. A clearer

impression of miR-34c-3p action should be achieved through Anti-miR™ transfections, but such data cannot be considered reliable due to its failure to reduce miR-34c-3p significantly within the cells. Although it would have been beneficial to also measure the levels of miRNA in the transfected HeLa cells, it would be anticipated that changes in miRNA levels would be similar in magnitude to those of the H295R cell experiments. Reporter construct studies are currently the best available method for assessing miRNA target-site validation. The *CYP17A1* reporter construct contains the full length 3'UTR sequence, thus giving a truer reflection of mRNA:miRNA interactions, compared to constructs with smaller segments inserted. Furthermore, in addition to the firefly luciferase gene used to assess the insert, this plasmid also contains a renilla luciferase gene, which acts as a control for transfection efficiency. This avoids possible transfection efficiency problems that may arise from having to co-transfect a separate control plasmid, particularly as small molecules also had to be transfected as part of the protocol. It may be appropriate to repeat these experiments using similar small hairpin molecules which require initial processing and Dicer cleavage by the cell itself. This may be more physiologically relevant; however, such molecules were not accessible at the time of these experiments having only recently become available. Further investigation of this miRNA would be needed to elucidate its mechanism of action on *CYP17A1* mRNA, with a detailed evaluation of other related target sites being a useful starting point. Given that expression levels in both types of adrenal tissue were significantly different, it is difficult to predict exactly what results would be expected from the *in vitro* systems used in this study. Published studies have implicated miR-34c-3p, as well as its family members miR-34a and miR-34b, as having a defined role in tumour development, through interaction with p53 (Hermeking 2010). From this perspective, it may be advantageous to study the role of this miRNA in the development of APA and other adrenal tumours rather than its effects on *CYP17A1*.

The miR-320a data presented in this chapter seem both promising and intriguing. Increased levels of miR-320a had no significant effect on basal H295R cells, but *CYP17A1* mRNA levels were raised following miR-320a inhibition. As discussed previously, the use of a specific miRNA inhibitor is probably more physiologically relevant than synthetic supplementation, and this pattern is typical of the

results seen when using these small molecules (Wood 2011). Upon stimulation with $(\text{Bu})_2\text{cAMP}$, significant increases in *CYP17A1* mRNA levels were observed. In the body, the presence of circulating ACTH activates cellular cAMP, which triggers a cascade of events stimulating the production of cortisol in the adrenal zona glomerulosa. When miR-320a mimics were transfected onto H295R cells, *CYP17A1* mRNA levels significantly reduced. Transfection with miR-320a inhibitor increased *CYP17A1* mRNA levels. The data described here are consistent with the hypothesis that miR-320a acts as a post-transcriptional negative regulator of *CYP17A1*. Reporter construct experiments, however, suggest that this effect does not occur through direct binding of miR-320a to the 3'UTR of *CYP17A1*. Bioinformatic analysis predicted a putative binding site for miR-320a within the 3'UTR of the *CYP11A1* gene, which encodes side chain cleavage enzyme, a key gene in the steroidogenic pathway. Data presented here show miR-320a modulates *CYP11A1* in a typical manner, although, it is still necessary to generate and conduct experiments using a *CYP11A1* 3'UTR reporter construct in order to confirm direct interaction. If direct miR-320a modulation of *CYP11A1* expression was confirmed, such regulation could potentially affect all downstream steroidogenesis, given the pivotal position of side-chain cleavage enzyme at the head of the pathway.

From the existing literature, it can be concluded that miRNAs act as part of a complex network so that, where one miRNA decreases expression of a gene, another may be present to compensate. The experiments involving the simultaneous supplementation or inhibition of both miRNAs within the same cells were designed to study this. In basal H295R cells, no significant effect on *CYP17A1* mRNA was observed, and the effects from single-miRNA were not replicated, although it is not immediately clear why. Potential explanations include the possibility that off-target effects are providing a compensatory mechanism, or that the presence of mimic or inhibitor in relatively high volumes has increased competition for cellular resources. It is also possible that the *in vitro* system is simply overloaded and transfection efficiency reduced. It is interesting, however, that the effect exerted by increased miR-320a on *CYP17A1* mRNA is maintained when transfected alone and in combination with miR-34c-3p in stimulated cells, and implies that miR-320a is a key regulator of *CYP17A1* expression. It would be ideal to measure *CYP17A1* protein levels in order to

corroborate mRNA data. In addition, measurement of the steroid products themselves would be of use in supporting this association.

Although the underlying mechanisms are unclear, *CYP17A1* expression is reported to be significantly decreased in APA tissue (Wang *et al.*, 2011). That publication only assessed mRNA abundance, however it assumed that this effect translated through to the protein level. On the basis of the evidence assembled here, the significant up regulation of miR-320a in APA tissue relative to normal adrenal tissue could, through inhibitory miRNA action, account for the reduced *CYP17A1* expression that the previous investigators observed. It is unlikely, however, that this would be the sole cause, since many miRNAs are likely to have fine-tuning effects on the steroidogenic pathway and the effects of numerous factors would probably be required to cause the -0.97 ± 0.41 fold decrease that they observed.

The data presented in this chapter provide the first analysis of miR-320a effects on the human adrenal gland at a molecular level. Previously, levels of mature miR-320a were found through microarray analysis to be significantly increased 1.5-fold in human adrenocortical carcinoma tissue compared to adrenocortical adenoma tissue, although this finding was not validated by qRT-PCR (Soon *et al.*, 2009). This reiterates the need for microarray analysis to be confirmed by qRT-PCR. The role of miR-320a in cancer appears to be a recurring theme within the literature. Microarray analysis revealed miR-320a to be overexpressed in the tumourigenesis of retinoblastoma (Zhao *et al.*, 2009), but a protective role for miR-320a has been suggested by other studies, including one showing it to be down regulated in prostate cancer tissue (Hsieh *et al.*, 2013). Furthermore, the authors of that study found that reducing the levels of mature miR-320a *in vitro* increased the formation of tumour spheres and other cellular cancerous properties. Subsequent cDNA microarray showed expression of several genes in the Wnt/ β -catenin pathway to be reduced in cells expressing miR-320a. Investigations similar to those conducted in this chapter using miRNA mimics, inhibitors and reporter constructs identified miR-320a as directly modulating expression of β -catenin (Sun *et al.*, 2012). Increased miR-320a levels have also been associated with reduced cell proliferation in a human leukaemia cell line (Schaar *et al.*, 2009). Studies which investigate the therapeutic potential of miR-320a are also now beginning to emerge. MiR-320a directly modulates the expression of Aquaporin 1 and 4, which play key roles in cellular water

homeostasis; changes in expression of these proteins associate with cerebral ischemia, and investigators have found that locally-administered anti-miR-320a significantly reduces infarct volume in rats (Sepmaniam *et al.*, 2010). Similarly, having been implicated in the regulation of cardiac ischaemia through its direct modulation of Heat Shock Protein 20, anti-miR-320a also reduces cardiac infarction size *in vivo* (Ren *et al.*, 2009). Although further work is required before the administration of anti-miRNA medicine is used clinically, its potential opens up an exciting field of research. The exact mechanisms and effects of miR-320a in the adrenal gland and its role in adrenal tumour pathology are yet to be fully elucidated. Local delivery of an anti-miRNA to the adrenal gland as a therapeutic treatment would be difficult, and risks off-target effects.

Regulation of Co-Factors by miRNA

Since miRNAs are capable of targeting thousands of genes in the genome, it is worth considering their effect on the co-factors of *CYP17A1* and how regulation and expression may be affected. For example, it is feasible to hypothesise that post-transcriptional regulation by miRNA may be responsible for the lack of *CYB5A* expression in the zona glomerulosa. Lists of adrenal miRNAs with putative binding sites on *POR* and *CYB5A* were generated but have not yet been investigated further. An initial point of investigation would be the influence of miR-21 and miR-24, as both have previously been implicated in the regulation of steroidogenesis (Section 1.5.1.6).

Overall Review

Common polymorphisms located in the 3'UTR of these – and indeed all – genes regulated by miRNAs, have the potential to inhibit or promote binding of the target site. Chapter 3 of this thesis found no variation in the 3'UTR of *CYP17A1* in the AFS Caucasian population studied, and *POR*, *CYB5A* and *CYP11A1* are yet to be assessed. Common variations found in other ethnic groups should be also considered.

In summary, these studies have identified and investigated putative miRNA binding sites on the 3'UTR of *CYP17A1* mRNA. While hsa-miR-320a has been shown to modulate *CYP17A1* expression in an adrenocortical cell line, this does

not occur through direct binding of *CYP17A1* transcripts. The effects of hsa-miR-34c-3p on *CYP17A1* expression are less convincing and require further clarification. A combination of bioinformatic analysis and *in vitro* studies has shown a possible direct modulatory effect of miR-320a on *CYP11A1* mRNA, but this is yet to be confirmed. In conclusion, this is the first study to investigate the regulatory effects exerted on *CYP17A1* by miRNA. Future work is required in order to fully unravel the complex system of miRNA regulation and draw definitive conclusions about the effects of miRNA on the regulation of *CYP17A1*.

7 General Discussion

Essential hypertension is a common disorder of complex aetiology affecting around one-third of adults worldwide and is a major risk factor for cardiovascular disease. It results from complex interactions between genetic and environmental factors, many of which are not fully understood. Genome-wide association studies (GWAS) have become the latest research tool to identify common genetic variants associated with hypertension and other diseases. Recent GWAS identified an association between a common genetic variant located in the human *CYP17A1* gene and increased systolic blood pressure. The *CYP17A1* gene encodes a dual-function enzyme critical in the adrenal corticosteroid biosynthesis pathway, a major candidate system already implicated in the development of essential hypertension, as outlined in Chapter 1. Therefore, increasing our knowledge of how this gene is regulated within this system should improve our understanding of essential hypertension.

The experimental work presented in this thesis was designed to investigate the hypothesis that there are functional polymorphisms in the *CYP17A1* gene, specifically the promoter region, that are co-inherited alongside the one highlighted by recent GWAS (rs1004467). In addition, the existence of a novel regulatory mechanism involving microRNAs was explored. Following a detailed examination of linkage disequilibrium patterns at the *CYP17A1* locus, I proceeded to analyse the effects of genotype on intermediate corticosteroid phenotype in a hypertension population and to identify possible functional variants *in vitro*. The resulting data presented here support the original hypothesis.

The detailed examination of *CYP17A1* in a normotensive Caucasian population (Chapter 3) found most variation to be in the promoter region and introns. This was achieved by direct sequencing of individual genomic DNA samples by the chain termination method. At the time, newer methods such as next-generation sequencing were not considered cost-effective. The method employed allowed the discovery of previously unreported SNPs. In fact, the polymorphism at position -1877 has only recently been assigned an official name (rs138009835), presumably as a result of the 1000 Genomes Project. While variants within introns may be functional, particularly if located at splice sites, priority was given to those located in the promoter region. Two distinct and unrelated blocks of SNPs in strong linkage disequilibrium warranted further exploration. One

block (LD Block 2) contained the polymorphism reported by the GWAS (rs1004467); hence its relationship with the SNP at -1877 was instantly attractive, since its location implied that it might alter transcriptional activity of the gene, while also supporting the original hypothesis.

Selected promoter SNPs were directly sequenced in a subset of the hypertensive BRIGHT cohort. While it would have been simpler to genotype utilising specific fluorescent probes (e.g. SNP genotyping by Taqman®), the DNA was not of sufficient quality to yield convincing results by such a method. Genotyping and subsequent LD and haplotype analysis found the distinction between the two blocks of SNPs to be less clear. The cohorts were not matched in terms of cases and controls but each was of Caucasian British descent and it would not be unreasonable to observe similar relationships between the SNPs and haplotype frequencies in both unless, of course, a particular haplotype is more strongly associated with the hypertensive or normotensive group. It would be desirable to examine this further in order to determine whether a 'risk' haplotype exists. Given that the SNP identified by GWAS associated with a small rise in systolic blood pressure, the effect from any 'risk' haplotype is also likely to be small. Personalised medicine is often discussed as the future of medicine and an individual who exhibits several 'risk' haplotypes within specific genes could benefit from alteration to their lifestyle choices.

Each of the selected SNPs in the promoter region was examined for association with intermediate corticosteroid phenotype (Chapter 4). It is clear from these studies that there is a case for analysing steroid excretion rates separately by gender. Cortisol excretion rates were significantly higher in males of AG genotype at position -362 than those of AA genotype (Table 4-12). Interestingly, studies of allele-dependent transcriptional activity *in vitro* (Chapter 5) found the G allele at this locus to exhibit significantly higher transcriptional activity compared to the A allele (Figure 5-6). It may be that increased transcription of *CYP17A1* leads to greater cortisol production, although why this is only seen in males is unclear. Furthermore, androgen metabolite excretion was similar between the two genotypes, possibly due to other transcriptional influences within the zona reticularis or to additional urinary androgen metabolite excretion from the testes. Higher cortisol excretion rates were also noted for females in the presence of the minor allele at positions -1204 and -2205. Similar

trends were observed for the other SNPs within this LD block. When transcriptional activity of each allele was assessed *in vitro* only the T allele at position -2205 resulted in significant increase. This is consistent with the idea that only one SNP within a LD block may be functional and that the others are merely markers co-inherited alongside it. This same block of SNPs has a clear association with the ratio of THDOC:THS. In females, the minor allele is associated with a lower ratio, indicative of increased 17 α -hydroxylase efficiency; the *in vitro* observations are relevant here also.

In examining the effects of an individual SNP separate from its haplotype block, the cumulative effect of the haplotype as a whole may be overlooked. In combination, a series of SNPs may have a more pronounced effect or, alternatively, the opposing effects of different SNPs may be negated. The combined effect of five strongly-related SNPs on urinary metabolite excretion was briefly explored here and would benefit from an increased number of participants to enable a comparison of the various genotype combinations at all seven SNP sites, as different factors may be interacting to influence transcription. Even in combination, genotype-dependent effect sizes are likely to be small and it is possible that actual effects within the urinary metabolite and *in vitro* studies were obscured by technical variability. In addition, rare polymorphisms have been excluded from these studies; these may also exert a physiological influence on blood pressure, albeit in a smaller number of individuals, and warrant further investigation.

One striking observation was that THAldo excretion rates were higher in the -1877 CC genotype group compared to the CT+TT group (Table 4-32). This polymorphic site was of interest due to its strong relationship with the GWAS SNP. However, it was not associated with altered excretion of the more obvious corticosteroids i.e. cortisol and androgens. Assessment of transcriptional activity at this site found activity of the C allele to be significantly higher than that of the T allele. An effect of ACTH on aldosterone production has previously been postulated (Freel *et al.*, 2007) and it may be that altered transcriptional activity of *CYP17A1* has an indirect effect on ACTH drive, although the underlying molecular mechanism is unclear.

This is the first study to examine directly the regulation of *CYP17A1* by miRNAs, and this was accomplished using both *in vitro* and *in silico* techniques. The studies presented in Chapter 6 utilised bioinformatic prediction algorithms to identify those miRNAs most likely to target *CYP17A1* mRNA. Post-transcriptional gene regulation by miRNA is a relatively new and rapidly developing field, and even over the course of this three-year research period, the algorithms within the databases have been extensively modified. Precise identification of all false-positive and false-negative results from bioinformatic prediction is difficult and would require a lot of time and expense. Even as our knowledge of miRNA target recognition improves, there will probably always be an inherent error associated with this type of analysis, given the imperfect base-pairing nature of miRNAs (Grimson *et al.*, 2007; Shin *et al.*, 2010). This study collated predictions from six separate databases in an attempt to compensate for the various algorithms and stringency levels, although such prediction lists will require updating as individual algorithms are refined. Those miRNAs differentially expressed in normal and diseased adrenal tissue were prioritised, and two miRNAs eventually selected for further study. Effects of these miRNAs on steroid secretion and *CYP17A1* protein levels remain to be explored. In addition, miR-7 and miR-376c were also predicted to bind to adrenal *CYP17A1* but have not yet been investigated *in vitro*. The manufacturer of the microarray used to detect the miRNAs in normal adrenal tissue advised a signal intensity cut-off of 500 arbitrary units (AU). Although a cut-off value is required to minimise experimental error and account for the lower detection limit of the scanner, it is possible that some miRNAs with intensity value marginally below 500 AU are important to adrenal physiology. There is also likely to be zone-specific expression of some miRNAs within the adrenal gland and, since the tissue samples analysed contain a heterogeneous adrenal cell population, their levels may be diluted within the whole sample. It would be beneficial to perform zonal micro-dissection and quantitative expression analysis to aid in the identification of such miRNAs, including miR-320a.

MiRNA expression profiling studies are quickly becoming a common research theme and have clear potential in the identification of biomarkers for the clinical diagnosis of a variety of disorders, including ovarian cancer and heart conditions (Chen *et al.*, 2013; Leptidis *et al.*, 2013). However, both practical and

ethical considerations make these types of studies on the adrenal glands of patients with essential hypertension impossible, and animal models are not ideal for a variety of reasons. Firstly, rodent adrenal physiology is not directly comparable to that of humans e.g. corticosterone is the major glucocorticoid in rat. Secondly, the similarity and conservation of the miRNA-mediated repression mechanisms across species are not fully understood.

In theory, targeting of specific miRNAs has enormous therapeutic potential. The control of aberrant disease-causing gene expression through manipulation of specific miRNA levels seems promising although, due to numerous potential targets a single miRNA may have, there is huge scope for side effects. Targeting tissues specifically may reduce such effects and the use of viral vectors for this purpose is ongoing. The delivery of anti-miR-122 to the liver of the African green monkey was successfully achieved and, subsequently, pharmaceutical companies have started early-stage clinical trials in humans. This year, Santaris Pharma announced enrolment completion of a Phase II clinical trial utilising anti-miRNA-based therapy as treatment for the Hepatitis C virus (Wartelle-Bladou *et al.*, 2012). Such trials for adrenal disorders are unlikely in the near future as further understanding of the role of miRNA in both normal and diseased adrenal pathology is required.

Aside from further *in vitro* suggested studies intended to develop a clearer understanding of the molecular basis of the allele-dependent changes in transcriptional activity (discussed in Section 5.4.4), it may be useful to examine the frequency of selected polymorphisms in other disorders where hypertension is a feature. The SNP at position -34 (rs743572) has been investigated for association with PCOS (Section 1.3.3.2) with inconsistent results. It would be interesting to assess the frequencies of the other promoter polymorphisms in a PCOS population and possibly derive a 'risk' haplotype. Similarly, other than the variation at position -34, polymorphisms have been largely ignored in association studies investigating hormone-related cancers and premature male baldness. Furthermore, regulation of the gene may be altered through other mechanisms and closer examination of the contribution of miRNA may aid understanding of PCOS development and treatment.

In conclusion, recent GWAS identified a common genetic variant in the *CYP17A1* gene that was associated with a small but significant rise in systolic blood pressure. It was hypothesised that a co-inherited SNP may be responsible. Several common polymorphisms in the promoter region have been identified and this is the first time that significant association with variations in the *CYP17A1* gene has been shown with corticosteroid intermediate phenotypes in a hypertensive population. Furthermore, evidence has been provided for allele-dependent alterations in transcriptional activity at a number of polymorphic locations. Early identification of subjects predisposed to hypertension and the future identification of susceptible genotypes at the *CYP17A1* locus and other known loci will allow early lifestyle and medicinal intervention. In addition, a regulatory role for miRNA has also been confirmed here, opening up new avenues of investigation into the fine control of corticosteroid secretion. It is expected that the improved understanding of how steroidogenic genes contribute to hypertension will aid the development of therapeutic interventions.

8 Appendices

8.1 Appendix 1

Table 8-1 Primers used to amplify and sequence 2.4kb of *CYP17A1* promoter in AFS and BRIGHT cohorts.

	Primer Name	Sequence 5'-3'	T _m (°C)	Cycling Conditions
PCR Primers (Expand High Fidelity PCR System)	cyp17promF2	ATGCAGTTCGATTGCAACAC	55.3	See Table 8-2
	cyp17promR2	TTGGGCCAAAACAAATAAGC	53.2	
Sequencing Primers	cyp17promF2	ATGCAGTTCGATTGCAACAC	55.3	BIGSEQ50
	cyp17promR2	TTGGGCCAAAACAAATAAGC	53.2	BIGSEQ50
	cyp17-1935F	AGCTGAGGCGTTAGATCAGG	59.4	BIGSEQ60
	cyp17-1525F	GTCACCTCAGGACCACTGTGA	59.8	BIGSEQ60
	cyp17-1213F	CCGCTCTGGGAATGTCTATC	59.4	BIGSEQ60
	cyp17-884F	TTGTCCTTCCCTCAGAAGC	57.3	BIGSEQ50
	cyp17-603F	GAAATATTGGGGTGGGTTTC	57.3	BIGSEQ50
	cyp17-159F	CCCAGATACCATTGCACTC	59.4	BIGSEQ60
	cyp17-1697R	GACTTCCCGCAACATCTCTC	59.4	BIGSEQ60
	cyp17-1388R	TGTTGTTTTCCCTTGTTC	55.3	BIGSEQ50
	cyp17-1021R	CAGCGGTGCACATACTGTCT	59.4	BIGSEQ60
	cyp17-720R	TACCCACCTGAGCCTCAAAC	59.4	BIGSEQ60
	cyp17-374R	TAAGGGCTGTGGGTTAATGG	57.3	BIGSEQ50
	cyp17-117R	CTCCCCATGCTTGAATGACT	57.3	BIGSEQ50
	cyp17+67R	GGCTACCCTGATCTTCACCTT	59.8	BIGSEQ60
	cyp17-112R	GTCAGTTGATCACCTCTGA	57.3	BIGSEQ50

Table 8-2 Expand high fidelity PCR system cycling conditions.

Time	Temperature	Cycles
2 min	94°C	1
15 sec	94°C	
30 sec	55°C	10
4 min	68°C	
15 sec	94°C	
30 sec	55°C	20
4 min (+5 sec every cycle)	68°C	
7 min	72°C	1

Table 8-3 Primers used to amplify and sequence exonic regions of *CYP17A1* in the AFS cohort.

Target Exon		Primer Name	Sequence 5'-3'	T _m (°C)	Cycling Conditions
Exon 1	PCR Primers	cyp17ex1_f1	CCACTGCTGTCTATCTTGCC	59.4	See Table 8-4
		cyp17ex1_r1	TGAAGACCTGAACAATCCCA	55.3	Annealing temp: 55°C
	Sequencing Primers	cyp17ex1_f1	CCACTGCTGTCTATCTTGCC	59.4	BIGSEQ60
		cyp17ex1_r1	TGAAGACCTGAACAATCCCA	55.3	BIGSEQ50
		17Exon1F	CAGAGGGTGATCAACTGAC	60.1	BIGSEQ60
		17Exon1R	CTAGGCATGGTCTGAAGAC	60.2	BIGSEQ60
Exons 2 & 3 (+ intron 2)	PCR Primers	cyp17ex2+3_f1	GGTGTGAGATTCTACAGCC	59.4	See Table 8-4
		cyp17ex2+3_r1	TCTACTAGAACCTGAAGGCAG	57.9	Annealing temp: 55°C
	Sequencing Primers	cyp17ex2+3_f1	GGTGTGAGATTCTACAGCC	59.4	BIGSEQ60
		cyp17ex2+3_r1	TCTACTAGAACCTGAAGGCAG	57.9	BIGSEQ50
		cyp17ex2_r1	TCCTAACCCCTTACCCCTG	56.0	BIGSEQ50
		cyp17ex3_f1	TGGTACAGAGAGGGGTAAG	59.4	BIGSEQ60
Exon 4	PCR Primers	cyp17ex4_f1	GGTGGAGTAGGAACTCCAG	59.4	See Table 8-4
		cyp17ex4_r2	TCCACCCTGCTCTGTGATT	57.3	Annealing temp: 59°C
	Sequencing Primers	cyp17ex4_f1	GGTGGAGTAGGAACTCCAG	59.4	BIGSEQ60
		cyp17ex4_r1	TGTGCCAGTTCTCTGCTTG	59.4	BIGSEQ60
		cyp17ex4_f2	AGCTAAGATCCGCCTCCAG	58.8	BIGSEQ50
		cyp17ex4_r2	TCCACCCTGCTCTGTGATT	57.3	BIGSEQ50
Exons 5 & 6 (+ intron 5)	PCR Primers	cyp17ex5+6_f1	TGGCAGGAGTGTACAGATG	59.4	See Table 8-4
		cyp17ex6_r1	TGAATGCATCATGGGGCTAG	57.3	Annealing temp: 60°C
	Sequencing Primers	cyp17ex5+6_f1	TGGCAGGAGTGTACAGATG	59.4	BIGSEQ60
		cyp17ex5_f1	GGCAGGAGTGTACAGATG	58.8	BIGSEQ50
		cyp17ex5_r1	TGGGGTCTAGGATCAATGAG	57.3	BIGSEQ50
		cyp17ex6_f1	ACACACTAGTACCTCCAAC	57.3	BIGSEQ50
cyp17ex6_r1	TGAATGCATCATGGGGCTAG	57.3	BIGSEQ50		
Exons 7 & 8 (+3'UTR)	PCR Primers	cyp17ex7+8_f1	TTCCTCTTCCACTCTGGAGC	59.4	See Table 8-4
		cyp17ex8utr_r1	GAATGAGTGAGCAAATGAATAC	54.7	Annealing temp: 58°C
	Sequencing Primers	cyp17ex7+8_f1	TTCCTCTTCCACTCTGGAGC	59.4	BIGSEQ60
		cyp17ex8utr_r1	GAATGAGTGAGCAAATGAATAC	54.7	BIGSEQ50
		cyp17ex7_r1	TTGGCAGAGGTGAAGGGGTA	59.4	BIGSEQ60
		cyp17ex7+8_r1	GCCACATAGGGTGACAGG	61.0	BIGSEQ60
cyp17ex8_f1	TCAACCAGGGCAGAACCATG	59.4	BIGSEQ60		
cyp17ex8_r1	TGTGTTGTGGGGCCACATAG	59.4	BIGSEQ60		

Table 8-4 Thermo-Start *taq* DNA polymerase PCR enzyme kit cycling conditions.

Time	Temperature	Cycles
15 min	94°C	1
15 sec	94°C	
30 sec	insert annealing temp	30
1 min	72°C	
1 min	72°C	1

Table 8-5 Primers used to amplify and sequence intronic regions of *CYP17A1* in the AFS cohort.

Target Intron		Primer Name	Sequence 5'-3'	T _m (°C)	Cycling Conditions
Intron 1	PCR Primers	intron1F	CACCAAGACTACAGTGATTG	55.3	See Table 8-4
		intron1R1	GTGCGCCAGAGTCAGCGAAG	63.5	Annealing temp: 57°C
	Sequencing Primers	intron1F	CACCAAGACTACAGTGATTG	55.3	BIGSEQ50
		intron1R1	GTGCGCCAGAGTCAGCGAAG	63.5	BIGSEQ60
		intron1s1f	CTTAGCCTAGCACCCAGCAC	61.4	BIGSEQ60
		intron1s1r	AGCTGGAAATAGCACCCAGGA	57.3	BIGSEQ50
		intron1s2f	CCAATCTCAGCTCACTGCAA	57.3	BIGSEQ50
		intron1s2r	CTAAGGTGGGAGGATCACGA	59.4	BIGSEQ60
		intron1s4f	ACCCTGTCAGCGAAAAGAAC	57.3	BIGSEQ50
		intron1s4r	TTGCCCTTACACCTCTGGTC	59.4	BIGSEQ60
intron1s3f	CTTCAGGGTCAGGAAATGGA	57.3	BIGSEQ50		
intron1s3r	AGGCTGAGGACTGCACAGAT	59.4	BIGSEQ60		
Intron 3	PCR Primers	cyp17ex3_f1	TGGTACAGAGAGGGGGTAAG	59.4	See Table 8-4
		cyp17ex4_r1	TGTGCCAGGTTCTCTGCTTG	59.4	Annealing temp: 59°C
	Sequencing Primers	Intron3s1f	TGGTTGAAGGTGAGATGCTG	57.3	BIGSEQ50
		Intron3s2f	AAGCATTCTATACGCATTCATCG	57.1	BIGSEQ50
		Intron3s1r	AAGCTCCTTAACCCCGCTAA	57.3	BIGSEQ50
		cyp17ex3_f1	TGGTACAGAGAGGGGGTAAG	59.4	BIGSEQ60
Intron3s2r	GACCTTCAGCCAGAATGGAA	57.3	BIGSEQ50		
Intron 4	PCR Primers	Intron4F1	AAGCAGAGAACCTGGCACAT	57.3	See Table 8-4
		Intron4R1	TCACTCCGGAATTTCTCCTG	57.3	Annealing temp: 57°C
	Sequencing Primers	Intron4F1	AAGCAGAGAACCTGGCACAT	57.3	BIGSEQ50
		Intron4R1	TCACTCCGGAATTTCTCCTG	57.3	BIGSEQ50
		Intron4s1r	CTTGCTGGCCTAGTTTTTG	57.3	BIGSEQ50
		Intron4s1f	CAGCTATTTGGGAGGCTGAG	59.4	BIGSEQ60
Intron 6	PCR Primers	cyp17ex6_f1	ACACACTAGTCACCTCCAAC	57.3	See Table 8-4
		cyp17ex7+8_r1	GCCACATAGGGTGGACAGG	61.0	Annealing temp: 60°C
	Sequencing Primers	Intron6s1f	GCTGGCCAACCTAAAGTCAG	59.4	BIGSEQ60
		Intron6s1r	ATCTTGGCTCACTGCAACCT	57.3	BIGSEQ50
		Intron6s2r	GGAAGCTCCTCTGGGAAGTC	61.4	BIGSEQ60
		intron6s3r	GGGACTTCGTA CTCCCTTCC	61.4	BIGSEQ60
Intron 7	PCR Primers	cyp17ex7+8_f1	TTCTCTTCCA CTCTGGAGC	59.4	See Table 8-4
		cyp17ex8utr_r1	GAATGAGTGAGCAAATGAATAC	54.7	Annealing temp: 55°C
	Sequencing Primers	cyp17ex8_r1	TGTGTTGTGGGGCCACATAG	59.4	BIGSEQ60
		cyp17ex7+8_r1	GCCACATAGGGTGGACAGG	61.0	BIGSEQ60
		intron7s1r	GCCCTTAACGACACAGAGGA	59.4	BIGSEQ60
		Intron7s2r	CAGGCCATGATGAGGAAGAG	59.4	BIGSEQ60

Table 8-6 Primers used for site-directed mutagenesis of pGL3-17 reporter construct.

SNP	Primer Name	Sequence 5'-3'	T _m (°C)	Base Change
-2205	t193c	ATGGGAAATGGTCAAAGGACACCTTCTGGGTAGGG	71.8	T → C
	t193c_antisense	CCCTACCCAGAAGGTGTCCTTTGACCATTTCCCAT	71.8	
-1877	c521t	AAGGGAGAGATGTTGTGGGAAGTCAGGGACC	70.8	C → T
	c521t_antisense	GGTCCCTGACTTCCCAACATCTCTCCCTT	70.8	
-1488	c910g	GAGAGAGGCTATAAATGGAGATGCAAGTAGGGAAGATAT	69.5	C → G
	c910g_antisense	ATATCTTCCCTACTTGCATCTCCATTTATAGCCTCTCTC	69.5	
-1204	t1194c	TGTTAAGGTGTTTATCAAGACAGTACGTGCACCGCTGAAC	71.4	T → C
	t1194c_antisense	GTTCCAGCGGTGCACGTAAGTCTTGTATAAACACCTTAAACA	71.4	
-804	g1594a	GTCTCTCTTTATTTCTCAGCCAGCTGACACTTATAGAAAGAAC	70.4	G → A
	g1594a_antisense	GTTCTTTCTATAAAGTGTGAGCTGGCTGAGAAATAAAGAGAGAC	70.4	
-362	a2036g	CCAGTGATTTTGATTTTGCAGCATGGAAAGTTCCAAGCCTT	70.4	A → G
	a2036g_antisense	AAGGCTTGAACTTCCATGCTGCAAAATCAAATCACTGG	70.4	
-34	c2364t	CAGCTCTTCTACTCCACTGCTGTCTATCTTGCCTG	71.8	C → T
	c2364t_antisense	CAGGCAAGATAGACAGCAGTGGAGTAGAAGAGCTG	71.8	

Table 8-7 Primers used for sequencing of pGL3-17 (and mutated) reporter constructs.

Primer name	Sequence 5'-3'	T _m (°C)
GLprimer2	CTTTATGTTTTGGCGTCTTCCA	57.1
RVprimer3	CTAGCAAATAGGCTGTCCC	57.3
RVprimer4	GACGATAGTCATGCCCCGCG	63.5
17_-2325R	GACTCATTAGCTGGTCCCA	59.4
17_-2288R	GTGTTGCAATCGAACTGCAT	55.3
17_-2107R	CCTGATCTAACGCCTCAGCT	59.4
17_-2414R	TTGGTGGAATTGCCTTAC	55.3
17_-2729R	TTGGACGTTTGATTGTTC	53.2
17_-2729F	TGAACAATCAAACCGTCCAA	53.2
17_-2595F	GGGAATCTTCCCCTCAGTA	59.4
17_-2900F	CTCGATTGCTTCTTACGG	57.3
17_-2815R	GGCTGGAGGTAAACAAAGCA	57.3
cyp17-1213F	CCGCTCTGGGAATGTCTATC	59.4
cyp17-1935F	AGCTGAGCGTTAGATCAGG	59.4
cyp17-1525F	GTCACCTCAGGACCACTGTGA	59.8
cyp17-457F	CACCGCTCCCCACAGCTTAGCAC	67.8
cyp17-117R	CTCCCATGCTTGAATGACT	57.3
cyp17+67R	GGCTACCCTGATCTTACCTT	59.8
cyp17-112R	GTCAGTTGATCACCTCTGA	57.3
cyp17promF2	ATGCAGTTCGATTGCAACAC	55.3
cyp17promF1	TGGGGACCAGCTAATGAGTC	59.4

Table 8-8 Primers used for sequencing of pEZX reporter constructs.

Primer name	Sequence 5'-3'	T _m (°C)
pEZX-MT01 For	GATCCGCGAGATCCTGAT	59.9
pEZX-MT01 Rev	TTGGCGTTACTATGGGAACAT	58.7

8.2 Appendix 2

Nucleotide sequences were obtained from Ensembl release 56 Sept 2009

Key:

CYP17A1 5' promoter region

CYP17A1 5' untranslated region (5'UTR)

CYP17A1 exons

CYP17A1 introns

CYP17A1 3' untranslated region (3'UTR)

TGGGCTAATTACAGTCACTGCACTGGCCACCCTGCCGGAGTGGCATTACACCAATCTATTCAAATGGCTAATTTTGTTAATGATTG
 GTAAGGCAATTCACCCAAATGTGGAATCCTCAACAAGGCATTGATCAAAAATTAGCTAATGATTTAAGACAGTCTGTTATTTGGCTT
 GGGGACCAGCTAATGAGTCTCGAACATCACATGCAAATGCAGTTCGATTGCAACACTTCTGATTTCTATAGCACACCATATTCCTACA
 ACGAGACTGATCATGGGAAATGGTCAAAGGACACCTTCTGGGTAGGGAAGATAATTTATCCTTGGACATAACTAAATTAAGAAAC
 AAATTTTGAAGCCTCTCAAGCTCATTATCCATTGTGCCTGGAGCTGAGGCGTTAGATCAGGTGGCAGAAAAGTCTTCTGGACTAAA
 CTCCACAACCTGGATTAAGTCTACTGGGGCTCCACTGTAGGAAATTTTGAATCATGTTTCTGTGTTAATCGGCTTGTTTTTAGTGT
 GCCAGACCAGTCAAAGAATCCTGCATCAAAACCGAGAGAACGAGCAAGCCTTCATCGCCACGGCAGCATTTATATAAAAAGAAAGGG
 AGAGATGTTGCGGGAAGTCAAGGACCCTGAATGGAGGGACTGGCTGGAGCCATGGCAGAGGAACATAAATGTGAAGATTTCAAT
 TTAATATGGACATTTATCAGTTCACCAATAATACTTTTATAATTTCTTATGCCTGTCTTACTTTAATCTCTTAATCCTGTTATCTTTGTA
 AGCTGAGGATGTTTGTCACTTCAGGACCCTGTGATAATTGTGTTAACTGTACAAATGATTGTAAGACATGTGTTTGAACAATGAA
 AATTAGTGCACCTGAAAAAGAACAGAATAAGAGCAATTTTGGGAACAAGGAAACAACCATAAAGTCTGACTGCCTGCAGGG
 TCGGGCAGAAAGAGCCATATTTTCTTCTGAGAGAGGCTATAAATGGACATGCAAGTAGGGAAGATATCACTAAATTTCTTTTCTTA
 GCAAGGAGTATTATTATAATACCCTGGGAAAGGAATGCATTCTGGGGGGAGGTCTATAAACAGCCGCTCTGGGAATGTCTATCTT
 GTGCAGTTGAGATAAGGACTGAGATACGCCCTGGTCTCCTGCAGTACCCTCAGGCTTACTAGGGTGGGGAAAAAATCCGCCCTGGT
 AAATTTGTGGTCAAGCCGTTCTCTGCTGTGCAACCCTGTTTGTCTGTTTAAAGGTGTTTATCAAGACAGTATGTGCACCCTGAAC
 ATAGACCCTCATCTGATGTTCTGCTTTTGCCTTTGCTGTGATCTTTGGACCCTTACAGTGGTCTGCTTTTGCCTTTGCTTT
 GTGATCTTTGTTGGCCTTATCGGTAGTTCTGCTTTTGCCTTTGCTTTTCCCTCAGAAGCATGTGATCTTTGTAGACACTTATTAG
 TAGTTCTGCTTTTGCCTTTGAAGCATGTGATCTTTGTACCTACTCCCTGTTCTTACACCCCTCCCTTTTGAACCCCTAATAAAAA
 CTTGCTGGTTGAGGCTCAGGTGGGTATCACAGTCTACCGATATGTGATGCCACCCCGCGGCCAGCTGTAAAATCCTCTCTTT
 ATACTGTCTCTTTATTTCTCAGCCGGCTGACACTTATAGAAAGAACCTACGTTGAAATATTGGGGGTGGGTTCCCCAGTACGCTA
 GTCCTGCTGATGAGCAAAGAAGGTGTTGATGGCATTGATCAACAAGAAATGTTATGAAACGGCCTCCACCTCTGGCATTCTAG
 TACTGACCTATCTCTCCCTCCCTCCACCGCTCCACAGCTTAGCACCCTTTCGTTCCCATACACATGTACATTTTTATTTGGGGA
 CCATTAACCCACAGCCCTTATCGCTGCCAAAACCATGGGCTGGAGGGCCAGGGCTGCATGGACAGTACACCACTGCACACCAG
 CCTGGTGTGAGCAAGACTCTGAAAAAAGAAAGCAAGCATAAAAGACCTTAAACAGTCCCTGCTACTTGTGACCTCCTGAATC
 TGTCATCTGTCCAGTGATTTTGATTTTGAACATGGAAAGTCCAAGCCTTGACTCCTGAGCCAGATACCATTCGCACTCTGGAGTC
 ATTCAAGCATGGGGAGCTCCTCAGAGGGTGTCAACTGACCTCCCTTACCTAGCTCCTCCTCCGGAGGTTTGCCTGGAGTTGAGCC
 AGCCCTTGAGGAGGCCTCACTCCACCGCCTCTCCCTTCTGGATATGAGTCAAGGCTCTTAAAGGCCTCTGTGCTTACAGTCTTCC
 AAGGAGATAACACAAAGTCAAGGTGAAGTCAAGGTCAGGCTAGCCCTTAAAGGCCTCTGTGCTTACAGTCTTCCACAGCTCTT
 CTACTCCACTGCTGTATCTTGTCTGCTGCGGACCCAGCCACTGTTGGGAGCTCGTGGCTCTTTGCTTACCCTAGCTTATTGTT
 TTTGGCCAAAGAGAAGGTGCCCTGGTGCCTAAGTACCCAAAGAGCCTCCTGTCCCTGCCCTGGTGGGCAGCCTGCCATTCTCCCA
 GACACGGCCATATGCATAAACAATCTTCAAGCTGCAGAAAAAATATGGCCCATCTATTGGTTGCTATGGGCACCAAGACTACAG
 TGATTGTGCGGCCACCACAGCTGGCCAAGGAGGTGCTTATTAAGAAGGGCAAGGACTTCTGTTGGCGGCTCAAATGTAAGTGGT
 GCCCATCTCTCCCTGCCCTTACCACCCCTGGGATTGTTCAAGTCTTACAGACTGCCTAGAATGGGGCTTCCAGCTCCAACAA
 CCTGTAATCTTCCAAAGTAGACTAGTGGGATGATGTGAAGGGAGTGAACCTTACAGACCCACCCAGCCTCTAAATAGGCAGGA
 AGAATTAAGGAATGTCTCTTACCAGGCTGCCAGGAGGTGGATGGGAGGACCACAGTGGTCTGAGGGGTCAAGGAATCCTC
 ACTCCACTCCTCTCTGAGCCTAGACTTCTAATGGACTGAGAAGGTGCATGTACAGCACTAGCCTAGCACCCAGCACAGTAAGT
 GCCCTTATACAGCCAGGATTCATGTTACTTTTATGGAATGGGGCAGTACTACTGCTCCATGAAAGCTGCTGGGGAGAAT
 TAGCCTAGCTATTGCAAGGCTGGGATTGCTGCTTCTGGTGTATTTCCAGCTACTCAGGCTCACAGGGGAGTCTTACAATGACA
 TTTCAAGGTTGCTGATGAGCCTCCACTCAGCAGGGCCCCCAGCCTCTCAGCATTTTTTTTTTTTTTTTTTTTTTTTGGAGACAGATCTC
 TCTGTGCGCCAGCCTGGAGTGCAGTGGCAATCTCAGCTCACTGCAACCTCTGCCTCCCGGTTCAAGTATTCTCCTGCCTCAGC
 CTCTGAGTACCTGGGACTACAGGAGCATGCCACCATGCCCGCTAATTTTTGTATTTTTAGTAGAGATGGTGTTCACCATGTTAGC
 CAGGATGGTCTCGATCTCCTGACCTCGTATCCTCCACCTTAGCCTCCAAAGTCTAGGATTATAGGCGTAAGCCACTGTGCCCTG
 CCAGCCTCTCAGCTTTGATCAAGCAAGGGTGGTTATTTTTCTTGGACCAATCAGCCAGGTCTGCTGACCAACTACCTAGCTCCCA
 CCTCTGCTGGCTTCTCCCGGGGAGAGAAAGATGGAGAAGGCTAGTCATGTGGATCTCAGGGTCAAGAAATGGAAAAGGGAGG
 CTTTGGACCCTTTGCTTTGGGGGACCTTAGGAGGAGGCGCTCGGCCAAGTCCAGACTGGGTAGACAAAACATCTGCACTCT
 CCAAATGTGGGCTTGTGGCTGGGTATGCAGGCTTGAATGGAAGGGTAAACCTGAGTGAAGTGAAGTGTGCTTTAGCTCAGCTAA
 GGGCTCAGGGAAAAGCAGAGATCTGTGAGTCTCAGCCTCAAGACTCACTGCTCCCTACCCTCTGGACAGGCATAGTTAGAG
 AGTTTATCCCATCCAGAGTTGCCCTCTGTGGTCAAGAACTGATGAGCAAAAAGAGCCAGAGGGCACCTGTGAGCGAAAAGAA
 CCCCATGTGCTGCATTCTAATTAAGGGTTCTTTCTTCTCTTATGATCTACTGTATTTCTGAAGGAATGGGAGTAGGAGGCCTTAG
 GGTCTGCTACCAAGTCTTGCAGTCATGGTGGAGTGCAGTGGGGCTGTGCCACATGGGAGTCAAGTGCAGGACCTGCCTT

TCCTCCAGGAAGGAAAGCAGGGACCAGAGGTGTAAGGGCAAGAGTGGGGTGGATGGTGTGAGATTCTACAGCCTTGCTGCTCT
 CTAAGGCAACTCTAGACATCGCGTCCAACAACCGTAAGGGTATCGCTTCGCTGACTCTGGCGCAGCTGGCAGCTGCATCGAAGG
 CTGGCGATGGCCACCTTTGCCCTGTTCAAGGATGGCGATCAGAAGCTGGAGAAGATCA GTGAGTGCCAGGCTGGCCCTGGGGCT
 GGGGCTGGATCCACAGGAGCTGCTGGAGGGAGAGGGGTTGGCAGGGGTAAGGGTTAGGACTAGAGCGCAATGCAGCCTTT
 TCTTGGCTACTGCTGCCATCTAGTGGCCATCTGCTATCTGTCCCCGCTCCTGTTAAGAGGCAACTGGTACAGAGAGGGGGTAAGGG
 TGCTGATTCATTTCCACCTCATGCCCCCTCTCCCTCAGTTTGT CAGGAAATCAGTACATTGTGTGATATGCTGGCCACCACAACG
 GACAGTCCATAGACATCTCTTTCTGTCTTCGTGGCGGTAACCAATGTCATCTCCTTGATCTGTTCAATACCTCTACAAGAATGGG
 GACCCTGAGTTGAATGTCATACAGAATTACAATGAAGGCATCATAGACAACCTGAGCAAAGACAGCCTGGTGGACCTAGTCCCTG
 GTTGAAGGTGAGATGCTGCCAGCCCTGCCTCAGGTTCTAGTAGACCCTGACATTGTCCCAATCTTCTTCTTTTACTTCCCTGCT
 CCAGCCGCAATGACCCATCTTTTCTGATTACCTCCGCCACTCTACCTCCTCTGCCACTAAAACCTTTGCCATTTCTCTGCAGAGAT
 AGATTTAGCCTTTTAAATTATGCACCTTAGTACTCCAGATAAGTACCTTCAATTTCTTTTCCAATTACCATGTGCCAGTAAAGCTTA
 TACGCATTCATCGCTGAATTTCCCTTGAAGTAGGTTTTATTATCCCATTTGTGCAGGTGAGAAGCAGGCTTAGCGGGTTAAGGAG
 CTTGTCTGAGCCTCAGGCTCATGTCTCTCACTCCTAAGGGCTGGACACATAGCAGAGTACAGCCTTGATGTTTATTGAATGGG
 GAAGGAGAGGTGGAGACCACGCCCTCTCCCTGTTTAGAATTGTCTTCGTCTCATGATAAACCCGTTCTGTGTCCCATCTTGCCT
 TCCATTCTGGCTGAAGGTCAGGGGTGGAGTAGGAATCCAGAGACAGAAAGCTAAGATCCGCTCCAGGAGAGACTCTGGCAGCT
 GGAGAAGCAAATGGAAGAAGGGTGGATTTAATTTCTTTTATTTCCAGATTTTCCCAACAAAACCTTGAAAAAATTAAGAG
 CCATGTTAAATACGAAATGATCTGCTGAATAAAAATACTTGAAAAATTACAAGGTAGGTGATAGAGCAGAAGAGAATATGAGTTAGG
 CTAAGGTAATCACAAGAGCAGGGTGGAGTCCATTCTACACACTGTAGAAGCTTCAAACCAAGCAGAGAACCTGGCAGATAGTAG
 GTGTACAATAAAAACTGACTTAAGGGCTGGGCGCGTGGCTCACGCCTGTAATCCCAACACTTTGGGAGGCGGAGGTGGGCAGATC
 AATTGAGGTGAGGATTCGAGATGAGCCTGGCCAATATGGTGAACCCCGTGTACTAAAAATACAAAACTAGGCCAGGCAAGA
 TGGCTCACACTGTAATCCCAACATTTGGGAGGCCAAGGTGGGCAGATCACCTGAGGTTGGGAGTTCGAGACCAGCCTGACCAAC
 ATGGAGAACTCTGTCTACTAAAAATACAAAATTAGCCGGCAGCGTGGCGCATGCCTATAATCCAGCTATTTGGGAGGCTGAG
 GCAGGAGACTCACTTGAACCCGAGAAGCAGAGGTTGCAGTGAGCTGAGATCATGCCATTGCACCTCCAGCTCCAGCTGGGCATTGCACCAAG
 ATTCTGTCTCAAAAAAAAAAAAAAAAAACTGACTCAAGGAGTTGGGATCGAAAAGTGAGAACTGAAGAGGATCTAGAAGAGACCT
 AACCTCTCCACCAATTTAAAGAGGGCCCGGGGCTGCCTCTACCTCCACAAGTTCTGAGGTCCTGCCAGACTTGCTCTACTTCCAA
 GTGGAAGGAGCCTTGTATCTCTAGTCAGGGACAGAAGTATGGCAGGAGTGTACAGATGGGGCTCCTTCTTATTAATGTCTCCA
 ACCTCACCAACCCAGGAGAAATTCGGAGTACTCTATCCAACATGCTGGACACACTGATGCAAGCCAAGATGAACTCAGATAA
 TGGCAATGCTGGCCAGATCAAGACTCAGAGCTGCTTTCAGATAAACCACATTCTCACCACCATAGGGGACATCTTTGGGGCTGGCGT
 GGAGACCACCCTCTGTGGTTAAATGGACCCTGGCCTCCTGCTGCACAATCCTCAGGTGTGCTTCCCTCATTGATCCTAGACCC
 CAGCCAGCCCAATCTCTGGGCTCCAGAGAAAGGGAGAGCAATCTCTCAGGCTTTCTGTGCAGGAAGACTAGGCCTGCCCTGCTCC
 TTACCAAGCAGTAGTTGGCTTTGACCCAGAGTAGAGCTGCCCATCTTCTGGAAGCCGGGCTGGGCCCCAGAGCCACTACTGG
 GAAGGGACTGGACAGGCTCTTCTCGATGTACAGTTGGATTCTTCTAAGCCCTTGCTTCTCTGGGCTTACACACACTAGTCACT
 CCAACCTACTCTGGTCTTTCAGGTGAAGAAGAAGCTCAGAGGAGATTGACCAGAATGTGGGTTTCAGCCGACCACTATCAGT
 AACCTGTAACCTCTCCTCCTGCTGGAGGCCACCTCCGAGAGTGTCTCGCTCAGGCCCTGACCTTCCCTCAGCCCAACG
 GCCAACCTGTTCCAGGTGTGTGCCTGCCCTCCAGTGACATCTAGCCCATGATGCATTCAACACTGCTTGCCAGCCACCTGGCTCC
 CCTACCCCGGCCCTGCTGGCCAACCTAAAGTCAGTCAACCTCAACTACTAAAAATCATCTGCCGGCCGGGCACGGTGGCTCA
 CACTGTATCCCAACACTTTGGGAGGTCGAGGGGGTGGATCATGAGGTGAGGGTTCAAGACCAGCCTGACCAATATGGTGAAA
 CCCCCTCTACTAAAAATACAAAATTAGCCATGCATCGTGGCGCTGCCTGTAGTCCAGCTACTCAGGAGGCTGAGGCAGGAG
 AATCACTGAACCAAGGCGGCGGAGGTTGCAGTAGCCAAGATTGCACCACTGCACTCCAGCCTGGGTGACAGAGCGGGACTCTGT
 CTCAAAATAAATAATTAATTAATTAATATAAAAATCATCCTGCCCCAGCCCCGTGGCTCCATGTCTCTACCACCTACAGACACGCAT
 TGACTCATCCACAGATCTGCCTGACTTCCCAGAGGAGCTTCTGTGCCCTCAGAGACATGTGGTCTGGGATGAAAGGCTGGGAGCT
 CCATGTTCCAACAGCTGCAGCACGCACATAACATGCGCTGCAGCTCAAACGCACACCACATACACTGCCAGACACCAAAGTCCA
 CAGACACAGGTGTTAGACAGAAAGCGCTGTTAGGAGGGAAGGGATGGAGAAGGGCTGGATTTAGGTTTATCTGGCAGAAGCTG
 AGGAAAACATGAGTGAGTGGGAATGAGGGAGTAAAGGGCATTTCCTCACGGCGGAAGAATGAGGGGGCATGAGGCTGAGCAAG
 GAAGGGAGTACGAAGTCCCAGACCCACTTTTCTCTTCACTCTGGAGCAGCATCGGTGAGTTTGTCTGGACAAGGCGCAGAAG
 TTATCATCAATCTGTGGGCGCTGCATCAATGAGAAGGAGTGGCACCAGCCGATCAGTTTCACTGCTGTGAGTCTGTCTGTCT
 GCGCCTGGGCCACACAGCGAGCCTGGACTCTGCTCCACCACCCAGTACCCCTTACCTCTGCCAAGCTTGTCTAGAAAACCTCTT
 GGCTCCAATAACGACCTGTTGACACCCTCATCTGCCATAGACTTACCAAACCTCTTACAGCTGGGTTTCCACGCTCTTCTTCC
 AACCAACTGCAAATTCACCCTCAAGAAGCCCTCTACGCCTGTCTGCCATTAAGTCTGTCCCTTCTCCCTCGGATGGTGTATTTT
 CATAGGTTAATTCATCTCTTTCCATCTTCTGAATATTTCACTTCTGTGTCTGTTAAGGGTACCTGAAAGCAGGGCTGTATCTC
 TCCCAGGCGGGGTTCCCCATAATAAGGCTACATCCTCAGATCAGGGTTCCTGGGCAGGGCCATGTCTCCCTCAACCAGGGC
 AGAACCATGCCTCTCTCCCTCCTGCCCTAACCCCTGGCTGATGCCACTCCTTGCCTGCAGAGCTTTCTTGAATCCAGCGGGGACCC
 AGCTCATCTCACCTCAGTAAGCTATTTGCCCTTCGGAGCAGGACCTCGCTCCTGTATAGGTGAGATCCTGGCCCGCAGGAGCTCT
 CCTCATCATGGCTGGCTGCTGCAGAGGTTGACCTGGAGGTGCCAGATGATGGGCAGCTGCCCTCCCTGGAAGGCATCCCAAGG
 TGGTCTTTCTGATCGACTTTTCAAAGTGAAGATCAAGGTGCGCCAGGCTGGAGGGAAAGCCAGGCTGAGGGTAGCACCTAAAGG
 CTGTAACCTACAGCCCCTGTCCACCTATGTGGCCCCACAACACAGATTTAGAGATAACAACCCCCACCCTTCTCCGCTTCTTCCCT
 ACTCCAACCCACTCTGCCTCTTTTTTTCAGCTTGTGGCAATGCCAGTGATGTGCATAAACAGTTTTTTTTTTTCCATAA

9 References

Achermann, J. C., M. Ito, P. C. Hindmarsh and J. L. Jameson (1999). "A mutation in the gene encoding steroidogenic factor-1 causes XY sex reversal and adrenal failure in humans." *Nat Genet* 22(2): 125-126.

Adrogué, H. J. and N. E. Madias (2007). "Sodium and potassium in the pathogenesis of hypertension." *N Engl J Med* 356(19): 1966-1978.

Allayee, H., T. W. de Bruin, K. Michelle Dominguez, L. S. Cheng, E. Ipp, R. M. Cantor, K. L. Krass, E. T. Keulen, B. E. Aouizerat, A. J. Lusis and J. I. Rotter (2001). "Genome scan for blood pressure in Dutch dyslipidemic families reveals linkage to a locus on chromosome 4p." *Hypertension* 38(4): 773-778.

Ambros, V., B. Bartel, D. P. Bartel, C. B. Burge, J. C. Carrington, X. Chen, G. Dreyfuss, S. R. Eddy, S. Griffiths-Jones, M. Marshall, M. Matzke, G. Ruvkun and T. Tuschl (2003). "A uniform system for microRNA annotation." *RNA* 9(3): 277-279.

Angius, A., E. Petretto, G. B. Maestrone, P. Forabosco, G. Casu, D. Piras, M. Fanciulli, M. Falchi, P. M. Melis, M. Palermo and M. Pirastu (2002). "A new essential hypertension susceptibility locus on chromosome 2p24-p25, detected by genomewide search." *Am J Hum Genet* 71(4): 893-905.

Attard, G., A. H. Reid, T. A. Yap, F. Raynaud, M. Dowsett, S. Settatree, M. Barrett, C. Parker, V. Martins, E. Folkard, J. Clark, C. S. Cooper, S. B. Kaye, D. Dearnaley, G. Lee and J. S. de Bono (2008). "Phase I clinical trial of a selective inhibitor of CYP17, abiraterone acetate, confirms that castration-resistant prostate cancer commonly remains hormone driven." *J Clin Oncol* 26(28): 4563-4571.

Auchus, R. J. and W. Arlt (2013). "Approach to the patient: the adult with congenital adrenal hyperplasia." *J Clin Endocrinol Metab* 98(7): 2645-2655.

Auchus, R. J., T. C. Lee and W. L. Miller (1998). "Cytochrome b5 augments the 17,20-lyase activity of human P450c17 without direct electron transfer." *J Biol Chem* 273(6): 3158-3165.

Auchus, R. J. and W. L. Miller (1999). "Molecular modeling of human P450c17 (17 α -hydroxylase/17,20-lyase): insights into reaction mechanisms and effects of mutations." *Mol Endocrinol* 13(7): 1169-1182.

Bair, S. R. and S. H. Mellon (2004). "Deletion of the mouse P450c17 gene causes early embryonic lethality." *Mol Cell Biol* 24(12): 5383-5390.

Banaszewska, B., R. Z. Spaczynski, M. Pelesz and L. Pawelczyk (2003). "Incidence of elevated LH/FSH ratio in polycystic ovary syndrome women with normo- and hyperinsulinemia." *Rocz Akad Med Białymst* 48: 131-134.

- Banerji, J., S. Rusconi and W. Schaffner (1981). "Expression of a beta-globin gene is enhanced by remote SV40 DNA sequences." *Cell* 27(2 Pt 1): 299-308.
- Barolo, S. and J. W. Posakony (2002). "Three habits of highly effective signaling pathways: principles of transcriptional control by developmental cell signaling." *Genes Dev* 16(10): 1167-1181.
- Barr, M., S. M. MacKenzie, E. C. Friel, C. D. Holloway, D. M. Wilkinson, N. J. Brain, M. C. Ingram, R. Fraser, M. Brown, N. J. Samani, M. Caulfield, P. B. Munroe, M. Farrall, J. Webster, D. Clayton, A. F. Dominiczak, J. M. Connell and E. Davies (2007). "Polymorphic variation in the 11beta-hydroxylase gene associates with reduced 11-hydroxylase efficiency." *Hypertension* 49(1): 113-119.
- Barrett, J. C., B. Fry, J. Maller and M. J. Daly (2005). "Haploview: analysis and visualization of LD and haplotype maps." *Bioinformatics* 21(2): 263-265.
- Bartel, D. P. (2009). "MicroRNAs: target recognition and regulatory functions." *Cell* 136(2): 215-233.
- Bassett, M. H., Y. Zhang, C. Clyne, P. C. White and W. E. Rainey (2002). "Differential regulation of aldosterone synthase and 11beta-hydroxylase transcription by steroidogenic factor-1." *J Mol Endocrinol* 28(2): 125-135.
- Basyuk, E., F. Suavet, A. Doglio, R. Bordonne and E. Bertrand (2003). "Human let-7 stem-loop precursors harbor features of RNase III cleavage products." *Nucleic Acids Res* 31(22): 6593-6597.
- Behm-Ansmant, I., J. Rehwinkel, T. Doerks, A. Stark, P. Bork and E. Izaurralde (2006). "mRNA degradation by miRNAs and GW182 requires both CCR4:NOT deadenylase and DCP1:DCP2 decapping complexes." *Genes Dev* 20(14): 1885-1898.
- Bernstein, E., S. Y. Kim, M. A. Carmell, E. P. Murchison, H. Alcorn, M. Z. Li, A. A. Mills, S. J. Elledge, K. V. Anderson and G. J. Hannon (2003). "Dicer is essential for mouse development." *Nat Genet* 35(3): 215-217.
- Betel, D., A. Koppal, P. Agius, C. Sander and C. Leslie (2010). "Comprehensive modeling of microRNA targets predicts functional non-conserved and non-canonical sites." *Genome Biol* 11(8): R90.
- Bhattacharyya, S. N., R. Habermacher, U. Martine, E. I. Closs and W. Filipowicz (2006). "Relief of microRNA-mediated translational repression in human cells subjected to stress." *Cell* 125(6): 1111-1124.
- Biglieri, E. G., M. A. Herron and N. Brust (1966). "17-hydroxylation deficiency in man." *J Clin Invest* 45(12): 1946-1954.
- Binder, A. (2007). "A review of the genetics of essential hypertension." *Curr Opin Cardiol* 22(3): 176-184.

Bird, I. M., N. A. Hanley, R. A. Word, J. M. Mathis, J. L. McCarthy, J. I. Mason and W. E. Rainey (1993). "Human NCI-H295 adrenocortical carcinoma cells: a model for angiotensin-II-responsive aldosterone secretion." *Endocrinology* 133(4): 1555-1561.

Biron, P., J. G. Mongeau and D. Bertrand (1976). "Familial aggregation of blood pressure in 558 adopted children." *Can Med Assoc J* 115(8): 773-774.

Bohnsack, M. T., K. Czaplinski and D. Gorlich (2004). "Exportin 5 is a RanGTP-dependent dsRNA-binding protein that mediates nuclear export of pre-miRNAs." *RNA* 10(2): 185-191.

Borchert, G. M., W. Lanier and B. L. Davidson (2006). "RNA polymerase III transcribes human microRNAs." *Nat Struct Mol Biol* 13(12): 1097-1101.

Burton, P. R., D. G. Clayton, L. R. Cardon, N. Craddock, P. Deloukas, A. Duncanson, D. P. Kwiatkowski, M. I. McCarthy, W. H. Ouwehand, N. J. Samani, J. A. Todd, P. Donnelly, J. C. Barrett, D. Davison, D. Easton, D. Evans, H. T. Leung, J. L. Marchini, A. P. Morris, C. C. A. Spencer, *et al.* (2007). "Genome-wide association study of 14,000 cases of seven common diseases and 3,000 shared controls." *Nature* 447(7145): 661-678.

Cartharius, K., K. Frech, K. Grote, B. Klocke, M. Haltmeier, A. Klingenhoff, M. Frisch, M. Bayerlein and T. Werner (2005). "MatInspector and beyond: promoter analysis based on transcription factor binding sites." *Bioinformatics* 21(13): 2933-2942.

Caulfield, M., P. Munroe, J. Pembroke, N. Samani, A. Dominiczak, M. Brown, N. Benjamin, J. Webster, P. Ratcliffe, S. O'Shea, J. Papp, E. Taylor, R. Dobson, J. Knight, S. Newhouse, J. Hooper, W. Lee, N. Brain, D. Clayton, G. M. Lathrop, *et al.* (2003). "Genome-wide mapping of human loci for essential hypertension." *Lancet* 361(9375): 2118-2123.

Chen, Y. and J. Pei (2010). "Factors influencing the association between CYP17 T34C polymorphism and the risk of breast cancer: meta-regression and subgroup analysis." *Breast Cancer Res Treat* 122(2): 471-481.

Chen, Y., L. Zhang and Q. Hao (2013). "Candidate microRNA biomarkers in human epithelial ovarian cancer: systematic review profiling studies and experimental validation." *Cancer Cell Int* 13(1): 86.

Chen, Z. J., H. Zhao, L. He, Y. Shi, Y. Qin, Z. Li, L. You, J. Zhao, J. Liu, X. Liang, X. Zhao, Y. Sun, B. Zhang, H. Jiang, D. Zhao, Y. Bian, X. Gao, L. Geng, Y. Li, D. Zhu, *et al.* (2011). "Genome-wide association study identifies susceptibility loci for polycystic ovary syndrome on chromosome 2p16.3, 2p21 and 9q33.3." *Nat Genet* 43(1): 55-59.

Chendrimada, T. P., K. J. Finn, X. Ji, D. Baillat, R. I. Gregory, S. A. Liebhaber, A. E. Pasquinelli and R. Shiekhattar (2007). "MicroRNA silencing through RISC recruitment of eIF6." *Nature* 447(7146): 823-828.

Cheng, A. M., M. W. Byrom, J. Shelton and L. P. Ford (2005). "Antisense inhibition of human miRNAs and indications for an involvement of miRNA in cell growth and apoptosis." *Nucleic Acids Res* 33(4): 1290-1297.

Cheng, L. C. and L. A. Li (2012). "Flavonoids exhibit diverse effects on CYP11B1 expression and cortisol synthesis." *Toxicol Appl Pharmacol* 258(3): 343-350.

Chobanian, A. V., G. L. Bakris, H. R. Black, W. C. Cushman, L. A. Green, J. L. Izzo, Jr., D. W. Jones, B. J. Materson, S. Oparil, J. T. Wright, Jr. and E. J. Roccella (2003). "Seventh report of the Joint National Committee on Prevention, Detection, Evaluation, and Treatment of High Blood Pressure." *Hypertension* 42(6): 1206-1252.

Chua, A. K., R. Azziz and M. O. Goodarzi (2012). "Association study of CYP17 and HSD11B1 in polycystic ovary syndrome utilizing comprehensive gene coverage." *Mol Hum Reprod* 18(6): 320-324.

Chung, B. C., J. Picado-Leonard, M. Haniu, M. Bienkowski, P. F. Hall, J. E. Shively and W. L. Miller (1987). "Cytochrome P450c17 (steroid 17 alpha-hydroxylase/17,20 lyase): cloning of human adrenal and testis cDNAs indicates the same gene is expressed in both tissues." *Proc Natl Acad Sci U S A* 84(2): 407-411.

Clouaire, T. and I. Stancheva (2008). "Methyl-CpG binding proteins: specialized transcriptional repressors or structural components of chromatin?" *Cell Mol Life Sci* 65(10): 1509-1522.

Clyne, C. D., Y. Zhang, L. Slutsker, J. M. Mathis, P. C. White and W. E. Rainey (1997). "Angiotensin II and potassium regulate human CYP11B2 transcription through common cis-elements." *Mol Endocrinol* 11(5): 638-649.

Cowley, A. W., Jr. (2006). "The genetic dissection of essential hypertension." *Nat Rev Genet* 7(11): 829-840.

Crawford, D. C., C. S. Carlson, M. J. Rieder, D. P. Carrington, Q. Yi, J. D. Smith, M. A. Eberle, L. Kruglyak and D. A. Nickerson (2004). "Haplotype diversity across 100 candidate genes for inflammation, lipid metabolism, and blood pressure regulation in two populations." *Am J Hum Genet* 74(4): 610-622.

Crick, F. (1956). Ideas on Protein Synthesis, Wellcome Library ref PP/CRI/H/2/6.

Danila, D. C., M. J. Morris, J. S. de Bono, C. J. Ryan, S. R. Denmeade, M. R. Smith, M. E. Taplin, G. J. Buble, T. Kheoh, C. Haqq, A. Molina, A. Anand, M. Koscuizka, S. M. Larson, L. H. Schwartz, M. Fleisher and H. I. Scher (2010). "Phase II multicenter study of abiraterone acetate plus prednisone therapy in patients with docetaxel-treated castration-resistant prostate cancer." *J Clin Oncol* 28(9): 1496-1501.

Denli, A. M., B. B. Tops, R. H. Plasterk, R. F. Ketting and G. J. Hannon (2004). "Processing of primary microRNAs by the Microprocessor complex." *Nature* 432(7014): 231-235.

Dhir, V., N. Reisch, C. M. Bleicken, J. Lebl, C. Kamrath, H. P. Schwarz, J. Grotzinger, W. G. Sippell, F. G. Riepe, W. Arlt and N. Krone (2009). "Steroid 17alpha-hydroxylase deficiency: functional characterization of four mutations (A174E, V178D, R440C, L465P) in the CYP17A1 gene." *J Clin Endocrinol Metab* 94(8): 3058-3064.

Diamanti-Kandarakis, E., M. I. Bartzis, E. D. Zapanti, G. G. Spina, F. A. Filandra, T. C. Tsianateli, A. T. Bergiele and C. R. Kouli (1999). "Polymorphism T-->C (-34 bp) of gene CYP17 promoter in Greek patients with polycystic ovary syndrome." *Fertil Steril* 71(3): 431-435.

Dickson, M. E. and C. D. Sigmund (2006). "Genetic basis of hypertension: revisiting angiotensinogen." *Hypertension* 48(1): 14-20.

Durkee, T. J., M. P. McLean, D. B. Hales, A. H. Payne, M. R. Waterman, I. Khan and G. Gibori (1992). "P450(17 alpha) and P450SCC gene expression and regulation in the rat placenta." *Endocrinology* 130(3): 1309-1317.

Duursma, A. M., M. Kedde, M. Schrier, C. le Sage and R. Agami (2008). "miR-148 targets human DNMT3b protein coding region." *RNA* 14(5): 872-877.

Dweep, H., C. Sticht, P. Pandey and N. Gretz (2011). "miRWalk--database: prediction of possible miRNA binding sites by "walking" the genes of three genomes." *J Biomed Inform* 44(5): 839-847.

Eberwine, J. (1999). Glucocorticoid and Mineralocorticoid Receptor as Transcription Factors. *Basic Neurochemistry: Molecular, Cellular and Medical Aspects*. A. B. Siegal GJ, Albers RW. Philadelphia, Lippincott-Raven.

Echiburu, B., F. Perez-Bravo, M. Maliqueo, F. Sanchez, N. Crisosto and T. Sir-Petermann (2008). "Polymorphism T --> C (-34 base pairs) of gene CYP17 promoter in women with polycystic ovary syndrome is associated with increased body weight and insulin resistance: a preliminary study." *Metabolism* 57(12): 1765-1771.

Edwards, C. R., P. M. Stewart, D. Burt, L. Brett, M. A. McIntyre, W. S. Sutanto, E. R. de Kloet and C. Monder (1988). "Localisation of 11 beta-hydroxysteroid dehydrogenase--tissue specific protector of the mineralocorticoid receptor." *Lancet* 2(8618): 986-989.

Ehret, G. B. and M. J. Caulfield (2013). "Genes for blood pressure: an opportunity to understand hypertension." *Eur Heart J* 34(13): 951-961.

Eulalio, A., E. Huntzinger and E. Izaurralde (2008). "GW182 interaction with Argonaute is essential for miRNA-mediated translational repression and mRNA decay." *Nat Struct Mol Biol* 15(4): 346-353.

Eystathioy, T., E. K. Chan, S. A. Tenenbaum, J. D. Keene, K. Griffith and M. J. Fritzler (2002). "A phosphorylated cytoplasmic autoantigen, GW182, associates with a unique population of human mRNAs within novel cytoplasmic speckles." *Mol Biol Cell* 13(4): 1338-1351.

Feinleib, M., R. J. Garrison, R. Fabsitz, J. C. Christian, Z. Hrubec, N. O. Borhani, W. B. Kannel, R. Rosenman, J. T. Schwartz and J. O. Wagner (1977). "The NHLBI twin study of cardiovascular disease risk factors: methodology and summary of results." *Am J Epidemiol* 106(4): 284-285.

Filipowicz, W., S. N. Bhattacharyya and N. Sonenberg (2008). "Mechanisms of post-transcriptional regulation by microRNAs: are the answers in sight?" *Nat Rev Genet* 9(2): 102-114.

Fire, A., S. Xu, M. K. Montgomery, S. A. Kostas, S. E. Driver and C. C. Mello (1998). "Potent and specific genetic interference by double-stranded RNA in *Caenorhabditis elegans*." *Nature* 391(6669): 806-811.

Fizazi, K., H. I. Scher, A. Molina, C. J. Logothetis, K. N. Chi, R. J. Jones, J. N. Staffurth, S. North, N. J. Vogelzang, F. Saad, P. Mainwaring, S. Harland, O. B. Goodman, Jr., C. N. Sternberg, J. H. Li, T. Kheoh, C. M. Haqq, J. S. de Bono and C.-A.-. Investigators (2012). "Abiraterone acetate for treatment of metastatic castration-resistant prostate cancer: final overall survival analysis of the COU-AA-301 randomised, double-blind, placebo-controlled phase 3 study." *Lancet Oncol* 13(10): 983-992.

Flück, C. E. and W. L. Miller (2004). "GATA-4 and GATA-6 modulate tissue-specific transcription of the human gene for P450c17 by direct interaction with Sp1." *Mol Endocrinol* 18(5): 1144-1157.

Foekens, J. A., A. M. Sieuwerts, M. Smid, M. P. Look, V. de Weerd, A. W. Boersma, J. G. Klijn, E. A. Wiemer and J. W. Martens (2008). "Four miRNAs associated with aggressiveness of lymph node-negative, estrogen receptor-positive human breast cancer." *Proc Natl Acad Sci U S A* 105(35): 13021-13026.

Franklin, S. S., M. G. Larson, S. A. Khan, N. D. Wong, E. P. Leip, W. B. Kannel and D. Levy (2001). "Does the relation of blood pressure to coronary heart disease risk change with aging? The Framingham Heart Study." *Circulation* 103(9): 1245-1249.

Fraser, R., M. C. Ingram, N. H. Anderson, C. Morrison, E. Davies and J. M. Connell (1999). "Cortisol effects on body mass, blood pressure, and cholesterol in the general population." *Hypertension* 33(6): 1364-1368.

Freel, E. M., M. Ingram, E. C. Friel, R. Fraser, M. Brown, N. J. Samani, M. Caulfield, P. Munroe, M. Farrall, J. Webster, D. Clayton, A. F. Dominiczak, E.

Davies and J. M. Connell (2007). "Phenotypic consequences of variation across the aldosterone synthase and 11-beta hydroxylase locus in a hypertensive cohort: data from the MRC BRIGHT Study." *Clin Endocrinol (Oxf)* 67(6): 832-838.

Friedman, R. C., K. K. Farh, C. B. Burge and D. P. Bartel (2009). "Most mammalian mRNAs are conserved targets of microRNAs." *Genome Res* 19(1): 92-105.

Funder, J. W., P. T. Pearce, R. Smith and A. I. Smith (1988). "Mineralocorticoid action: target tissue specificity is enzyme, not receptor, mediated." *Science* 242(4878): 583-585.

Gazdar, A. F., H. K. Oie, C. H. Shackleton, T. R. Chen, T. J. Triche, C. E. Myers, G. P. Chrousos, M. F. Brennan, C. A. Stein and R. V. La Rocca (1990). "Establishment and characterization of a human adrenocortical carcinoma cell line that expresses multiple pathways of steroid biosynthesis." *Cancer Res* 50(17): 5488-5496.

Geller, D. H., R. J. Auchus and W. L. Miller (1999). "P450c17 mutations R347H and R358Q selectively disrupt 17,20-lyase activity by disrupting interactions with P450 oxidoreductase and cytochrome b5." *Mol Endocrinol* 13(1): 167-175.

Gibbs, R. A., J. W. Belmont, P. Hardenbol, T. D. Willis, F. Yu, H. Yang, C. a. L. Y., W. Huang, B. Liu, Y. Shen, P. K. H. Tam, L. C. Tsui, M. M. Y. Waye, J. T. F. Wong, C. Zeng, Q. Zheng, M. S. Chee, L. M. Galver, S. Kruglyak, S. S. Murray, *et al.* (2003). "The International HapMap Project." *Nature* 426(6968): 789-796.

Gomez-Rubio, P., M. M. Meza-Montenegro, E. Cantu-Soto and W. T. Klimecki (2010). "Genetic association between intronic variants in AS3MT and arsenic methylation efficiency is focused on a large linkage disequilibrium cluster in chromosome 10." *J Appl Toxicol* 30(3): 260-270.

Goodwin, J. E. and D. S. Geller (2012). "Glucocorticoid-induced hypertension." *Pediatr Nephrol* 27(7): 1059-1066.

Greco, T. L. and A. H. Payne (1994). "Ontogeny of expression of the genes for steroidogenic enzymes P450 side-chain cleavage, 3 beta-hydroxysteroid dehydrogenase, P450 17 alpha-hydroxylase/C17-20 lyase, and P450 aromatase in fetal mouse gonads." *Endocrinology* 135(1): 262-268.

Griffiths-Jones, S. (2004). "The microRNA Registry." *Nucleic Acids Res* 32(Database issue): D109-111.

Griffiths-Jones, S. (2006). "miRBase: the microRNA sequence database." *Methods Mol Biol* 342: 129-138.

Griffiths-Jones, S., R. J. Grocock, S. van Dongen, A. Bateman and A. J. Enright (2006). "miRBase: microRNA sequences, targets and gene nomenclature." *Nucleic Acids Res* 34(Database issue): D140-144.

- Griffiths-Jones, S., H. K. Saini, S. van Dongen and A. J. Enright (2008). "miRBase: tools for microRNA genomics." *Nucleic Acids Res* 36(Database issue): D154-158.
- Grimson, A., K. K. Farh, W. K. Johnston, P. Garrett-Engele, L. P. Lim and D. P. Bartel (2007). "MicroRNA targeting specificity in mammals: determinants beyond seed pairing." *Mol Cell* 27(1): 91-105.
- Gu, S. and M. A. Kay (2010). "How do miRNAs mediate translational repression?" *Silence* 1(1): 11.
- Guo, H., N. T. Ingolia, J. S. Weissman and D. P. Bartel (2010). "Mammalian microRNAs predominantly act to decrease target mRNA levels." *Nature* 466(7308): 835-840.
- Guyton, A. C. (1991). "Blood pressure control--special role of the kidneys and body fluids." *Science* 252(5014): 1813-1816.
- Guyton, A. C., T. G. Coleman and H. J. Granger (1972). "Circulation: overall regulation." *Annu Rev Physiol* 34: 13-46.
- Hahm, J. R., D. R. Kim, D. K. Jeong, J. H. Chung, M. S. Lee, Y. K. Min, K. W. Kim and M. K. Lee (2003). "A novel compound heterozygous mutation in the CYP17 (P450 17alpha-hydroxylase) gene leading to 17alpha-hydroxylase/17,20-lyase deficiency." *Metabolism* 52(4): 488-492.
- Hajjar, I. and T. Kotchen (2003). "Regional variations of blood pressure in the United States are associated with regional variations in dietary intakes: the NHANES-III data." *J Nutr* 133(1): 211-214.
- Haller, F., A. von Heydebreck, J. D. Zhang, B. Gunawan, C. Langer, G. Ramadori, S. Wiemann and O. Sahin (2010). "Localization- and mutation-dependent microRNA (miRNA) expression signatures in gastrointestinal stromal tumours (GISTs), with a cluster of co-expressed miRNAs located at 14q32.31." *J Pathol* 220(1): 71-86.
- Hanley, N. A., W. E. Rainey, D. I. Wilson, S. G. Ball and K. L. Parker (2001). "Expression profiles of SF-1, DAX1, and CYP17 in the human fetal adrenal gland: potential interactions in gene regulation." *Mol Endocrinol* 15(1): 57-68.
- Hansson, J. H., C. Nelson-Williams, H. Suzuki, L. Schild, R. Shimkets, Y. Lu, C. Canessa, T. Iwasaki, B. Rossier and R. P. Lifton (1995). "Hypertension caused by a truncated epithelial sodium channel gamma subunit: genetic heterogeneity of Liddle syndrome." *Nat Genet* 11(1): 76-82.
- Hermeking, H. (2010). "The miR-34 family in cancer and apoptosis." *Cell Death Differ* 17(2): 193-199.
- Holleman, A., M. L. den Boer, M. H. Cheok, K. M. Kazemier, D. Pei, J. R. Downing, G. E. Janka-Schaub, U. Gobel, U. B. Graubner, C. H. Pui, W. E. Evans

and R. Pieters (2006). "Expression of the outcome predictor in acute leukemia 1 (OPAL1) gene is not an independent prognostic factor in patients treated according to COALL or St Jude protocols." *Blood* 108(6): 1984-1990.

Horrocks, P. M., A. F. Jones, W. A. Ratcliffe, G. Holder, A. White, R. Holder, J. G. Ratcliffe and D. R. London (1990). "Patterns of ACTH and cortisol pulsatility over twenty-four hours in normal males and females." *Clin Endocrinol (Oxf)* 32(1): 127-134.

Hsieh, I. S., K. C. Chang, Y. T. Tsai, J. Y. Ke, P. J. Lu, K. H. Lee, S. D. Yeh, T. M. Hong and Y. L. Chen (2013). "MicroRNA-320 suppresses the stem cell-like characteristics of prostate cancer cells by downregulating the Wnt/beta-catenin signaling pathway." *Carcinogenesis* 34(3): 530-538.

Huang, C. C. and H. H. Yao (2010). "Inactivation of Dicer1 in Steroidogenic factor 1-positive cells reveals tissue-specific requirement for Dicer1 in adrenal, testis, and ovary." *BMC Dev Biol* 10: 66.

Huang, N., A. Dardis and W. L. Miller (2005). "Regulation of cytochrome b5 gene transcription by Sp3, GATA-6, and steroidogenic factor 1 in human adrenal NCI-H295A cells." *Mol Endocrinol* 19(8): 2020-2034.

Iwai, N., K. Kajimoto, H. Tomoike and N. Takashima (2007). "Polymorphism of CYP11B2 determines salt sensitivity in Japanese." *Hypertension* 49(4): 825-831.

James, P. A., S. Oparil, B. L. Carter, W. C.ushman, C. Dennison-Himmelfarb, J. Handler, D. T. Lackland, M. L. Lefevre, T. D. Mackenzie, O. Ogedegbe, S. C. Smith, Jr., L. P. Svetkey, S. J. Taler, R. R. Townsend, J. T. Wright, Jr., A. S. Narva and E. Ortiz (2013). "2014 Evidence-Based Guideline for the Management of High Blood Pressure in Adults: Report From the Panel Members Appointed to the Eighth Joint National Committee (JNC 8)." *JAMA*.

Jeunemaitre, X. (2008). "Genetics of the human renin angiotensin system." *J Mol Med (Berl)* 86(6): 637-641.

Jeunemaitre, X., F. Soubrier, Y. V. Kotelevtsev, R. P. Lifton, C. S. Williams, A. Charru, S. C. Hunt, P. N. Hopkins, R. R. Williams, J. M. Lalouel and et al. (1992). "Molecular basis of human hypertension: role of angiotensinogen." *Cell* 71(1): 169-180.

Jimenez, P., K. Saner, B. Mayhew and W. E. Rainey (2003). "GATA-6 is expressed in the human adrenal and regulates transcription of genes required for adrenal androgen biosynthesis." *Endocrinology* 144(10): 4285-4288.

John, B., A. J. Enright, A. Aravin, T. Tuschl, C. Sander and D. S. Marks (2004). "Human MicroRNA targets." *PLoS Biol* 2(11): e363.

Kahsar-Miller, M., L. R. Boots, A. Bartolucci and R. Azziz (2004). "Role of a CYP17 polymorphism in the regulation of circulating dehydroepiandrosterone sulfate levels in women with polycystic ovary syndrome." *Fertil Steril* 82(4): 973-975.

Kapp, L. D. and J. R. Lorsch (2004). "The molecular mechanics of eukaryotic translation." *Annu Rev Biochem* 73: 657-704.

Kefas, B., J. Godlewski, L. Comeau, Y. Li, R. Abounader, M. Hawkinson, J. Lee, H. Fine, E. A. Chiocca, S. Lawler and B. Purow (2008). "microRNA-7 inhibits the epidermal growth factor receptor and the Akt pathway and is down-regulated in glioblastoma." *Cancer Res* 68(10): 3566-3572.

Kelly, J. J., A. Martin and J. A. Whitworth (2000). "Role of erythropoietin in cortisol-induced hypertension." *J Hum Hypertens* 14(3): 195-198.

Khaw, K. T., S. Bingham, A. Welch, R. Luben, E. O'Brien, N. Wareham and N. Day (2004). "Blood pressure and urinary sodium in men and women: the Norfolk Cohort of the European Prospective Investigation into Cancer (EPIC-Norfolk)." *Am J Clin Nutr* 80(5): 1397-1403.

Khvorova, A., A. Reynolds and S. D. Jayasena (2003). "Functional siRNAs and miRNAs exhibit strand bias." *Cell* 115(2): 209-216.

Kiiveri, S., J. Liu, M. Westerholm-Ormio, N. Narita, D. B. Wilson, R. Voutilainen and M. Heikinheimo (2002). "Differential expression of GATA-4 and GATA-6 in fetal and adult mouse and human adrenal tissue." *Endocrinology* 143(8): 3136-3143.

Kristjansson, K., A. Manolescu, A. Kristinsson, T. Hardarson, H. Knudsen, S. Ingason, G. Thorleifsson, M. L. Frigge, A. Kong, J. R. Gulcher and K. Stefansson (2002). "Linkage of essential hypertension to chromosome 18q." *Hypertension* 39(6): 1044-1049.

Krone, N. and W. Arlt (2009). "Genetics of congenital adrenal hyperplasia." *Best Pract Res Clin Endocrinol Metab* 23(2): 181-192.

Kruger, J. and M. Rehmsmeier (2006). "RNAhybrid: microRNA target prediction easy, fast and flexible." *Nucleic Acids Res* 34(Web Server issue): W451-454.

Lander, E. S., L. M. Linton, B. Birren, C. Nusbaum, M. C. Zody, J. Baldwin, K. Devon, K. Dewar, M. Doyle, W. FitzHugh, R. Funke, D. Gage, K. Harris, A. Heaford, J. Howland, L. Kann, J. Lehoczky, R. LeVine, P. McEwan, K. McKernan, *et al.* (2001). "Initial sequencing and analysis of the human genome." *Nature* 409(6822): 860-921.

Landthaler, M., A. Yalcin and T. Tuschl (2004). "The human DiGeorge syndrome critical region gene 8 and its *D. melanogaster* homolog are required for miRNA biogenesis." *Curr Biol* 14(23): 2162-2167.

Langenfeld, M. R., R. Veelken, H. P. Schobel, A. Friedrich and R. E. Schmieder (1997). "Is endogenous erythropoietin a pathogenetic factor in the development of essential hypertension?" *Nephrol Dial Transplant* 12(6): 1155-1160.

Lau, N. C., L. P. Lim, E. G. Weinstein and D. P. Bartel (2001). "An abundant class of tiny RNAs with probable regulatory roles in *Caenorhabditis elegans*." *Science* 294(5543): 858-862.

Lee, R. C., R. L. Feinbaum and V. Ambros (1993). "The *C. elegans* heterochronic gene *lin-4* encodes small RNAs with antisense complementarity to *lin-14*." *Cell* 75(5): 843-854.

Lee, Y., C. Ahn, J. Han, H. Choi, J. Kim, J. Yim, J. Lee, P. Provost, O. Radmark, S. Kim and V. N. Kim (2003). "The nuclear RNase III Drosha initiates microRNA processing." *Nature* 425(6956): 415-419.

Lee, Y., M. Kim, J. Han, K. H. Yeom, S. Lee, S. H. Baek and V. N. Kim (2004). "MicroRNA genes are transcribed by RNA polymerase II." *EMBO J* 23(20): 4051-4060.

Leptidis, S., H. El Azzouzi, S. I. Lok, R. de Weger, S. Olieslagers, N. Kisters, G. J. Silva, S. Heymans, E. Cuppen, E. Berezikov, L. J. De Windt and P. da Costa Martins (2013). "A deep sequencing approach to uncover the miRNOME in the human heart." *PLoS One* 8(2): e57800.

Levy, D., A. L. DeStefano, M. G. Larson, C. J. O'Donnell, R. P. Lifton, H. Gavras, L. A. Cupples and R. H. Myers (2000). "Evidence for a gene influencing blood pressure on chromosome 17. Genome scan linkage results for longitudinal blood pressure phenotypes in subjects from the framingham heart study." *Hypertension* 36(4): 477-483.

Levy, D., G. B. Ehret, K. Rice, G. C. Verwoert, L. J. Launer, A. Dehghan, N. L. Glazer, A. C. Morrison, A. D. Johnson, T. Aspelund, Y. Aulchenko, T. Lumley, A. Kottgen, R. S. Vasan, F. Rivadeneira, G. Eiriksdottir, X. Guo, D. E. Arking, G. F. Mitchell, F. U. Mattace-Raso, *et al.* (2009). "Genome-wide association study of blood pressure and hypertension." *Nat Genet* 41(6): 677-687.

Lewis, B. P., C. B. Burge and D. P. Bartel (2005). "Conserved seed pairing, often flanked by adenosines, indicates that thousands of human genes are microRNA targets." *Cell* 120(1): 15-20.

Lewontin, R. C. (1960). "The Evolutionary Dynamics of Complex Polymorphisms." *Evolution* 14(4): 458-472.

Li, A., R. Tedde, Z. S. Krozowski, A. Pala, K. X. Li, C. H. Shackleton, F. Mantero, M. Palermo and P. M. Stewart (1998). "Molecular basis for hypertension in the "type II variant" of apparent mineralocorticoid excess." *Am J Hum Genet* 63(2): 370-379.

Li, Y., F. Liu, S. Luo, H. Hu, X. H. Li and S. W. Li (2012). "Polymorphism T-->C of gene CYP17 promoter and polycystic ovary syndrome risk: a meta-analysis." *Gene* 495(1): 16-22.

Lifton, R. P., R. G. Dluhy, M. Powers, G. M. Rich, S. Cook, S. Ulick and J. M. Lalouel (1992a). "A chimaeric 11 beta-hydroxylase/aldosterone synthase gene causes glucocorticoid-remediable aldosteronism and human hypertension." *Nature* 355(6357): 262-265.

Lifton, R. P., R. G. Dluhy, M. Powers, G. M. Rich, M. Gutkin, F. Fallo, J. R. Gill, Jr., L. Feld, A. Ganguly, J. C. Laidlaw and et al. (1992b). "Hereditary hypertension caused by chimaeric gene duplications and ectopic expression of aldosterone synthase." *Nat Genet* 2(1): 66-74.

Lin, C. J., J. W. Martens and W. L. Miller (2001). "NF-1C, Sp1, and Sp3 are essential for transcription of the human gene for P450c17 (steroid 17alpha-hydroxylase/17,20 lyase) in human adrenal NCI-H295A cells." *Mol Endocrinol* 15(8): 1277-1293.

Lin, D., J. A. Harikrishna, C. C. Moore, K. L. Jones and W. L. Miller (1991). "Missense mutation serine106----proline causes 17 alpha-hydroxylase deficiency." *J Biol Chem* 266(24): 15992-15998.

Liu, C., H. Li, Q. Qi, L. Lu, W. Gan, R. J. Loos and X. Lin (2011). "Common variants in or near FGF5, CYP17A1 and MTHFR genes are associated with blood pressure and hypertension in Chinese Hans." *J Hypertens* 29(1): 70-75.

Livak, K. J. and T. D. Schmittgen (2001). "Analysis of relative gene expression data using real-time quantitative PCR and the 2(-Delta Delta C(T)) Method." *Methods* 25(4): 402-408.

Longini, I. M., Jr., M. W. Higgins, P. C. Hinton, P. P. Moll and J. B. Keller (1984). "Environmental and genetic sources of familial aggregation of blood pressure in Tecumseh, Michigan." *Am J Epidemiol* 120(1): 131-144.

Lu, J., G. Getz, E. A. Miska, E. Alvarez-Saavedra, J. Lamb, D. Peck, A. Sweet-Cordero, B. L. Ebert, R. H. Mak, A. A. Ferrando, J. R. Downing, T. Jacks, H. R. Horvitz and T. R. Golub (2005). "MicroRNA expression profiles classify human cancers." *Nature* 435(7043): 834-838.

Lund, E., S. Guttinger, A. Calado, J. E. Dahlberg and U. Kutay (2004). "Nuclear export of microRNA precursors." *Science* 303(5654): 95-98.

Luo, X., Y. Ikeda and K. L. Parker (1994). "A cell-specific nuclear receptor is essential for adrenal and gonadal development and sexual differentiation." *Cell* 77(4): 481-490.

Madhani, H. D. and C. Guthrie (1994). "Dynamic RNA-RNA interactions in the spliceosome." *Annu Rev Genet* 28: 1-26.

Mangelsdorf, D. J., C. Thummel, M. Beato, P. Herrlich, G. Schutz, K. Umesono, B. Blumberg, P. Kastner, M. Mark, P. Chambon and R. M. Evans (1995). "The nuclear receptor superfamily: the second decade." *Cell* 83(6): 835-839.

Marszalek, B., M. Lacinski, N. Babych, E. Capla, J. Biernacka-Lukanty, A. Warenik-Szymankiewicz and W. H. Trzeciak (2001). "Investigations on the genetic polymorphism in the region of CYP17 gene encoding 5'-UTR in patients with polycystic ovarian syndrome." *Gynecol Endocrinol* 15(2): 123-128.

Martin, R. M., C. J. Lin, E. M. Costa, M. L. de Oliveira, A. Carrilho, H. Villar, C. A. Longui and B. B. Mendonca (2003). "P450c17 deficiency in Brazilian patients: biochemical diagnosis through progesterone levels confirmed by CYP17 genotyping." *J Clin Endocrinol Metab* 88(12): 5739-5746.

Maston, G. A., S. K. Evans and M. R. Green (2006). "Transcriptional regulatory elements in the human genome." *Annu Rev Genomics Hum Genet* 7: 29-59.

McManus, F. (2012) "Regulation of the aldosterone synthase gene- role in human hypertension and adrenal corticosteroid production" *University of Glasgow PhD*

McManus, F., W. Sands, L. Diver, S. M. MacKenzie, R. Fraser, E. Davies and J. M. Connell (2012). "APEX1 regulation of aldosterone synthase gene transcription is disrupted by a common polymorphism in humans." *Circ Res* 111(2): 212-219.

Miller, W. L. (1988). "Molecular biology of steroid hormone synthesis." *Endocr Rev* 9(3): 295-318.

Miller, W. L. (2005a). "Disorders of androgen synthesis--from cholesterol to dehydroepiandrosterone." *Med Princ Pract* 14 Suppl 1: 58-68.

Miller, W. L. (2005b). "Minireview: regulation of steroidogenesis by electron transfer." *Endocrinology* 146(6): 2544-2550.

Miyoshi, Y. and S. Noguchi (2003). "Polymorphisms of estrogen synthesizing and metabolizing genes and breast cancer risk in Japanese women." *Biomed Pharmacother* 57(10): 471-481.

Monno, S., H. Ogawa, T. Date, M. Fujioka, W. L. Miller and M. Kobayashi (1993). "Mutation of histidine 373 to leucine in cytochrome P450c17 causes 17 alpha-hydroxylase deficiency." *J Biol Chem* 268(34): 25811-25817.

Mononen, N. and J. Schleutker (2009). "Polymorphisms in genes involved in androgen pathways as risk factors for prostate cancer." *J Urol* 181(4): 1541-1549.

Mountjoy, K. G., I. M. Bird, W. E. Rainey and R. D. Cone (1994). "ACTH induces up-regulation of ACTH receptor mRNA in mouse and human adrenocortical cell lines." *Mol Cell Endocrinol* 99(1): R17-20.

- Mune, T. and P. C. White (1996). "Apparent mineralocorticoid excess: genotype is correlated with biochemical phenotype." *Hypertension* 27(6): 1193-1199.
- Nakajin, S. and P. F. Hall (1981). "Microsomal cytochrome P-450 from neonatal pig testis. Purification and properties of A C21 steroid side-chain cleavage system (17 alpha-hydroxylase-C17,20 lyase)." *J Biol Chem* 256(8): 3871-3876.
- Nakamura, Y., H. X. Gang, T. Suzuki, H. Sasano and W. E. Rainey (2009). "Adrenal changes associated with adrenarche." *Rev Endocr Metab Disord* 10(1): 19-26.
- Napoli, C., C. Lemieux and R. Jorgensen (1990). "Introduction of a Chimeric Chalcone Synthase Gene into Petunia Results in Reversible Co-Suppression of Homologous Genes in trans." *Plant Cell* 2(4): 279-289.
- NCEP (2002). "Third Report of the National Cholesterol Education Program (NCEP) Expert Panel on Detection, Evaluation, and Treatment of High Blood Cholesterol in Adults (Adult Treatment Panel III) final report." *Circulation* 106(25): 3143-3421.
- Nelson, D. R., D. C. Zeldin, S. M. Hoffman, L. J. Maltais, H. M. Wain and D. W. Nebert (2004). "Comparison of cytochrome P450 (CYP) genes from the mouse and human genomes, including nomenclature recommendations for genes, pseudogenes and alternative-splice variants." *Pharmacogenetics* 14(1): 1-18.
- Neres, M. S., R. J. Auchus, C. H. Shackleton and C. E. Kater (2010). "Distinctive profile of the 17-hydroxylase and 17,20-lyase activities revealed by urinary steroid metabolomes of patients with CYP17 deficiency." *Arq Bras Endocrinol Metabol* 54(9): 826-832.
- New, M. I. (2003). "Inborn errors of adrenal steroidogenesis." *Mol Cell Endocrinol* 211(1-2): 75-83.
- Newton-Cheh, C., T. Johnson, V. Gateva, M. D. Tobin, M. Bochud, L. Coin, S. S. Najjar, J. H. Zhao, S. C. Heath, S. Eyheramendy, K. Papadakis, B. F. Voight, L. J. Scott, F. Zhang, M. Farrall, T. Tanaka, C. Wallace, J. C. Chambers, K. T. Khaw, P. Nilsson, *et al.* (2009). "Genome-wide association study identifies eight loci associated with blood pressure." *Nat Genet* 41(6): 666-676.
- Nieman, L. K. and I. Ilias (2005). "Evaluation and treatment of Cushing's syndrome." *Am J Med* 118(12): 1340-1346.
- Ntais, C., A. Polycarpou and J. P. Ioannidis (2003). "Association of the CYP17 gene polymorphism with the risk of prostate cancer: a meta-analysis." *Cancer Epidemiol Biomarkers Prev* 12(2): 120-126.
- O'Donnell, C. J., K. Lindpaintner, M. G. Larson, V. S. Rao, J. M. Ordovas, E. J. Schaefer, R. H. Myers and D. Levy (1998). "Evidence for association and genetic linkage of the angiotensin-converting enzyme locus with hypertension and blood

- pressure in men but not women in the Framingham Heart Study." *Circulation* 97(18): 1766-1772.
- Org, E., S. Eyheramendy, P. Juhanson, C. Gieger, P. Lichtner, N. Klopp, G. Veldre, A. Doring, M. Viigimaa, S. Sober, K. Tomberg, G. Eckstein, P. Kelgo, T. Rebane, S. Shaw-Hawkins, P. Howard, A. Onipinla, R. J. Dobson, S. J. Newhouse, M. Brown, *et al.* (2009). "Genome-wide scan identifies CDH13 as a novel susceptibility locus contributing to blood pressure determination in two European populations." *Hum Mol Genet* 18(12): 2288-2296.
- Orom, U. A., F. C. Nielsen and A. H. Lund (2008). "MicroRNA-10a binds the 5'UTR of ribosomal protein mRNAs and enhances their translation." *Mol Cell* 30(4): 460-471.
- Ozbay, T., A. Rowan, A. Leon, P. Patel and M. B. Sewer (2006). "Cyclic adenosine 5'-monophosphate-dependent sphingosine-1-phosphate biosynthesis induces human CYP17 gene transcription by activating cleavage of sterol regulatory element binding protein 1." *Endocrinology* 147(3): 1427-1437.
- Packer, A. N., Y. Xing, S. Q. Harper, L. Jones and B. L. Davidson (2008). "The bifunctional microRNA miR-9/miR-9* regulates REST and CoREST and is downregulated in Huntington's disease." *J Neurosci* 28(53): 14341-14346.
- Papadopoulos, G. L., M. Reczko, V. A. Simossis, P. Sethupathy and A. G. Hatzigeorgiou (2009). "The database of experimentally supported targets: a functional update of TarBase." *Nucleic Acids Res* 37(Database issue): D155-158.
- Park, J. M., E. J. Lee, S. Ramakrishna, D. H. Cha and K. H. Baek (2008). "Association study for single nucleotide polymorphisms in the CYP17A1 gene and polycystic ovary syndrome." *Int J Mol Med* 22(2): 249-254.
- Patterson, E. E., A. K. Holloway, J. Weng, T. Fojo and E. Kebebew (2011). "MicroRNA profiling of adrenocortical tumors reveals miR-483 as a marker of malignancy." *Cancer* 117(8): 1630-1639.
- Payne, A. H. and D. B. Hales (2004). "Overview of steroidogenic enzymes in the pathway from cholesterol to active steroid hormones." *Endocr Rev* 25(6): 947-970.
- Perusse, L., T. Rice, C. Bouchard, G. P. Vogler and D. C. Rao (1989). "Cardiovascular risk factors in a French-Canadian population: resolution of genetic and familial environmental effects on blood pressure by using extensive information on environmental correlates." *Am J Hum Genet* 45(2): 240-251.
- Pesi, R., S. Allegrini, M. G. Careddu, D. N. Filoni, M. Camici and M. G. Tozzi (2010). "Active and regulatory sites of cytosolic 5'-nucleotidase." *FEBS J* 277(23): 4863-4872.

- Petersen, C. P., M. E. Bordeleau, J. Pelletier and P. A. Sharp (2006). "Short RNAs repress translation after initiation in mammalian cells." *Mol Cell* 21(4): 533-542.
- Phillips, A. C., D. Carroll, C. R. Gale, J. M. Lord, W. Arlt and G. D. Batty (2010). "Cortisol, DHEAS, their ratio and the metabolic syndrome: evidence from the Vietnam Experience Study." *Eur J Endocrinol* 162(5): 919-923.
- Pusalkar, M., P. Meherji, J. Gokral, S. Chinnaraj and A. Maitra (2009). "CYP11A1 and CYP17 promoter polymorphisms associate with hyperandrogenemia in polycystic ovary syndrome." *Fertil Steril* 92(2): 653-659.
- Quandt, K., K. Frech, H. Karas, E. Wingender and T. Werner (1995). "MatInd and MatInspector: new fast and versatile tools for detection of consensus matches in nucleotide sequence data." *Nucleic Acids Res* 23(23): 4878-4884.
- Rafiq, S., S. Anand and R. Roberts (2010). "Genome-wide association studies of hypertension: have they been fruitful?" *J Cardiovasc Transl Res* 3(3): 189-196.
- Rainey, W. E., I. M. Bird and J. I. Mason (1994). "The NCI-H295 cell line: a pluripotent model for human adrenocortical studies." *Mol Cell Endocrinol* 100(1-2): 45-50.
- Ramos Cirilo, P. D., F. E. Rosa, M. F. Moreira Ferraz, C. A. Rainho, A. Pontes and S. R. Rogatto (2012). "Genetic polymorphisms associated with steroids metabolism and insulin action in polycystic ovary syndrome." *Gynecol Endocrinol* 28(3): 190-194.
- Reddy, S. D., K. Ohshiro, S. K. Rayala and R. Kumar (2008). "MicroRNA-7, a homeobox D10 target, inhibits p21-activated kinase 1 and regulates its functions." *Cancer Res* 68(20): 8195-8200.
- Reinhart, B. J., F. J. Slack, M. Basson, A. E. Pasquinelli, J. C. Bettinger, A. E. Rougvie, H. R. Horvitz and G. Ruvkun (2000). "The 21-nucleotide let-7 RNA regulates developmental timing in *Caenorhabditis elegans*." *Nature* 403(6772): 901-906.
- Ren, X. P., J. Wu, X. Wang, M. A. Sartor, J. Qian, K. Jones, P. Nicolaou, T. J. Pritchard and G. C. Fan (2009). "MicroRNA-320 is involved in the regulation of cardiac ischemia/reperfusion injury by targeting heat-shock protein 20." *Circulation* 119(17): 2357-2366.
- Robertson, S., S. M. Mackenzie, S. Alvarez-Madrazo, L. A. Diver, J. Lin, P. M. Stewart, R. Fraser, J. M. Connell and E. Davies (2013). "MicroRNA-24 Is a Novel Regulator of Aldosterone and Cortisol Production in the Human Adrenal Cortex." *Hypertension*.
- Rodriguez, A., S. Griffiths-Jones, J. L. Ashurst and A. Bradley (2004). "Identification of mammalian microRNA host genes and transcription units." *Genome Res* 14(10A): 1902-1910.

Rodriguez, H., D. W. Hum, B. Staels and W. L. Miller (1997). "Transcription of the human genes for cytochrome P450_{scc} and P450_{c17} is regulated differently in human adrenal NCI-H295 cells than in mouse adrenal Y1 cells." *J Clin Endocrinol Metab* 82(2): 365-371.

Romero, D. G., M. W. Plonczynski, C. A. Carvajal, E. P. Gomez-Sanchez and C. E. Gomez-Sanchez (2008). "Microribonucleic acid-21 increases aldosterone secretion and proliferation in H295R human adrenocortical cells." *Endocrinology* 149(5): 2477-2483.

Sabatti, C., S. K. Service, A. L. Hartikainen, A. Pouta, S. Ripatti, J. Brodsky, C. G. Jones, N. A. Zaitlen, T. Varilo, M. Kaakinen, U. Sovio, A. Ruukonen, J. Laitinen, E. Jakkula, L. Coin, C. Hoggart, A. Collins, H. Turunen, S. Gabriel, P. Elliot, *et al.* (2009). "Genome-wide association analysis of metabolic traits in a birth cohort from a founder population." *Nat Genet* 41(1): 35-46.

Saito, T. and P. Saetrom (2010). "MicroRNAs--targeting and target prediction." *N Biotechnol* 27(3): 243-249.

Sarai, A. and H. Kono (2005). "Protein-DNA recognition patterns and predictions." *Annu Rev Biophys Biomol Struct* 34: 379-398.

Sato, A., H. Suzuki, M. Murakami, Y. Nakazato, Y. Iwaita and T. Saruta (1994). "Glucocorticoid increases angiotensin II type 1 receptor and its gene expression." *Hypertension* 23(1): 25-30.

Schaar, D. G., D. J. Medina, D. F. Moore, R. K. Strair and Y. Ting (2009). "miR-320 targets transferrin receptor 1 (CD71) and inhibits cell proliferation." *Exp Hematol* 37(2): 245-255.

Schmitz, K. J., J. Helwig, S. Bertram, S. Y. Sheu, A. C. Suttorp, J. Seggewiss, E. Willscher, M. K. Walz, K. Worm and K. W. Schmid (2011). "Differential expression of microRNA-675, microRNA-139-3p and microRNA-335 in benign and malignant adrenocortical tumours." *J Clin Pathol* 64(6): 529-535.

Schonemann, M. D., M. O. Muench, M. K. Tee, W. L. Miller and S. H. Mellon (2012). "Expression of P450_{c17} in the human fetal nervous system." *Endocrinology* 153(5): 2494-2505.

Seitz, H., J. S. Tushir and P. D. Zamore (2011). "A 5'-uridine amplifies miRNA/miRNA* asymmetry in *Drosophila* by promoting RNA-induced silencing complex formation." *Silence* 2: 4.

Sepramaniam, S., A. Armugam, K. Y. Lim, D. S. Karolina, P. Swaminathan, J. R. Tan and K. Jeyaseelan (2010). "MicroRNA 320a functions as a novel endogenous modulator of aquaporins 1 and 4 as well as a potential therapeutic target in cerebral ischemia." *J Biol Chem* 285(38): 29223-29230.

Sethi, A. A., B. G. Nordestgaard, M. L. Gronholdt, R. Steffensen, G. Jensen and A. Tybjaerg-Hansen (2003). "Angiotensinogen single nucleotide polymorphisms, elevated blood pressure, and risk of cardiovascular disease." *Hypertension* 41(6): 1202-1211.

Sewer, M. B. and S. Jagarlapudi (2009). "Complex assembly on the human CYP17 promoter." *Mol Cell Endocrinol* 300(1-2): 109-114.

Sewer, M. B., V. Q. Nguyen, C. J. Huang, P. W. Tucker, N. Kagawa and M. R. Waterman (2002). "Transcriptional activation of human CYP17 in H295R adrenocortical cells depends on complex formation among p54(nrb)/NonO, protein-associated splicing factor, and SF-1, a complex that also participates in repression of transcription." *Endocrinology* 143(4): 1280-1290.

Sewer, M. B. and M. R. Waterman (2002). "Adrenocorticotropin/cyclic adenosine 3',5'-monophosphate-mediated transcription of the human CYP17 gene in the adrenal cortex is dependent on phosphatase activity." *Endocrinology* 143(5): 1769-1777.

Sewer, M. B. and M. R. Waterman (2003). "cAMP-dependent protein kinase enhances CYP17 transcription via MKP-1 activation in H295R human adrenocortical cells." *J Biol Chem* 278(10): 8106-8111.

Shibata, H., Y. Ikeda, T. Mukai, K. Morohashi, I. Kurihara, T. Ando, T. Suzuki, S. Kobayashi, M. Murai, I. Saito and T. Saruta (2001). "Expression profiles of COUP-TF, DAX-1, and SF-1 in the human adrenal gland and adrenocortical tumors: possible implications in steroidogenesis." *Mol Genet Metab* 74(1-2): 206-216.

Shibata, H., I. Kurihara, S. Kobayashi, K. Yokota, N. Suda, I. Saito and T. Saruta (2003). "Regulation of differential COUP-TF-coregulator interactions in adrenal cortical steroidogenesis." *J Steroid Biochem Mol Biol* 85(2-5): 449-456.

Shin, C., J. W. Nam, K. K. Farh, H. R. Chiang, A. Shkumatava and D. P. Bartel (2010). "Expanding the microRNA targeting code: functional sites with centered pairing." *Mol Cell* 38(6): 789-802.

Singh, P., P. S. Soon, J. J. Feige, O. Chabre, J. T. Zhao, N. Cherradi, E. Lalli and S. B. Sidhu (2012). "Dysregulation of microRNAs in adrenocortical tumors." *Mol Cell Endocrinol* 351(1): 118-128.

Sookoian, S., T. F. Gianotti, C. D. Gonzalez and C. J. Pirola (2007). "Association of the C-344T aldosterone synthase gene variant with essential hypertension: a meta-analysis." *J Hypertens* 25(1): 5-13.

Soon, P. S., L. J. Tacon, A. J. Gill, C. P. Bambach, M. S. Sywak, P. R. Campbell, M. W. Yeh, S. G. Wong, R. J. Clifton-Bligh, B. G. Robinson and S. B. Sidhu (2009). "miR-195 and miR-483-5p Identified as Predictors of Poor Prognosis in Adrenocortical Cancer." *Clin Cancer Res* 15(24): 7684-7692.

Souter, I., I. Munir, P. Mallick, S. R. Weitsman, D. H. Geller and D. A. Magoffin (2006). "Mutagenesis of putative serine-threonine phosphorylation sites proximal to Arg255 of human cytochrome P450c17 does not selectively promote its 17,20-lyase activity." *Fertil Steril* 85 Suppl 1: 1290-1299.

Sparkes, R. S., I. Klisak and W. L. Miller (1991). "Regional mapping of genes encoding human steroidogenic enzymes: P450scc to 15q23-q24, adrenodoxin to 11q22; adrenodoxin reductase to 17q24-q25; and P450c17 to 10q24-q25." *DNA Cell Biol* 10(5): 359-365.

Stamler, J., G. Rose, R. Stamler, P. Elliott, A. Dyer and M. Marmot (1989). "INTERSALT study findings. Public health and medical care implications." *Hypertension* 14(5): 570-577.

Stark, A., J. Brennecke, N. Bushati, R. B. Russell and S. M. Cohen (2005). "Animal MicroRNAs confer robustness to gene expression and have a significant impact on 3'UTR evolution." *Cell* 123(6): 1133-1146.

Stuiver, M., S. Lainez, C. Will, S. Terry, D. Gunzel, H. Debaix, K. Sommer, K. Kopplin, J. Thumfart, N. B. Kampik, U. Querfeld, T. E. Willnow, V. Nemecek, C. A. Wagner, J. G. Hoenderop, O. Devuyst, N. V. Knoers, R. J. Bindels, I. C. Meij and D. Muller (2011). "CNNM2, encoding a basolateral protein required for renal Mg²⁺ handling, is mutated in dominant hypomagnesemia." *Am J Hum Genet* 88(3): 333-343.

Sun, J. Y., Y. Huang, J. P. Li, X. Zhang, L. Wang, Y. L. Meng, B. Yan, Y. Q. Bian, J. Zhao, W. Z. Wang, A. G. Yang and R. Zhang (2012). "MicroRNA-320a suppresses human colon cancer cell proliferation by directly targeting beta-catenin." *Biochem Biophys Res Commun* 420(4): 787-792.

Suzuki, H. I., K. Yamagata, K. Sugimoto, T. Iwamoto, S. Kato and K. Miyazono (2009). "Modulation of microRNA processing by p53." *Nature* 460(7254): 529-533.

Takeuchi, F., M. Isono, T. Katsuya, K. Yamamoto, M. Yokota, T. Sugiyama, T. Nabika, A. Fujioka, K. Ohnaka, H. Asano, Y. Yamori, S. Yamaguchi, S. Kobayashi, R. Takayanagi, T. Ogiwara and N. Kato (2010). "Blood pressure and hypertension are associated with 7 loci in the Japanese population." *Circulation* 121(21): 2302-2309.

Tee, M. K., Q. Dong and W. L. Miller (2008). "Pathways leading to phosphorylation of p450c17 and to the posttranslational regulation of androgen biosynthesis." *Endocrinology* 149(5): 2667-2677.

Tremblay, J. J. and R. S. Viger (2001). "GATA factors differentially activate multiple gonadal promoters through conserved GATA regulatory elements." *Endocrinology* 142(3): 977-986.

Unger, T. (2002). "The role of the renin-angiotensin system in the development of cardiovascular disease." *Am J Cardiol* 89(2A): 3A-9A; discussion 10A.

Unsal, T., E. Konac, E. Yesilkaya, A. Yilmaz, A. Bideci, H. Ilke Onen, P. Cinaz and A. Menevse (2009). "Genetic polymorphisms of FSHR, CYP17, CYP1A1, CAPN10, INSR, SERPINE1 genes in adolescent girls with polycystic ovary syndrome." *J Assist Reprod Genet* 26(4): 205-216.

Valencia-Sanchez, M. A., J. Liu, G. J. Hannon and R. Parker (2006). "Control of translation and mRNA degradation by miRNAs and siRNAs." *Genes Dev* 20(5): 515-524.

Van Cauter, E., R. Leproult and D. J. Kupfer (1996). "Effects of gender and age on the levels and circadian rhythmicity of plasma cortisol." *J Clin Endocrinol Metab* 81(7): 2468-2473.

Veldhuis, J. D., A. Iranmanesh, M. L. Johnson and G. Lizarralde (1990). "Amplitude, but not frequency, modulation of adrenocorticotropin secretory bursts gives rise to the nyctohemeral rhythm of the corticotropic axis in man." *J Clin Endocrinol Metab* 71(2): 452-463.

Venter, J. C., M. D. Adams, E. W. Myers, P. W. Li, R. J. Mural, G. G. Sutton, H. O. Smith, M. Yandell, C. A. Evans, R. A. Holt, J. D. Gocayne, P. Amanatides, R. M. Ballew, D. H. Huson, J. R. Wortman, Q. Zhang, C. D. Kodira, X. H. Zheng, L. Chen, M. Skupski, *et al.* (2001). "The sequence of the human genome." *Science* 291(5507): 1304-1351.

Via, M., C. Gignoux and E. G. Burchard (2010). "The 1000 Genomes Project: new opportunities for research and social challenges." *Genome Med* 2(1): 3.

Vollmer, W. M., F. M. Sacks, J. Ard, L. J. Appel, G. A. Bray, D. G. Simons-Morton, P. R. Conlin, L. P. Svetkey, T. P. Erlinger, T. J. Moore and N. Karanja (2001). "Effects of diet and sodium intake on blood pressure: subgroup analysis of the DASH-sodium trial." *Ann Intern Med* 135(12): 1019-1028.

Walker, B. R. (2007). "Glucocorticoids and cardiovascular disease." *Eur J Endocrinol* 157(5): 545-559.

Walker, B. R., R. Best, C. H. Shackleton, P. L. Padfield and C. R. Edwards (1996). "Increased vasoconstrictor sensitivity to glucocorticoids in essential hypertension." *Hypertension* 27(2): 190-196.

Wallerath, T., K. Witte, S. C. Schafer, P. M. Schwarz, W. Prellwitz, P. Wohlfart, H. Kleinert, H. A. Lehr, B. Lemmer and U. Forstermann (1999). "Down-regulation of the expression of endothelial NO synthase is likely to contribute to glucocorticoid-mediated hypertension." *Proc Natl Acad Sci U S A* 96(23): 13357-13362.

Wang, L. H., S. Y. Tsai, R. G. Cook, W. G. Beattie, M. J. Tsai and B. W. O'Malley (1989). "COUP transcription factor is a member of the steroid receptor superfamily." *Nature* 340(6229): 163-166.

Wang, T., F. Satoh, R. Morimoto, Y. Nakamura, H. Sasano, R. J. Auchus, M. A. Edwards and W. E. Rainey (2011). "Gene expression profiles in aldosterone-producing adenomas and adjacent adrenal glands." *Eur J Endocrinol* 164(4): 613-619.

Wang, Y., J. R. O'Connell, P. F. McArdle, J. B. Wade, S. E. Dorff, S. J. Shah, X. Shi, L. Pan, E. Rumpersaud, H. Shen, J. D. Kim, A. R. Subramanya, N. I. Steinle, A. Parsa, C. C. Ober, P. A. Welling, A. Chakravarti, A. B. Weder, R. S. Cooper, B. D. Mitchell, *et al.* (2009). "From the Cover: Whole-genome association study identifies STK39 as a hypertension susceptibility gene." *Proc Natl Acad Sci U S A* 106(1): 226-231.

Wang, Y. H., M. K. Tee and W. L. Miller (2010). "Human cytochrome p450c17: single step purification and phosphorylation of serine 258 by protein kinase a." *Endocrinology* 151(4): 1677-1684.

Ward, R. (1990). Familial aggregation and genetic epidemiology of blood pressure. *Hypertension: Pathophysiology, Diagnosis and Management*. B. B. JH Laragh. New York, Raven Press. 1: 81-100.

Wartelle-Bladou, C., G. Le Folgoc, M. Bourliere and L. Lecomte (2012). "Hepatitis C therapy in non-genotype 1 patients: the near future." *J Viral Hepat* 19(8): 525-536.

Wei, L., T. M. MacDonald and B. R. Walker (2004). "Taking glucocorticoids by prescription is associated with subsequent cardiovascular disease." *Ann Intern Med* 141(10): 764-770.

Wells, S. E., P. E. Hillner, R. D. Vale and A. B. Sachs (1998). "Circularization of mRNA by eukaryotic translation initiation factors." *Mol Cell* 2(1): 135-140.

Whelton, P. K., J. He, J. A. Cutler, F. L. Brancati, L. J. Appel, D. Follmann and M. J. Klag (1997). "Effects of oral potassium on blood pressure. Meta-analysis of randomized controlled clinical trials." *JAMA* 277(20): 1624-1632.

White, P. C. and L. Slutsker (1995). "Haplotype analysis of CYP11B2." *Endocr Res* 21(1-2): 437-442.

Whitworth, J. A., G. J. Mangos and J. J. Kelly (2000). "Cushing, cortisol, and cardiovascular disease." *Hypertension* 36(5): 912-916.

Whitworth, J. A., P. M. Williamson, G. Mangos and J. J. Kelly (2005). "Cardiovascular consequences of cortisol excess." *Vasc Health Risk Manag* 1(4): 291-299.

Wickenheisser, J. K., P. G. Quinn, V. L. Nelson, R. S. Legro, J. F. Strauss, 3rd and J. M. McAllister (2000). "Differential activity of the cytochrome P450 17alpha-hydroxylase and steroidogenic acute regulatory protein gene promoters in

normal and polycystic ovary syndrome theca cells." *J Clin Endocrinol Metab* 85(6): 2304-2311.

Wightman, B., I. Ha and G. Ruvkun (1993). "Posttranscriptional regulation of the heterochronic gene *lin-14* by *lin-4* mediates temporal pattern formation in *C. elegans*." *Cell* 75(5): 855-862.

Williamson, C., P. Jeemon, C. E. Hastie, L. McCallum, S. Muir, J. Dawson, M. Walters, W. Sloan, D. Morrison, A. F. Dominiczak, J. Pell and S. Padmanabhan (2013). "Family history of premature cardiovascular disease: blood pressure control and long-term mortality outcomes in hypertensive patients." *Eur Heart J*.

Wilson, F. H., S. Disse-Nicodeme, K. A. Choate, K. Ishikawa, C. Nelson-Williams, I. Desitter, M. Gunel, D. V. Milford, G. W. Lipkin, J. M. Achard, M. P. Feely, B. Dussol, Y. Berland, R. J. Unwin, H. Mayan, D. B. Simon, Z. Farfel, X. Jeunemaitre and R. P. Lifton (2001). "Human hypertension caused by mutations in WNK kinases." *Science* 293(5532): 1107-1112.

Wood, S. (2011) "Regulation of Adrenal Corticosteroidogenesis: the role of microRNAs in the control of aldosterone synthase and 11 β -hydroxylase" *University of Glasgow PhD*

Wood, S., S. MacKenzie, R. Fraser, J. Connell and E. Davies (2011). "Dicer-Dependent miRNAs Regulate Adrenal Steroidogenesis." *Endocrine Reviews* 32.

Wu, L., J. Fan and J. G. Belasco (2006). "MicroRNAs direct rapid deadenylation of mRNA." *Proc Natl Acad Sci U S A* 103(11): 4034-4039.

Wu, L., B. Xi, M. Zhang, Y. Shen, X. Zhao, T. Wang, H. Cheng, D. Hou, G. Liu, X. Wang and J. Mi (2012). "A sex-specific effect of the CYP17A1 SNP rs11191548 on blood pressure in Chinese children." *J Hum Hypertens* 26(12): 731-736.

Wurtman, R. J. and J. Axelrod (1965). "Adrenaline synthesis: control by the pituitary gland and adrenal glucocorticoids." *Science* 150(3702): 1464-1465.

Yanase, T., H. Sasano, T. Yubisui, Y. Sakai, R. Takayanagi and H. Nawata (1998). "Immunohistochemical study of cytochrome b5 in human adrenal gland and in adrenocortical adenomas from patients with Cushing's syndrome." *Endocr J* 45(1): 89-95.

Yi, R., Y. Qin, I. G. Macara and B. R. Cullen (2003). "Exportin-5 mediates the nuclear export of pre-microRNAs and short hairpin RNAs." *Genes Dev* 17(24): 3011-3016.

Zehavi, L., R. Avraham, A. Barzilai, D. Bar-Ilan, R. Navon, Y. Sidi, D. Avni and R. Leibowitz-Amit (2012). "Silencing of a large microRNA cluster on human chromosome 14q32 in melanoma: biological effects of mir-376a and mir-376c on insulin growth factor 1 receptor." *Mol Cancer* 11: 44.

Zhang, L., S. Volinia, T. Bonome, G. A. Calin, J. Greshock, N. Yang, C. G. Liu, A. Giannakakis, P. Alexiou, K. Hasegawa, C. N. Johnstone, M. S. Megraw, S. Adams, H. Lassus, J. Huang, S. Kaur, S. Liang, P. Sethupathy, A. Leminen, V. A. Simossis, *et al.* (2008). "Genomic and epigenetic alterations deregulate microRNA expression in human epithelial ovarian cancer." *Proc Natl Acad Sci U S A* 105(19): 7004-7009.

Zhang, L. H., H. Rodriguez, S. Ohno and W. L. Miller (1995). "Serine phosphorylation of human P450c17 increases 17,20-lyase activity: implications for adrenarche and the polycystic ovary syndrome." *Proc Natl Acad Sci U S A* 92(23): 10619-10623.

Zhao, J. J., J. Yang, J. Lin, N. Yao, Y. Zhu, J. Zheng, J. Xu, J. Q. Cheng, J. Y. Lin and X. Ma (2009). "Identification of miRNAs associated with tumorigenesis of retinoblastoma by miRNA microarray analysis." *Childs Nerv Syst* 25(1): 13-20.